# Weathering Extremes: Medieval Climate Change at Caerlaverock Castle

**Final Report to the Castle Studies Trust and Historic Environment Scotland**

**June 2022**

**Richard Tipping with contributions from Eileen Tisdall, Busie Gisranin, Jason Jordan, Tim Kinnaird, Neil McDonald, Stefan Sagrott and Aayush Srivastava**

## Summary

This reports details the work undertaken since July 2021 at and around Old Caerlaverock Castle. It describes the results of LiDAR-aided geomorphological mapping, systematic sediment coring and description, quantitative sedimentological analyses, distom analyses, luminescence profiling and OSL dating, and AMS $^{14}$C dating.

The later prehistoric and early historic coastline at Caerlaverock is a low degraded cliff cut in soft sediments. Seaward of this is an exceptional coastal landform called a prograding strandplain (prograding means advancing seaward). Much larger examples are known in Scotland, dating to around 4500 BC. Relative sea level fall is usually invoked to explain them through coastal sediment being stranded as the waves retreat, to be re-deposited as sandy plains and beaches. The Caerlaverock example is different because it started to form much later, around 200 BC, and was not formed in response to falling relative sea level. Instead, greatly increased sediment supply driven by extreme storm events encouraged both progradation and erosion, called barrier breaching. Strandplains are recognised as key indicators of past storminess and storm surges.

At Caerlaverock later Iron Age and probably Roman Iron Age storms created a minimum of five major storm surges, building elongate fine gravel and sand barrier beaches parallel to the coast, hundreds of metres long and tens of metres wide. These periods are not ones of heightened storminess in north west Europe. Gravels and sands were probably derived from glacial deposits in the valley of the River Nith 2-3km to the west. Their increased supply to the estuary may have been through accelerated fluvial erosion. Gravel was then pushed east to Caerlaverock by longshore drift currents in the form of very large gravel spits. They probably extended east across the coast where the Old Caerlaverock Castle was later built. Lagoons formed behind these barrier beaches, filled with mud from erosion of the pre-existing soft sediment coast. From the altitudes of the surfaces of lagoons, minimal water depths in the storm surges were 2-3m above contemporary spring tides. These events made the coast wider through progradation by some 200m. The ‘harbour’ at the Old Castle was constructed in a former tidal creek which had accumulated sediment from before 4000 BC. There is nothing in the very fine-grained mud of the tidal creek to indicate sediment deposition during storm surges. Hiatuses in sedimentation are identified in ‘harbour’ sediment in this period which may be storm surge indicators.

The eastern ends of these spits and lagoons were then eroded and truncated by a much larger storm event/s. This is not dated. It is loosely estimated to have been in the first half of the 1st millennium AD, but the extraordinary scale of this event makes it most parsimonious to think of this as the earliest surge impact on the Old Castle moat system (below). This event generated waves perpendicular (swash-aligned) to the coast. A 200m deep embayment was created by barrier breaching which reached the later prehistoric cliff, probably eroding it. One archaeological structure, the so-called ‘park pale’, built on remnants of earlier salt marsh, was partially destroyed. Beach gravel was thrown 20m inland on top of and beyond the cliff. Some gravel was reworked from eroding spits but most of it was ripped from the bedrock foreshore as it was exposed by wave erosion. The bedrock surface may have been lowered by 1.5m in this event/s, a prodigious amount.

After this, progradation resumed in response to major storms. They formed a second strandplain parallel to the first. This filled the embayment in a minimum of four ridge-forming events. These events were from swash-aligned storms: longshore drift was not involved. Beach ridges were made of gravel re-deposited from the barrier-breaching event. These events are only dated to before the later 16th century: they are assumed to relate to Medieval as well as later events. The second strandplain grew directly in front of the Old Castle and its ‘harbour’, eventually some 200m wide.

Construction of the 'harbour' cannot be identified from analyses of 'harbour' sediment: it may be represented by one of several hiatuses prior to AD1200-1300. The 'harbour' was not a harbour: its probable floor at any time in the historic period was higher than normal spring tides. It may have been a fish pond. Sediments in the 'harbour' that formed after AD1200-1300 contain no evidence for deposition of coarse sand and fine gravel deposited in barrier beaches in storm surge events happening only tens of metres away. To explain this it is necessary to assume that people blocked the exit of the Old Castle Burn because coarse sand and fine gravel were deposited a few metres inland of the 'harbour' at different times in the ditches of the moat system around the Old Castle.

The outer ditch of the moat system formed before c. AD1250. The basal peat in the moat system dates to AD1287-1342 (*c*. AD1300). This is younger than the accepted date of moat construction from dendro-dating (AD1229-30): one interpretation is that the wood was used long after felling, but another is that the basal peat marks the time when the function of the Old Castle changed. Some though not all coarse sand and fine gravel deposits in the moat system are established from diatom analyses to have been associated with salinities significantly higher than the fresh water that would normally have been the source of water to the moat system. At least three such inundations impacted the moat system (a) between *c*. AD1300 and *c*. AD1330, (b) after *c*. AD1330 and before *c*. AD1400, (c) tentatively around *c*. AD1400 and (d) around AD1475. All these inundations occurred at times of heightened storminess in north west Europe. The earliest surge raised the water surface around the Old Castle to at least 8m OD, 3-3.5m above contemporary high water spring tides. Whether the earlier events provoked abandonment of the Old Castle is unknown but is still feasible. Storm surges ceased to affect the surroundings of the Old Castle after *c*. AD1600.

The last lagoon to form was isolated from wave action at around AD1570. It was isolated by a 1600m long recurved spit transporting gravel from the Nith estuary that re-established longshore drift as a significant factor in coastal development. By the mid-18th century salt marsh began to accumulate at Caerlaverock, probably through climate change. This impeded longshore drift and cut off the supply of gravel from the Nith. Storm surges have at times impacted the salt marsh.

# 1. Introduction

In Martin Brann's (2004) monograph on Old Caerlaverock Castle Tipping *et al* examined landscape-shaping events associated in time with construction of the Old Castle, exploring the ppossibility that major coastal storms and floods had impacted deleteriously on the Old Castle and its environs in the high Medieval period. Radiocarbon dating of organic sediments in the outer ditch of the castle suggested that this feature pre-dated the Old Castle by, possibly, several hundred years. Sedimentological and diatom analyses suggested that the outer ditch, and thus the environs of the Old Castle more generally, experienced marine flooding from *c*. AD900 to *c*. AD1250. The moat system around the Old Castle had at times been filled on all but the eastern side, furthest from the coast, by comparatively coarse-grained sediment probably deriving from the coast. Marine inundation, possibly by storm surge events, might have been a reason to abandon the Old Castle and rebuild further inland and slightly higher at the New Castle. Tipping (unpublished) gained SMC in 2004 to core sediment filling the south side of the outer ditch of the New Castle. Around the causeway leading to Castle Wood still-water organic mud was found to be interrupted by bands of silt and clay up to 30cm thick and to a consistent altitude of 8.5-8.6 m OD, potentially indicating storm surges at least a metre higher than could be demonstrated at the Old Castle.

Seaward of the early Medieval coast, seven or so elongated ridges and intervening basins were mapped in difficult ground conditions and thought to be storm-generated barrier beaches with intervening back-barrier lagoons. Tipping and Adams (2007) suggested that some gravels in a few ridges were derived from a source west of the Nith Estuary. They dated peat formed before deposition of the final barrier beach to AD1290-1420.

There remained some fundamental chronological problems, however. Radiocarbon samples were not short-lived single entities but 2.0cm thick samples of peat or organic mud inherently imprecise in slowly accumulating sediment. Different organic fractions were dated, making temporal correlations difficult. Bayesian modelling, necessary in the historic period, was almost unknown in 2004. The age and function of the 'harbour', the likely conduit for storm surges, remained completely unknown. New LiDAR imagery in 2019 showed how inadequately the series of ridges and basins, barrier and back-barrier environments, had been mapped and how poorly dated they were.

This report presents all the data and interpretations of work conducted since July 2021. **Section 2** introduces Caerlaverock and the Solway Firth and what we already knew. **Section 2.1** focuses on what is known of the inner Solway Firth, its sediments and the dynamic processes that shape them, and attempts from archival data to reconstruct its recent sedimentological history, which is otherwise unknown**. Section 2.2** describes the probable sources of sediment to the coastal landforms at Caerlaverock. **Section 2.3** describes what is known of long-term coastal evolution, and **Section 2.4** pulls together archival evidence for Medieval and post-Medieval landscape change.

The context of coastal change at Carleverock is given in **Section 2.5** where prograding strandplains are explained. Their association with storm surges, coastal floods and climate change is detailed in **Section 2.6**: *Figure 6 is new*. The very limited evidence from archival data for coastal floods in the Solway Firth and beyond is reviewed in **Section 2.7**.

**Section 3** describes the methods used in the analyses at Caerlaverock. The report first discusses the new evidence for late Holocene coastal evolution at Caerlaverock (**Section 4.1**) describing and detailing all the evidence from fieldwork and laboratory analyses of the different landforms mapped by new LiDAR imagery, the sediments associated with them and their dating. **Section 4.1.13** attempts to synthesise what we now know of the events that shaped the Caerlaverock coast before

and after the Middle Ages. *This section has been extensively revised, relating the chronology of storm surges to their climate drivers*.

We then systematically follow the sedimentological impacts of storm surges inland by understanding sediments formed in relation to archaeological features. **Section 4.2.1** describes the work undertaken on environmental change in the 'harbour' of the Old Castle. *Section 4.2.1.4, defining chronologically the environmental changes, has been extensively revised*. Then the work undertaken to understand environmental change in (a) the moat system that surrounds the Old Castle,in **Sections 4.2.3 to 4.2.6** and (b) an outer 'defence', the outer ditch, in **Section 4.2.7,** is assessed. The chronological relation between these is evaluated in **Section 4.2.8**. Sediments in a previously mis-understood feature, the bailey, are described in **Section 4.2.9**, and the environmental context of the New Castle outlined in **Section 4.2.10**.

**Section 4.3** synthesises the new data from archaeological features by setting out the chronology of what seems to have happened around the Old and New Castles. *This section has been extensively revised*.

**Section 4.4** returns to the LiDAR imagery to enumerate and discuss the chronology of archaeological structures that were built in recent centuries on the prograding strandplain. **Section 4.5** is a more adventurous examination of the implications of the work for our understanding of the archaeology, before **Section 5** makes recommendations for future work. *Section 6 defines the final conclusions*.

# 2. The study area

## 2.1. The setting

The two castles at Caerlaverock are south east of Dumfries, east of the River Nith where it enters the inner Solway Firth estuary near Blackshaw Bank (Figures 1a, 1b).

The inner Solway Firth is a macro-tidal estuary with very large tidal ranges of 3.4 to 7.4m at Carsethorn (Figure 1a). Mean High Water Springs (MHWS) is at 4.6m OD and Mean Low Water Springs (MLWS) is at -3.0m OD at Southerness. The maximum fetch, of around 180km, is from the south-south-west (200$^{o}$): the coast at Caerlaverock is almost square on to this. It scores highly (8.75-9.00) on Dyer *et al*'s (2000) exposure scale. Though Caerlaverock is protected from south-westerly winds by the promontory of Southerness (Harvey and Allan 1998), and the Solway Firth is protected to a degree from North Atlantic storm tracks by the island of Ireland (Harrison 1997), extreme sea level events affect this coast, driven by south west or southerly winds from storm centres which lie northwest of Ireland and track north of Scotland (Haigh *et al* 2016: see also Zong and Tooley 2003). From storm surges affecting the British west coast between 1920 and 1955, Lennon (1963a) described major surge generation (e.g. 1.46 to 1.95m surges at Liverpool) arising not from stable uni-directional winds but from deepening secondary depressions to the south of the Icelandic Low which move from south west to north east at high speed. Lennon (1963b) went on to estimate the frequency of abnormally high tides along the British west coast. Silloth (MHWS 4.42m OD) is the nearest station to Caerlaverock (Figure 1a), though with a short (25 yr) record to 1960 and sea level determined from relatively imprecise observations of a tide pole. Tides 0.6m above MHWS occurred 37% of the time, tides 1.2m above MHWS occurred 2% of the time, and tides 2.3m above MHWS occurred only 0.16% of the time, the last close to a 200-yr event.

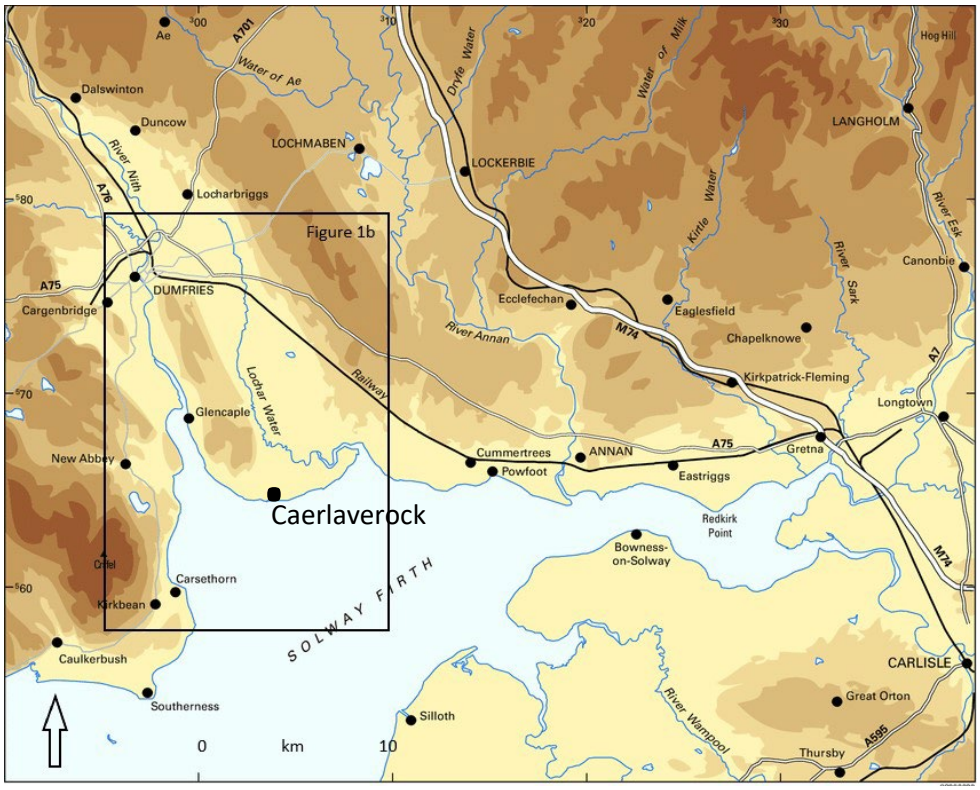

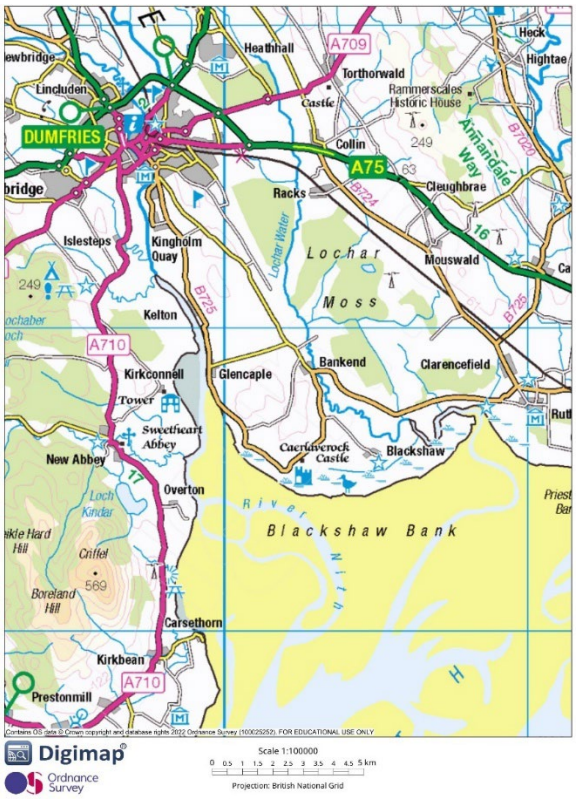


*Figure 1. The topographic setting of Caerlaverock: (a) the inner Solway Firth, north east of a line between Southerness in Scotland and Silloth in England; (b) Caerlaverock in relation to Dumfries, the River Nith and the Lochar Water.*

The firth is a flood-dominant estuary with semi-diurnal tides, an asymmetric tidal cycle with flood tides rising over two hours and ebb tides falling over six hours, with a five-hour slack period at low water. Tides rise very quickly. The Minister for Cummertrees parish, east of Caerlaverock, described the rising tide driven by south or south westerly storms (Gordon 1845a, 246) which may explain part of the name of Caerlaverock ('noisy' or 'chattery': James unpublished):

"*When the tide is coming in these angry moods, its loud roaring is heard by people along the shore for upwards of twenty miles before it reaches them. … before the first wave is discernible from the shore, there is seen a cloud of spray whirling and dashing forward; then a long curved white and flowing surf, and on a sudden, the large wave itself appears throwing forward its speckled body three feet abreast with awful impetuosity*".

The firth has high tidal energies, with flows up to 2.5ms$^{-1}$ off Southerness Point. Flood tide speeds exceed the ebb tide by 0.77ms$^{-1}$. At the entrance to the inner firth, waves >1m occurred (1991-1992) 40% of the year, the maximum significant wave height was 3.9m and waves >3m occurred mainly during the winter. A uni-directional wave climate from the south west, and the south westerly direction of the most common winds coincide with the longest length of fetch to make the inner firth a sediment trap. Suspended inorganic particulate matter (turbidity) in the inner firth is the highest in Scotland. The sea floor in the inner estuary is almost everywhere <10m deep. Storm surge risk is elevated because of this. Surface currents are thought to be seaward but currents near the floor of the firth, and wave-induced currents, push sediment upstream where it is trapped in intertidal sandbanks, mudflats and as salt marsh on the northern shore. Sediments are overwhelmingly fine and very fine sand with silt though locally, medium sand can form 1/3 of the sand-sized fraction. In summer sandflats can be delicately laminated by algal stromatolites that form at low flow. Intertidal sandflats contain significant shell material, much fragmented by feeding birds,

and shell banks occur. Sediment coarsens slightly towards shallow (up to 2.5m deep) intertidal channels. Channels transport clay as well as silt and sand. Tidal scour of mudflats and sandbanks rarely result in erosion of more than a few centimetres of sediment, but major channel migration can mean the complete reworking of several metres of sediment. Gravel other than in anthropogenic deposits is not found. Though the Caerlaverock shore is classified as erosional in relation to other Scottish coasts, salt marshes greatly soften coastal impacts (Wilson 1965; Bridges and Leeder 1976; Mowbray 1983; Garbutt 1993; Solway Firth Partnership 1996; Brampton, Lees and Ramsay 1999; Firth, Collins and Smith 2000; Harvey 2000; Axelsson *et al* 2006; McMillan *et al* 2011, 28; Ball, Edwards and Werritty 2014; Garcia-Oliver, Tabor and Djordjevic 2014; Fitton, Hansom and Rennie 2016; Moffat *et al* 2020: accessed 24/12/21).

Sandbanks and mudflats extend at low tide for several kilometres. Documentary and cartographic evidence suggest that extensive intertidal sandbanks have characterised the inner firth since at least the Middle Ages. Scars or scaurs are Norse terms for exposed bedrock within sandbanks and salt marshes (Nielson 1899). Bowhouse Scar south of Castle Wood at Caerlaverock must have been exposed around the 10th century AD. The word 'Solway' is derived from 'sul' for mud and 'wath' a ford though this need not apply west of the ford at Sulwath, near Carlisle, used by Edward I in 1300. The '*Siege of Caerlaverock'*, a contemporary description of Edward's siege of the New Castle in 1300 (Scott-Giles transl. 1960), calls the sea "*la mer de Irlande*" (Nielson 1899). However, Medieval salt panning along the northern shore of the Solway implies the presence of contemporary salt marsh (Neilson 1899; McIntire 1942; Cranstone 2006; Oram 2012). The term 'Solway' was applied from the 16th century to all the inner firth (Nielson 1899). in 1545 the English garrison at Caerlaverock could be supplied only by 'litle boottis' of shallow draught. In earlier centuries supplies from England by ship were preferentially landed at the riverine ports of Dumfries and Annan (Brown unpublished). Henry Bullock's (1552) map of the 'debateable land' (Mackenzie 1951) shows sandflats at the east end of the firth, and *A Platt of the opposete Borders of Scotland to ye west marches of England* in 1590 shows all the inner firth filled with sediment, as does Winter's chart of 1742 (Moore 1983). In a military report of 1563x1566, "*The mouthe of the water of Nytht* [Nith] [is] *a schallow revere; noo weshalles* [no vessels] *can come furtht of England in yt but at the ful sea, and that at the crope of the tyde; soo that thei mon pas the Longrake sande, in the myddes of Sulwaye*" (Watson 1923, 29). This probably implies the presence then of sandbanks in the estuary because, although the Nith was also made shallow through erosion-resistant sandstone bedrock, this was at Dumfries and not at its mouth (McDowall 1906, 488, 693).

In the estuary, the course of the River Nith can change significantly between easily eroded intertidal sandflats (Marshall 1961; Wilson 1965, 140-43; Bridson 1979). In 1775/6 (Figure 4), 1855 and 1956 the Nith flowed east, immediately south of Castle Wood. The Nith was fordable south of Glencaple (Gordon 1845b, 349) before the river was canalised and deepened by mid-19th century training walls. The River Nith is the largest river in south west Scotland with a mean discharge (28.24 cumecs: $m^3s^{-1}$) six times that of neighbouring rivers on the north shore of the inner firth. The Nith is tidal to Dumfries: it has a tidal bore. East of Caerlaverock, the Lochar Water (Figure 1b) is a far less significant river. It is tidal only to Bankend although the valley floor is lower than 10.0m OD north of Heathhall (Figure 1b). Its valley at Racks is nearly 4km wide, filled with several metres of raised bog, the Lochar Moss complex (Figure 2b; Nichols 1967). Between these rivers and north of Caerlaverock is a long sandstone ridge to Dumfries, rising to 90m OD between Glencaple and Bankend at Ward Law, the traditional gathering place for Maxwells and the site of a Roman camp and earlier, Iron Age hill forts.

## 2.2. Geology

The bedrock geology underlying Holocene sediments at Caerlaverock comprise early Permian Locharbriggs Sandstone (Sst.), distinctively red fine to medium grained aeolian sandstones, siltstone and mudstones, and slightly older Doweel Breccia alluvial fan deposits interbedded with fluvial and aeolian sandstone (Brookfield 1979, 1980; McMillan *et al* 2011). The Doweel Breccia underlies Castle Wood at Caerlaverock and also outcrops within thin recent salt marsh sediments on Bowhouse Scar at Caerlaverock (Tipping and Adams 2007). At the few localities measured it has a south-westerly 15$^{o}$ dip (Geological Survey of Scotland 1879). McMillan *et al* (2011) reported clasts (pebbles) of Silurian origin and of Galloway Granitic Suite (GGS) Criffel granodiorite. Tipping and Adams (2007) quantified clast lithologies in the Doweel Breccia at Bowhouse Scar (NY 0023 6893), recording 67% GGS granodiorite, 22% Silurian greywacke and 5% Locharbriggs Sst. in clasts >4mm diameter.

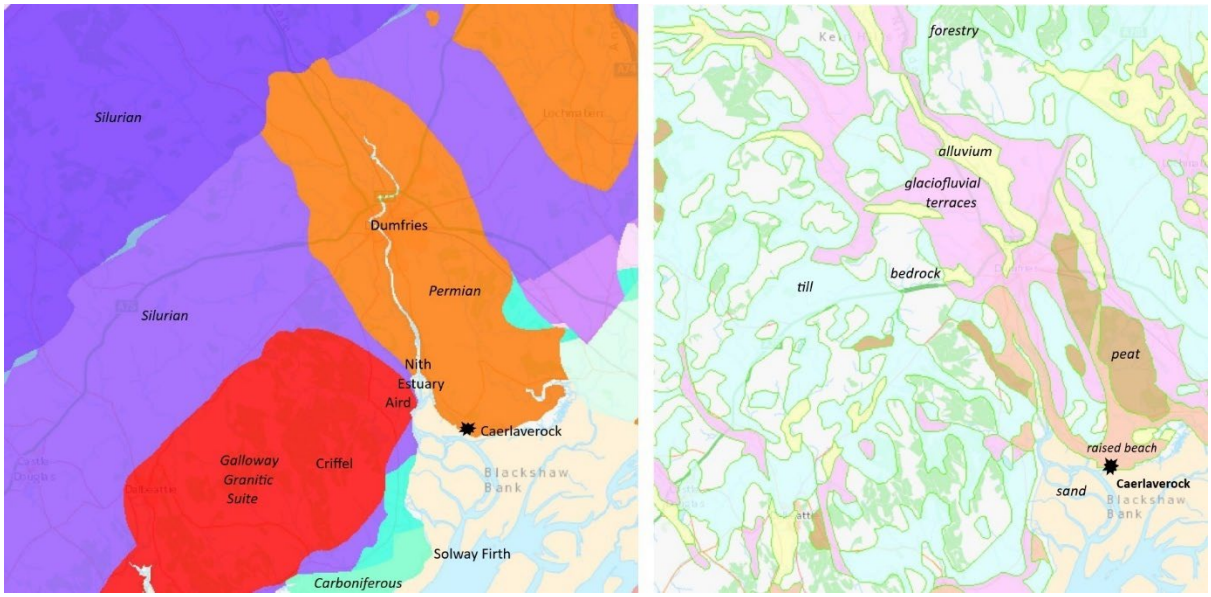


*Figure 2. Solid and superficial geology around Caerlaverock.*

Figure 2b shows the distribution north and west of Caerlaverock of Quaternary sediments deposited during and after the last glaciation of the British-Irish Ice Sheet. Glacial till smears the higher ground between areas of bedrock. This was derived from the Southern Uplands to the north and the Galloway Hills to the north west. Locally, the slopes of Ward Law, north of Caerlaverock, are covered in thin glacial till called the Irish Sea Coast Glacigenic Subgroup (British Geological Survey 2005; McMillan *et al* 2011, 14). It contains abundant Silurian clasts, smaller proportions of Permian clasts and rare GGS clasts. On the west side of the River Nith, the Southern Uplands Glacigenic Subgroup has clasts predominantly of Silurian lithologies and GGS granite and granodiorite, the last locally predominant around Criffel, with Carboniferous lithologies on the west coast of the Nith estuary (British Geological Survey 2005; McMillan *et al* 2011, 20). Livingstone *et al* (2008) and Evans *et al* (2009) recorded a complex sequence of ice flow regimes in the Solway lowlands east of the River Nith. The earliest was from west to east. Brookfield, Merritt and McMillan (2010) reported a glacially striated boulder pavement exposed at low tide on Priestside Bank east of the Lochar Water (Figure 1b) which comprised 95% Silurian clasts, 5% Permian clasts and some GGS (Criffel) granodiorite, though much less than 1%. The underlying till also contained 95% Silurian clasts and 4% Permian clasts but no GGS granodiorite. Further east, Trotter (1929) recorded erratics of Criffel granodiorite and Galloway granites from an early phase of the last glaciation in glacial till and glaciofluval gravel in the Vale of Eden near Carlisle: proportions were not quantified. Galloway granites were described as

"very abundant" in only one section: the suggestion is that they were few. Tipping and Adams (2007) did not record GGS clasts in till at Glencaple, but this may have been a younger deposit.

## 2.3. Holocene coastal evolution

South of Bowhouse Park and the New Castle (Figure 3) is a 'raised beach' of postglacial age, a level surface above 9 to 9.4m OD. It is called the New Castle Terrace in Figure 3. This widens east from Bowhousepark. Old Caerlaverock Castle and surrounding earthworks were constructed on or cut into this surface. It is widespread throughout the inner firth (Jardine 1980). The deposit underlying this terrace surface is largely a silt-rich fine sand, the product of tidal, inter-tidal and salt marsh sediments accumulating in the early to mid-Holocene Epoch (Greenlandian-Northgrippian Stages) as relative sea level (RSL) rose (Jardine 1975, 1980; Lloyd *et al* 1999; Smith *et al* 2003a; Tipping, Haggart and Milburn 2007). Jardine (1980) provides detailed records of its sediments and depositional environments. The deposit can be 11m thick. It is ubiquitously called 'carse', an informal Scots term meaning 'fen, low wet land' (Hough 2020). This name is problematic as a geological term when the 'carse' is diachronous, as it is in the inner Solway Firth (Dawson *et al* 1999; Lloyd *et al* 1999; Smith *et al* 2012). Tipping *et al* (2004) called the 'carse' outcropping in the study area the New Castle Terrace (NCT) fill (Figure 3).

In the Nith estuary immediately west of Caerlaverock, Smith *et al* (2003a) identified two marine shoreline terrace surfaces, the more extensive around 7.6-10.2m OD (N1) and a second forming small discontinuous fragments at 6.0-7.8m OD (N2). RSL rose in the lower Nith valley from 6750-6470 BC, culminating between 6640-6440 BC and 4540-4270 BC in shoreline N1: the original age estimates are re-calibrated. Shoreline N2 is younger but undated in the inner Solway Firth. It is correlated with the Blairdrummond Shoreline dated to between 2000 and 1000 BC (Smith *et al* 2012). RSL then fell to around 5m OD. Smith *et al* (2006, 2012) recognised a later, small, poorly defined, and undated RSL rise they called the Wigtown Shoreline.

Their youngest dated RSL change is from the base of a peat at Preston west of Southerness at 4.9m OD (with an altitudinal precision estimated at 3.8–6.0m OD), covering a surface of estuarine silt at 1760±70 $^{14}$C BP (AD120-440: Beta-84193: Smith *et al* 2003a). This age estimate is thought to be the time when present sea level, understood to relate to Mean High Water Springs (MHWS or MHWOST) tides, was attained. MHWS today at Southerness (Figure 1) is 4.6m OD. There is only one other $^{14}$C dated sea-level index point in the Solway Firth younger than AD1 listed in the most recent compilation of RSL data-points (Shennan, Bradley and Edwards 2018), but this is also at Preston where Jardine (1980) dated peat at 5.3m OD to 1850±95 $^{14}$C BP (I-5069), re-calibrated in 2022 to 1BC-AD409, interpreted to represent "the withdrawal of the sea to approximately its present position" prior to this date (ibid, 53). This observation is critical in discussion of the archaeological features at Caerlaverock. Small short-term fluctuations in RSL, with amplitudes of a few centimetres, have been claimed for the Medieval and post-Medieval in Britain (Tooley 1978; Lamb 1977, 1995; Orford *et al* 2000), but such fluctuations are usually interpreted today as products of storm-related coastal modification (e.g. Van Vliet-Lanoë *et al* 2014a). Changing RSL at centennial scales is not supported for the historic period in northern Britain (Long *et al* 1998; Dawson, Smith and Dawson 2001; Orford, Murdy and Freel 2006; Barlow *et al* 2014; Gehrels and Shennan 2015) where RSL has been stationary until, perhaps, the last few decades (Rennie and Hansom 2011). The evidence suggests that RSL in the Solway Firth, on the boundary between rising and subsiding coasts (Lloyd *et al* 1999) has been stable in the historic period.

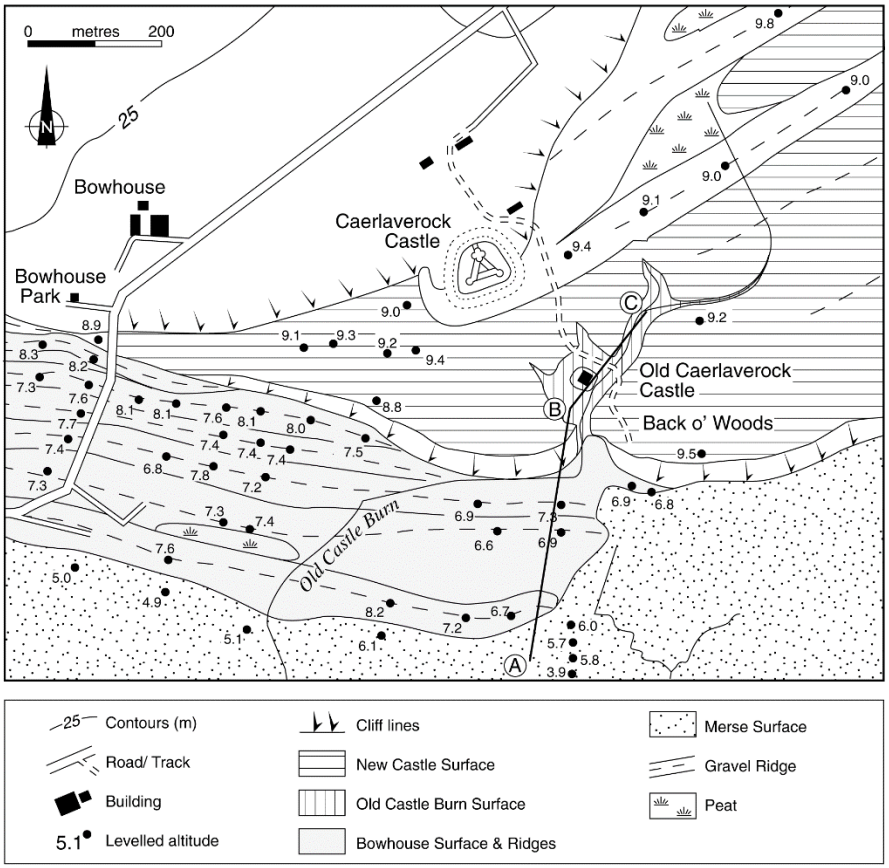


*Figure 3. Superficial sediments around the Old and New Caerlaverock Castles. The gravel ridges were mapped in difficult ground conditions and are not accurate.*

Sediments beneath the Old Castle Burn terrace surface in Figure 3 are younger than the NCT surface and largely fluvial. The landforms and sediments of the Bowhouse fill and surface are the subjects of this study.

In some places, though not at Caerlaverock, the higher of the marine shoreline terrace surfaces (N1) is capped by up to 3m of blown sand. Jardine (1980, 17, 24) and Dawson *et al* (1999) give $^{14}$C ages, again re-calibrated, of 4780-4260 BC, 2130-1580 BC and 390-60 BC for peat beneath sand in coastal sections near Annan (Figure 1a). Smith *et al* (2003a) dated blown sand forming after 120-440 AD on peat near Southerness.

At much lower altitudes than the NCT fill is the 'merse' (Figures 3, 5), a local term for fine sandy intertidal and salt marsh sediments forming close to HWMS, often vegetated, flooded occasionally (Jardine 1980), still accumulating (Fridlington *et al* 1998; Harvey and Allan 1998; Tyler 1999) but changing frequently in extent (Steers 1973; Rowe 1978; Bridson 1979). Smith *et al* (2003a) recorded values for the merse surface of 4.5-5.6m OD but there are three surfaces, separated by low cliffs, around the inner firth (Marshall 1961, 1962a, b). At Caerlaverock these surfaces are at 5.8–6 m OD, 5.4 m OD and 5.3m OD (Tipping *et al* 2004). Marshall (1961, 1962b) argued that river erosion eroded the merse, creating the low cliffs separating the three merse surfaces, but marine erosion best explains the spatial scale of these features. The highest merse fill is up to 3.5m thick north of the sea wall marked on Figure 7a. Seaward of the sea wall the average thickness of the highest merse is around 1.2m thick. Bedrock is at around 3.5m OD but its altitude is variable, being 4.2m OD at Bowhouse Scar, south of Castle Wood.

## 2.4. Archival evidence for the Caerlaverock landscape

From the '*Siege of Caerlaverock'* (trans. Scott-Giles 1960) we seem to have a vivid description of the local landscape in AD1300:

> *"I believe there never was seen a castle more beautifully situated, for at once could be seen the Irish sea towards the west, and to the north a fine country, surrounded by an arm of the sea, so that no creature born could approach it on two sides, without putting himself in danger of the sea.*
>
> *Towards the south it was not easy, because there were numerous dangerous defiles of wood, and marshes, and ditches, where the sea is on each side of it, and where the river reaches it; and therefore it was necessary for the host to approach it towards the east, where the hill slopes"*

except that the Irish Sea is to the south and there was no more than 200m of marsh and wood between the coast and the New Castle (Tipping *et al* 2004). The 'fine country' stretches eastward, not north, 'surrounded' by the Lochar Water. There are tidal waters on three sides of the peninsula (Section 2.1). Perhaps the marsh and wood and ditches lay principally west towards the Nith estuary, and Edward advanced down the slope from the north. Reference in 1545 by English march wardens to Caerlaverock, "standdithe in a gret strenght of crikes and mosse" (Brown unpublished) might refer to the marshy ground and burns of the impermeable NCT surface south of the New Castle and around the Old Castle.

Stone (1973) considered Timothy Pont's *c*. 1596 Nithsdale manuscript map (Pont 35) 'realistic' despite being "noticeably different to the present configuration (Stone 1968, 167). Pont 35 depicts the peninsula at large scale, and a castle is mapped (almost certainly the New Castle) some distance from the mapped coast. The outline of the peninsula south of the castle appears exaggerated compared to subsequent maps, particularly Pont's depiction of a pronounced 'bulb' of land extending south from "Carlaverock" but this might be the low dome of bedrock called Bowhouse Scar, now concealed by thin salt marsh sediment. Salt marsh is not depicted by Pont. Tipping *et al* (2004, table 2.1) suggested that Pont had depicted open water where the highest and oldest merse is today. The 1545 comment that Caerlaverock "standeth uppon the see side" (Brown unpublished) might also imply that the merse had not then formed. Tipping *et al* (2004) described a Caerlaverock estate plan of 1746 (now mislaid) that depicted the sea wall extending east from the coastal ridges (Figure 7a). This need not have been the time the sea wall was constructed, but north of the sea wall was a field called 'The Flooders' (Marshall 1962b), newly formed merse, sometimes under water and probably affected by tides. Tipping *et al* (2004) $^{14}$C dated the basal 1.0cm of a 30cm thick peat overlying merse in this field, north of the sea wall at grid ref 302820 565190 (high merse borehole: Figure 7d). This is a minimal age for merse formation here. The calibrated age in 2004 (AD1660-1960) was unhelpful in defining this but re-calibration gives an age of AD1670-1800 for peat inception. This age-range might be narrowed to before 1800 by assuming that the sea wall, built before 1746, encouraged peat inception by reducing tidal influence.

Wells' 1775-6 plan of Castle Wood (Figure 4) shows the merse around 50m wide south of Castle Wood, widening to 170m east of Castle Wood in 'The Flooders', the merse forming the left bank of an east-flowing River Nith or a branch thereof. The New Castle was "far from the sea" when Pennant saw it in 1772 (Pennant (1774) 1998, 93). To the west at Lantonside and the east at Lands there was no merse: farmland formed the left bank of the river. However, by 1795 the church minister at Ruthwell, east of Annan (Figure 1a) had noted the expansion of merse "almost a mile further than it

did some years ago" (Sinclair 1794, 219), and at Kirkbean near Southerness at the west end of the inner firth (Figure 1a) "many acres are now excellent salt pasture, which not long ago the tides covered, when they consisted of beach and sand" (Sinclair 1795, 129). The low rock dome of Bowhouse Scar was exposed in Newell's detailed plan of 1845, then called Greenhead Point, giving in plan a peninsula not dissimilar to Pont's depiction 250 years earlier. The merse extended no further than in Well's plan (Figure 4).

*Figure 4. Wells' 1775-6 estate plan of Castle Wood, Wood Back and Greenhead (https://maps.nls.uk/view/217626568)*

## 2.5. Gravel ridges and strandplains: the context of coastal evolution at Caerlaverock

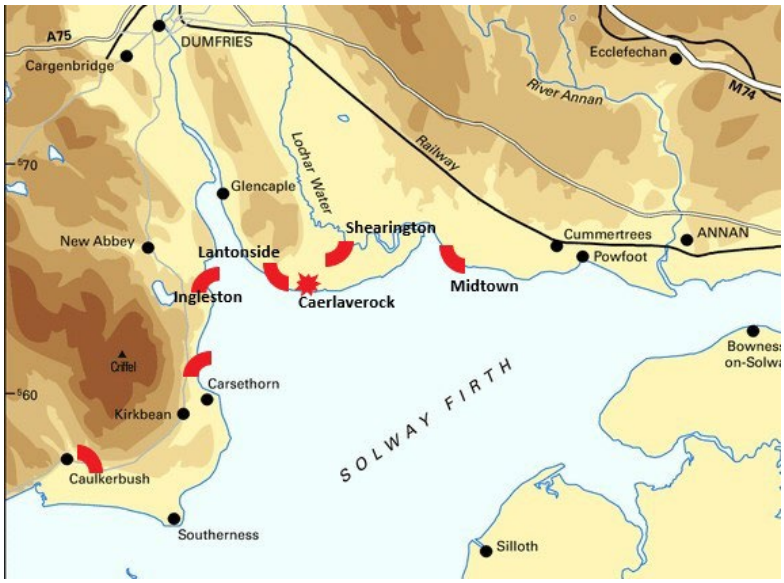


*Figure 5. Distribution and approximate orientations of coastal gravel ridges on the Scottish side of the Solway Firth mapped by Jardine (1980) and Smith* et al *(2003a)*

Jardine (1980) and Smith *et al* (2003a) mapped gravel ridges or groups of parallel ridges, spits or barrier beach systems that originally projected from the coast between Annan and Caulkerbush (Figure 5). Orientations align with present tidal flows (south west to north east) except one at Midtown that Jardine (1980) depicted as having grown northward: Hughes (1995) considered the Midtown ridges to be swash-aligned (e.g. parallel to the coast) barrier beaches. A few of these ridge systems overlie the NCT fill and most are surrounded by it, leading to the interpretation that most formed during the early-mid Holocene RSL rise or close to its culmination. None, however, have been dated. The Shearington ridges north of Caerlaverock New Castle rise above 10m OD and are probably of early-mid Holocene age: two Early Bronze Age flat axes were recovered from their lateral equivalent at the New Castle (Figure 3) at NY 0251 6551 (Yates 1979). Jardine (1980) thought the ridges at Carsethorn (not mapped by Smith *et al* 2003a) were comparatively young because they apparently lay on an eroded surface of the NCT, and Hickey (1997, 429) suggested a date of AD1425 for their formation, but they have Mesolithic and Neolithic flints on their surfaces (CANMORE ID 65479).

Parallel elongate beach ridges like these are called prograding strandplains: they prograde (advance) seaward. Those in the inner Solway Firth, including that at Caerlaverock, are small in extent compared to the major accumulations elsewhere in Scotland, the largest at the 15km$^2$ Morrich More on the Dornoch Firth and the 24 km$^2$ Culbin Sands (Comber 1993, 1995; Firth *et al* 1995; Hansom 2003; May and Hansom 2003), or the vast 250km$^2$ of the Dungeness foreland in south east England (Long, Waller and Plater 2007). Beach ridges are coastal barriers and form a spectrum from single beaches backed by the mainland to barrier islands isolated from the mainland. Prograding strandplains contain many such barriers. They can comprise only elongated beach ridges of sand or sand and gravel (Roy *et al* 1994; Otvos 2020), but those in Scotland have lower-lying parallel troughs or swales between beach ridges, usually filled with sand. Shoreward of barrier beaches at lower altitudes can be found back-barrier environments with finer-grained sediments, marshy and organic or under water.

Prograding strandplains are found on wave-dominated coasts. They result from a combination of allogenic (external) factors; sediment source, sediment supply, sea-level fluctuations, regional geological framework, topography and nearshore bathymetry combined with autogenic (internal) feedbacks; variations in hydrodynamic and weather conditions, transmitted sediment volumes and changing depth and slope of the adjacent seafloor (Otvos 2020). British and Irish examples demonstrate some of these factors.

Scottish and Irish strandplains are poorly dated but seem to have been initiated during or soon after the mid-Holocene RSL maximum, which culminated *c*. 4500 BC. Before this time, easily erodible coasts tended to retreat inland with rising RSL and wave action. Rising RSL (transgression) from below 0m OD at the beginning of the Holocene pushed sediment onshore, depending on bathymetry, rate of RSL rise and effective wave-base. The sediment is most commonly assumed to have been glacigenic, transported during glaciation and deglaciation by glaciers and glacial rivers and deposited offshore (Hansom 2001). Barrier beaches formed during transgressions are propelled shoreward as sediment facing the sea is eroded and deposited shoreward. Barrier beaches are said to 'rollover'. RSL rise thus created sediment surpluses at the coast by the middle of the Holocene (Hansom 1999; Hansom and McGlashan 2004). As RSL rise slowed from around 5000 BC and stabilised, some sediment was blown onshore to form sand dunes (Hansom and McGlashan (2004): blown sand at Annan dated after 4776-4251 BC (Jardine 1980) may relate to this phase, as might the earliest dunes in Brighouse Bay (Wells *et al* 1999) and Glen Luce (Smith *et al* 2020) to the west.

In the absence of significant seaward sediment supply, or where sediment supply failed, shoreward sediment movement (transgression) continued (Carter and Orford 1984; Carter *et al* 1987). Where sediment supply continued to be high or was increased, either from offshore or from terrestrial sources (e.g. Spencer *et al* 1998 at Dungeness), sediment stores were reworked by tidal processes and strandplains were initiated (Carter and Orford 1984). This process was aided by falling RSL which isolated nearshore sediment stores, allowing their reworking. Falling RSL may be recorded in the altitudes of gravel ridge crests although these will have been higher than contemporary MHWS and are in detail products of the strength of individual storm surges (Goslin and Clemmensen 2017). At the Morrich More, ridge crests fall from 8.6 to 1.4m OD (May and Hansom 2003). At Culbin they fall from 10.9 to 3.7m OD (May and Hansom 2003) though ridge crests lie above 9m OD for almost all of a *c*. 900m long transect, probably formed before *c*. 2500 BC (Comber 1995). Waves oblique to the shore added sediment by longshore drift, as on the Moray coast (Hansom 2021). Little is known in detail of the rate of progradation of most Scottish strandplains. The Morrich More, initiated before *c*. 4400 BC, is around 8km wide (May and Hansom 2003). The Culbin strandplain was initiated around 3300 BC (Comber 1995; Hansom 1999) with a maximum width of some 2.5km, and at Tentsmuir, south of the Tay estuary, gravels have prograded over 3.5km in the last *c*. 5000 years (Hansom and McGlashan 2004). Such ages are common in other parts of the world where RSL change has been similar (Roy *et al* 1994). Once initiated on a slowly falling or stable RSL, accretion and progradation will continue for thousands of years. Roy *et al* (1994) give values for progradation in Australian strandplains of between 0.24 and 0.6m/yr.

Broadly parallel, elongated coarse clastic ridges (gravel or shingle: well-rounded pebbles with grain sizes ~2 to ~64mm) represent high-energy storm deposits, times when there was excessive sediment supply (Carter and Orford 1984; Clayton in May and Hanson 2003; Donnelly *et al* 2004; Nott *et al* 2009; Otvos 2020). The recognition of this has made palaeoclimatologists focus on strandplains as less ambiguous signals of past storms than, for instance, blown sand accumulations (Goslin and Clemmensen 2017; below). There are prograding strandplains that formed much later than *c*. 6000 years ago and over much shorter timescales. Small mixed sand and gravel strandplains are thought generally to complete a lifecycle in a matter of a few centuries or millennia, dictated by a finite sediment supply rather than RSL change (Orford *et al* 1991; Forbes *et al* 1995). They have rarely been analysed, though. Nielsen *et al* (2006) OSL dated ridges in northern Jutland that formed between *c*. AD 700 and 1000, estimating that each ridge formed over *c*. 15 years at around 2m/yr.

Ridges form barriers, “supratidal nearshore and inshore landforms that separate high salinity marine waters from brackish inshore bodies”, with varying relations with the coast (Otvos 2020). They reduce wave erosion and mitigate storm-induced inundations. They create and protect back-barrier environments, low-lying, wet, brackish lagoons to freshwater ponds that become marsh at different rates and to different end points not necessarily related to barrier growth (Plater, Stupples and Roberts 2009). It is not clear whether single ridges represent multiple storm events. Goslin and Clemmensen (2017) argued they do, but Haslett and Bryant (2007) concluded that those they saw in section were formed by single events. Storms can be destructive of coastal landforms (Poirier, Tessier and Chaumillon 2017), but coarse clastic ridges have high preservation potential because they are relatively stable from wave attack, do not leak sediment seaward (Carter and Orford 1984) and they adjust only slowly to less energetic coastal processes (Trenhaile 1997). Ridges can be of sand also, as with the 50 or so at the Morrich More, each 1-1.5m high and spaced every 100m or so (May and Hansom 2003), but these are not comparable to coarse clastic forms (Carter and Orford 1984).

Barriers can be breached during storm events (Fruergaard *et al* 2013), forming channels connecting back-barrier environments to coastal processes, shoreward sediment transfer as overwash fans (Carter and Orford 1981; Donnelly, Kraus and Larson 2006) and re-distribution sometimes to form storm-swash terraces 1-10m above contemporary high water mark (McKenna, Cooper and Jackson 2012). Formation of coarse clastic barriers can slow, and they can be broken down in the long term when, for instance, progradation enters deeper water or sediment supply is reduced. Coarse-grained sediment is then exported seaward and stored in inter-tidal or sub-tidal deposits (Sorrel *et al* 2009; Van Vliet-Lanoë *et al* 2014a; Poirier *et al* 2017).

RSL fall in the later Holocene led to the coast becoming more compartmentalised. Headlands intercepted longshore sediment movement (Carter and Orford 1984) and confined areas of offshore sediment within smaller coastal cells (Brampton *et al* 1999). Where bodies of offshore sediment could not be replenished, they were depleted, leading to sediment starvation and shorelines increasingly vulnerable to erosion (Hansom 1999, 2001).

## 2.6. Proxy records of later Holocene storminess along the Atlantic façade and the North Sea

Prograding strandplains were considered until quite recently as products largely of RSL fluctuations (Carter 1983; Carter *et al* 1987, 1989; Carter and Orford 1988; Oliver, Thom and Woodroffe 2016), with sea level change seen to control sediment supply. Scottish examples were interpreted in such terms (Firth *et al* 1995; May and Hansom 2003). Because RSL change is usually slow, strandplains prograded slowly. The barrier beaches that punctuate them are clearly products of exceptional storm events (Carter and Orford 1984) but they received less attention as indicators of environmental change until theoretical frameworks changed from process- to event-oriented (Schumm 1976; Nott *et al* 2009), and concerns for near-future climate change required an understanding of past coastal storm frequency and magnitude. Increasing confidence in new dating techniques, particularly optically stimulated luminescence (OSL) which directly dates the sediment deposited, allowed for the first time the complex minerogenic sediment accumulations that characterise strandplains to be dated (Nielsen *et al* 2006; Reimann *et al* 2011).

Chronologies of past storminess from coarse clastic (gravel-rich) sediment bodies are the most significant because they are the least ambiguous: they are the products of very major storm events (or of extreme waves: Hansom and Hall 2009) and parts of their morphology, if preserved, are precise indicators of water depth (Goslin and Clemmensen 2017). Analyses along the coast facing the Atlantic Ocean are still comparatively few and some chronologies of major events and episodes in the later Holocene are not well-constrained (13th century AD: Plater *et al* 1999; AD600-650: Plater *et al* 2009; AD1100 to younger than AD1800: Haslett and Bryant 2007; AD750-1000: Billeaud *et al* 2009; AD400-600, AD700-1100 and after AD1300: Hanson and Hall 2009; AD1-300, AD1050-1200: Roberts and Plater 2007; AD300-700, AD1300-1600: Sorrel *et al* 2009; AD1700-1750; Cunningham *et al* 2011; 200 BC–AD150, AD200, AD300–400; Van Vliet-Lanoë *et al* 2014a; AD600-800, AD900-1100, AD1200-1650; Poirier *et al* 2017).

Most studies have focused on the deposition of wind-blown (aeolian) sand forming dunes or sheets, initially from the $^{14}C$ dating of peat associated with these, and later from OSL dating. Peats provide limiting dates only for events. The continuity of record is a problem in dune-derived storm chronologies. The environmental significance of thin sand layers is an interpretative issue, as are ambiguities as to the cause of blown sand activation (Delaney and Devoy 1995). Anthropogenic activities, direct or indirect, can either retard or accelerate sand-blow (Bateman and Godby 2004; Clarke and Rendell 2006; de Jong *et al* 2006; Reimann *et al* 2011; Brown 2015; Orme *et al* 2016), and

Jackson, Costas and Guisado-Pintado (2019) have suggested that dune construction in the 'little ice age' was driven not primarily by storms but by lower temperatures inducing shorter growing seasons for plants that would otherwise stabilise sand. Archaeological sites buried by sand have been considered (Brown 2015; Griffiths 2015) although their dating is problematic and the interval between initial sand-blow and settlement abandonment can be large.

For all sediment bodies and archaeological sites, preservation decreases with increasing age, so that debate about how climate determines storm frequency and magnitude has focused on the last *c*. 1000 years. In this period the North Atlantic Oscillation (NAO) is the dominant mode of atmospheric circulation in the North Atlantic Ocean and is the principal determinant of north west European weather and climate, particularly in winter months (Hurrell 1995). The NAO is the air pressure difference between a persistent high-pressure cell over the Azores and a low-pressure cell over Iceland. When differences are greatest, NAO values are high, often described as positive, and *vice versa*. Positive NAO winters are characterised in northern Europe and the British Isles by increased temperature, precipitation and the strength and frequency of westerly winds (Tsimplis *et al* 2005). The NAO is a fundamental control on storminess.

The NAO varies at all timescales. Proxy measures of long-term, centennial change in the NAO based on proxy records of temperature, precipitation and storminess now extend across the last millennium. Using proxy records of temperature and precipitation, the last millennium has been, simplistically, divided in two periods, the Medieval Climate Anomaly (MCA) and the 'little ice age' (LIA). The timing of these episodes depends on geography, chronological precision and techniques used in reconstruction. The MCA probably began around AD1000 (Büntgen *et al* 2011) though some suggest as early as *c*. AD800 (McDermott *et al* 2001; Trouet *et al* 2009) or as late as AD1150 (Ortega *et al* 2015). For some workers the MCA-LIA boundary is as early as *c*. AD1200 to *c*. AD1350 (Glueck and Stockton 2001; Brazdil *et al* 2005; Lund, Lynch-Steiglitz and Curry 2006; Masse *et al* 2008; Sicre *et al* 2008; Büntgen *et al* 2011; Graham *et al* 2011; Olsen, Anderson and Knudsen 2012; Cunningham et al 2013; Faust *et al* 2016). Miller *et al* (2012) reported an abrupt start to the LIA between AD1275 and AD1300 with substantial intensification AD1430-1455 (see also Ogilvie and Farmer 1997; Dugmore *et al* 2007; Ortega *et al* 2015; Anchukaitis *et al* 2019). Anchukaitis *et al* (2019) described the 1450s as a decadal-scale period of sustained colder sea surface temperatures and atmospheric anomalies similar to the negative phase of the NAO. *Circa* AD1400 is a significant date for changes in western Scotland in precipitation (Proctor *et al* 2000), sea surface temperature (Cage and Austin 2010) and the sign (+/-) of the NAO index (Proctor *et al* 2006; Baker *et al* 2015). Neither period was climatically stable (Pfister *et al* 1998). Within the LIA, in Scotland after *c*. AD1400, there were short positive NAO phases. Those defined by Cook (2003) between AD1500 and AD1800 are estimated at 1490–1510, 1520–1535, 1555–1590, 1610–1625, 1690–1705, 1715–1730, 1755–1760 and 1770–1810. Those defined by Ortega *et al* (2015) from their $NAO_{mc}$ ensemble between AD1400 and AD1800 are estimated before 1425, 1480–1600 and 1630–1670. Alheit and Hagen's (2002) analysis of Norwegian herring populations emphasised their abundance to have been determined by negative modes of the NAO and minimal frequencies of south westerly winds along the European seaboard *c*. AD970-1020, *c*. 1110-1130, the end of the 12th to the mid-13th centuries, *c*. 1307-1330, the mid-15th century, 1556-1589, 1660-1680 and 1747-1809.

There is a positive relation between winds and extreme sea levels and the NAO index (Woodworth *et al* 2007; Phillips, Rees and Thomas 2013). Kreutz *et al* (1997) and Meeker and Mayewski (2002) identified a major, abrupt (*c*. 20 year) increase in storminess in the Greenland GISP2 ice-core record at ~AD1400 (AD1425: Dugmore *et al* 2007). This was linked to records in north west Europe and to the behaviour of the NAO. Dawson *et al* (2003, 2004, 2007) argued for a prolonged positive NAO

phase to have characterised the LIA, enhanced by North Atlantic storm tracks pushed south by expanding sea-ice cover in the Arctic. The centuries prior to AD1400, the MCA (~AD1000-1400), were said to be characterised by 'dormant NAO' conditions (Dawson *et al* 2007). This interpretation was challenged by reconstructions which concluded that the MCA was characterised by persistent positive NAO conditions and the LIA by weaker, negative NAO conditions (Seager *et al* 2007; Trouet *et al* 2009; Cage and Austin 2010; Graham *et al* 2011; Baker *et al* 2015). Trouet, Scourse and Raible (2012) tried to reconcile these positions by characterising the coldest parts of the LIA, though a negative NAO phase, as experiencing fewer but more intense storms. It is still uncertain from model simulations whether the NAO can 'flip' persistently for long periods (Lehner, Raible and Stocker 2012; Ortega *et al* 2015). As we have seen, Jackson *et al* (2019) have argued that storm strength is not the prime determinant of sand-blow events in the LIA.

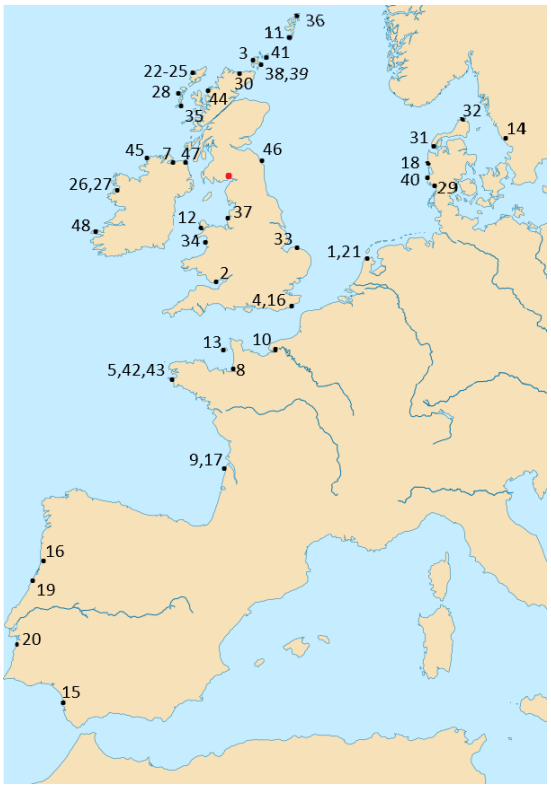

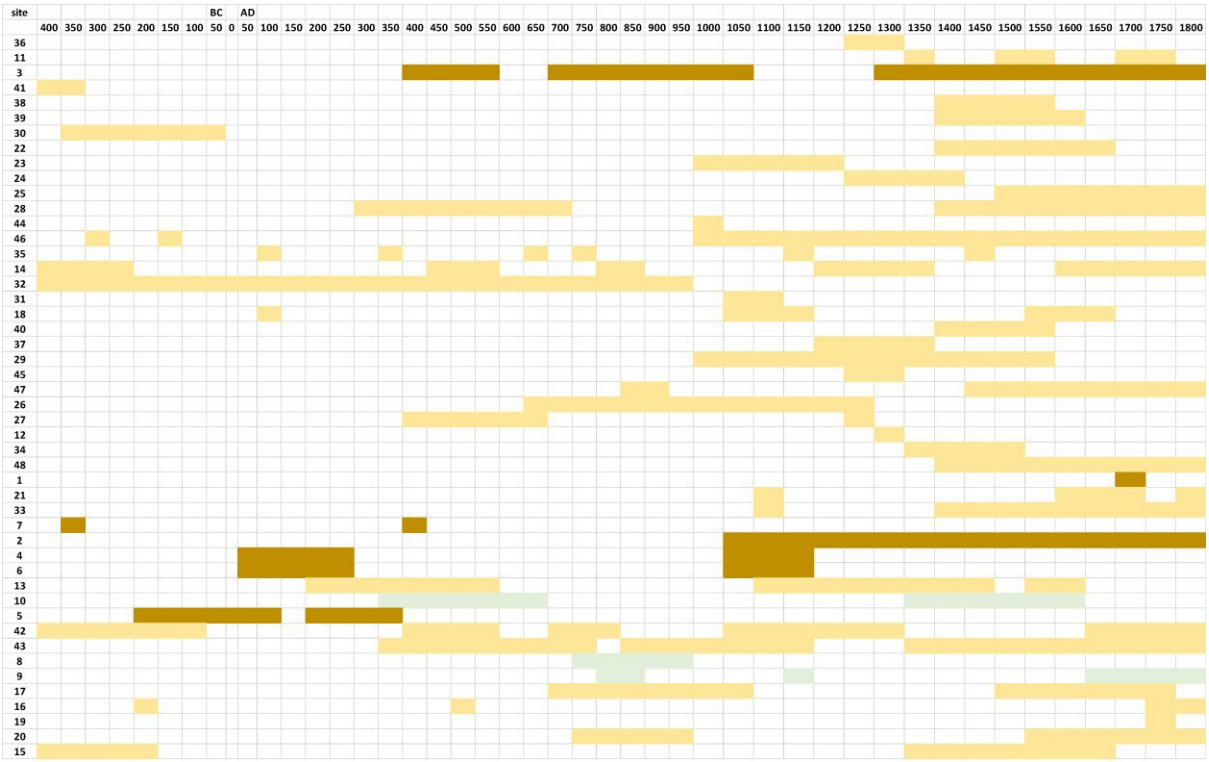


*Figure 6. (a) the distribution along the coastal Atlantic façade of dated (rounded to 50 years) natural sediment accumulations between 400BC and AD1800 argued by the authors to describe past storminess:*

***coarse clastic sediments*** *: (1) Cunningham* et al *(2011); (2) Haslett and Bryant (2007); (3) Hansom and Hall (2009); (4) Roberts and Plater (2007); (5) Van Vliet-Lanoë* et al *(2014a); (6) Plater* et al *(1999, 2009); (7) Wilson and McKenna (1996):* ***subtidal and intertidal sediments*** *(8) Billeaud et al (2009); (9) Poirier et al (2017); (10) Sorrel* et al *(2009):* ***wind-blown sand*** *(11) Bampton* et al *(2017); (12) Bailey* et al *(2001); (13) Bailiff* et al *(2013); (14) Bjorck and Clemmensen (2004), de Jong* et al *(2006, 2007); (15) Borja* et al *(1999); (16) Clarke and Rendell (2006); (17) Clarke* et al *(2002); (18) Clemmensen* et al *(2009); (19) Costa* et al *(2021); (20) Costas* et al *(2016); (21) Cunningham* et al *(2011); (22-25) Dawson, S.* et al *2004, 2011; (26-27) Delaney and Devoy (1995); (28) Gilbertson* et al *(1999); (29) Madsen* et al *(2010); (30) McIlvenny* et al *(2013); (31) Murray and Clemenssen (2001); (32) Nielsen* et al *(2006); (33) Orford* et al *(2000); (34) Orme* et al *(2015); (35) Orme* et al *(2016); (36) Preston* et al *(2020); (37) Pye and Neal (1993); (38) Sommerville* et al *(2003); (39) Sommerville* et al *(2007); (40) Szkornik* et al *(2008); (41) Tisdall* et al *(2013); (42) Van Vliet-Lanoë* et al *(2014b); (43) Van Vliet-Lanoë* et al *(2016); (44) Wilson (2002); (45) Wilson and Braley (1997); (46) Wilson* et al *(2001); (47) Wilson* et al *(2004); (48) Wintle* et al *(1998). The red dot in Figure 6a is Caerlaverock. Base Map: LeBret.CC BY-SA 30 via Wikimedia Commons.*

Figure 6 summarises data from many sources from late prehistory to AD1800. Few extend beyond AD1000, a product partly of the debate over storminess in the last 1000 years and partly because the youngest sediments, particularly in sand dunes, are the best preserved and most easily sampled. Records do not sample changing environments continuously: they are episodic. Geomorphic activity is better recorded than phases of inactivity. And most records are less well-dated than they appear in Figure 6.

Some records that span both the MCA and the LIA have tended to suggest, confusingly, increased storminess in either the MCA or the LIA, notwithstanding that the MCA-LIA boundary is often defined differently. The evidence for increased storminess in the MCA is less abundant (Pye and Neal 1993; Wilson and Braley 1997; Plater *et al* 1999; Murray and Clemmensen 2001; de Jong *et al* 2006; de Jong, Schoning and Bjorck 2007; Nielsen *et al* 2006). A few studies have found no change in frequency (Delaney and Devoy 1995; Wilson, McGourty and Bateman 2004; Clemmensen *et al* 2009; Bailiff *et al* 2013; Preston *et al* 2020). Many more workers have found storms increasing in frequency in the LIA (Devoy *et al* 1996; Kreutz *et al* 1997; Gilbertson *et al* 1999; Bailey *et al* 2001; Wilson *et al*

2001; Clarke *et al* 2002; Gottshalk in de Kraker 2002; Meeker and Mayewski 2002; Dawson *et al* 2003, 2004, 2007; Bateman and Godby 2004 (describing an absence of storms in the MCA); Bjorck and Clemmensen 2004: Dawson, S. *et al* 2004; Clarke and Rendell 2006, 2009; Somerville *et al* 2007; Dawson, Dawson and Jordan 2011; Brown 2015; Orme, Davies and Duller 2015; Orme *et al* 2016; Bampton *et al* 2017; Jackson *et al* 2019; Moskalewicz *et al* 2020; Costa *et al* 2021).

Further back in time, climatic interpretations are more circumspect because atmospheric circulation patterns are less easily reconstructed. Thus Goslin *et al* (2018, 1) argued that Holocene sand-blow events have been driven by large shifts in the latitudes of Atlantic westerlies "akin to present-day NAO patterns", which have been increasingly negative since the 1940s (Ortega *et al* 2015) with strong westerly winter winds. Sand-blow events, they argued, have been periodic, not random, at millennial (~2200 year) and centennial (~450, 36y0 and 200 year) cycles, in the later Holocene at 2450–1850 BC and 1350-850 BC: their record stops before the historic period. Sorrel *et al* (2012) defined later Holocene peaks of sand-blow events on the Atlantic façade at about 2350 BC, 850 BC, AD550 and AD1550, at times when North Atlantic westerly winds strengthened because Arctic sea-ice pushed the Icelandic Low circulation cell south, as in the LIA (Lamb 1979). Van Vliet-Lanoë *et al*'s (2014b) ambitious interpretation can be argued to have identified later Holocene storminess virtually all the time so that it is easier to define phases longer than 100 years when storminess was significantly reduced, between 550 and 450 BC, 350 and 150 BC, AD450-600 and around AD1385. They also saw cold Arctic winters as necessary conditions for heightened storminess but coupled with Atlantic hurricanes made more vigorous by warm tropical Atlantic sea surface temperatures. In and after the MCA, they suggest that storms were most severe during solar minima spanning AD950-1040, 1050-1080 and 1645-1715, the last called the Maunder Minimum and the nadir in west-central Europe of the LIA. Storms were not more frequent or severe in in the Medieval solar minimum at AD1100-1250 or the better-known Wolf minimum AD1280-1350 or the Spörer minimum AD1450-1550, however: solar minima are periods of reduced solar irradiance. Sorrel *et al* (2012) rejected this association.

## 2.7. Archival analyses of coastal floods

### 2.7.1. Caerlaverock

There is no mention of coastal floods in the otherwise exhaustive history, the *Book of Carlaverock* (Fraser 1873). Both volumes are on-line and searchable through the National Library of Scotland, but searching for 'Solway', 'inundation' (there are two reported but elsewhere in Scotland), 'flood', 'storm', tempest', 'coast' and 'Nith' generated nothing. There are some intriguing problems, though. The observation by the Revd. Gillies in the Second Statistical Account that the New Castle "is not many feet above high water-mark" (Gordon 1845c, 351), and the oft-quoted myth that "the outer moat of the Mediaeval Castle was filled by the sea at high tide" (Reid 1946, 68; Marshall 1962b; Steers 1973, 116) are problematic because ordinary high tides do not reach the Old Castle, let alone the new one. Marshall (1961) thought the origin of this description to derive from the contemporary description of the '*Siege of Caerlaverock'* (Scott-Giles 1960) in 1300:

> *"Mighty was Caerlaverock Castle. Siege it feared not. scorned surrender —wherefore came the King in person. Many a resolute defender, well supplied with stores and engines, 'gainst assault the fortress manned. Shield-shaped, was it. corner-towered, gate and draw-bridge barbican'd. strongly walled, and girt with ditches filled with water brimmingly."*

If so, it is very unclear how this description came to be interpreted as referring to the tide. There is no discussion by MacIvor *et al* (1999) concerning the source of water in the New Castle moat. It is

not fed by streams as with the Old Castle moat (below: Section 4.2.3). The New Castle straddles the geological boundary between Permian sandstone in the north and the NCT fill in the south, and a series of springs supply water to the moat. A sluice controls the water level (Valerie Bennett pers comm). The dry valley which fed the Old Castle moat (Section 4.2.3) probably originated in this spring line. Marine-brackish ostracods from the moat of the New Castle are modern in age, but it is unclear how they got there (Kontrowitz and Griffiths 2009).

As perplexing, not least in its ambiguity, is Fraser's (1873, 1, 55) comment that "In recent years, there was discovered in the inner fosse a strong sluice, formed of oak and bound with iron, by which the waters of the Solway at high tide could be admitted." It is utterly unclear to which castle he referred. The comment was made in discussion of the "castle built by Sir Robert Maxwell" (i.e. the New Castle) but this was said to be "erected on the site of the present ruins" (Fraser knew both castles, saw the ruins of the Old Castle but may have considered the New Castle to be ruinous). MacIvor *et al* (1999, 170) recognised the need for a sluice in the moat of the New Castle to allow installation of bridges but made no mention of Fraser's find. Neither did Martin Brann at the Old Castle (2004).

**2.7.2. The Solway Firth**

Ogilvie and Farmer (1997) and de Kraker (2002) both counselled caution in drawing on archival records before AD1500 as a chronology of events. For example, though Haslett and Bryant (2008) suggested that a tsunami impacted the Solway Firth in 1014 there is no contemporary description, but one made in 1746! At Carlisle in 1292 "There was … such a tremendous inroad of an unusually high tide as to overflow the ancient landmarks of the country [in a degree] beyond all memory of old people" (Maxwell 1913, 87-88), and "violent storms" in 1365 (Wilson 1905). The inundation by the sea of the 11km$^2$ Moricambe Bay on the north west Cumbrian coast, 14km south east of Caerlaverock in *c*. 1304 has been seen as catastrophic (Grainger and Collingwood 1929; Cracknell 2005) but most recent analyses (Bellhouse 1962; Jones 1980; Singh 1996; Fletcher and Miller 1997; Clare 2004) accept that Moricambe was an embayment long before the Middle Ages. Skinburness, the port south of Moricambe Bay apparently ruined by the disaster, continued after this event as the main English port supplying the north Solway coast (Nielson 1899; Reid 1946). The Lanercost Chronicle recorded floods on the River Nith, not necessarily coastal, in 1268 and 1282 (Britton 1937), the latter "such that no-one there remembered the like" (ibid, 70) though it was only 14 years after the former. Britton (1937) did not record the 1304 event at Skinburness. Lamb (1977, 120) records one coastal flood in the Solway Firth in 1302 but with no other detail: this may be the Moricambe Bay flood. Searching Marusek's (2010) remarkable compilation for inundations by/of/from the sea in western Britain north of Wales identified events affecting the River Dee in Cheshire in 387, 415, 649, 885 and 1753, and Glasgow in 738 (or 758): Marusek does not list floods in 1268, 1282, 1292 or 1304. All these events remain only sporadic descriptions, not a time-series. The paucity of the Scottish evidence may explain why Cracknell (2005, 265) thought Scotland appeared least affected by storms from the 15th century.

In later centuries to AD1800 the documentary record for storms affecting the inner Solway Firth remains sporadic despite thorough searches of the *Transactions* of both the Cumberland and Westmorland and Dumfries and Galloway Societies. Graham and Truckell (1976-7, 110) made the point that "however violent may have been the worst of the weather in the Firth, … ports were not called upon to face anything comparable with the North Sea storms" and they make no reference to Medieval and later harbours in Dumfries and Galloway being affected by storms or siltation save at New Abbey in 1788. Yet in the 1650s "The badness of coming into the river [Nith] upon whiche it [Dumfries] lyes … hinders … theyr commerce by sea" (Hume Browne 1891, 180) through siltation,

and the harbours of Ayr were “being clogged and filled with sand, which the Westerne Sea and the winds … beate up in to it” (Hume Brown 1891, 179).

Hickey (1997, 429) reported a personal communication from A.E Truckell (Dumfries Museum) describing an event affecting all of the inner Solway Firth in 1425 when shingle ridges are thought to have formed in Kirkbean parish, probably at Carsethorn (Figure 2). In November 1627 a coastal inundation of the northern Solway shore, including Caerlaverock (ibid, 79) Caerlaverock, was driven by a “south wind, blowing directly from the Isle of Man” (Stevenson 1753 in Macleod 2001, 6; Chambers 1855, 231), killing 13 salt-panners at Ruthwell and flooding the ground floor of Cockpool Castle (NY 0699 6766: CANMORE ID 66067). "The highest Sea Tide for the last fifty Years" was reported by the Rev. Hutton of Beetham in Morecambe Bay on 28 October 1795 (Tufnell 1983, 145). All the Solway ports suffered serious damage from a coastal flood on January 24th 1796 (McIntire 1943).

**2.7.3. The British Isles**

The documentary record is fuller for England, particularly for the North Sea coast (Britton 1937; Brooks 1949; Lamb 1977, 120-126, 1982; Bailey 1991; Lamb and Frydendahl 1991; Brown 2001, 204-255; Cracknell 2005; Galloway 2009; Marusek 2010; Brown 2015, 2019; Griffiths 2015). Lamb (1977, table 3.13) lists coastal floods affecting parts of the British west coast in 520 (Wales), 1554 and 1720 (Lancashire). He also identified persistent anticyclonic high pressure cells over Europe, which would weaken westerly winds, in the 1260s, 1310-19, the 1370s, 1400-09, the 1430s, the 1490s and in the 1780s (ibid, 451). Archival sources are too few before AD1600 to critically assess the clustering of coastal storms in Scotland. After this, Hickey’s data (1997, figure 4.5) might suggest clusters of events AD1613-1642, AD1653-1670 and AD1791-1800. Lamb and Frydendahl (1991, table 2) defined in 50 year intervals from AD1500 the most severe storms to have affected north west Europe. To AD1800 they were: 1570-99 = 6; 1600-1649 = 3; 1650-1699 = 1; 1700-1749 = 2; 1750-1799 = 2. They noted (p. 33) clusters of storms from the 1570s to the 1620s, the 1690s to the early 1700s and in the 1790s.

# 3. Methods

Archaeological features were surveyed in 2004 (Brann 2004). Geomorphological mapping of natural features was undertaken from multi-directional hillshaded LiDAR imagery at 16 ppm (points per metre) horizontal resolution and vertical resolution ± 15cm, with limited ground-truthing due to the density of trees inside Castle Wood. Altitudes were taken from transects of LiDAR data at 0.5m intervals. Sediments in archaeological and natural features were described in the field along transects from 1.0m long, 3.0cm diameter Eijelkamp peat gouge cores: colours and particle sizes were estimated. Boreholes are numbered consecutively. Boreholes in archaeological features were normally stopped when the fill of the NCT (the 'natural') was recorded. In natural features some boreholes hit bedrock. Rock, stone and gravel were distinguished by feel and sound.

Sediments for laboratory analyses and dating programmes were sampled with a 1.0m long, 6.5cm diameter closed-chamber Russian-type corer, a 65.0cm long, 5.0cm diameter Abbey piston corer, or a 0.5m long, 10.0cm diameter modified golf-hole corer, and in deep sediment in the 'harbour' with a Wink vibracorer in 1.5m long, 4.0cm diameter Perspex tubes wrapped in black plastic. Sediment sampled by piston corer and vibracorer were corrected for compression. Sampled sediments were logged in the laboratory. Munsell colours were recorded on moist sediment under artificial light.

Samples for clast lithological analysis were taken with a 15cm long, 13cm wide post-hole auger, but with jaws that limit the size of clasts sampled to those with a-axes ~5-6cm. Sampled sediment was weighed in the field with a spring balance to ~100gm. It was then sieved through a 16.0mm mesh metal sieve and all retained clasts counted and weighed. Sampling stopped when the number of clasts reached around 50. Clasts were washed in the laboratory. All clasts in the sample were identified, a-axes measured, and roundness estimated by reference to fig. 7 of Hodgson (1976). Proportions of (a) Galloway Granitic Suite (GGS: cf. Criffel Granodiorite), (b) Permian Locharbriggs Sst. and (c) Silurian Gala and Hawick Group sediments are discussed. Tipping and Adams' (2007) data on clasts >16.0mm from these three lithologies are included.

In sampled sediments, organic contents were measured on 1.0cm thick sub-samples by loss-on-ignition (l-o-i) at 550$^{o}$C for 4 hours. Particle size distributions were determined by laser interferometry using a Coulter LS230 instrument after deflocculation with sodium hetamexaphosphate from the mineral residues of sub-samples after l-o-i and sieving through a 2.0mm sieve. Particle size distributions are reported using the Udden-Wentworth scale. Peat in borehole 101 at Basin 2 contained visible rock clasts with a-axes >1mm to 5.25mm. These were concentrated by being picked from oven-dried and gently ground 1cm thick, 10cm diameter (*c*. 80cm$^{3}$) slices of peat and examined under a low power (x20) stereo microscope, estimating a-axis length to the nearest 0.25mm. In borehole 13 in the Outer Ditch, wood macrofossils were quantified from 1.0cm thick slices of uniform volume following gentle excavation of moist sediment.

Sub-samples for luminescence profiling from coastal basins were *c*. 1.0cm thick sediment slices cut from the centres of intact 10.0cm modified golf-hole cores split vertically under red-light conditions. Sub-samples from sediment in the 'harbour' were similarly prepared. A SUERC portable reader (Sanderson and Murphy 2010) at St. Andrews University, operated in continuous wave mode, measured net signal intensities (photon counts released in 120s) under infra-red stimulated luminescence (IRSL) and optically stimulated luminescence (OSL), and IRSL and OSL depletion. IRSL:OSL ratios were calculated. For selected sub-samples, apparent doses were measured on two sediment sub-samples at the same depth (aliquots) in the size-range 90-250µm and etched with hydrofluoric acid to isolate quartz. Using luminescence profiles and data from paired aliquot assays,

three samples from 'harbour' sediment and two samples from sediment in Basins 3 and 6 were selected for OSL dating (Srivastava, Kinnaird and Bates 2022).

Sub-samples of 0.5cm thickness were cut from Russian core samples in the western moat (32 samples from 4.25 to 50.50cm depth) and piston-core samples in the outer ditch (32 samples from 5.40 to 91.00cm depth) for diatom analyses by conventional techniques.

20 sub-samples for AMS $^{14}$C dating were taken from sediment cores in the laboratory 1-2 days after being sampled, wrapped in aluminium foil and stored at 4$^{o}$C. Horizontal and likely to be bedded, small diameter twigs were sought as short-lived single entity samples (Ashmore 1999). Where these or other plant macrofossils were absent, samples were 1cm thick sediment slices of peat. Cellulose from samples of twigs and the humic acid fraction of peat samples were dated at the Scottish Universities Environmental Research Centre (SUERC: Dunbar *et al* 2016). Unless stated, all $^{14}$C age estimates are calibrated using Oxcal 4.4 (Bronk Ramsey 2009) with INTCAL20 (Reimer *et al* 2020) and expressed at 95.4% probability.

# 4. Results and discussion

## 4.1. Coastal Evolution at Caerlaverock

### 4.1.1. LiDAR imagery and geomorphic mapping

Figure 7a is a Lidar MHS image of Castle Wood and surroundings, south and west of the Old and New Castles. The Old Castle Burn in the east flows through the eastern moat of the Old Castle and the 'harbour'. It is now a drainage ditch between the 'harbour' and the salt marshes ('merse'). A second channel to the west, now dry, is called the New Castle Burn. The image shows several other drainage ditches. Figure 7b is the interpretation of geomorphological features. The base of a degraded cliff formed the coast prior to the events described in this study. West of Bowhousepark the cliff is around 10m high, cut in glacial till. Within Castle Wood it is cut in the thick early-mid Holocene estuarine fill of the NCT. East of the 'harbour' it is again cut in till.

Figure 7a shows a series of broadly east-west trending ridges. Figure 7b delineates and numbers these (R1–14) and basins which intervene (B1–8). The term 'basin' is used because they are sediment traps fronted by ridges, although they were originally terraces. B3 is a valley, its surface falling east over 260m from 7.4 to 7.0m OD, rather than a basin.

R1 and 2 are in bedrock. Other ridges are in sand or gravelly sand (below: Section 4.1.8). These and sedimentary basins are numbered in the probable relative order they formed. For most features the relative order is clear because shoreward basins and ridges have to have formed before more seaward ones. The ridges and basins represent a prograding strandplain, probably a mainland-anchored strandplain (Otvos 2020) since most gravel ridges are anchored to bedrock ridges (below), though not to the cliff. In the west the order is: B2 > R4 > B3 > R5 > R6 > B4 > R7 > R8 > B6 > R14. In the east the suggested order (B1 > R3 > R9 > B5 > R10 > R12 > B7 > R11 > R13 > B8 > R14) is less clear morphologically. Relative ordering also drew on differences in the gravel composition of ridges and, more cautiously, altitude, evaluated below (Sections 4.1.4; 4.1.8). Channels, mostly dry, that cut ridges are shown in Figure 7c. Figure 7d shows the series of sediment-stratigraphic transects of boreholes across the basins, locations of samples taken for analyses of gravel composition on ridges and the line of transect made by Tipping and Adams (2007).

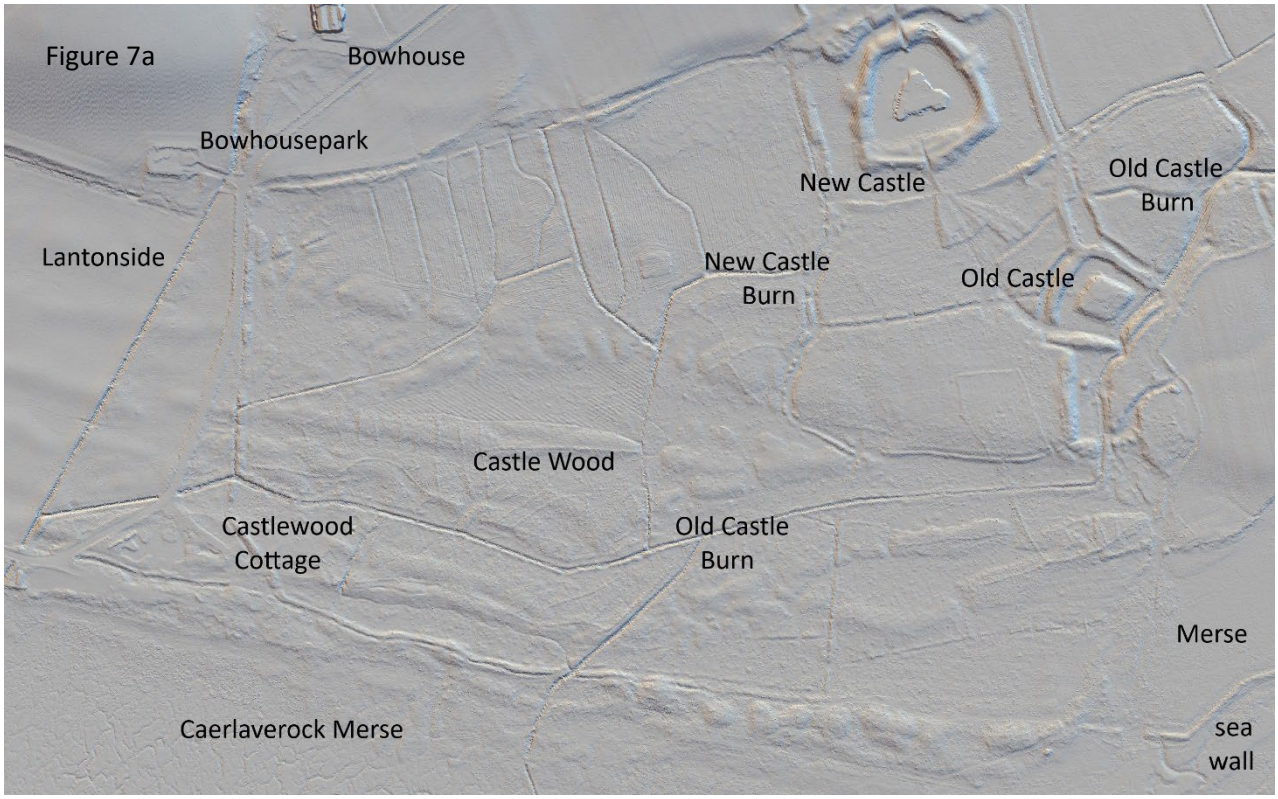
Figure 7a
Bowhouse
Bowhousepark
Lantonside
New Castle
Old Castle Burn
New Castle Burn
Old Castle
Castle Wood
Castlewood Cottage
Old Castle Burn
Merse
Caerlaverock Merse
sea wall

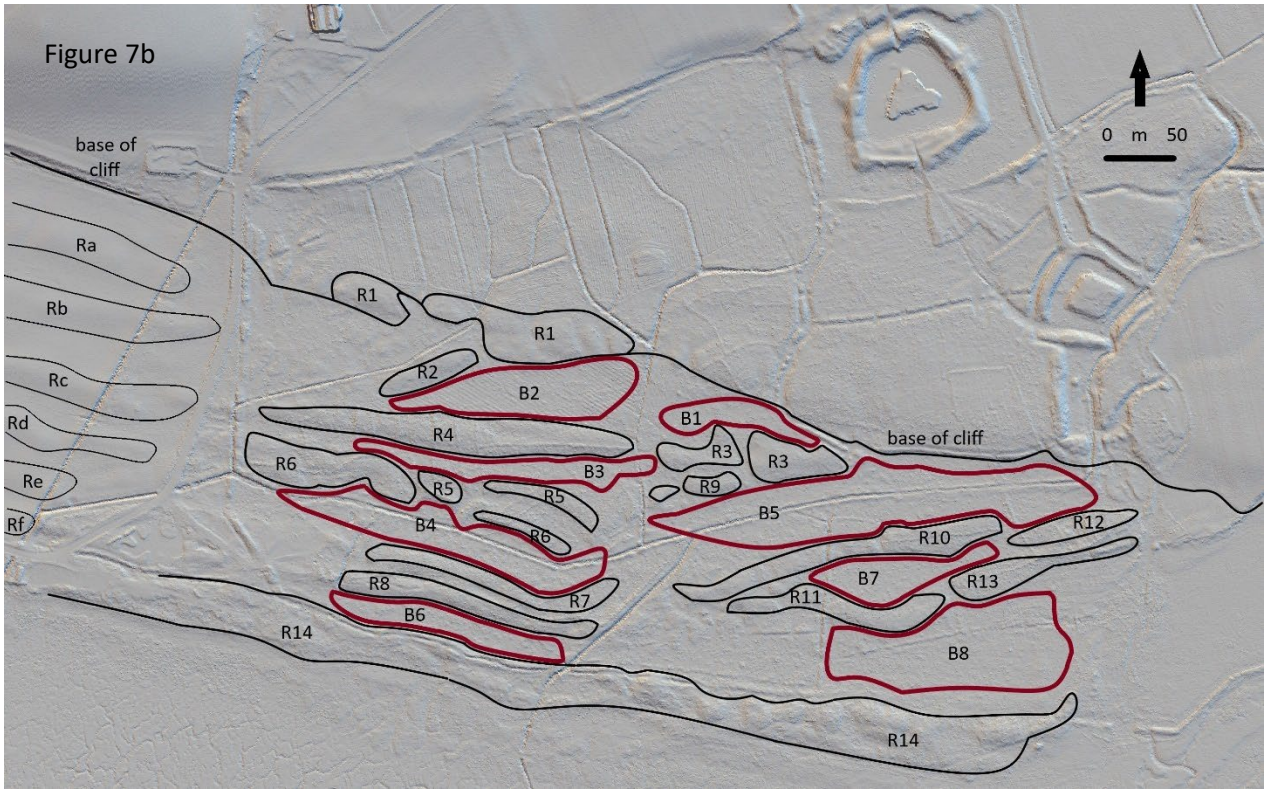
Figure 7b
base of cliff
0 m 50
Ra
Rb
Rc
Rd
Re
Rf
R1
R1
R2
B2
B1
R4
R3
R3
base of cliff
R6
B3
R5
R9
R5
B5
B4
R6
R10
R12
R8
R7
B7
R13
R11
B6
R14
B8
R14

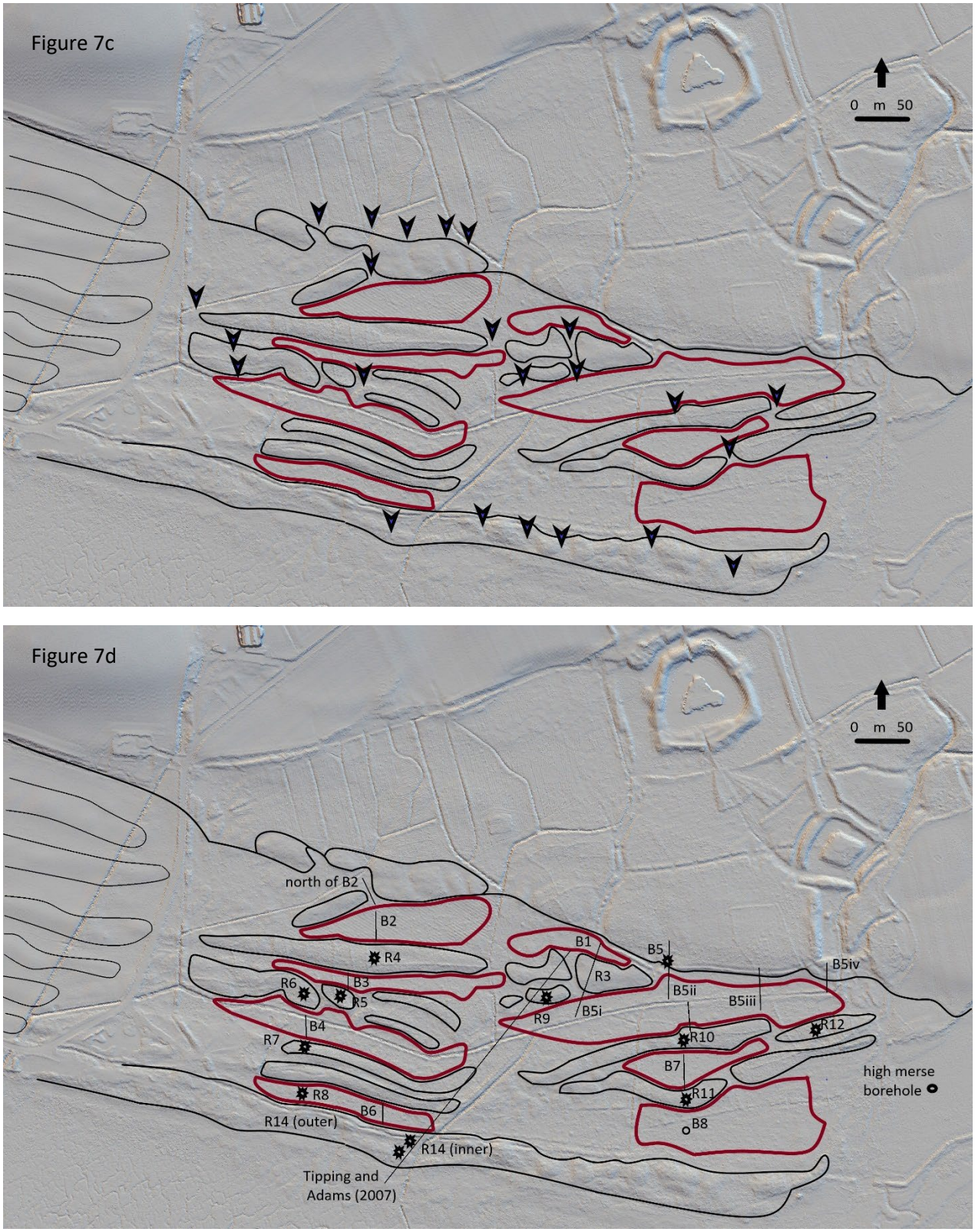


*Figure 7. (a) a LiDAR MHS image of the topography of Castle Wood and surroundings, identifying the features named in this work; (b) interpretation of the topography of Castle Wood and surroundings showing the cliff-line that was the coast prior to the events in this work, basins B1 to B8 and ridges R1 to R14 that define them, and the subdued ridges Ra to Rf at Lantonside; (c) natural channels that cut ridges; (d) the locations of sediment-stratigraphic transects across the basins and of gravel samples in ridges, with the single transect reported by Tipping and Adams (2007: figure 3).*

### 4.1.2. Buried bedrock ridges

There are no exposures of rock in Castle Wood. North of B2 (Figure 7b), the bedrock ridges R1 and R2 protect from erosion a capping of *in situ* NCT fill north of them with a surface at 9.0-9.5m OD. The steep southern slopes of R1 (8-9% gradient) formed the coastline prior to the events described in this study. The slopes have probably been washed free of superficial sediment by waves. R1 is cut by shallow north-south valleys or channels (Figure 7c). A sediment-stratigraphic transect north of Basin 2 (Figure 7d) found above bedrock, 110cm of mineral sediment with the characteristics of the NCT fill in borehole 91 to 7.74m OD (see also Figure 9).

South of the degraded cliff, sixty-two hand-sunk Eijelkamp boreholes encountered bedrock beneath younger sediment. Most boreholes are on a composite north-south transect from north of B2 to R14 (Figure 7b). In Figure 8a these are plotted for clarity along arbitrary distances: the actual length of the transect is 300m. South of B2, R4, R6, R7 and R8 form a level surface or platform at 7m OD. Because the Doweel Breccia is not horizontally bedded, but has a south-westerly dip (Section 2.2), this surface is an erosional feature of some antiquity.

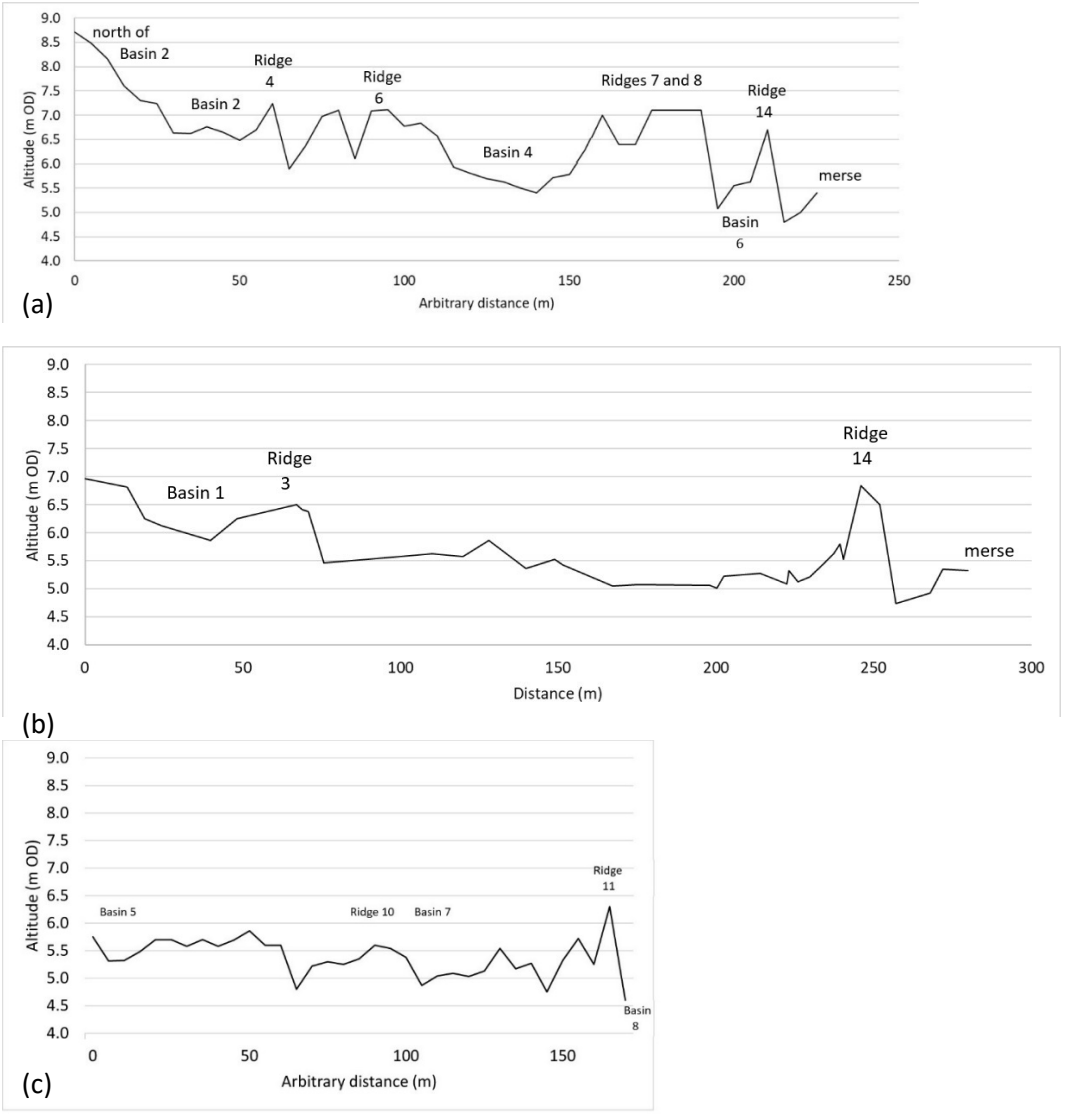


*Figure 8. Altitudes (m OD) of buried bedrock surfaces encountered along north-south sediment-stratigraphic transects (a) from north of Basin 2 to Ridge 14 in the west, (b) along Tipping and Adams' (2007) transect and (c) from Basin 5 to Basin 8 in the east.*

Tipping and Adams (2007) recorded depths to bedrock on a transect east of that in Figure 8a (Figure 7d) where a surface or platform at 5-5.5m OD is recorded (Figure 8b), also seen underlying younger sediments further east beneath B5 and B7 and on the R10 (Figure 8c). These last two transects show that the fall in altitude eastward is not a slope.

**4.1.3. Bedrock basins**

Depths to bedrock in the basins were recorded from transects of Eijelkamp boreholes. Not all boreholes were deep enough to record rock. No attempt was made in B1 because 3m deep boreholes along the New Castle Burn to the north did not encounter rock.

Where encountered in the basins, the rock surface (rockhead) is generally horizontal (Table 1). In B5 along transect (ii)N, rockhead is deeper in the north, beneath the cliff (Figures 11b, 12a). Where rockhead was met, the basal fill (described in Section 4.1.4) is uniformly thick (64±16cm overall) in most basins (Table 1). That in B2 thins southward. Upper surfaces of the basal fills are horizontal and except in B1 and B2, the oldest basins, were described as sharp (Table 1).

The upper surfaces of the basal minerogenic fills in B1 to B3 fall southward from 7.35 to 5.96m OD as basins get younger (column 4; Table 1). It is not clear why. Falls in altitude need not reflect changes in base level such as falling RSL except to say that this pattern could not be preserved under rising RSL. Ground surfaces of B5 to B8 also fall southward but differences are much smaller and may not be significant. Because the mechanism whereby therse surfaces fall in altitude is unclear, altitudinal correlation is a weak predictor of the relative order of construction, but deposition in B2 and B3 may have occurred at broadly the same time, followed by B4 and then B5 even though this basin is shoreward of B4 (Figure 7b). This may imply that the eastern ends of R6, R7 and R8 and the 7m OD buried bedrock platform (above: Figure 8a) were truncated before B5 was formed. In this large embayment R10 to R13 (Figure 7b) have different orientations to ridges in the west. This may reflect wave refraction around the eroded barrier of Ridge 8 rather than a change in direction of waves and sediment transport. B1 is different because it is not a lagoon shoreward of a barrier beach, and its altitude does not reflect elevated storm surge RSL.

The overlying, predominantly more organic, more varied fill (below: Section 4.1.10) is also quite uniform in thickness (33±10cm overall; column 6: Table 1). Column 7 (Table I) defines the altitudes of the ground surfaces of basins from LiDAR data. They are much lower than altitudes of the NCT fill north of the coastline at 9-9.5m OD but also considerably higher than the estimated contemporary sea level at MHWS of around 5m OD (Smith *et al* 2003a). They do not coincide with the altitudes of underlying bedrock ridges (Figure 8) so were not ponded by them.

| Basin | rockhead (m OD) | basal fill (cm) | upper surface of the basal fill (m OD) | upper boundary | overlying fill (cm) | ground surface (m OD) |
|---|---|---|---|---|---|---|
| 1 | not met | | 7.35±0.05 (n 5) | sharp 0% (n 5) | 16±4 (n 5) | 7.40±0.07 (n 305) |
| 2 | 6.67±0.40 (n 6) | 57±15 (n 6) | 7.21±0.15 (n 11) | sharp 28% (n 11) | 30±10 (n 11) | 7.41±0.12 (n 439) |
| 3 | | | 6.79±0.09 (n 11) | sharp 82% (n 11) | 34±7 (n 11) | |
| 4 | 5.66±0.16 (n 7) | 67±11 (n 7) | 6.34±0.06 (n 7) | sharp 87% (n 8) | 25±11 (n 7) | 6.69±0.11 (n 441) |
| 5 | 5.61±0.26 (n 6) | 64±17 (n 6) | 6.07±0.09 (n 8) | sharp 100% (n 8) | 40±6 (n 8) | 6.51±0.10 (n 177) |
| 6 | 5.42±0.24 (n 3) | 63±18 (n 6) | 5.96±0.13 (n 8) | sharp 87% (n 8) | 39±7 (n 8) | 6.44±0.18 (n 125) |
| 7 | 5.16±0.24 (n 12) | not present | | | | 6.12±0.05 (n 287) |
| 8 | 1 borehole | | | | | 6.06±0.10 (n 421) |

*Table 1. Mean altitudes and single standard deviations of Basins 1-2 and 4-8 inc. B3 slopes east.*

### 4.1.4. Basal minerogenic fills in basins

Sediments filling the basins were recorded along transects of Eijelkamp boreholes. Figure 9 depicts the sediment stratigraphies in B1 and B2; Figure 10 shows those in B3; Figure 11 shows those in B3 and B4. Figure 12 shows sediment stratigraphies in B5 along three transects and Figure 13 shows that in B5 along transect 5(ii). Figures 13 and 14 show those along B6, B7 and B8.

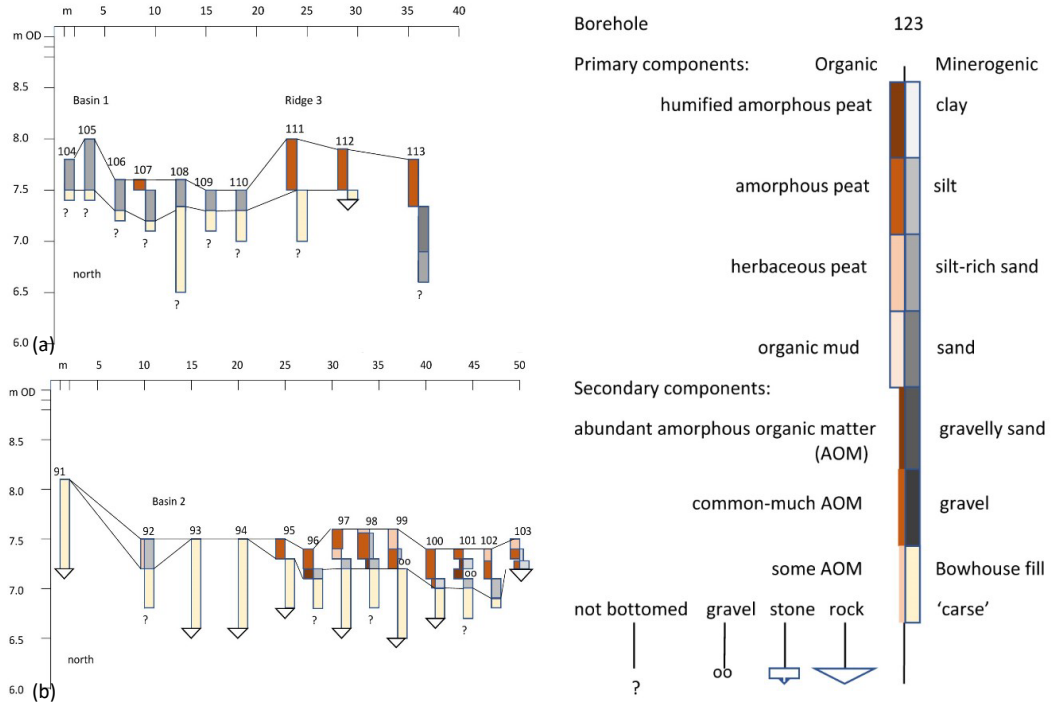


*Figure 9. Sediment-stratigraphic borehole transects across (a) Basin 1 (boreholes 104 to 110) and Ridge 3 (boreholes 111 to 113), and (b) north of Basin 2 (borehole 91) and across Basin 2 (boreholes 92 to 103).*

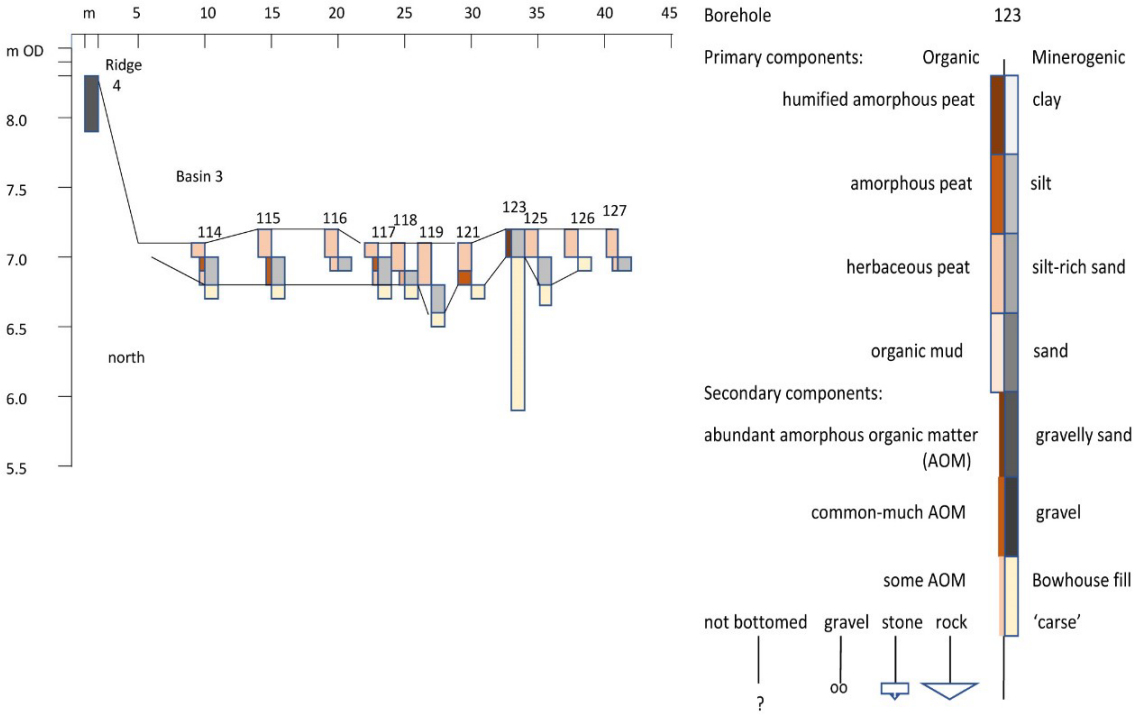


*Figure 10. Sediment-stratigraphic borehole transects across Basin 3 (boreholes 114 to 127).*

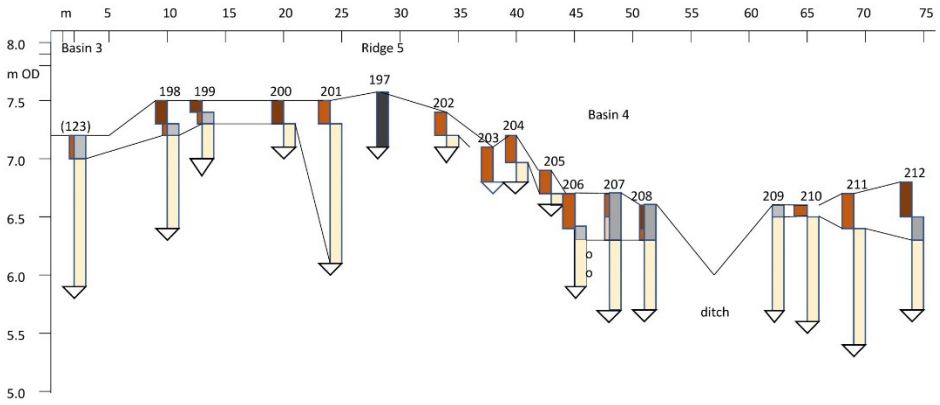


*Figure 11. Sediment-stratigraphic borehole transects across Basin 3 (boreholes 123 and 198 to 201), Ridge 5 (boreholes 197 and 202 to 205) and Basin 4 (boreholes 206 to 212). See Figure 10 for key.*

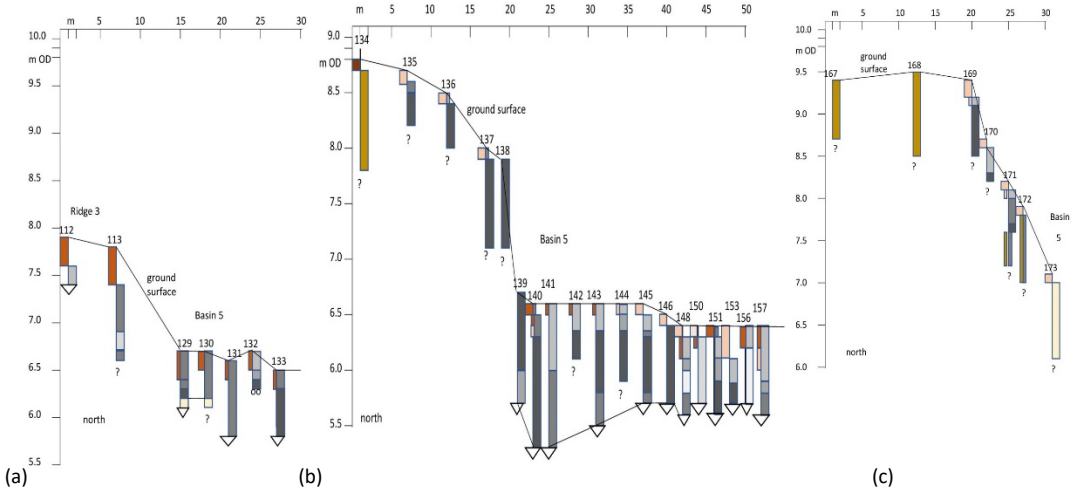


*Figure 12. Sediment-stratigraphic borehole transects across Basin 5 along three north-south transects, arranged from west to east (see Figure 7d): (a) transect 5(i) from Ridge 3 (boreholes 112–113) south; (b) transect 5(ii)N is north of the Old Castle Burn from the cliff north of Basin 5 (boreholes 134 to 138) across Basin 5 (boreholes 139 to 157); (c) transect 5(iii) from the cliff (boreholes 167 to 172) to Basin 5 (borehole 173). See Figure 10 for key.*

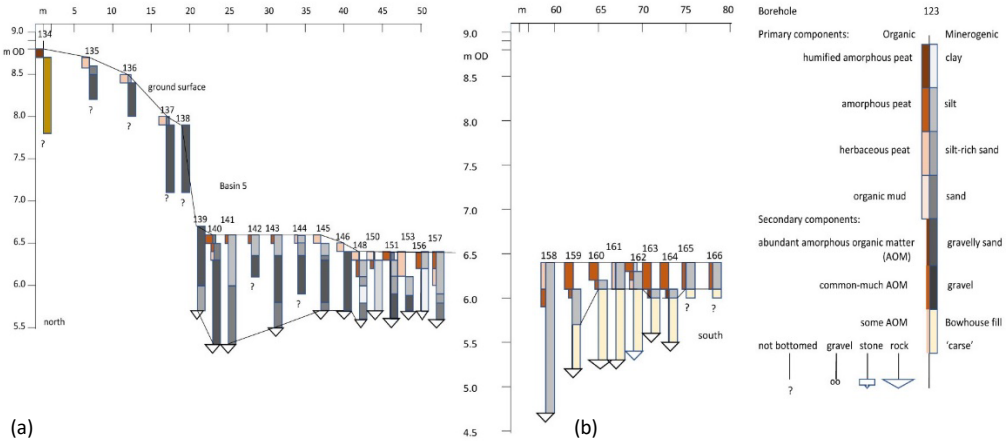


*Figure 13. Sediment-stratigraphic borehole transect across Basin 5 at transect 5(ii) showing the relation between sediments (a) north of the Old Castle Burn and (b) south of the Old Castle Burn (see Figure 7d).*

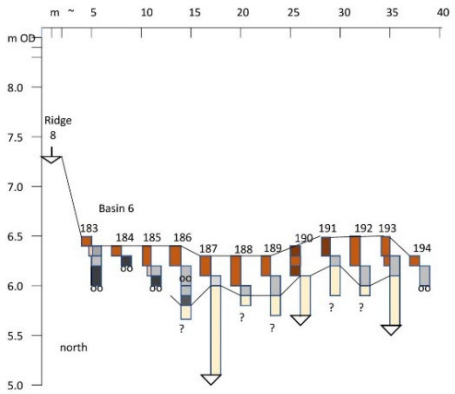


*Figure 14. Sediment-stratigraphic borehole transect from Ridge 8 across Basin 6 (boreholes 183 to 194). See Figure 13 for key.*

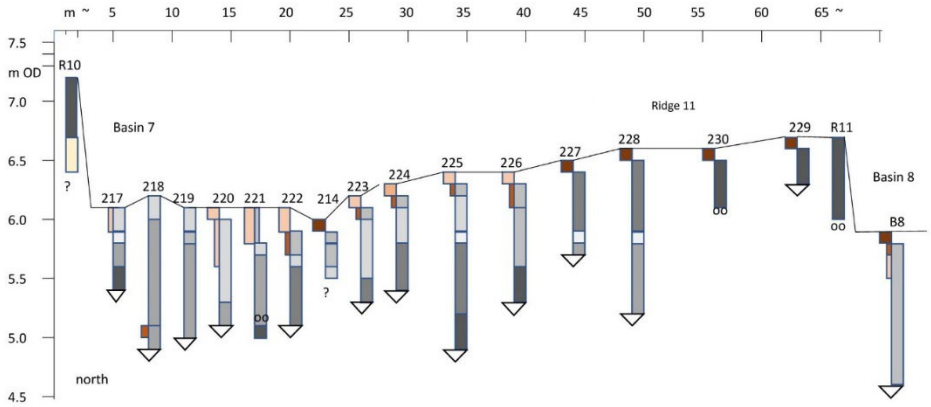


*Figure 15. Sediment-stratigraphic borehole transect across Ridge 10, Basin 7 (boreholes 217 to 224), Ridge 11 (boreholes 225 to the modified golf-hole corer boreholes R11 and B8. See Figure 13 for key.*

The uppermost *c*. 50cm of sediment were sampled from typical boreholes in B2, B3 and B5-B8 inclusive with a modified golf-hole corer. Sediment in B3 was poorly sampled because it is indurated. B4 was not sampled because there was no potential for $^{14}C$ dating. Table 2 gives the boreholes sampled and presents sediment descriptions recorded in the laboratory. Figure 16 shows photographs of the sediment cores: that in B6 was not photographed.

Bed 1 in each basin is the basal minerogenic fill overlying rock. It is uniformly inorganic, usually pale brown or pale grey structureless silt and fine sand, distinguished from overlying sediment by the absence of organic matter The basal fill of Basin 7 is different to that in other basins in being stratified, comprising bedded clays, silts and sands with a fining-up trend reflecting highly variable depositional energies and environments. Basal minerogenic fills are identical in appearance to the NCT fill and in the field were often recorded as 'carse'.

| Bed | Depth cm | Description **Basin 2: borehole 101** |
|---|---|---|
| 7 | 0-3 | Leaf litter; gradual to |
| 6 | 3-7 | Dark brown stratified amorphous peat with common fine to coarse wood fragments and some fine fleshy stems; sharp to |
| 5 | 7-17 | Very dark grey structureless silt with abundant amorphous organic matter; sharp to |
| 4 | 17-27 | Very dark brown to black structureless amorphous peat with very rare vertical fine fleshy stems and a clear, discontinuous band of pale brown silt, with sharp upper and lower boundaries at 20-22cm depth; gradual to |

| | | |
|---|---|---|
| 3 | 27-37 | Mid-dark brown amorphous peat with very rare vertical fine fleshy stems and disseminated, matrix-supported, well-sorted >2mm subrounded grit/fine pebbles, rare 30.0-31.5cm depth, common 31.5-34.0cm depth and rare 34.0-37.0cm depth; sharp to |
| 2 | 37-42 | Mid-dark grey structureless silt with rare amorphous organic matter; sharp to |
| 1 | 42-48 | Pale brown structureless silt |
| | | |
| Bed | Depth cm | Description **Basin 3: borehole 123** |
| 3 | 0-5 | Very dark brown friable, crumb-structured amorphous peat with common fine fleshy stems; gradual to |
| 2 | 5-23 | Dark grey structureless silt with abundant amorphous organic matter; sharp to |
| 1 | 23-39 | Pale brown structureless silt |
| | | |
| Bed | Depth cm | Description **Basin 5 (south): borehole 162** |
| 4 | 0-10 | Dark brown amorphous peat with rare-some fine fleshy stems and some mineral matter; gradual to |
| 3 | 10-23 | Mid-brown structureless silt with common amorphous organic matter and rare fine fleshy stems; gradual to |
| 2 | 23-31 | Mid-brown structureless silt with some amorphous organic matter; sharp to |
| 1 | 31-45 | Pale grey structureless silt with clay, clay increasing down-unit |
| | | |
| Bed | Depth cm | Description **Basin 6: borehole 187** |
| 5 | 0-11 | Black to very dark brown amorphous peat with common fine fleshy stems and rare coarse fleshy stems; gradual to |
| 4 | 11-22 | Dark brown amorphous peat with some small wood fragments and some mineral matter; gradual to |
| 3 | 22-31 | Black to very dark brown amorphous peat with common fine fleshy stems and rare small roundwood (twigs), abundant 29-31cm depth, with one large (2.5cm diameter) roundwood, clearly intrusive, visible at 31cm depth; sharp to |
| 2 | 31-33 | Well-stratified pale brown to pale yellow bands of silt; sharp to |
| 1 | 33-44 | Mid-grey structureless silt |
| | | |
| Bed | Depth cm | Description **Basin 7: borehole 214** |
| 4 | 0-8 | Very dark brown to black herb peat with much amorphous organic matter; gradual to |
| 3 | 8-21 | Mid- to dark grey structureless silt with rare horizontal fine fleshy stems; sharp to |
| 2 | 21-39 | Pale brown to mid-grey structureless silt with large wood fragments at the upper boundary; gradual to |
| 1 | 39-46 | Pale brown to mid-grey stratified clay with silt |
| | | |
| Bed | Depth cm | Description **Basin 8** |
| 5 | 0-12 | Very dark brown to black coarse herb peat with abundant small roundwood (twigs) and common small wood fragments; gradual to |
| 4 | 12-22 | Dark grey structureless silt with common amorphous organic matter and some vertical fine fleshy stems; gradual to |
| 3 | 22-38 | Mid-grey structureless silt with some amorphous organic matter and some vertical fine fleshy stems; gradual to |
| 2 | 38-40 | Mid-brown structureless silt with common amorphous organic matter; gradual to |
| 1 | 40-46 | Pale grey structureless silt |

*Table 2. Sediment descriptions of modified golf-hole cores in B2, B3 and B5 (south) to B8.*

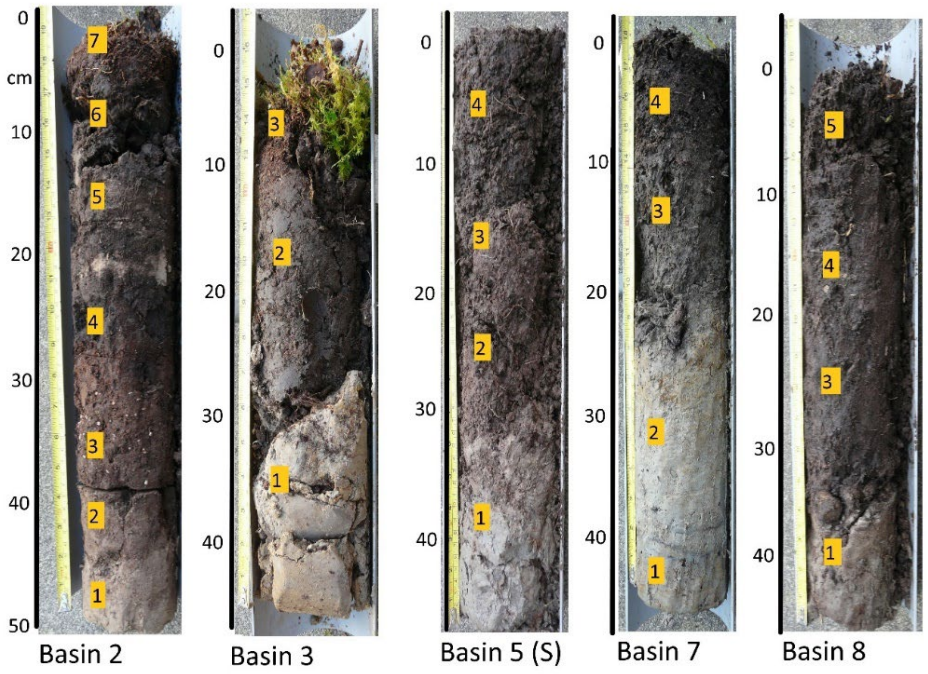


*Figure 16. Photographs of the sediment in B2 at borehole 101 (Figure 9), B3 at borehole 123 (Figure 10), B5 (south) at borehole 162 (Figure 13), B7 at borehole 214 (Figure 12) and B8 (Figure 12).*

### 4.1.5. Luminescence patterns, ages and age estimates of the basal minerogenic fills

Table 3 presents luminescence profiling data from the uppermost basal minerogenic sediments, between 10 and 15cm below their upper boundaries, at B2, B3 and B5-8. Between four and six samples per core were measured, at 2 to 5cm intervals (column 1). Columns 3 and 5 in Table 3 are mean, rounded net signal intensities. These are energies released by the sample exposed to two types of stimulation, infra-red (IRSL) and optical (OSL), measured as photons counted by a portable OSL reader (Sanderson and Murphy 2010) over 120 seconds. Samples are of heterogeneous mineralogies with different particle size distributions, weights and geometries. They can, however, when the sampled sediments are so similar, be most informative on how sediment has accumulated. Measurement errors in net signal intensity data are 1.40±0.76 and are not given in Table 3. Column 8 presents the ratios of IRSL to OSL net signal intensities. IRSL net signal intensities are largely derived from feldspar grains and OSL net signal intensities principally from quartz grains (Sanderson and Murphy 2010). The IRSL:OSL ratio is a measure of changing mineralogy, but in these samples, it is unchanging with a mean ratio of all samples of 0.21±0.01. The luminescence signal is dominantly as OSL from quartz grains.

Figure 17 shows changes with depth of OSL net signal intensities in the uppermost *c.* 15cm of basal minerogenic fills. There are differences in the way each basin accumulated their uppermost sediments. Patterns in which samples decline in net signal intensity up-profile represent conformably accumulating sediment (e.g., B2, B5, B7 above 35cm depth). Hiatuses are suggested by large differences between samples (B2 between 48 and 45cm depth). Patterns in which samples exhibit no change (e.g., B3, B6) accumulated conformably and rapidly. In Basin 8, conformable sedimentation is affected at 35cm depth by deposition of sediment not fully bleached of its luminescence.

| 1 | 2 | 3 | 4 | 5 | 6 | 7 | 8 | 9 | 10 | 11 | 12 |
|---|---|---|---|---|---|---|---|---|---|---|---|
| Depth | Laboratory No. | IRSL net signal intensity | IRSL Depletion Index | OSL net signal intensity | OSL Depletion Index | IRSL:OSL Depletion Index | IRSL:OSL ratio | Aliquot 1 | | Aliquot 2 | |
| (cm) | (cersa) | (counts) | | (counts) | | | | De (Gy) | error | De (Gy) | error |
| Basin 2 | | | | | | | | | | | |
| 37.5 | 742/1 | 1354 | 1.45 | 5753 | 1.64 | 0.88 | 0.24 | 1.22 | 0.08 | 0.94 | 0.05 |
| 39.5 | 742/2 | 1783 | 1.28 | 7357 | 1.74 | 0.73 | 0.24 | | | | |
| 41.5 | 742/3 | 2100 | 1.36 | 8108 | 1.73 | 0.79 | 0.26 | | | | |
| 43.5 | 742/4 | 9250 | 1.37 | 40187 | 1.70 | 0.80 | 0.24 | 3.25 | 0.14 | 2.38 | 0.12 |
| 45.5 | 742/5 | 11323 | 1.41 | 43192 | 1.70 | 0.83 | 0.26 | | | | |
| 47.5 | 742/6 | 23542 | 1.40 | 98662 | 1.74 | 0.80 | 0.24 | | | | |
| Basin 3 | | | | | | | | | | | |
| 23.5 | 743/1 | 25591 | 1.37 | 111425 | 1.78 | 0.77 | 0.23 | 5.04 | 0.24 | 4.05 | 0.24 |
| 28.5 | 743/2 | 26702 | 1.39 | 115776 | 1.85 | 0.75 | 0.23 | | | | |
| 33.5 | 743/3 | 22078 | 1.43 | 97181 | 1.78 | 0.80 | 0.23 | | | | |
| 38.5 | 743/4 | 34077 | 1.44 | 136839 | 1.86 | 0.77 | 0.25 | 4.13 | 0.16 | 4.05 | 0.18 |
| Basin 5 | | | | | | | | | | | |
| 31.5 | 744/1 | 6547 | 1.28 | 28154 | 1.65 | 0.77 | 0.23 | | | | |
| 34.5 | 744/2 | 4912 | 1.36 | 24290 | 1.73 | 0.79 | 0.20 | 2.91 | 0.18 | 2.68 | 0.17 |
| 37.5 | 744/3 | 8959 | 1.26 | 43723 | 1.72 | 0.73 | 0.20 | | | | |
| 40.5 | 744/4 | 7755 | 1.60 | 56897 | 1.93 | 0.83 | 0.14 | | | | |
| 44.5 | 744/5 | 14373 | 1.40 | 69606 | 1.87 | 0.75 | 0.21 | 3.38 | 0.14 | 2.88 | 0.16 |
| Basin 6 | | | | | | | | | | | |
| 33.5 | 747/1 | 3596 | 1.43 | 17112 | 1.65 | 0.87 | 0.21 | 1.07 | 0.07 | 0.85 | 0.07 |
| 36.5 | 747/2 | 3654 | 1.47 | 16219 | 1.74 | 0.84 | 0.23 | | | | |
| 39.5 | 747/3 | 3653 | 1.54 | 17160 | 1.72 | 0.90 | 0.21 | | | | |
| 43.5 | 747/4 | 3258 | 1.44 | 16277 | 1.71 | 0.84 | 0.20 | 1.52 | 0.10 | 1.59 | 0.09 |
| Basin 7 | | | | | | | | | | | |
| 24.5 | 745/1 | 8713 | 1.39 | 46132 | 1.85 | 0.75 | 0.21 | 1.92 | 0.11 | 2.13 | 0.10 |
| 29.5 | 745/2 | 12281 | 1.41 | 64948 | 1.93 | 0.73 | 0.19 | | | | |
| 34.5 | 745/3 | 21145 | 1.34 | 114133 | 1.89 | 0.71 | 0.19 | | | | |
| 38.5 | 745/4 | 10723 | 1.31 | 61894 | 1.85 | 0.71 | 0.17 | 2.49 | 0.12 | 3.09 | 0.17 |
| Basin 8 | | | | | | | | | | | |
| 34.5 | 746/1 | 4105 | 1.41 | 21273 | 1.77 | 0.80 | 0.19 | 1.38 | 0.13 | 1.42 | 0.12 |
| 38.5 | 746/2 | 1548 | 1.39 | 8615 | 1.64 | 0.85 | 0.18 | | | | |
| 42.5 | 746/3 | 5645 | 1.33 | 31707 | 1.76 | 0.75 | 0.18 | | | | |
| 45.5 | 746/4 | 8562 | 1.32 | 46880 | 1.73 | 0.76 | 0.18 | 2.54 | 0.12 | 2.17 | 0.14 |

*Table 3. Luminescence data from B2, B3, and B5-8 inclusive.*

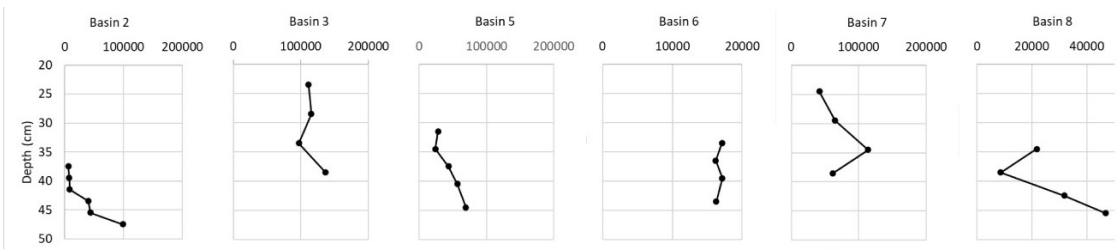


*Figure 17. OSL net signal intensities in the uppermost* c*. 15cm of the basal minerogenic fill in Basins 2, 3 and 5-8 inc. plotted against depth in core (see Table 2). Note changes in horizontal scale.*

Based on these profiles, 12 samples were selected, and paired aliquots measured (using standard SAR protocol) to define more precisely their apparent doses (Section 3). Samples were from immediately beneath the upper surfaces of basal minerogenic fills (Tables 2, 3). The data are in columns 9-12 of Table 3. Mean measurement errors for aliquot 1 are 5.60±1.50% of the dose and for aliquot 2 are 5.98±1.20% of the dose. Apparent doses (Table 3: columns 9-12) are more precise measures of luminescence, sufficient to compare them more closely. Apparent doses are not absolute ages. Of the paired aliquots, only five of the 12 samples overlap (CERSA-743/4, 744/2, 747/5, 745/1 and 746/1: Table 3), indicating caution in interpretation. Apparent doses in Table 5 are calculated as percentages of the maximum apparent dose in any of the basins as a measure of relative age: this was at 38.5cm depth in B3 (Table 3). The % max is given in Table 5 for both aliquots 1 and 2. There is again some inconsistency between aliquots in the ordering of samples, indicating further caution in interpretation. The two samples selected for OSL dating characterise the end-members of the range in apparent doses (Srivastava *et al* 2022: Tables 4, 5).

| CERSA | Basin | Depth (cm) | K (%) | U (ppm) | Th (ppm) | Cosmic dose contribution | Beta (Gy ka$^{-1}$) | Gamma (Gy ka$^{-1}$) | Total (Gy ka$^{-1}$) | Burial dose (Gy) | Total effective dose rate (Gy ka$^{-1}$) | Age (ka) | Years (BC/AD) |
|---|---|---|---|---|---|---|---|---|---|---|---|---|---|
| 743/4 | 3 | 38.5 | 1.51 ± 0.08 | 1.31 ± 0.07 | 5.63 ± 0.28 | 0.20 ± 0.02 | 1.23 ± 0.05 | 0.69 ± 0.03 | 2.12 ± 0.06 | 4.62 ± 0.08 | 2.12 ± 0.06 | 2.18 ± 0.07 | 160 ± 70 BC |
| 747/1 | 6 | 33.5 | 1.37 ± 0.07 | 1.82 ± 0.09 | 6.40 ± 0.32 | 0.20 ± 0.02 | 1.22 ± 0.05 | 0.75 ± 0.03 | 2.18 ± 0.06 | 1.00 ± 0.04 | 2.18 ± 0.06 | 0.46 ± 0.02 | AD 1560 ± 20 |

*Table 4. ICP-MS and ICP-OES determinations of K (%), U and Th (ppm) concentrations, cosmic dose contributions, effective beta and gamma dose rates (wet) following water correction, burial doses, total effective environmental dose rates and corresponding depositional ages of two sediment samples in B3 and B6.*

| B2 | | B3 | | | B5 | | B6 | | | B7 | | B8 | |
|---|---|---|---|---|---|---|---|---|---|---|---|---|---|
| depth cm (altitude m OD) | % max ali 1 (ali 2) | depth cm (altitude m OD) | % max ali 1 (ali 2) | age (BC/AD) | depth cm (altitude m OD) | % max ali 1 (ali 2) | depth cm (altitude m OD) | % max ali 1 (ali 2) | age (BC/AD) | depth cm (altitude m OD) | % max ali 1 (ali 2) | depth cm (altitude m OD) | % max ali 1 (ali 2) |
| | | | | | | | 33.5 (5.94) | 26 (21) | **AD1560 ±20** | | | | |
| 37.5 (7.02) | 30 (23) | | | | | | | | | | | | |
| | | | | | | | | | | | | 34.5 (5.55) | 33 (35) |
| | | | | | | | 43.5 (5.84) | 37 (39) | | | | | |
| | | | | | | | | | | 24.5 (5.75) | 46 (53) | | |
| | | | | | | | | | | 38.5 (5.61) | 60 (76) | | |
| | | | | | | | | | | | | 45.5 (5.44) | 61 (54) |
| | | | | | 34.5 (6.05) | 70 (66) | | | | | | | |
| 43.5 (6.96) | 79 (59) | | | | | | | | | | | | |
| | | | | | 44.5 (5.95) | 82 (71) | | | | | | | |
| | | 23.5 (6.77) | not used (100) | | | | | | | | | | |
| | | 38.5 (6.92) | 100 (100) | **160±70 BC** | | | | | | | | | |

*Table 5. Comparisons in apparent doses from aliquots 1 and 2 between B2, B3 and B5-8 inclusive calculated as percentages of the maximum apparent dose in any basin (see text) and plotted by increasing % max, with depths and altitudes of the samples. Ages BC/AD are OSL age estimates (Table 4).*

Pairs of samples in basins in Table 5 are in stratigraphic order except in B3, apparent doses being smaller at shallower depths. B3 has the highest apparent doses: although in aliquot 1 apparent doses are inverted and are not used in Table 5, they are the same in aliquot 2 (Table 3). Sediment at

38.5cm depth, 16cm below the upper surface of the basal minerogenic fill (Table 2) is dated to 160 ± 70 BC. By inference from aliquot 2, sediment of a very similar age was deposited just beneath the upper surface of the basal minerogenic fill (Bed 1) at 23.5cm depth.

The dated samples in B3 and B6 (Table 5) suggest that 1% of the maximum apparent dose approximates to 20-22 years but the apparent dose data cannot be used as a precise chronological tool. The uppermost 13cm of basal minerogenic fill in B5 is likely to have accumulated after that in B3 (Table 5) although aliquots 1 and 2 agree only in sample CERSA 744/2 at 34.5cm depth (Table 3). So seemingly did sediment in B2 at 43.5cm depth (Table 5), at the top of Bed 1 (Table 2) although B2 is shoreward of B3 and should have formed first: the two aliquots in this sample (CERSA-742/4: Table 3) do not agree and interpretation is uncertain. B5 may have formed in the first half of the 1st millennium AD, but might be later.

It is probable that Beds 1-3 in B8 (45.5 to 34.5cm depth: Table 2) accumulated close in time to comparable sediment in the shoreward B7 (Bed 2: Table 2) and in B6 at 43.5cm depth, possibly in the high Middle Ages. Most anomalous is the apparent dose of sediment at 37.5cm depth in B2, which appears to have been deposited long after B6 was accumulating, which is probably not correct. The highest dated sediment in the basal minerogenic fill at B6 (33.5cm depth in Bed 2) formed at AD1560 ± 60.

B1 is not a surge-related lagoon. It is assumed to have been a salt marsh. It's position against the prehistoric cliff indicates it, and R3, to be the earliest preserved landforms of the Bowhouse Fill. R3 is higher than B1 only because it has a thick mor horizon formed under recent conifers. Their upper surfaces are around 7.35m OD. Assuming that this surface was close to contemporary MHWS (Section 2.3), B1 and R3 may date to around 2500 BC (cf. Figure 29: below).

**4.1.6. Beaches in basin sediments**

Eijelkamp boreholes did not record beach sediment in B2, B3 or B4. Banks of poorly sorted medium-coarse sand with fine pebbles and rare clasts with a-axes >16.0mm were recorded at the northern (shoreward) sides of B5 and B6 that are interpreted as beach deposits, pushed against the coast in B5 or against the earlier-formed R8 in B6. On transect B5(ii) the *c.* 1m beach deposite can be picked out morphologically between boreholes 139 and 148 over some 20m width (Figure 13a); that at B6 is 15m wide and much shallower, rising up onto the underlying impenetrable gravel of R8 (Figure 14). They were probably formed from swash-aligned waves perpendicular to the coast. The need for sustained sediment supply in their formation may imply they were formed before their barrier beaches (R10, R14 respectively) to seaward or very high rates of overwash deposition.

On transect 5(i), in the west of Basin 5 (Figure 10a), boreholes 131-133 stop on gravel coarser than that able to be sampled. Sand underlies organic soil to 7.4m OD at borehole 113. On transect 5(ii) 80m to the east, the fine-grained basal minerogenic fill recorded in the southern side of the basin (5(ii)S: Figure 13b) was eroded at and north of borehole 158 and replaced to the north by coarse-grained sand, gravelly sand and fine gravel lying directly on rock (Figure 12b, 12a). Some 80cm+ of coarse sand with rare clasts having a-axes >16.0mm was also thrown to 8.5m OD onto the existing cliff cut in NCT fill (boreholes 135 to 138). Surviving NCT fill in borehole 134 on transect 5(ii)N is a metre lower than the intact surface away from the cliff and erosion probably reduced the height of the cliff before gravelly sand was emplaced. Gravelly sand was pushed north beyond the cliff some 12m to borehole 135 (Figure 12b). On transect 5(iii) the ground falling steeply from the cliff at 9.5m OD to 7.0m OD had poorly sorted sand with rare fine grit pushed against it, impenetrable at 90cm depth in borehole 169: Figure 12c) but sediment was not thrown landward to boreholes 168 and

167: beach sand has not been preserved at borehole 173. A few boreholes at transect 5(iv) show a very limited extent of beach sand on the floor of Basin 5 (not shown).

Interpretation of Figures 17 and 18 suggests a sequence of events in the creation of B5. To the west, R3 and R9 were not entirely eroded during the erosion that created B5. Protected by these ridges, existing archaeological features were preserved at the base of the cliff at the eastern end of Basin 1, in the lee of Ridge 3. The earthwork is a pronounced bank with an internal ditch and a 4m wide entrance (Figure 20). This entrance implies access to land to the south which was probably more extensive than the remnant of R3 that survives and is indicative of the extent of shoreward erosion that took place in the creation of B5. This bank is the lower of two (Figure 19). East of the entrance, this bank has been lost to coastal erosion. B5 was created in this erosional event. The fine-grained basal minerogenic fill was scoured out on the south side of B5. A beach formed against the cliff. The cliff was lowered by wave action. To the north, lateral erosion lowered by up to a metre the level NCT surface for some 40-50m, identified from the gap between the line of the original cliff and the intact NCT surface. This gap narrows eastward (Figure 18), suggesting the impact of the event weakened eastward. Beach gravels were then thrown onto and beyond the line of the original cliff (above). The cliff was probably steepened (Figures 11b, c) in a later phase. The boundary represented by the bank and ditch was then restored but not on the floor of B5. Instead, a shallow ditch was dug into gravels on top of the cliff, creating an upper bank on the cliff (Figure 19). The upper bank continues east to the 'harbour' (Figure 18). This boundary is what Brann (2004, 18) cautiously likened to a 'park pale' (Figure 30), which would make it broadly Medieval, but Richard Oram (pers comm) thinks the Caerlaverock example to be too small to be a Medieval boundary. The 'park pale' pre-dates the events that created Basin 5.

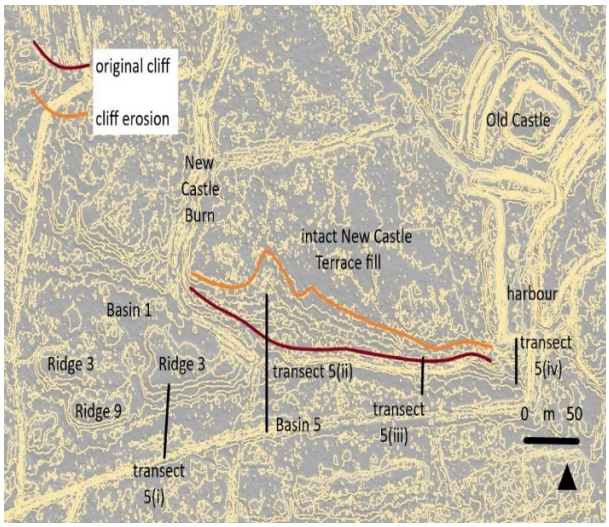


*Figure 18. A contoured LiDAR image (0.25m intervals) of the ground around Basin 5 showing geomorphological features, some archaeological features, the locations of Transects 5(i) to 5(iv) and the conjectured extent of erosion of the NCT fill on the north side of Basin 5.*

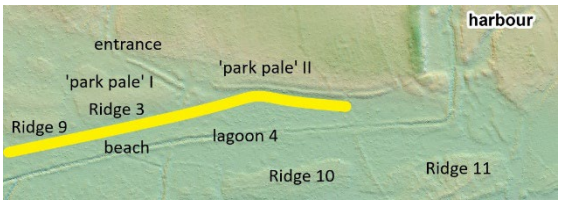


*Figure 19. Natural and archaeological features at and east of Ridge 3*


*Figure 20. A photograph looking east from the crest of the lower bank, with the ditch to the north and with the staff in the entrance gap in the bank.*

B6 has a fine gravel beach at its northern side extending for 10m in boreholes 183 to 186 (Figure 14), coarsening below the sediment able to be sampled. B7 is like B5 in that bedrock is directly overlain by coarse sediment (Figure 15). At the base of borehole 218 is a structureless mix of organic and mineral sediments capped by 2cm of amorphous organic matter that may be a soil developed in bedrock. Poorly sorted coarse sand and grit form the basal deposit in B7 only in boreholes 217, 221 and 225-226. Better sorted structureless sand overlie this and is widespread. South of B7, Basin 8 is understood only from one golf-hole core (Figure 15).

**4.1.7. Barrier Beaches**

Most often, but not in every case, a barrier beach was deposited seaward of each basin (Figure 7b). They were not dated by OSL because the taphonomy of sand trapped in or forming them is likely to be complex (Fruergaard *et al* 2013). They most likely formed towards the end of the events that led to sediment deposition on bedrock terraces (Sections 4.1.4 and 4.1.5) and slightly later coarse-grained beach deposits to shoreward (Section 4.1.6). The barrier beaches formed basins out of what had been terraces. Waning stages of sediment accumulation in basins (Section 4.1.9) are assumed to form because barrier beaches isolated basins from coastal processes. Having said that, R5 and 6, and R7 and 8, accumulated with no intervening basin (Figure 7b). R3 is not a barrier beach: thick peat is underlain by a fine-grained minerogenic sediment fill, not dated but possibly the NCT fill, at the same altitude as the fine-grained fill of Basin 1 to the north (Figure 9a).

The crests of R4 to R8 do not fall southward. Nor do those on R9–R11, but those on R12–R13 are significantly lower. Ridges are between 40 and 1600m long and between 8 and 30m wide. Ridge crest orientations change from west-east in R3-R9 to south west-north east in R11-R13. From their preserved lengths, most ridges are straight, but the eastern ends of R4-R8 have been truncated. R7, R8 and R11 may be recurved at their east ends, suggesting drift alignment. Ridge crests can be level with basins to shoreward (preserved heights (a): Table 6) but can be 2m higher.

| Ridge | Altitude (m OD) of highest preserved crest | Preserved length m | Orientation º | Shape | Preserved width m | Preserved height (a) cm | Type | Sediment | Preserved height (b) cm |
|---|---|---|---|---|---|---|---|---|---|
| 3 | *c.* 8.0 | 150 | 95-275 | straight | 24 | 0 to B1 | | NCT fill | *c.* 130 to B5 |
| 4 | 8.1±0.2 | 300 | 94-274 | straight | 24-32 | *c.* 200 to B2 | barrier beach | sand with grit and some clasts | B3 slopes east |
| 5 | 7.5±0.1 | 175 | 90-270 | straight? | 12-15 | *c.* 60 to B3 | barrier beach | sand | |
| 6 | 7.6±0.2 | 340 | 100-280 | straight | 5-8 | | beach | sand with grit and some clasts | *c.* 90 to B4 |
| 7 | 7.4±0.1 | 240 | 108-288 | recurved | 10-20 | *c.* 90 to B4 | barrier beach | sand with grit and common clasts | |
| 8 | 8.1±0.1 | 230 | 100-280 | recurved | 15-20 | | barrier beach | sand with grit and | *c.* 190 to B6 |

| | | | | | | | | | |
|---|---|---|---|---|---|---|---|---|---|
| | | | | | | | | common clasts | |
| 9 | 7.2±0.2 | 40 | 90-270 | ? | 15 | | beach | sand with grit and some clasts | *c.* 120 to B5 |
| 10 | 7.1±0.1 | >120 | 78-258 | straight | 18-25 | *c.* 100 to B5 | barrier beach | sand with grit and rare clasts | *c.* 100 to B7 |
| 11 | 7.1±0.1 | 100 | 83-263 | recurved | 24-30 | *c.* 120 to B7 | barrier beach | sand with grit and very rare clasts | *c.* 95 t0 B8 |
| 12 | 6.6±0.1 | 80 | 85-265 | straight | 15-20 | *c.* 60 to B5 | barrier beach | sand with grit and some clasts | |
| 13 | 6.5±0.1 | 160 | 85-265 | straight | 15-20 | *c.* 100 to B7 | barrier beach | Sand with grit | |
| 14 | 8.0±0.2 | 1600 | 95-275 | recurved | 15-35 | *c.* 200 to B6 | barrier beach | sand with grit and very common clasts | |

*Table 6. Characteristics of R3 to R14: preserved height (a) is the height of the ridge above the surface of the basal minerogenic fill in the basin to shoreward; preserved height (b) is the height of the ridge above the surface of the basal minerogenic fill in the basin to seaward.*

All ridge crests are eroded to a considerable extent. The west ends of R7 and R8 are disturbed by landscaping. Others (R4, R10, R11, R12) terminate close to later drainage ditches. The east ends of R7 and R8 are argued to have been truncated by wave erosion (below: Section 4.1.8; 4.1.13). The long profile of R4 (Figure 21a) suggests that it might be composite or that the eastern 125m has been eroded. R10 is truncated on its west and east ends by channels. R12 has been truncated at its east end where it abuts the highest and oldest 'merse' surface (Figure 21c).

LiDAR data show that ridge crests are not asymmetrical in cross-profile and have no preserved storm scarps, probably through the concentration of subsequent farming activities on their dry surfaces (below: Section 4.4). Most ridge crests have been cut by north-south trending channels (Figure 7c): on R6 (Figure 21b) they have incised a metre and more into gravelly sand and removed this entirely in places. There are many more north-south channels cutting R6 than R5 (Figure 7c). They may have been cut by wave action. Subsequent ground disturbance has destroyed evidence, if it existed, for features like washover fans (Carter and Orford 1984).

R14 is the youngest preserved ridge. It extends west of Castle Wood for 1600m (Smith *et al* 2003a). The orientation of this ridge is similar to that in R4 to R8. Within Castle Wood the ridge is heavily modified by footpaths and pierced by north-south channels, now dry, and the ditched channel of the Old Castle Burn. There are two crests to the ridge west of the Old Castle Burn, reaching 7.7m OD. This is lower than the crest eastward which reaches 8.2m OD. The ridge west of the Old Castle Burn may be different in age. Tipping and Adams (2007) called the ridge west of the Old Castle Burn, Ridge Two. This is around a metre of stoneless sand perched on a bedrock ridge rising to 6.7m OD. The sand of Ridge 2 is pierced by many channels (Figure 21d). Gravel sampled by Tipping and Adams

(2007) is younger, 40cm thick, overlying at 6m OD a fine-grained minerogenic fill and stacked against the bedrock ridge on its southern side to 6.4m OD.

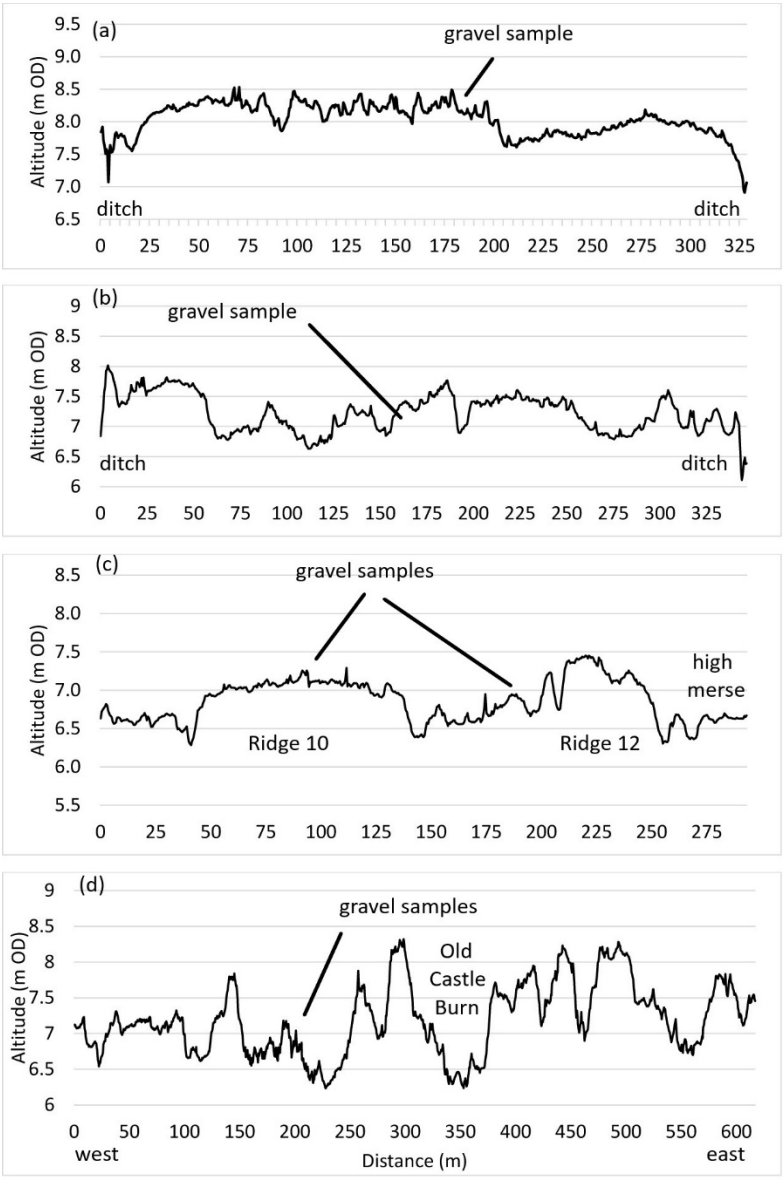


*Figure 21. Plots of LiDAR-defined long profiles (west-east) on (a) R4, (b) R6, (c) along R10 and R12 and (d) along 600m, within Castle Wood, of R14.*

Smith *et al* (2003a; fig. 7)) mapped a series of 10 ridge crests in the fields west of Castle Wood and south of the cliff at Lantonside. They described three groups: crests 1-4 in the west were parallel, oriented 135-315$^{o}$. Crests 2-4 were then overridden by crests 5-7, and then these were overlain by crests 8-10 with orientations broadly 90-270$^{o}$. Smith's mapping ended west of the ridges Ra to Rf in Figure 7b. South of Bowhousepark, six ridges (1, 5, 6 and 8-10) are preserved. Interpretation of a 2018 aerial photograph (Figure 22) suggests the pattern of ridges is much simpler than described by Smith *et al* (2003a), with six broadly parallel ridges curving gently from 135-315$^{o}$ in the west to 90-270$^{o}$ eastward as they approach Castle Wood.

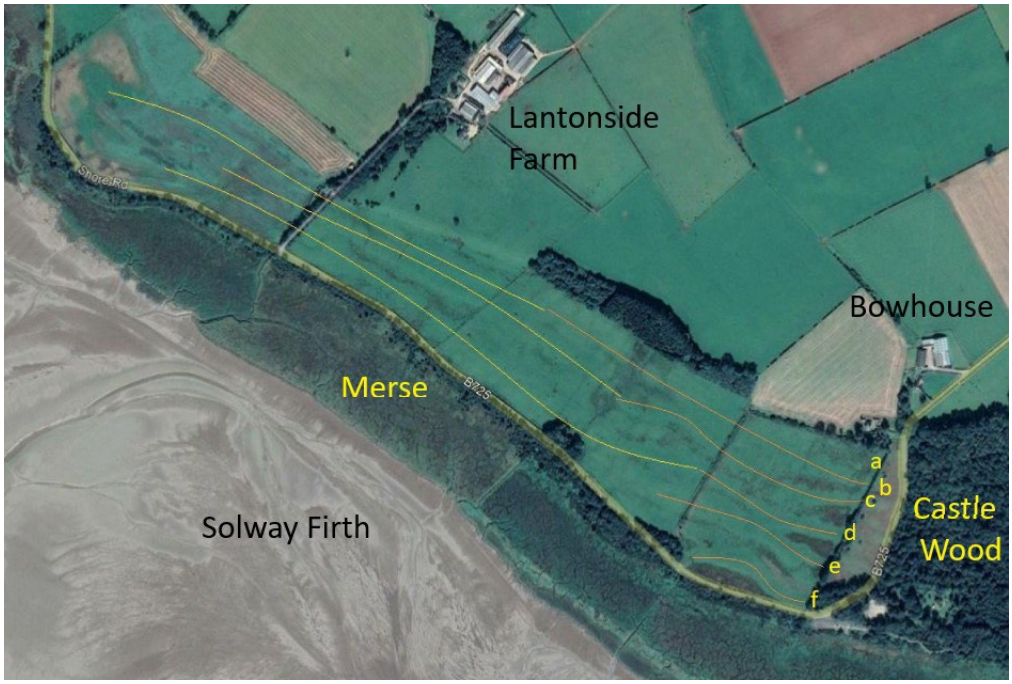


*Figure 22. 2018 aerial photograph of the fields west of Castle Wood at Lantonside with the interpretation of subdued ridge crests and their appearance (a-f) on the LiDAR image of Figure 7b.*

Table 7 attempts correlation between the Lantonside ridges and those in the west of Castle Wood, spatially via their appearance south of Bowhousepark (Figure 7b) and on altitude.

| Spatial correlation | | | Altitudinal correlation | | | |
|---|---|---|---|---|---|---|
| Lantonside | Bowhousepark | Castle Wood | Lantonside | | Castle Wood | |
| 1 | a | | 1 | 8.93±0.3 (n 24) | | |
| 5 | b | | | | R4 | 8.1±0.2 |
| 6 | c | R4 | 5 | 7.72±0.4 (5) | R5 | 7.5±0.1 |
| 8 | d | R5+R6 | 6 | 7.35±0.2 (6) | R6 | 7.6±0.2 |
| | | | | | R7 | 7.4±0.1 |
| 9 | e | R7? | 8 | 7.9 (2) | R8 | 8.1±0.1 |
| 10 | f | R8? | 9 | 7.3 (2) | | |
| | | | 10 | 7.0 (1) | | |

*Table 7. Spatial and altitudinal correlation of the Lantonside ridges (Smith* et al *2003a) and those in Castle Wood (this study).*

Both types of correlation suggest that Lantonside 1 has no correlative in Castle Wood: it is older than any analysed in this study. R4 in Castle Wood should be spatially correlated with Bowhousepark Rc and Lantonside R6 (Figure 7b). Altitudinal correlation suggests no correlative at Lantonside, but altitudinal correlation is of less value because (a) ridge crests are determined by storm energy and not RSL, and (b) ridge crests at Lantonside are heavily ploughed out in contrast to those in Castle Wood. R5 to R7 in Castle Wood may correlate altitudinally to Lantonside R5 and R6 but the truncated western end of R6 aligns with Lantonside Rd. Lantonside R9 and R10, and Bowhousepark Re and Rf, may spatially be correlated with R7 and R8 in Castle Wood, and both are older than R14 in Castle Wood, but landscaping in Castlewood Cottage (Figure 7a) restricts comparisons. Tipping and Adams (2007) could see little reason to equate the Lantonside ridges with those in Castle Wood, but this was before the LiDAR imagery used in this study. It seems highly likely that the same processes affected the coast everywhere between the River Nith and Caerlaverock at the same time.

### 4.1.8. Sediments forming the barrier beaches

The sediment forming most ridges is a poorly sorted medium to very coarse sand with matrix-supported fine gravel. Clasts with a-axes >16.0mm comprise between 0.4 and 37.8% by weight (Table 8). Thicknesses of this sediment were difficult to gauge because they proved impenetrable at depth to augers: it is thought that gravel became coarser with depth. R6, R7 and R8 lie directly on buried bedrock ridges at 7.60, 7.30 and 7.20m OD respectively. It may be that most ridges were anchored on bedrock ridges seaward of the coastline. Sediment was met underlying R9 and R10, though. At both there was *c*. 30cm of structureless silt or fine sand, not bottomed, with upper surfaces at 6.8m OD.

Tipping and Adams (2007) found thicknesses of gravelly sand of 50cm in R14 and 90cm in R8. Thicknesses of gravelly sand are around 90cm in R9 and 55cm in R10. It is a minimal 35cm thick at R4, 65cm at Ridge 5, 50cm at R6 and 95cm at R7 (Table 8). Mean a-axis length of clasts with a-axes >16.0mm in ridges are not significantly different (Table 8), but the post-hole auger cannot sample larger clasts than those retained.

| Ridge | UK Grid Ref | Altitude (m OD) | Proven thickness (cm) | Total wt (gms) | Σ clasts >16.0mm | Wt >16.0mm (gms) | % >16.0mm | Mean a-axis length (mm) |
|---|---|---|---|---|---|---|---|---|
| 4 | 302183 565340 | 8.1 | 20–35 | 9400 | 46 | 800 | 8.5 | 31.4 ± 9.3 |
| 5 | 302183 565281 | 7.6 | 30–45 | 4400 | 8 | not measured | | |
| 6 | 302164 565300 | 6.9 | 10-45 | 9500 | 48 | 725 | 7.6 | 33.4 ± 13.4 |
| 7 | 302132 565246 | 7.3 | 0-24 | 3900 | 56 | 575 | 14.7 | 28.3 ± 8.1 |
| 8 | 302129 565219 | 7.2 | 0-24 | 5000 | 51 | 610 | 12.2 | 29.8 ± 8.7 |
| 9 | 302348 565290 | 7.7 | 20–60 | 10800 | 59 | 550 | 5.1 | 27.5 ± 8.3 |
| Basin 5(ii) | 302550 565320 | 7.5 | 0-80 | 17400 | 66 | 460 | 2.6 | 26.2 ± 6.8 |
| 10 | 302590 565255 | 7.1 | 20-50 | 3500 | 49 | 100 | 2.9 | 28.7 ± 8.7 |
| 11 | 302575 565180 | 6.8 | 20-55 | 6800 | 20 | 25 | 0.4 | 26.6 ± 5.3 |
| 12 | 302684 565260 | 6.9 | 20-55 | 10800 | 71 | 500 | 4.6 | 27.2 ± 7.3 |
| 14 (inner) | 302244 565135 | 6.4 | 20-50 | 2080 | 59 | 450 | 21.6 | 31.1 ± 8.3 |
| 14 (outer) | 302235 565122 | 6.4 | 10-50 | 3180 | 66 | 1200 | 37.8 | 32.4 ± 10.9 |

*Table 8. Details of gravel sampling sites on ridges and of samples: thickness is the thickness of the augered sample.*

Clasts of three lithologies from at least 50 clasts with a-axes >16.0mm were recorded from samples on the crests of R4 and R6–R12 and on the beach in B5 (Section 3): (a) Criffel granodiorite from the Galloway Granitic Suite (GGS), (b) Permian sandstone and breccia, and (c) Silurian sandstone, siltstone, and mudstone. Section 2.2 described the distributions of source rocks and Quaternary sediments around Caerlaverock.

| Ridge | % GGS | % Permian | % Silurian |
|---|---|---|---|
| 4 | 2.2 | 4.3 | 93.5 |
| 6 | 0.0 | 4.9 | 95.1 |
| 7 | 7.7 | 5.8 | 86.5 |
| 8 | 22.9 | 6.3 | 70.8 |
| 9 | 3.6 | 25.0 | 71.4 |
| Basin 5(ii) | 48.4 | 17.7 | 33.9 |
| 10 | 31.8 | 0.0 | 68.2 |
| 11 | 42.1 | 0.0 | 57.9 |
| 12 | 52.1 | 8.5 | 39.4 |
| 14 (inner) | 5.7 | 0.0 | 94.3 |
| 14 (outer) | 1.5 | 0.0 | 98.5 |

*Table 9. Percentages of GGS, Permian and Silurian clasts in ridges and beaches.*

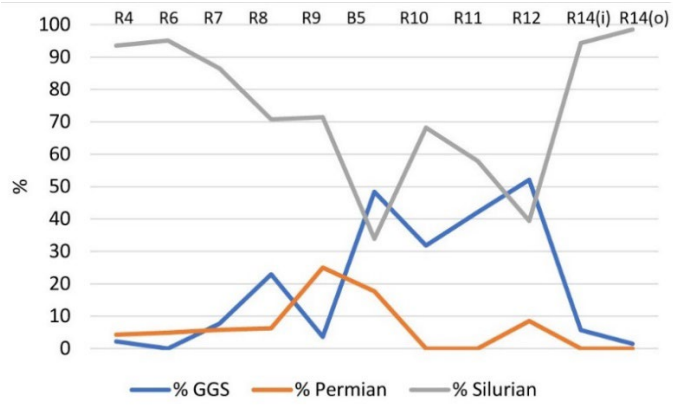


*Figure 23. Percentages of GGS, Permian and Silurian clasts in ridges and beaches.*

Table 9 and Figure 23 show changes through time in these clast lithologies from the earliest sampled ridge, R4, to the most recent, R14. R4 to R9 are dominated by Silurian clasts, though percentages fall as percentages of GGS clasts rise to 23% in R8. R9 has few GGS clasts, being replaced proportionally by Permian clasts. GGS and Silurian clasts characterise the beach in B5 and R10 to R12. Permian clasts are absent after their deposition on the beach in B5 save for R12. Silurian clasts dominate again in R14.

Clasts of these three lithologies have markedly different shape characteristics (Table 10). Clasts from Silurian sediments are significantly more rounded because the sediments are uniformly erodible and have passed through several stages of transport since glaciation (McMillan et al 2011). GGS clasts are neither angular nor rounded. They have a complex mineralogy, with quartz resistant to weathering and feldspar susceptible to weathering. They have short distances to travel from bedrock sources on the high ground of Airds opposite Glencaple and the Criffel or from fluvial gravels deriving from them at New Abbey, south of Aird (Figure 2a). GGS clasts are also commonly found in the Doweel Breccia at Caerlaverock (Tipping and Adams 2007) but clast shape was not recorded. Permian clasts are local and are not resistant to erosion. Their angularity is taken to imply limited transport from bedrock in and immediately around Castle Wood.

| | % angular | % subangular | % subrounded | % rounded | n |
|---|---|---|---|---|---|
| GGS | 3.8 | 40.6 | 52.8 | 2.8 | 108 |
| Permian | 15.4 | 25.6 | 38.5 | 20.5 | 38 |
| Silurian | 3.8 | 18.0 | 26.3 | 51.9 | 338 |

*Table 10. Shape characteristics in the three recorded lithologies of all clasts with a-axes >16.0mm.*

Table 11 describes changes in shape of all clasts and the three lithologies although only Silurian clasts are represented in sufficient numbers to allow assessment of change in nearly all samples.

| Ridge | % all clasts | | | | % GGS clasts | | | | % Permian clasts | | | | % Silurian clasts | | | |
|---|---|---|---|---|---|---|---|---|---|---|---|---|---|---|---|---|
| | ang | suba | subr | r'nd | ang | suba | subr | r'nd | ang | suba | subr | r'nd | ang | suba | subr | r'nd |
| R4 | nm | | | | | | | | | | | | | | | |
| R6 | 4 | 29 | 37 | 29 | | | | | | | | | 3 | 26 | 39 | 32 |
| R7 | 11 | 20 | 25 | 45 | | | | | | | | | 13 | 18 | 22 | 47 |
| R8 | 0 | 16 | 31 | 53 | 0 | 9 | 64 | 27 | | | | | 0 | 15 | 24 | 62 |
| R9 | 3 | 42 | 29 | 25 | | | | | 7 | 50 | 29 | 14 | 3 | 44 | 26 | 28 |
| B5(ii) | 14 | 32 | 38 | 17 | 10 | 33 | 57 | 0 | 27 | 36 | 27 | 9 | 14 | 24 | 14 | 48 |
| R10 | 0 | 31 | 29 | 41 | 0 | 43 | 57 | 0 | | | | | 0 | 19 | 32 | 48 |
| R11 | 0 | 30 | 40 | 30 | 0 | 38 | 63 | 9 | | | | | 0 | 27 | 18 | 55 |
| R12 | 7 | 39 | 35 | 18 | 3 | 45 | 52 | 0 | | | | | 7 | 21 | 25 | 46 |
| R14 (inner) | 0 | 5 | 24 | 71 | | | | | | | | | 0 | 0 | 29 | 71 |
| R14 (outer) | 0 | 4 | 28 | 68 | | | | | | | | | 0 | 2 | 26 | 72 |

*Table 11. Percentages of angular (ang), subangular (suba), subrounded (subr) and rounded (r'nd) clasts in all clasts, GGS, Permian and Silurian clasts with a-axes >16.0mm.*

GGS clasts in R8 are subrounded and rounded, but many in B5 and R10–R12 are subangular. When comparatively abundant, in R9 and B5, Permian clasts are more angular than rounded. Silurian clasts are more angular and subangular in R9 and B5. Values are more consistent in Ridges 10 and after. Silurian clasts are markedly more rounded in R14.

| Ridge | % All clasts | | | | | % GGS clasts | | | % Permian clasts | | | % Silurian clasts | | |
|---|---|---|---|---|---|---|---|---|---|---|---|---|---|---|
| | mean | mode | 16-25 | 25-50 | >50 | 16-25 | 25-50 | >50 | 16-25 | 25-50 | >50 | 16-25 | 25-50 | >50 |
| R4 | nm | | | | | | | | | | | | | |
| R6 | 33.42±13.3 | 38 | 36 | 51 | 13 | | | | | | | 36 | 51 | 13 |
| R7 | 28.3±8.0 | 25 | 26 | 70 | 5 | | | | | | | 26 | 70 | 5 |
| R8 | 29.8±8.6 | 27 | 24 | 71 | 4 | 27 | 73 | 0 | | | | 24 | 71 | 6 |
| R9 | 27.5±8.2 | 23 | 41 | 56 | 4 | | | | 21 | 71 | 7 | 48 | 50 | 3 |
| B5(ii) | 26.2±6.8 | 24 | 48 | 51 | 2 | 67 | 44 | 0 | 30 | 60 | 10 | 29 | 71 | 0 |
| R10 | 28.7±8.6 | 44 | 32 | 66 | 2 | 64 | 36 | 0 | | | | 20 | 77 | 3 |
| R11 | 26.6±5.1 | 29 | 42 | 58 | 0 | 50 | 50 | 0 | | | | 36 | 64 | 0 |
| R12 | 27.2±7.7 | 23 | 60 | 36 | 4 | 43 | 54 | 3 | | | | 39 | 57 | 4 |
| R14 (inner) | 31.1±8.2 | 27 | 23 | 71 | 6 | | | | | | | 23 | 71 | 6 |
| R14 outer) | 32.4±10.8 | 23 | 13 | 85 | 2 | | | | | | | 13 | 85 | 2 |

*Table 12. Mean and modal a-axis values (mm) for all clasts and percentages of all clasts and those of Galloway Granitic Suite, Permian and Silurian lithologies in three divisions: a-axis lengths 16-25mm, 25-50mm and >50mm.*

Clasts are further classified by a-axis length in Table 12. There is no bias in a-axis length in the three lithologies recorded. Mean a-axis length of all clasts does not significantly change though it is highest in R6 and R14. There are high modal values for all clasts in R6 and R10. Proportions of all clasts with a-axes 16-25mm tend to increase after R8, peaking in B5 and R12 before falling sharply in R14. These are principally GGS clasts. Proportions of clasts 25-50mm fluctuate over time with no trend: they dominate gravel in R14. More clasts with a-axes >50mm are recorded in R6 than in younger deposits: all are Silurian.

**Synthesis**

The significance of the gravelly sand deposits is that clasts cannot derived from the NCT fill, which is overwhelmingly fine-grained (Jardine 1980). Clasts this size are also not present in surface sediment offshore in the inner firth (Axelsson *et al* 2006; McMillan *et al* 2011). Because proportions of lithologies vary markedly over time (Figure 23), clasts are also unlikely to have derived from offshore glacigenic (glacial or glaciofluvial) stores where sediment is well mixed. They are interpreted as deriving from discrete sources around the inner firth (above) and cannibalised from earlier ridges in younger ridges.

The earliest ridges, R4 and R6 (R5 is almost stoneless) contain only 8% clasts >16.0mm. R7 and R8 were, on this basis, more energetic events or more gravel was available (Table 8). Ridges R4 to R7 are similar in their being dominated by Silurian clasts (Table 9; Figure 23). Several in R6 are very large (Table 12): all with a-axes >40mm are rounded or subrounded. They are likely to have been derived from glaciofluvial gravels in the lower Nith valley. Their deposition eastward implies easterly longshore transport and drift-aligned deposition. There is a consistent but small proportion of Permian clasts from local bedrock.

The gravel in R8 differs sharply from these with a much-increased proportion of GGS clasts. These are much more rounded than GGS clasts in younger deposits. Glacigenic sediment in the Irish Sea Coast Glacigenic Subgroup on the east side of the River Nith has rare GGS clasts (Section 2.2; McMillan *et al* 2011), so a source near Criffel on the west side of the estuary might seem likely. Another source is the Permian Doweel Breccia at Caerlaverock where 2/3 of the clasts, though much

smaller than sampled in this study, were of the GGS (Tipping and Adams 2007). Here they are cemented into a sandstone matrix, but Tipping and Adams (2007, 117) described how clasts were readily separated from this. None of the GGS clasts measured in the present study had matrix adhering to it but this is easily eroded and many GGS clasts were subangular and heavily abraded.

Gravel on R9 formed following barrier-breaching, truncation of R4-R8 and extensive shoreward erosion to form an embayment almost to the pre-existing cliff-line. Despite the energy of this event, gravels >16.0mm are small percentages of the sediment (Table 8). R9 and the succeeding gravel beach in B5 and above it on the cliff at B5(ii), share a high representation of Permian clasts, the only times this occurs. Many of these are angular (Table 11). Seventy % of these in R9, and 70% in B5, are >25mm long. They were probably eroded from bedrock surfaces on the foreshore at Caerlaverock exposed by wave-base erosion during shoreward erosion. Silurian clasts in R9 are much more subangular than in other deposits (Table 11), suggestive of high abrasion during transport. Clasts are not larger in R9, however (Table 12), probably because they were cannibalised from R4–R8. This injection of locally derived material in R9 may have suppressed the proportion of GGS clasts in R9, but more likely is that the beach in B5 was the first deposit to receive a major influx of GGS clasts. Almost half the GGS clasts in B5 and in R10–R12 are subangular and angular. The simplest interpretation of these observations is that GGS clasts were derived from the Doweel Breccia, as were Permian clasts, as a rock platform underlying the embayment underwent severe truncation and bevelling by wave action and abrasion.

Permian clasts are not recorded in R10 and 11, from which it is assumed that foreshore erosion did not continue. GGS clasts are common to abundant in B5 to R12 (Table 9), though not more so than in B5. Silurian clasts are again abundant in R10 (Table 9; Figure 23) and comparatively few are subangular and none are angular (Table 11), suggesting limited abrasion. Both may have been cannibalised and reworked.

R14 has very high proportions of coarse gravel. It also represents a final change in clast composition. Silurian clasts dominate (Table 9; Figure 23). They are much more rounded than in earlier deposits (Table 11). This may reflect the erosion and transport of clasts from a different source, perhaps again from erosion of glaciofluvial gravels in the Nith valley. The reduction in proportions of GGS clasts reflects this injection of Silurian clasts from drift-aligned longshore transport.

Relevant to this interpretation is the result of clast lithological analyses of the fine-grained sediment fill beneath the two highest and oldest merse surfaces sampled in 2007. Two 10.0cm diameter cores sampled around 120cm of silt-rich fine sand. Four bands at 24-25, 29-30, 107-108 and 116-117cm depth contained a total of 540 pebbles, almost certainly storm driven: the sediments were not dated but they are younger than the mid-18th century (Sections 2.5, 4.1.1). All but two clasts had a-axes <<16.0mm (mean 4.2±1.9mm). They cannot in size be compared to samples from ridge crests in this study, but they are comparable in size to clasts sampled from Bowhouse Scar (Tipping and Adams 2007). Of 177 GGS, Permian and Silurian clasts, 85% were from the GGS, 7% from Permian sources, including the Doweel Breccia, and 8% from Silurian lithologies. In recent centuries, then, small GGS clasts have dominated storm sediments at Caerlaverock, derived from local sources probably in swash-aligned deposition, and longshore drift as in R14 has not occurred.

**4.1.9. Waning stages of sediment accumulation in the basins**

There is very little minerogenic sediment accumulation overlying beach deposits in B5, B6 and B7 (Figures 11-14) but in some boreholes in B5 and B7 these are overlain by bedded or laminated silts and sands. These may be washover deposits but they lack shells (Sedgwick and Davis 2003). In B5(ii)

there is 10cm of bedded sand on top of the eroded cliff at 8.6m OD, suggesting a considerable depth of water there. Thin beds of clay are also recorded within post-beach sediments in B5 and throughout B7, some in B7 thick enough to be depicted in Figure 12, but in no other basin. Scouring and removal of the basal minerogenic fills in B5 and B7 probably created accommodation space sufficient to trap sediment. These clays indicate periods of still-water sedimentation not disturbed by waves. Basins were isolated from coastal processes by bedrock ridges (R11, R14: Figure 8) and barrier beaches, becoming back-barrier environments (Goslin and Clemmensen 2017), probably lagoons, although diatom analyses have not been undertaken to test this.

### 4.1.10. Organic matter accumulation in basins and a $^{14}$C chronology of basin isolation

Figures 8-14 record in six basins the sealing of surfaces of the basal minerogenic fill or coarser beach sediments by a capping of organic-rich silt or peat (see also Table 2). B1 does not show this (Figure 9) but B1 is the only basin not to be enclosed by bedrock ridges or barrier beaches.

Peat can be traced across B3 and B6 (Figures 9, 13) but in B2, B4, B5 and B7 it fills only the southern sides because beach deposits thicken northward (Figures 8-12, 14). In B2 (Figure 9) there is no beach, the northern side of the basin being a surface in the NCT fill. The thicknesses of organic sediment (25-30cm) are uniform within and between basins.

In only one basin, B2, is there evidence for minerogenic sediment deposition contemporary with peat growth. Bed 3 contains abundant clasts of very coarse sand and very fine gravel disseminated within the peat (Table 2; Figure 16). Clasts with a-axes >1.0mm were measured to the nearest 0.25mm. Almost all are rounded or subrounded in shape. Faceted clasts suggestive of aeolian origin were not seen.

| | 35-36cm | 34-35cm | 33-34cm | 32-33cm | 31-32cm | 30-31cm | 29-30cm | 28-29cm | 27-28cm |
|---|---|---|---|---|---|---|---|---|---|
| n | 153 | 329 | 465 | 376 | 469 | 426 | 284 | 27 | 10 |
| n/gm$^{-1}$ | 3.06 | 4.11 | 4.65 | 4.18 | 5.21 | 4.73 | 3.16 | 0.30 | 0.11 |
| max (mm) | 3.00 | 4.00 | 5.00 | 4.00 | 3.75 | 5.25 | 4.00 | 2.75 | 2.5 |
| mode (mm) | 1.50 | 1.50 | 1.50 | 1.50 | 1.50 | 1.50 | 1.50 | 1.00 | 1.00 |
| mean (mm) | 1.64 | 1.77 | 1.69 | 1.69 | 1.63 | 1.75 | 1.65 | 1.56 | 1.59 |
| SD (mm) | 0.48 | 0.58 | 0.57 | 0.56 | 0.54 | 0.59 | 0.61 | 0.52 | 0.51 |
| D10 (mm) | 1.00 | 1.25 | 1.00 | 1.00 | 1.00 | 1.25 | 1.00 | 1.00 | 1.00 |
| D50 (mm) | 1.75 | 2.00 | 1.75 | 1.75 | 1.75 | 2.00 | 1.75 | 1.51 | 1.75 |
| D90 (mm) | 2.50 | 2.75 | 2.50 | 2.75 | 2.50 | 2.75 | 3.00 | 2.67 | 2.00 |
| %<2.0mm | 86 | 79 | 84 | 79 | 86 | 79 | 83 | 89 | 75 |
| %>2.0mm | 14 | 21 | 16 | 21 | 14 | 21 | 17 | 11 | 25 |
| kurtosis | 0.01 | 1.13 | 1.51 | 0.32 | 0.86 | 2.91 | 1.97 | 0.22 | -0.84 |
| skewness | 0.61 | 0.89 | 1.06 | 0.73 | 0.90 | 1.12 | 1.24 | 0.85 | 0.4 |

*Table 13. Descriptive statistics of minerogenic clasts with a-axes >1.0mm in Bed 3, borehole 101, Basin 2.*

Table 13 summarises the data in nine contiguous 1.0cm thick samples. Clasts increase in abundance (measured as clasts gm$^{-1}$) to 31.5cm depth and are very rare above 29.5cm depth. Single clasts only were seen above 27.0cm depth. Most clasts are very coarse sand (<2.0mm). The maximum length of clast recorded increases to 30.5cm depth but all other size measures show no significant change. The NCT fill is not a source for these clasts (Jardine 1980). Clasts of this size are >1% of the offshore sediment today only in the deeper water of the outer estuary west of Southerness (Axelsson *et al* 2006, appendix 4): this is unlikely to be an immediate source. They are thought to have been thrown by waves onto the growing peat surface, though the grains are far too coarse to represent wave-spray deposits described by Cooper and Jackson (1999). Two AMS $^{14}$C assays, at 35-36 and 24-25cm

depth in the same core give a modern age or a $^{14}$C age too young to be calibrated respectively (SUERC-101783, -101779: Table 14), younger than the OSL age of B6 (AD1560 ± 20: CERSA 743/4: Section 4.1.5) some 200m to the south, however. These might discount such an origin, except to note that the youngest basal minerogenic fill in B2 at 37.5cm depth has an apparent OSL dose close to that in the youngest OSL dated basin, B6 (Section 4.1.5; Table 5), immediately beneath the deepest sample in Table 13.

Peat inception In B3 was dated by a single stratified short-lived *Alnus* twig to AD1675-1942 (SUERC-101784), too young to be precisely calibrated. Peat inception in B6 was also dated by a single stratified short-lived twig too young to be calibrated (SUERC-101786). Tipping and Adams (2007) dated the humic acid fraction of basal peat at a shallower depth in B6, though not in the same location, to AD1290-1410 (AA-521534: Table 14). The difference between these $^{14}$C assays, and between both and the OSL age on the underlying basal minerogenic fill are not easily explained. The OSL age is accepted. In B7, bedded clays and silts (Bed 1) and similar but structureless silt (Bed 2) only gradually stored organic matter (Bed 3: Figure 16; Table 2). At the top of Bed 2 a wood fragment unidentified to taxon, weathered and stratified, gave a date too young to be calibrated (SUERC-101785: Table 14).

| Site | Borehole | Depth (cm) | Bed | Material | Description | Wt. (gms) | SUERC No. | $^{14}$C BP | $\delta^{13}$C (‰) | Cal BC/AD (95.4%) |
|---|---|---|---|---|---|---|---|---|---|---|
| B2 | 101 | 24-25 | base of 4 | amorphous peat | humic acid | 12.7 | 101783 | 143 ±28 | -28.9 | AD1670- … |
| B2 | 101 | 35-36 | base of 3 | wood (*Alnus*) | one 4cm long horizontal, weathered, short-lived twig | 0.34 | 101779 | | -27.4 | modern |
| B3 | 123 | 22-23 | base of 2 | wood (*Alnus*) | one 5x1cm horizontal roundwood | 3.06 | 101784 | 130 ±28 | -28.4 | AD1675-1942 |
| B6 | (2007) | 18-20 | | herb peat | humic acid | | AA-51534 | 610 ±45 | -29.4 | AD1290-1410 |
| B6 | 187 | 30.5 | base of 3 | wood (unid.) | One 3.5x0.75cm horizontal, weathered and compressed short-lived twig | 2.09 | 101786 | 178 ±28 | -27.8 | AD1658- … |
| B7 | 214 | 21-22 | top of 2 | wood (unid.) | one 7x2cm horizontal, weathered short-lived wood fragment | 10.30 | 101785 | 204± 28 | -30.0 | AD1645- … |

*Table 14. Details of AMS 14C assays in B2, B3, B6 and B7, and from B6 (Tipping and Adams 2007), calibrated using Oxcal 4.4 (Bronk Ramsey 2009) with INTCAL20 (Reimer et al 2020) and expressed at 95.4% probability (… represents a calibrated age that extends to the present).*

The $^{14}$C assays in Table 14 are minimal ages for the processes creating the basal minerogenic sediments and for barrier beach construction. However, assays other than AA-51534 in Table 14 are thought to relate to paludification (peat formation) unrelated to coastal processes. Assay SUERC-101779 is presumed to date an intrusive, modern twig albeit at considerable depth: its weathered appearance was taken as an indication of some antiquity, but its age indicates the opposite. None of these age estimates capture the timing of storm surges.

### 4.1.11. Other gravel ridges in the inner firth

Of the six beach ridges at Ingleston, five formed to altitudes >9m OD as the NCT fill accumulated to 9.4m OD, the youngest to altitudes >8.5m OD, comparable to the Lantonside ridges that have been equated to the Castle Wood ridges (above: Section 4.1.7).

Jardine's (1980) gravel bar at Midtown is actually a series of 9-10 subdued curving ridges, almost certainly swash-aligned (Hughes 1995), nearly 600m wide, with elongated peat basins separating some ridges, seaward of Priestside Flow between 6 and 7m OD, cut into the early-mid Holocene 'carse' (NCT fill) described and $^{14}$C dated by Lloyd *et al* (1999) east of Nethertown. They are later Holocene in age. The ridges are in turn eroded west of Nethertown, the embayment thus created filled with younger 'carse', subsequently fringed with 'merse'. In the younger 'carse' at Mid Upper Priestside was found an anchor described as Roman (CANMORE ID 66560). The Midtown ridges are likely to be contemporary with those in Castle Wood.

### 4.1.12. Formation of the oldest merse at Caerlaverock

The eastern edge of the suite of features B5 to R14 is sharply defined (Figure 7b). R12 is truncated by a track. R14 may be a recurved spit. East of these the strandplain is cut into by an embayment filled by the highest and oldest merse. This straddles the sea wall (Figure 7a) and lies against a cliff cut in glacial till some 150m north of the east end of R14. Bedrock at around 3.5m OD underlies the oldest merse in the embayment. If the embayment was originally filled with sea water, these ridges may have ended naturally in deep water but it is thought most likely that they were truncated by erosion of their eastern ends. This is dated to between the sealing of B8 by R14 and after B6 was formed by R14 at AD1560 ± 20 (above: Section 4.1.5), and the earliest surviving merse, dated from cartographic and $^{14}$C dating to before the mid-18th century (above: Section 2.4).

The embayment created is comparable in size and shape to the embayment eroded during formation of B5. A possible control on why erosion occurred where it did is given by the location of the bedrock mound of Bowhouse Scar south of Castle Wood, protecting ridges to its north and forcing currents either side (Marshall 1962b). While erosion may have been through wave action, it is hard to explain why erosion was only partial. Both embayments may have been cut by east-flowing channels of the River Nith pushed north by storms.

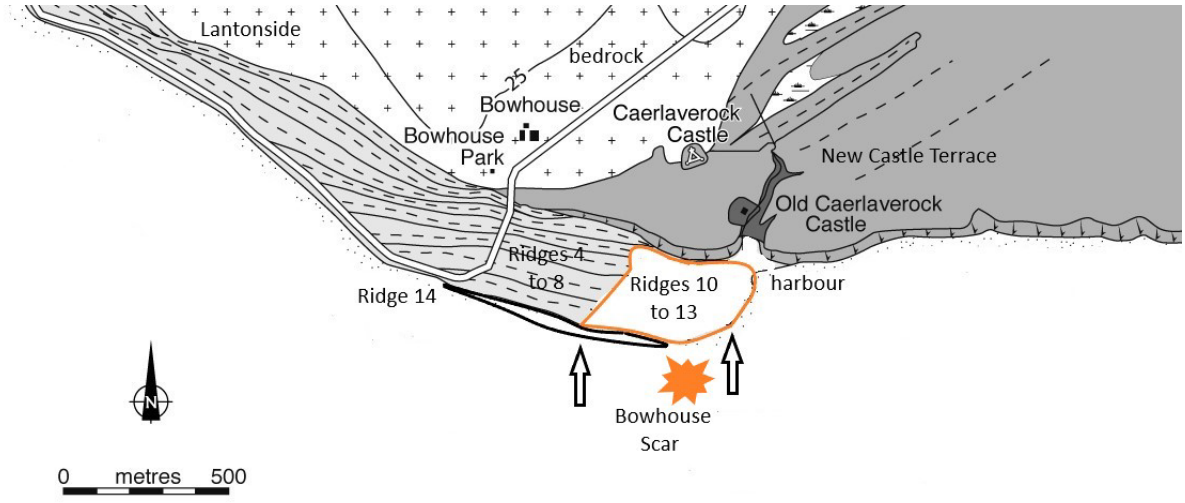


*Figure 24. Map of the Caerlaverock coast as it may have been between the 17th and 18th centuries, showing prominent buildings, the Shore Road, areas of bedrock and of the New Castle Terrace north of the Lantonside storm beaches and their continuation in Castle Wood (only schematically represented), emphasising the area east of R4 to R8 that was eroded after*

*their formation and the area east of the subsequent R10 to R13 that was eroded after their formation (arrowed) and the position of Bowhouse Scar as surveyed by the Ordnance Survey in 1851: modified from Brann (2004) figure 2.1.*

it is possible that merse sedimentation was linked to changes in climate and sediment supply, explored in Section 4.1.13.

**4.1.13. Late Holocene evolution of the Caerlaverock strandplains**

The New Castle Terrace (NCT fil) aggraded before *c*. 4500 BC to between 8 and 10m OD (Section 2.3). As it accumulated, it buried a pre-existing landscape of Permian sandstone and breccia bedrock ridges and shallow bedrock basins (Sections 4.1.2, 4.1.3). By the later Iron Age, the coast at Caerlaverock was marked by a *c*. 2m high degraded cliff cut in glacial till and in the soft, easily eroded NCT fill. The cliff-top was in part the upper surface of the NCT fill. Salt marsh probably extended seaward of the cliff for an unknown distance: B1 and R3 probably represent the surviving remnant of that marsh, forming a ground surface at around 7.3m OD (Section 4.1.3).

The oldest preserved barrier beach is Lantonside 1 (Smith *et al* 2003a) to the west of those studied in Castle Wood. It lies at the foot of the cliff and is anchored to the mainland. Its crest is at almost 9m OD, but this has been lowered by ploughing. This ridge is not dated. It might be considerably older than R5-6 in Castle Wood, which date to 160 ± 70 BC and may relate in age to spits at Shearington to the east of Caerlaverock (Jardine 1980; Smith *et al* 2003a: Section 2.5).

Probably shortly before 160 ± 70 BC (Section 4.1.5) the coast was impacted by the first preserved later Holocene storm surge of R4. The date of 160 ± 70 BC relates to the deposition of R5. R4 and R6 may also have formed close in time to this. This earliest preserved strandplain at Caerlaverock began to form much later than larger strandplains elsewhere in the British Isles (Section 2.5). Storm surges eroded almost all the pre-existing salt marsh sediment at Caerlaverock, making sea water highly turbid but dominated by reworked, uniformly mixed silt, very fine and fine sand. They exhumed the bedrock topography. Cliff retreat cannot be demonstrated but seems likely. Extreme storm events created barrier beaches, a series of straight, elongated sand and gravel ridges parallel to the cliff, several hundred metres long, tens of metres wide and up to two metres above surrounding sediment. Ridges were not anchored to the mainland but were barrier islands, perhaps all anchored on underlying bedrock ridges that they buried (Section 4.1.2). They were cut by wave-eroded channels perpendicular to the coast (Section 4.1.7). Successive beach ridges formed to seaward and the strandplain prograded (advanced) south some 150m. If each ridge is assumed to have formed in a single event there were a minimal five surge events (R4, R5, R6, R7 and R8). Where measured the ridges are between 50 and 90cm thick (Section 4.1.8). The sediments forming R4 to R8 are poorly sorted medium to very coarse sands with matrix-supported fine gravel: clasts with a-axes >16.0mm are consistently 8% (R6) to 15% (R7) of the fill by weight (Section 4.1.7).

Most barrier beach ridges R4-R8 at Carlaverock ponded ‘lagoons’ to shoreward. Around 60cm of entirely minerogenic uniform silts and fine sands accumulated on bedrock terraces shoreward of barrier beach ridges (Sections 4.1.3, 4.1.4). They are collectively called basal minerogenic fills. They are not well-understood because until pOSL profiling showed them to be young (Section 4.1.5) they were assumed to comprise truncated early-mid Holocene NCT fill. The sediment is re-deposited NCT fill derived from sea water charged with mud held in suspension by wave action. Whether the bedrock was eroded immediately prior to sediment deposition (i.e. during storm surges) is not known. Over how long the 60cm of basal minerogenic fill accumulated is not known because the earliest fills were not dated. What the depositional environments of the basal minerogenic fills were is not known because sedimentological and diatom analyses were not undertaken. Only their uppermost *c*. 15cm or so are understood, and that only partially (Section 4.1.5). From pOSL analyses

there is no consistency in how these youngest sediment fills accumulated: in B2, B5 and B7 sediment accumulated conformably, in B3 and B6 very rapidly; hiatuses occur in B2; deposition of reworked, partially bleached sediment indicative of turbulent deposition occurred only in B8. Some of these traits suggest high-energy depositional environments, though not particle size. The youngest basal minerogenic fill of B3 is OSL dated to 160 ± 70 BC (Section 4.1.5). Measurements of apparent OSL doses (Table 5), though they are not age estimates, suggest that the youngest basal minerogenic fill in B2, which has to be older than B3, was formed close in time to B3. Maximal ages for basal minerogenic fills from AMS $^{14}$C dating of overlying organic sediment (Section 4.1.10) are very young and probably date only late-stage paludification. The youngest basal minerogenic fill in B2 is at 7.2m OD and that in B3 at 6.8m OD (section 4.1.3). MHWS is estimated to have been stable in the Solway Firth at 4.6-5m OD at AD120-440 (Section 2.3; Smith *et al* 2003), though it is not known how long this had been established before the first millennium AD. This $^{14}$C dated fragment of salt marsh at West Preston was probably forming when storm surges impacted 12km to the north at Caerlaverock, an interesting contrast in coastal environments. Assuming that the upper surfaces of basal minerogenic fills in lagoonal basins at Caerlaverock had some relation to the sea water surface that formed the seaward barrier beach, a minimal water depth of 2-2.5m above contemporary MHWS was generated by these first storm surges. This corresponds, from Lennon (1963, table 2) to a *c*. 210 yr flood. Luminescence properties of the basal minerogenic fill of B4 were not measured but it is probably close in age to B3. A minimal water depth 1.3-1.8m above contemporary MHWS is inferred. R5 and R6, and R7 and R8 were built with no intervening 'lagoon' having formed.

Under a stable RSL, progradation occurs when sediment supply to the coast is increased. The dominance of Silurian clasts in R4-R8 strongly suggests a source for the gravel in glacigenic sediment stores in the Nith valley (Section 4.1.8). However, this is not straightforward. Glaciofluvial terrace fills, the Kirkbean Sand and Gravel Formation (McMillan *et al* 2011) are preserved today in the Nith valley at the surface only in Dumfries itself, 10km north of the mouth of the estuary (British Geological Survey 2005). There are small, isolated deposits of the Kirkbean Sand and Gravel Formation at Carsethorn (Figure 1a) but too restricted to be a source. Downstream of Dumfries, early to mid Holocene estuarine-marine sediments ('carse'; the NCT fill) bury them and fill the valley to 10m OD (Smith *et al* 2003a). Only with falling RSL could fluvial processes move gravel towards the estuary. Sediment supply from the River Nith may have increased through increased river discharge, climatically induced (Macklin, Johnstone and Lewin 2005; Macklin, Jones and Lewin 2010) or as a consequence of late Iron Age land use change (Dumayne and Barber 1994; Tipping 1997), making gravel easier to transport. Accelerated fluvial activity is known at this time in the region (Tipping 1995, 1999; Tipping, Milburn and Halliday 1999) and can be expected on the River Nith, though there is no evidence on the lower Nith for later Holocene alluvium to be gravel-rich. Ignorance of the sediment stratigraphy of the inner firth (McMillan *et al* 2011) limits analysis but glaciofluvial terraces, if they survive, are even more deeply buried: offshore sediment is an unlikely source unless the inner firth was then completely different to the last millennium when fine-grained muds and sands have dominated (Section 2.1).

Ridges 4-8, and ridges b-f at Lantonside, probably formed as spits extending from the mouth of the River Nith, driven eastward by longshore drift to Caerlaverock. Younger Lantonside ridges can be correlated with R4 to R8 in Castle Wood where preservation is much better (Section 4.1.1). They cannot be traced west of Lantonside because they were subsequently eroded by cliff retreat (ridges mapped by Smith et al (2003a) and the British Geological Survey (2005) close to Glencaple are higher than 10m OD and so are older). We do not know how far east R4–R8 extended because they were truncated by later barrier-breaching (below) although the shallow bedrock surface at around 5m OD, and the later eastward extension of R14 implies that they would not have been prevented from

forming. Eastward drift is today's circulation pattern on the northern shore of the inner firth, but because spits do not form today, longshore drift is assumed to have been stronger then. However, R4-R8 do not include significant numbers of GGS (Criffel granodiorite) clasts from and near its outcrop west of the River Nith.

Stronger longshore drift should have been a response to changing climate: this is assumed in our general interpretations. It is hard to demonstrate for the period when R4 and R5 were constructed, however. From *c*. 400 BC to *c*. AD250 is the Roman Warm Period (Büntgen *et al* 2011), not a period of rapid climate change (Mayewski *et al* 2004), warm in western Ireland (McDermott *et al* 2001) and very dry in northern Britain (Baker *et al* 1999; Charman *et al* 2006) and Ireland (Swindles *et al* 2013). Sea surface temperatures reconstructed for western Scotland fell abruptly to very low after *c*. 100BC, recovering consistently after *c*. AD50 before falling from *c*. AD250 to c. AD600 towards the Dark Ages Cold Period (Eiríksson *et al* 2006), also called the Late Antique Little Ice Age (Büntgen *et al* 2016). North Atlantic storminess was limited (O'Brien *et al* 1995). Baker *et al* (2015) suggested the NAO to have been in a negative phase, which would imply lower strengths and frequencies of westerly winds. Though high energy storm surges breached coarse clastic barrier breaches on the Brittany coast from *c*. 200 BC (Van Vliet-Lanoë et al 2014ab) and generated sand dunes there (Van Vliet-Lanoë *et al* 2014b), and in northernmost Scotland (McIlvenny, Muller and Dawson 2013), Northumberland (Wilson *et al* 2001) and Denmark (Nielsen *et al* 2006), there is no generally significant increase in wind-blown sand at this time along the Atlantic façade (Sorrel *et al* 2012; Goslin *et al* 2018). North Atlantic deep water formation was enhanced (Oppo, McManus and Cullen 2003), sea-ice west of Ireland negligible (Bond *et al* 1997) and sea surface temperatures west of Mull perhaps cooler than in the warm 20th century (Wang, Surge and Mithen 2011). What climatic patterns were like when R7 and R8 were deposited must wait for their dating.

An exceptional barrier breach event, caused by a much higher-energy storm or storms occurred after deposition of R8 and before deposition of R9. This event is defined in relative time by the composition of gravels contrasting with those in R4-R8 (Section 4.1.8). Gravel deposits in R9-R12 have very large proportions of clasts of Criffel granodiorite (GGS). In this event/s, R3 to R8 and B4 were truncated on their eastern sides (Figure 7b). The south west trending canalised Old Castle Burn (Figure 7a) broadly follows this line, probably because the absence of gravel ridges made digging it easier. It is not clear why coastal erosion occurred along this line: Section 4.1.12 attempts to account for it by forced migration of an east-flowing River Nith but there is no evidence for this, and west of Lantonside the proximal ends of R4-R8 were also eroded. The line of attack in these event/s means that they were swash-aligned, coming directly from the south to south west. Longshore drift ceased to be effective.

Shoreward erosion of around 75m created a large embayment. The eastern side of R4 may have been lowered by erosion (Figure 21); B3 may slope east because its eastern end was invaded by the eroding sea. At R9 erosion stopped against the probable salt marsh of B1 and R3 but further east it eroded to the early Medieval coast and eroded the bank and ditch boundary of an enclosure that was built on the salt marsh (Section 4.1.6). The sharp change in gravel composition in R9 is explained by lateral erosion of Permian Doweel Breccia, introducing highly abraded angular and sub-angular clasts of sandstone matrix and Criffel granodiorite clasts (Section 4.1.8). There may have been significant vertical erosion as well. Beneath R4–R8 is a bedrock surface at around 7m OD; in the embayment there is a bedrock surface at 5.5m OD (Section 4.1.2). This may be a storm abrasion surface (cf. Retallack and Roering 2012; Van Vliet-Lanoë *et al* 2014a) lowered by some 1.5m. As well as R9 being built and then much-eroded, the minerogenic fill of B5 also contains on its northern side a beach developed in coarse sand with gravel (Section 4.1.6). The cliff was eroded and lowered and

gravel thrown onto and beyond it to 9m OD. This is a minimal water depth: the upper surface of the basal minerogenic fill of B5 is 6m OD (Section 4.1.3), a metre higher than contemporary MHWS. This indicates only that minimal water depths estimated from such measurements are very much minimal. Erosion seems to have lessened eastward to the 'harbour' of the Old Castle. R10 was constructed seaward of B5. Apparent OSL dose measurements in B5 might suggest this event happened in the first half of the 1st Millennium AD (Section 4.1.5) but this is very uncertain, and instead this event may be related to the earliest storm surge impacts at the Old Castle in the early 14th century AD.

A second strandplain was constructed, infilling the embayment, directly seaward of the 'harbour' to the Old Castle. These formed between the barrier-breaching event and the late 16th century. The strandplain incorporates B5, R10, R12, B7, R13 and R11, B6 and B8 (Figure 7b). B5, B6 and B7 contain beaches on their shoreward edges (Section 4.1.6), probably because waves were now swash-aligned rather than drift-aligned. Depositional events in the formation of B7 are particularly complex and suggestive of higher-energy sedimentation. The orientations of these ridges are south west-north east (Section 4.1.7), in part caused by refraction around the R4–R8 headland but probably also because these barrier beaches were all swash-aligned (Section 4.1.6). They are again heavily channelled. R10, R11 and R12 each have common Criffel granodiorite (GGS) clasts, with Silurian clasts equally common but rare to no Permian clasts, best explained by the continued cannabilisation of earlier eroded ridges (Section 4.1.8). These ridges also have lower abundances of clasts (Section 4.1.8: R13 is almost stoneless), and the crests of R12 and R13 are lower (Section 4.1.7), suggesting that some storm surges preserved in this strandplain were of lower magnitude. The upper surfaces of basal minerogenic fills in B5 and B6 are also at altitudes only just above contemporary MHWS (Section 4.1.3). The lower altitude of the bedrock surface under these deposits (Section 4.1.2), only just above contemporary MHWS at 5.5m OD, implies that lower magnitude storms could make as significant a geomorphological and topographic impact as reflected in R4–R8 where the bedrock surface was 1.5m higher.

Another change in the style of basin and ridge deposition occurred after formation of R11 and R13. Though inadequately explored because of the density of scrub woodland, B8 is comparable in location and altitude to B6, though separate (Figure 7b), and these represent the first landforms to span the lengths of both strandplains. Both are protected from erosion by the extraordinary development of the 1600m long R14. R14 is dated by OSL from the youngest basal minerogenic fill in B6 to AD1560±20 (Section 4.1.5). This is much younger than the AMS $^{14}$C assay of AD1290-1420 obtained by Tipping and Adams (2007) on peat directly overlying this fill (Section 4.1.10) but much older than others in comparable stratigraphic contexts reported in Section 4.1.10. Its meaning is unclear: it is unlikely that these age estimates imply diachroneity in the isolation from wave processes in B6.

The shape of R14 strongly suggests that it extended east as a spit, a drift-aligned barrier with a recurved eastern end. The abundance of Silurian clasts in it might suggest that the spit originated in the estuary of the River Nith (Section 4.1.8), much like, it is assumed, the earlier strandplain of R4-R8 (above). Clast lithologies might suggest derivation from R4-R8 but clast shape (Table 11) and size (Table 12) do not support this. Defining a precise source of clasts is difficult, however, as in discussion of R4-R8 (above), and though increased fluvial sediment supply delivering more coarse sediment to the estuary is possible (cf. Macklin and Rumsby 2007), the evidence is lacking. As in R4-R8, eastward longshore drift is likely to have strengthened. This, then, is a major change in barrier formation from the swash-aligned R9-R13. Both sets of ridges lie on bedrock close to the ground

surface, and bedrock extends beneath the merse south of Castle Wood in Bowhouse Scar (Figure 24), so water depth did not constrain development of the swash-aligned R9-R13 strandplain.

The spit of R14 may have accumulated time-transgressively, morphological changes along it (Section 4.1.7) signifying different times and rates of progradation (cf. Reimann *et al* 2011), such that the age estimate at B6 may pertain only to the spit here. Assuming that the age estimate is significant, R14 formed within the LIA. This is characterised generally as having a strongly negative NAO (Section 2.6: Trouet *et al* 2012; Baker *et al* 2015). Cook (2003) defined the interval AD1555-1590 as a short-lived positive NAO phase, however, as did Ortega *et al* (2015) between AD1480 and 1595, and Luterbacher *et al* (2002) suggested winter values close to 0 between 1575 and 1590. In tropical Atlantic latitudes, hurricane activity is throught to have risen from the mid-15th century to peak at AD1600 (Burn and Palmer 2015). An abrupt warming of the sea surface in western Scotland AD1540-1600 has been suggested to represent strengthening of the winter NAO (Cage and Austin 2010). The interval 1556-1589 saw a boom in the Norwegian herring trade, though, associated by Alheit and Hagen (2002) with negative NAO (Section 2.6). A positive NAO implies strong westerly winds, probably with wave-induced strengthening of the eastward longshore drift on the northern side of the inner firth. Lamb (1977, 444-445) reconstructed winter westerly storm tracks in the second half of the 16th century affecting all of the eastern Atlantic coast, and (ibid, 467) cyclonic depressions between 56$^{o}$and 62$^{o}$N, over Scotland, 80-85% of the summers between 1586 and 1605. The years 1570-1599 stood out as stormy in Lamb and Frydendahl's (1991) analysis (Section 2.7.3), with the summer 1588 storms that scattered the *armada* an example of "jet stream winds at the limit of, or beyond, the maximum speeds expected from modern experience" (Lamb 1995, 218): Hickey (1997), however, reported only one 16th century archival reference to a storm in Scotland. There are very few sedimentological records at this time (Figure 7), or British coastal archaeological sites reviewed by Brown (2015) and Griffiths (2015) that do not show heightened geomorphological activity at this time.

It is not known if the recurved eastern end of R14 ended naturally in deep water or whether it and the ridges and basins forming the second strandplain were truncated at their eastern ends by later erosion: they are disturbed and terminate in swamp. Section 4.1.12 suggests truncation and a mechanism for this but there is no field evidence for this. There is no evidence for coarse clastic landforms to have been constructed at Caerlaverock after the 16th century. The absence of actively accreting spits on the northern shore of the firth today suggests a regionally significant reduction in coarse clastic sediment transport. Figure 7 suggests that evidence is rare for wind-blown sand accumulation after *c*. AD1600 between south Wales and northernmost Ireland. The dated coarse clastic barrier ridges at Caerlaverock are more assured indicators of storminess and support this interpretation of regionally reduced storm activity. Marine inundations still occurred, as in 1627 (Section 2.7.2) but they appear to have left no geomorphological trace. Most storm tracks may have bifurcated to south and north of this region. Why this happened is unclear. Cage and Austin (2010) reconstruct declining sea surface temperatures off western Scotland after *c*. AD1600 to the mid-20th century. Across the north east Atlantic, sea surface temperatures fell from *c*. AD1570 but only to *c*. AD1700: the 18th century was warmer than centuries either side (Cunningham *et al* 2013).

East and south of the strandplains of the Bowhouse fill is the merse, actively forming salt marsh. The merse is a fundamentally different sediment and landform to the high-energy marine deposits that preceded it at Caerlaverock. Salt marshes in the outer firth and the headwaters of the inner firth are confined to the fringes of estuaries but at Caerleverock they are on an open coast (cf. Allen 2000; Harvey and Allen 2000). Formation of merse in the inner forth is diachronous. It is at least 700 years old behind the barrier beaches of Moricambe Bay; Kirkconnel Flow in the Nith estuary began to form

behind the Nith Navigation Commission's river training wall in the 19th century (Morss 1927). But correspondents with Sir John Sinclair in the First Statistical Account suggest the merse on open coasts in the inner firth expanded in area in the years before 1795-6 (Section 2.4). The merse at Caerlaverock is estimated from several lines of evidence to have begun to form from the mid-18th century (Section 2.4), significantly earlier than and not associated with the work of the Nith Navigation Commission in the 19th century (cf. Steers 1973, 317).

Formation of the merse at Caerlaverock was also unconnected to the cessation of longshore drift-generated spits from the Nith: they were separate events. It is also significantly later and so also unconnected to the earliest record of siltation in the River Nith, in 1563x1566 (Watson 1923, 29: Section 2.1) and in the mid-17th century (Hume Brown 1891, 190). In the First Statistical Account of Scotland, the Rev. Little of Colvend and Southwick Parish reported that "Excessive falls of rain, brought by violent southerly or south-westerly winds, blowing in from the neighbouring Atlantic, have of late years been severely felt here". "The sudden and loud gusts of south-westerly winds, several of which have been experienced in this part of the country, [have been] uncommonly violent within these last 12 years" and "the roughness of the sea in the cod-fishing season [autumn-winter], render[s] the use of boats in fishing dangerous, and almost impracticable" (Sinclair 1796, 101-104). Southerly and south westerly winds are implicated in the rare archival records of inundations in the inner Solway Firth (Stevenson 1753 in MacLeod 2001; Sinclair 1796, 101-2; Hickey 1997). These descriptions suggest climatic causation in formation of the merse *via* an increased strengthening of south westerly winds and storms driving fine-grained sediment into the inner firth and onto its shores (Section 4.1.12). The Rev. Little stated that change occurred in the 1780s. The observations of the Rev. Little are, however, not supported by Mossman's record of gale days experienced in Edinburgh, which begins in 1770. From 50 days in 1770, they decline to <15 in the mid-1780s (Dawson *et al* 1997). Kington (1988) demonstrated that westerly winds over the Btitish Isles were unusual in the 1780s, blocked by persistent high pressure cells over the European continent. Extreme high water levels at Liverpool were very high in the 1770s but low in the 1780s (Woodworth and Blackman 2002). The reconstructed NAO was strongly negative from *c*. 1750 to after 1800 (Luterbacher *et al* 2002; Cook 2003; Ortega *et al* 2015) or even all of the 18th century (Baker *et al* 2015). A positive NAO and strong westerly winds prior to *c*. 1750 might have promoted merse formation at Caerlaverock, but not generally. It seems probable that the Rev. Little was over-interpreting events in the 1780s or that storms were more rare than they appeared to him.

However, in the 1790s the church ministers of Kirkbean and neighbouring Colvend and Southwick, near Caulkerbush (Figure 1a) both described recent increases in size and height of offshore sandbanks, with the firth "gradually shutting up. … The navigation of the frith they [local fishermen] find is becoming daily more difficult; new sand-banks frequently appear" (Sinclair 1795, 129), "The navigation … of the Solway Frith is every day becoming more difficult and hazardous, by the large sand banks which lie in its channel …; and which within these few years have risen much higher, and extended themselves much farther out towards its mouth, seeming to threaten, at no very distant period, to shut it up altogether." (Sinclair 1796, 101). These changes were more immediate and ongoing. Whether the two ministers independently observed these changes is unknown, and it might be expected that local fishermen would exaggerate conditions, but the reports are intriguing. Intertidal sandbanks and merse are closely linked today, sandbanks feeding sediment to the merse. And though the reconstructed NAO phase remained negative (above), Lamb and Frydendahl (1991, 22) and Hickey (1997) for Scotland reported the 1790s as a decade of heightened storminess, though not in Edinburgh (Dawson *et al* 1997) and the frequency of extreme high water levels at Liverpool rose (Woodworth and Blackman 2002).

Storms did impact merse sediments also, of course. Four undated but different storms deposited thin bands of small-diameter clasts in the oldest two merse surfaces (Section 4.1.8). All are dominated by GGS clasts. Their origin is unclear. They may have been reworked from R12 and others to the west or exposure of bedrock scars on the foreshore continued to be common.

Throughout the later Holocene development of the coast at Caerlaverock there was no inland aeolian accumulation of sand. Jardine (1980) mapped 'young' dunes at Blackshaw Bank east of Caerlaverock but these are sleeching mounds associated with salt making (Cranstone 2006). The absence of wind-blown sand must relate to the predominance of much finer-grained sediment released by coastal erosion of the NCT fill. In this regard, the nearshore sediment store differed from that in the mid-Holocene, when some sand dunes formed (Section 2.5).

## 4.2. Sediments in archaeological features

### 4.2.1. The 'harbour'

Figure 25 is a LiDAR contoured image of the archaeological features at and around the Old Castle.

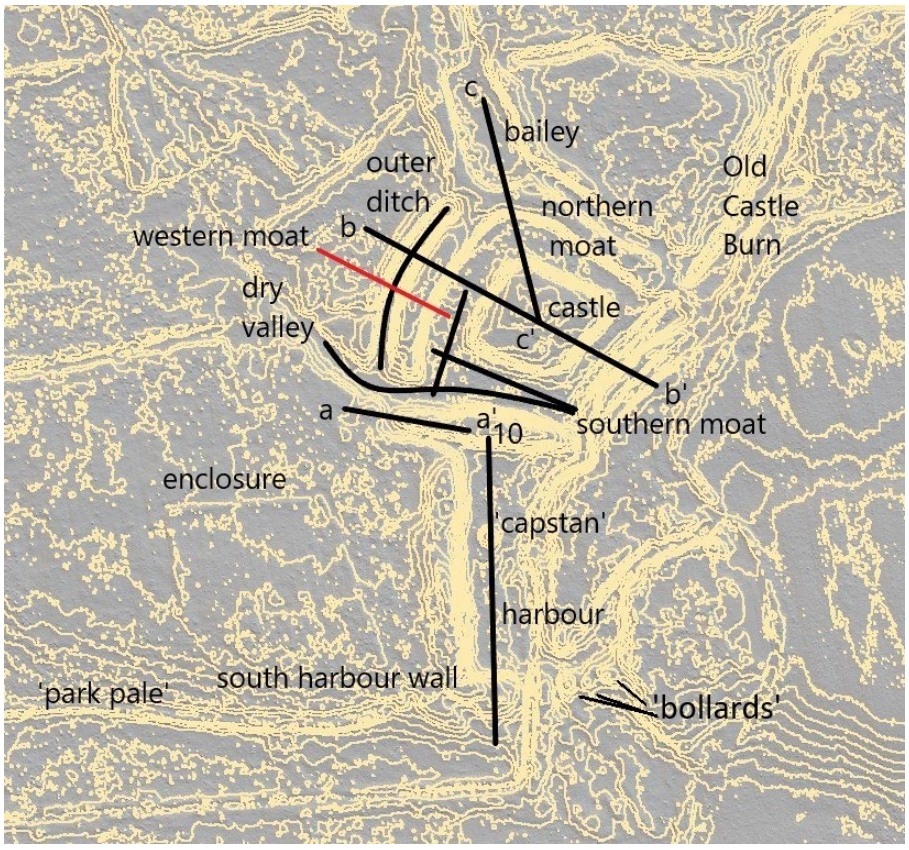


*Figure 25. Archaeological features at and around Old Caerlaverock Castle picked out by contours at 0.25m intervals. North is to the top.*

The 'harbour' is south of the Old Castle. It is a rectangular depression some 70m long, narrowing southward from around 35m to 25m wide with an area of around 0.2 ha. The northern side rises to around 9.5-9.7m OD and separates the 'harbour' from the southern moat of the Old Castle (Figures 24, 25). Brann (2004, 15-16) excavated this wall in a 10.0x1.5m trench. He recorded natural sediments from the base of the trench at 6.8m OD to 8.2m OD, capped by a turf-line: this was not dated. The upper part is artificial, comprising upcast of re-deposited natural silt and clay. Cut into the western end of the northern wall (a-a': Figure 25), where the crest of the wall is lower at around

9m OD, is a 10m wide, 1m deep ditch crossing the wall. It connects the 'harbour' to the moat system. However, the base of the ditch at 8m OD is 0.5m above the surfaces of both the 'harbour' and the dry valley.

The upper parts of the western and eastern walls are also probably of upcast, falling around a metre away from the 'harbour' to the level surface of the NCT at 9m OD (Figure 25). The southern wall has a crest around 9.5m OD. Brann (2004, 15) saw this as a man-made bank some 2m high, though extraordinarily, his reconstruction (Figure 13.2) omits the southern wall. Reid (1946) described it as a sea wall with the implication that it was man-made. Simpson (1953) ignored the southern wall, claiming the 'harbour' was open to the sea. It is not: there is only a narrow (*c.* 2m) gap through which the Old Castle Burn flows. To the east of the burn are three linear mounds on the line of the southern wall around 7, 12 and 16m east of the Old Castle Burn , called 'bollards' in Figure 25. Their origin and meaning are unknown. Figure 25 also shows that the pre-existing coastline at the 'park pale' broadens and becomes much less steep near and at the southern wall of the 'harbour'. One borehole on this south-facing slope (borehole 174) recorded only NCT fill, and although it is not possible from the sediment stratigraphy to detect whether this is re-deposited, it is thought that the southern wall of the 'harbour' is formed from natural (NCT) sediment.

Figure 26 shows two parallel LiDAR transects across the basin floor from north to south: (a) is T10 (Figure 25); (b) is to the east. In the north the floor is level at around 7.5m OD but in the south, it is 30-50cm lower, channelled and eroded. The channels may relate to the Old Castle Burn if the burn was ever outside the ditch that constrains it now. The burn passes through the 'harbour' on its extreme east. Brann (2004, 15) is almost certainly right in thinking that construction of the basin modified the existing valley of the Old Castle Burn. Figure 25a also shows the 1m high prominence called the 'capstan'. A 70cm deep borehole from its top recorded the NCT fill: the 'capstan' appears to have been sculpted as the valley was widened and deepened to make the 'harbour'.

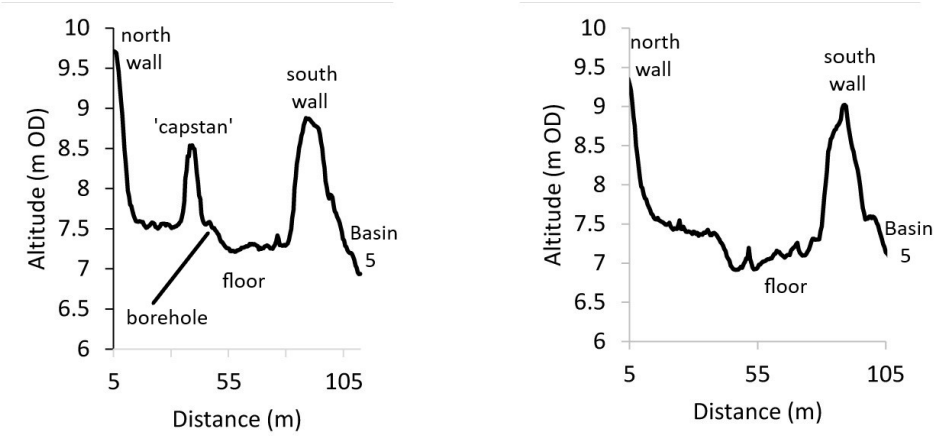


*Figure 26. LiDAR transects at 0.5m intervals across the floor of the 'harbour' from north to south at (a) Transect 10 (Figure 25) and (b) to the east.*

#### 4.2.1.1. Sediment sampling and description

Tipping *et al* (2004, figure 2.3) recorded *c.* 3m of silt-rich sand from six Eijelkamp boreholes along the floor of the basin, each bottoming on bedrock at 3.85±0.15m OD. Beneath a more organic 20-30 cm soil, the uppermost 40-60 are silty clays, mottled and pedogenically altered, overlying a well sorted, internally structureless and featureless fine-medium sand. Sediment recovery was difficult, though, because the sediment was fluid. A borehole was cored with a vibracorer in October 2021 at NY 02688 65380 from the surface of the basin at 7.5m OD, on its west side, away from the Old Castle

Burn, and just south west of the 'capstan'. The coring site is unaffected by erosion (Figure 26). Some 3.23m of sediment was retrieved above bedrock at 4.27m OD. Core 1 (18-168cm depth) was very compressed at 47cm length: depths were corrected uniformly in this core by a factor of 3.16 from the top of the core at a known depth. Core 2 in a second borehole (173-323cm depth) was not at all compressed. That this difference might reflect a significant sedimentological boundary was tested by two further Eijelkamp boreholes cored close by in April 2022: they did not record more compact sediment at any depth. Luminescence data demonstrate that there is no overlap between the two cores. The sediment stratigraphy was described from very dry cores in 2022. It is given in Table 15.

| Depth cm | Description |
|---|---|
| 18-38 | Pale-mid grey structureless silt with some amorphous organic matter; gradual boundary to |
| 38-168 | Pale grey to cream-yellow structureless silt with fine sand; boundary not seen to |
| 173-184 | Cream-yellow structureless silt with fine sand; gradual boundary to |
| 184-248 | Cream structureless fine sand with silt; very gradual boundary to |
| 248-291 | Cream structureless fine sand with silt with common mica flakes and few mafic minerals, common 263-269cm depth; gradual boundary to |
| 291-296 | Cream structureless fine sand with silt with common mica flakes and common mafic minerals; sharp to |
| 296-323 | Cream structureless fine sand with silt with common mica flakes and rare mafic minerals |

*Table 15. Sediment stratigraphy of the sediment core from the 'harbour'.*

Nineteen samples showed the sediment to be a very fine sand (Figure 27) , largely unchanging except between 147 and 72cm depth when fine and medium sand increases, and above 42cm when silt dominates. Apparent dose estimates (below: Table 16) were obtained on the very fine sand fraction (90-150µm).

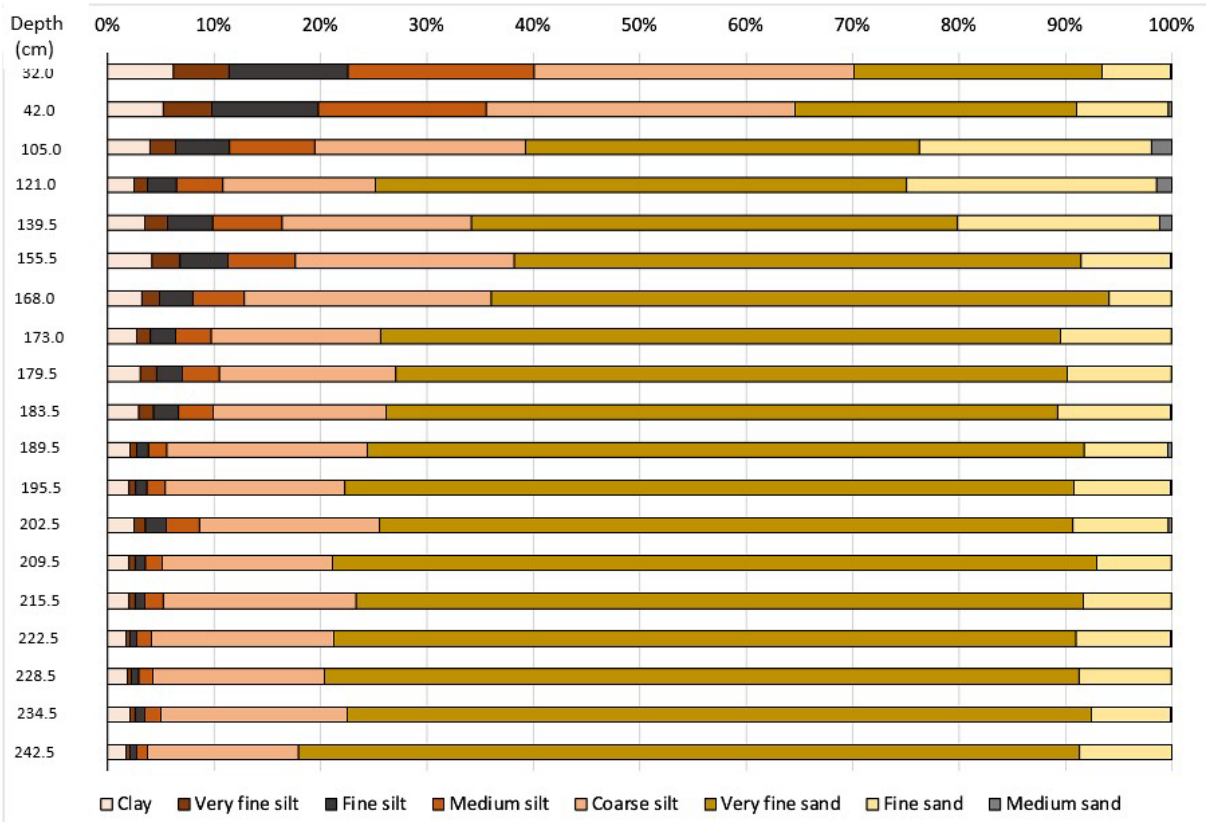


*Figure 27. Particle size distributions in harbour sediment.*

### 4.2.1.2. Luminescence patterns and sediment accumulation in the 'harbour'

Table 16 and Figure 28 present the luminescence data from the sediment surface to bedrock in the cores sampled by vibracorer, at depths corrected for compression: this correction creates the 12cm intervals in core 1. Sediment between 158 and 120cm depth was sampled contiguously in 2cm thick slices to reduce the sampling interval here. Columns 3 and 5 in Table 16 are mean, rounded net signal intensities. Measurement errors in net signal intensity data decline from 13% to <1% by 158.5cm depth and below and are not given in Table 16. Net signal intensities are energies released by the sample exposed to two types of stimulation, infra-red (IRSL) and optical (OSL), measured as photons counted by a portable OSL reader over 120 seconds (Sanderson and Murphy 2010). Samples are of heterogeneous mineralogies with different particle size distributions, weights and geometries. They can, however, when the sampled sediments are comparable, be most informative on how sediment accumulated. The uniform silt-rich fine sand in the basin (Table 15) allows this assumption to an extent.

Based on these data, 23 samples were selected, and paired aliquots prepared and measured to define more precisely the first approximations of apparent doses (Grays (Gy): Srivastava *et al* 2022). The data are in columns 9-12 of Table 16. Mean measurement errors for aliquot 1 are 3.28±0.75% of the dose, significantly higher above 121cm depth and for aliquot 2 are 3.42±1.37% of the dose, significantly higher above 42cm depth.

| 1 | 2 | 3 | 4 | 5 | 6 | 7 | 8 | 9 | 10 | 11 | 12 |
|---|---|---|---|---|---|---|---|---|---|---|---|
| Depth | Lab No. | IRSL net signal intensity | IRSL depletion index | OSL net signal intensity | OSL depletion index | IRSL:OSL depletion ratio | IRSL/OSL ratio | Aliquot 1 | | Aliquot 2 | |
| (cm) | (cersa) | (counts) | | (counts) | | | | De (Gy) | error | De (Gy) | error |
| Core 1 | | | | | | | | | | | |
| 20.0 | 739/1 | 288 | 1.22 | 2287 | 1.52 | 0.80 | 0.13 | | | | |
| 32.0 | 739/2 | 374 | 1.34 | 2946 | 1.62 | 0.83 | 0.13 | 0.58 | 0.03 | 0.59 | 0.05 |
| 42.0 | 739/3 | 553 | 1.06 | 2791 | 1.49 | 0.71 | 0.20 | 0.66 | 0.03 | 0.48 | 0.03 |
| 57.5 | 739/4 | 610 | 1.21 | 3819 | 1.62 | 0.75 | 0.16 | | | | |
| 73.5 | 739/5 | 1259 | 1.66 | 7398 | 1.60 | 1.03 | 0.17 | | | | |
| 92.5 | 739/6 | 2357 | 1.28 | 14347 | 1.69 | 0.75 | 0.16 | | | | |
| 105.0 | 739/7 | 3049 | 1.38 | 17203 | 1.62 | 0.85 | 0.18 | 1.50 | 0.07 | 1.66 | 0.08 |
| 121.0 | 739/8 | 7451 | 1.06 | 37529 | 1.58 | 0.67 | 0.20 | 2.39 | 0.12 | 2.27 | 0.12 |
| 124.5 | 739/12 | 12446 | 1.44 | 55595 | 1.65 | 0.87 | 0.22 | | | | |
| 128.3 | 739/13 | 9631 | 1.42 | 46769 | 1.65 | 0.86 | 0.21 | | | | |
| 135.9 | 739/14 | 26016 | 1.48 | 127313 | 1.78 | 0.84 | 0.20 | | | | |
| 139.5 | 739/9 | 41741 | 1.33 | 242112 | 1.72 | 0.77 | 0.17 | 6.17 | 0.20 | 2.15 | 0.06 |
| 143.6 | 739/15 | 57473 | 1.42 | 300656 | 1.83 | 0.78 | 0.19 | | | | |
| 151.5 | 739/16 | 88094 | 1.48 | 441139 | 1.89 | 0.79 | 0.20 | | | | |
| 155.5 | 739/10 | 77725 | 1.30 | 486007 | 1.73 | 0.75 | 0.16 | 12.99 | 0.40 | 10.44 | 0.33 |
| 158.6 | 739/17 | 47923 | 1.36 | 251578 | 1.68 | 0.81 | 0.19 | | | | |
| 161.8 | 739/18 | 60569 | 1.43 | 291617 | 1.81 | 0.79 | 0.21 | | | | |
| 168.0 | 739/11 | 75854 | 1.31 | 416919 | 1.70 | 0.77 | 0.18 | 11.51 | 0.30 | 10.28 | 0.26 |
| Core 2 | | | | | | | | | | | |
| 173.5 | 740/1 | 81583 | 1.33 | 387566 | 1.67 | 0.80 | 0.21 | 8.48 | 0.24 | 9.07 | 0.22 |
| 179.5 | 740/2 | 75786 | 1.31 | 362702 | 1.65 | 0.79 | 0.21 | 8.71 | 0.25 | 9.73 | 0.28 |
| 183.5 | 740/3 | 89728 | 1.32 | 426801 | 1.68 | 0.79 | 0.21 | 9.17 | 0.27 | 8.52 | 0.23 |
| 189.5 | 740/4 | 136962 | 1.34 | 735057 | 1.80 | 0.75 | 0.19 | 9.07 | 0.25 | 10.36 | 0.29 |
| 195.5 | 740/5 | 100633 | 1.30 | 555284 | 1.70 | 0.76 | 0.18 | 10.55 | 0.27 | 9.04 | 0.26 |
| 202.5 | 740/6 | 115510 | 1.32 | 677626 | 1.76 | 0.75 | 0.17 | 8.95 | 0.27 | 11.28 | 0.38 |
| 209.5 | 740/7 | 114075 | 1.30 | 676192 | 1.69 | 0.77 | 0.17 | 12.73 | 0.36 | 12.12 | 0.42 |
| 215.5 | 740/8 | 146453 | 1.34 | 868839 | 1.86 | 0.72 | 0.17 | 9.49 | 0.27 | 10.21 | 0.28 |
| 222.5 | 740/9 | 135381 | 1.32 | 788641 | 1.81 | 0.73 | 0.17 | 9.94 | 0.31 | 9.84 | 0.26 |
| 228.5 | 740/10 | 140021 | 1.32 | 825782 | 1.79 | 0.74 | 0.17 | 10.50 | 0.32 | 9.86 | 0.25 |
| 234.5 | 740/11 | 154940 | 1.33 | 854376 | 1.79 | 0.74 | 0.18 | | | | |
| 242.5 | 740/12 | 125167 | 1.36 | 735819 | 1.75 | 0.78 | 0.17 | | | | |
| 248.5 | 740/13 | 138408 | 1.32 | 790785 | 1.79 | 0.73 | 0.18 | | | | |
| 255.5 | 740/14 | 131470 | 1.32 | 734733 | 1.81 | 0.73 | 0.18 | | | | |
| 262.5 | 740/15 | 121388 | 1.34 | 694652 | 1.78 | 0.75 | 0.17 | | | | |
| 269.5 | 740/16 | 123549 | 1.31 | 707617 | 1.77 | 0.74 | 0.17 | | | | |
| 275.5 | 740/17 | 128867 | 1.32 | 732325 | 1.81 | 0.73 | 0.18 | | | | |
| 282.5 | 740/18 | 134814 | 1.33 | 763688 | 1.88 | 0.71 | 0.18 | 10.07 | 0.24 | 10.70 | 0.32 |
| 290.5 | 740/19 | 122770 | 1.32 | 701042 | 1.84 | 0.72 | 0.18 | 10.03 | 0.37 | 10.42 | 0.31 |
| 298.5 | 740/20 | 127631 | 1.32 | 725555 | 1.80 | 0.73 | 0.18 | 8.57 | 0.23 | 8.56 | 0.21 |
| 305.5 | 740/21 | 96349 | 1.31 | 564486 | 1.79 | 0.73 | 0.17 | 9.66 | 0.32 | 10.34 | 0.37 |
| 314.5 | 740/22 | 98398 | 1.29 | 576024 | 1.77 | 0.73 | 0.17 | 9.37 | 0.35 | 11.01 | 0.34 |
| 322.5 | 740/23 | 103692 | 1.31 | 566258 | 1.79 | 0.73 | 0.18 | 10.44 | 0.29 | 10.20 | 0.29 |

*Table 16. Luminescence data from sediments in the 'harbour'.*

Column 8 presents the ratios of IRSL to OSL net signal intensities. IRSL net signal intensities are largely derived from feldspar grains and OSL net signal intensities principally from quartz grains (Sanderson and Murphy 2010). The IRSL:OSL ratio is a measure of changing mineralogy (Figure 28, column a). The mean IRSL:OSL ratio of all samples is 0.17±0.06. The luminescence signal is dominantly as OSL from quartz grains, but ratios above 200cm depth are much more erratic than below this. Periodically, sediment accumulating above 200cm depth has had a higher feldspar content. Since feldspar is much more easily weathered in nature than quartz, the sediment deposited above 202cm depth sometimes experienced less weathering than that accumulating

earlier. It is particularly less weathered between 189 and 168, at 121 and at 42cm depth. Sediment above 42cm depth has very low IRSL:OSL ratios and thus little feldspar.

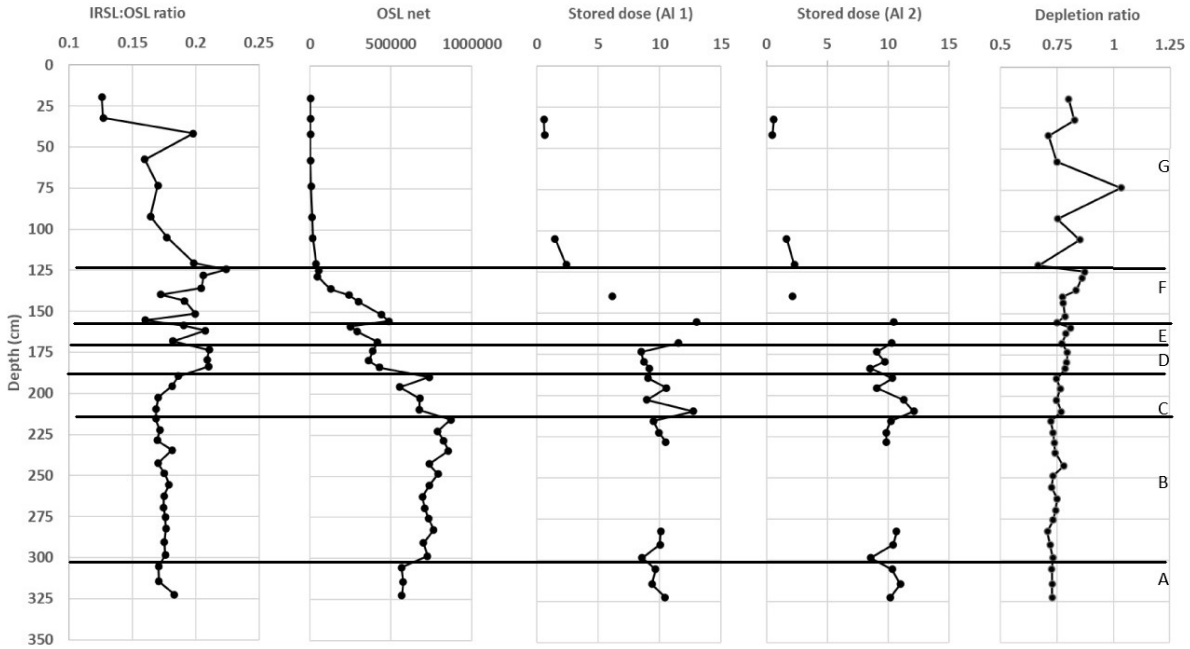


*Figure 28. (a) IRSL:OSL ratios, (b) OSL net signal intensities, (c) and (d) apparent doses of selected aliquots, and (e) IRSL:OSL depletion ratios plotted against depth and showing Zones A-G.*

Nevertheless, the OSL signal dominates. Column B in Figure 28 depicts changes in OSL net signal intensities. Up-profile changes in net signal intensities have five characteristic patterns (Munyikwa, Kinnaird and Sanderson 2021):

(a) when net signal intensities consistently decline up-profile, they reflect deposition of sediment fully bleached (zeroed) of pre-existing luminescence and undergoing slow, conformable burial, absorbing background radiation from surrounding sediment

(b) similar net signal intensities up-profile represent the same process but with rapid burial so that the time-difference between deeper and shallower sediment is negligible

(c) when net signal intensities consistently increase up-profile, they reflect deposition of sediment not fully bleached of pre-existing luminescence such that it retains some pre-existing luminescence as well as luminescence absorbed after deposition

(d) profiles with scattered or mixed net signal intensities have been attributed to bioturbation (Muñoz-Salinas *et al* 2011) but a more likely origin in sediment is the pulsed delivery of variably bleached grains

(e) hiatuses in sediment accumulation are recognised by abrupt reductions in net signal intensities.

Columns 9-12 of Table 16 (columns c and d, Figure 28) present apparent doses, which are more refined and precise measures of luminescence intensity. They endorse and accentuate the patterns in OSL net signal intensities. The possibility that grains can be partly or entirely unbleached, however, means that these patterns are less straightforwardly explained. The IRSL:OSL depletion ratio (Table 16: column 7), derived from dose depletion indices (columns 4 and 6) have been suggested as measures of how well bleached luminescent grains are (Munyikwa *et al* 2021): higher ratios imply well bleached sediment. The mean depletion ratio for samples in Table 16 is 0.76±0.06. Figure 28e shows that sediment below 140cm depth is uniformly bleached. Samples at 105, 73 and 32cm depth lie outwith 1.0SD of the mean and are very well bleached, and that at 20cm depth is well bleached. The two highest samples are from close to the ground surface. Sediment at 121cm

depth is outwith 1.0SD of the mean and so very poorly bleached, and that at 42cm depth is poorly bleached, probably because sediment was transported and buried very rapidly.

#### 4.2.1.3. OSL dating

Three samples were selected for OSL dating (Table 17) after interpretation of the luminescence data and agreement in apparent dose estimates between paired aliquots (Table 16). Assay CERSA 750 is from core 1; assays CERSA 751 and -752 are from core 2.

| CERSA | Depth (cm) | K (%) | U (ppm) | Th (ppm) | Cosmic dose contribution | Beta (Gy ka$^{-1}$) | Gamma (Gy ka$^{-1}$) | Total (Gy ka$^{-1}$) | Burial dose (Gy) | Total effective dose rate (Gy ka$^{-1}$) | Age (ka) | Years (BC/AD) |
|---|---|---|---|---|---|---|---|---|---|---|---|---|
| 750 | 152.5 | 1.55 ± 0.08 | 1.81 ± 0.09 | 7.25 ± 0.36 | 0.17 ± 0.02 | 1.42 ± 0.06 | 0.89 ± 0.02 | 2.48 ± 0.07 | 1.89 ± 0.12 | 2.48 ± 0.07 | 0.76 ± 0.05 | AD 1250 ± 50 |
| 751 | 173.0 | 1.50 ± 0.08 | 1.33 ± 0.07 | 5.46 ± 0.27 | 0.17 ± 0.02 | 1.25 ± 0.05 | 0.75 ± 0.03 | 2.17 ± 0.06 | 11.80 ± 0.29 | 2.17 ± 0.06 | 5.44 ± 0.21 | 3420 ± 210 BC |
| 752 | 215.5 | 1.46 ± 0.07 | 1.16 ± 0.06 | 4.83 ± 0.24 | 0.16 ± 0.02 | 1.20 ± 0.05 | 0.67 ± 0.03 | 2.03 ± 0.06 | 12.13 ± 0.18 | 2.03 ± 0.06 | 5.99 ± 0.21 | 3970 ± 210 BC |

*Table 17. ICP-MS and ICP-OES determinations of K (%), U and Th (ppm) concentrations, cosmic dose contributions, effective beta and gamma dose rates (wet) following water correction, burial doses, total effective environmental dose rates and corresponding depositional ages of three sediment samples from the 'harbour'.*

Because of the evidence for hiatuses (Table 16; Figure 28), these OSL ages do not describe conformable sediment accumulation. No estimates of rates of sedimentation or ages interpolated between OSL ages can be made. The two lowest dated samples are later prehistoric in age. They have the sedimentological characteristics of the NCT fill (Table 15) and are likely to be naturally accumulating sediments. They cannot, however, be assumed to represent the typical sandflat or salt marsh environments of the NCT fill because the samples plot on Figure 29, the RSL curve developed for the lower Nith valley (Smith *et al* 2003a), between 3.5 and 3m below the RSL for these times. Although Figure 29 has only one $^{14}$C dating control after 6500 BP, the gradual fall in RSL is replicated in other RSL curves and models of glacio-isostatic uplift through time for this region (Shennan *et al* 2018). An explanation for this may lie in the location of the 'harbour' being in a tidal creek (Figure 25). Tidal creeks do not grade to MHWS: they probably grade to something like mean tidal level. Assuming the present tidal range in the inner Solway Firth to apply in prehistory, mean tidal level was and is around 4m lower than MHWS.

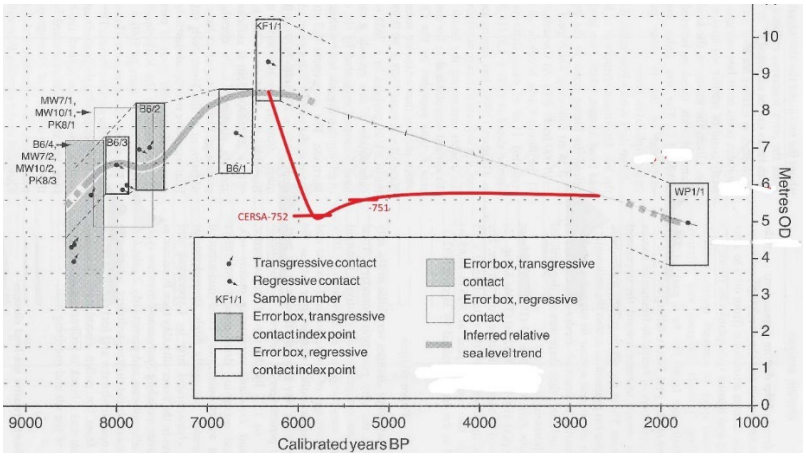


*Figure 29 [draft]. Age (BP) - altitude curve of Holocene RSL change in the lower Nith valley (modified from Smith* et al *2003a; Figure 16) with the altitudes and age-ranges of OSL ages CERSA-752 and -751 and apparent change in RSL at these times shown in red.*

#### 4.2.1.4. Environmental change recorded in 'harbour' sediments

1. Bedrock at the base of the vibrocores is at 323cm depth (around 4.3m OD). Elsewhere in the 'harbour', bedrock is at a similar depth (*c*. 3m; 4.5m OD). The bedrock surface was effectively a level rock platform.

2. The NCT fill started to cover this platform when RSL rose higher than 4.5m OD, at *c*. 6500 BC (Figure 29). Zone A (323-301cm depth: Figure 26) records sediment that rapidly accumulated to 4.5m OD, probably because RSL was also rising. The tidal creek need not have existed: sediment was probably deposited on a salt marsh surface. RSL rose above 4.3m OD about 7000 BC (9000 BP), not dated in the lower Nith valley (Figure 29) but in the Cree valley to the west and equidistant from the centre of glacio-isostatic uplift (Smith *et al* 2003b). RSL rose very rapidly for a time after 7000 BC (Lawrence *et al* 2016).

3. Above 301cm depth to 215cm depth (5.35m OD) in Zone B, higher OSL net signal intensities suggest deposition of consistently partially bleached sediment, with no trend, perhaps because sediment was re-deposited rapidly from a single eroding sediment source. The sediment is a uniform very fine sand, corresponding to the NCT fill, suggesting that the NCT fill was being eroded and re-deposited. Stable IRSL:OSL ratios indicate no mineralogical change in the sediment. Depletion ratios suggest that sediment was uniformly weathered. Sediment at 215.5cm depth is dated to 4180-3760 BC (CERSA-752: Table 17; 6200-5780 BP).

4. Because the catchment of the Old Castle Burn is entirely within the NCT fill, the tidal creek need not have existed until RSL stabilised at around 4500 BC and began to fall (Figure 29). The tidal creek was initially small with virtually no gradient.

5. As RSL fell after *c*. 4300 BC, the tidal creek began to incise into the NCT fill. Because the NCT fill is a cohesive sediment and because tidal creeks are scoured by wave action on the flood tide, the tidal creek was probably narrow and deep. By 4180-3760 BC (CERSA-752) the creek was some 3m below the surface of the NCT fill (Figure 29), deeper than the contemporary salt marsh: tidal creeks do not grade to HWMS but to lower parts of the tidal cycle.

6. Between 215 and 186cm depth, in Zone C (Figure 28: 5.35 to 5.64m OD), after 4180-3760 BC, the sediment is a uniform very fine sand, corresponding to the NCT fill (Figure 27). Sedimentation in the tidal creek was from luminescence profiling (Figure 28) largely conformable, with declining OSL net signal intensities and apparent doses up-profile, with no change in depletion ratios, but a trend above 200cm depth (5.50m OD) to higher IRSL:OSL ratios which suggests an increasing proportion of feldspar in the sediment. Hiatuses are apparent at the base of the zone and at 200cm depth, and others may exist unseen because only four samples span the long duration represented.

7. Zone D (186-170cm depth: *c*. 5.7m OD) also has few samples. The sediment is a uniform very fine sand, corresponding to the NCT fill, which was the source of re-deposited sediment. Sediment at 173.0cm depth is dated to 3630-3210 BC (CERSA 751: Table 17). Around 550 years is covered by 13cm of sediment, indicating that hiatuses were of substantial duration, but particle size distributions, though few, do not change (Figure 27). Assuming that sedimentation was continuous and uniform at 13 years/cm in the 550 years between *c*. 3970 and *c*. 3420 BC, and extrapolating this rate forward, the surface of the tidal creek would have risen to around 9m OD by AD1250. The tidal creek would have filled to the altitude of the NCT surface. But there were hiatuses. They may have removed substantial thicknesses of sediment from the 'harbour' and yet left no sediment.

8. Above another hiatus at the base of Zone D, OSL net signal intensities suggest that sediment above 179.5cm depth was only partially bleached. The trend in Zone C to increasing proportions of feldspar peaks in Zone D. The preservation of rapidly weathered feldspar in sediment affected by hiatuses implies that the hiatuses were erosional, removing sediment, and not non-depositional, as exposure would have led to weathering of feldspars. Depletion ratios in this zone are slightly higher, suggesting that re-deposited sediment was better-bleached. The upper zone boundary at 170cm depth coincides with the marked change from compact to overlying highly compressible sediment (Section 4.2.1.1; Table 15). This boundary is almost certainly a hiatus.

9. In and after 3630-3210 BC is a period (Zone E: 170-155cm depth) when OSL net signal intensities increase in a band of partially or fully unbleached, more weathered sediment was eroded from elsewhere, almost certainly from the sea, possibly from different sources since IRSL:OSL ratios are erratic, to be re-deposited in the tidal creek. The particle size distribution of sediments do not change significantly, however, only proportions of coarse silt increasing (Figure 27). There is a mean 4600-year difference in age between sediments at 173.0cm depth (3630-3210 BC: CERSA 751) and 152.5cm depth (AD1200-1300: CERSA 750) such that the partial bleaching of sediment must conceal very large hiatuses. During this long period, RSL fell from around 9m OD to 4.6-5m OD (Figure 29). Smith *et al* (2003a) estimated that MHWS throughout the historic period (after AD 120-440) has been unchanged at 4.6-5m OD. Some hiatuses hidden in zone E thus broadly coincide with the period when RSL fell below the altitude of the sediment surface in the tidal creek (Figure 29) so that one explanation for them is through tidal scour. Younger hiatuses in Zone E may be from storm surges that formed after *c*. 170 BC including the major barrier-breaching event that impacted the coast just west of the 'harbour' (above). There is no coarse sediment in Zone E, however, only hiatuses in sedimentation that were probably erosional.

10. There was then a period (Zone F: 155-121cm depth: *c*. 6 to 6.3m OD) when conformable sediment deposition took place. A close sampling interval shows a strongly linear trend in OSL net signal intensities not demonstrably interrupted by hiatuses and with no evidence for sediment reworking (Figure 28). IRSL:OSL ratios fluctuate wildly, with a general trend up-profile to higher ratios and higher amounts of feldspar, despite depletion ratios suggesting that sediment was more weathered above 143cm depth (*c*. 6m OD). OSL age estimate CERSA-750 dates sediment just after the beginning of Zone F at 152cm depth (*c*. 6m OD) to AD1200-1300 (Table 17: 820-720 BP). Zone F includes the time when the Old Castle and its moat system were built (below): the age of sediment at the upper zone boundary at 121cm depth cannot be interpolated between the 13th century and the present day (a) because the sediment accumulation rate changed in overlying Zone G and (b) the ground surface in the 'harbour' is not currently being formed by sedimentation. Proportions of fine and medium sand increased above *c*. 147cm and below *c*. 72cm depth (Figure 27). By AD1200-1300 the sediment in the 'harbour' was around 1-1.5m higher than contemporary HWMS, so that coastal sediment may have been deposited only rarely. There is no sedimentological evidence (Table 15) for the sediment accumulating then to be at all impacted by coarser grain sizes or disturbance associated with storm surge events.

11. Above 121cm depth (6.3m OD) pOSL characteristics change (121-20cm depth: Zone G: Figure 28). The lower zone boundary is undated. OSL net signal intensities suggest that sediment accumulated conformably and rapidly, undisturbed by hiatuses, very probably waterlain. The silt-sized fraction dominates (Figure 27). The sediment source must have been inland, in fresh water. Why deposition accelerated is unknown. It is tempting to suggest that this reflected the abandonment of water-control structures like sluices that formerly ponded water in the moat system.

Water depth cannot be estimated. IRSL:OSL ratios suggest that proportions of feldspar in the sediment generally fall over time, indicating that weathering was increasingly effective. The very low IRSL:OSL ratios above 42cm depth are probably derived from weathering during pedogenesis (soil formation) on a dry 'harbour' floor. Depletion ratios (Figure 28) are very erratic, unlike any earlier sediment, though they are centred around the mean value of these sediments. The initially very low depletion ratio does not distort OSL net signal intensities, hard to explain if low depletion ratios relate to the relative ineffectiveness of bleaching of luminescent grains by sunlight (Munyikwa *et al* 2021). The very high depletion ratio at 73.5cm depth may indicate a degree of bleaching far more thorough than at any other time, and this, like the declining IRSL:OSL ratios, might suggest that sediment was fully exposed on a dry 'harbour' floor. Geochemical data on the degree of pedogenesis would help here, but the interpretation is that sediment in Zone G was increasingly affected by complete bleaching despite its rapid accumulation, possibly through there being many short, possibly seasonal hiatuses in deposition. Immediately to the south (Figure 26a), the uppermost 0.25-0.5m of sediment has been scoured out. The Old Castle Burn was probably a more active agent in sediment formation. Above 42cm depth (7.1m OD) the sediment in the borehole became more of a soil, probably as the Old Castle Burn was confined to the incised channel it now occupies, incision being a consequence of the burn cutting deeper as it left the 'harbour'. The 'harbour' was almost certainly part of the land by Roy's Military Survey of *c*. 1750 and certainly was by 1775-6 (Figure 4).

**4.2.2. The connection between the 'harbour' and the moat system**

The present ground surface of the 'harbour' at its northern end where it is not eroded is around 7.5m OD. OSL assay CERSA 750 (above) indicates that the ground surface in the 'harbour' contemporary with the Old Castle was around 6m OD. The floor of the southern moat in its south east corner (borehole 66: below) is around 6.24m OD. With more than 0.24m water depth, the 'harbour' could supply water to the moat, but the sedimentological evidence in the 'harbour' suggests the 'harbour' may not have contained water. The next sections discuss the sediment fills in the moat around the Old Castle and the outer ditch and show that to cover the western moat and the outer ditch with water required the water surface to exceed 8m OD. To maintain water above this would have required a dam or sluice at the lowest, south east corner of the moat (RCAHMS 1920), at least to 8m OD, between the north bank of the 'harbour', which rises to 9m OD and the surface of the NCT fill at around 9.5m OD to the east. There is no archaeological evidence for such a structure, and one is not depicted in the reconstruction drawing of the Old Castle (Brann 2004, Figure 13.2).

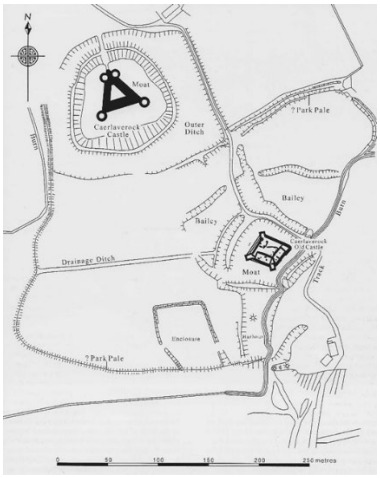


*Figure 30. Surveyed earthworks (fig. 1.2 of Brann 2004).*

### 4.2.3. Sediments in the dry valley and the southern moat

North of the 'harbour' is the southern side of the moat system (Figure 25). The southern moat is trumpet-shaped, narrowing between the southern bank and the castle platform eastward from around 24m to around 11m. At its western end, the southern moat is not embanked. It is open, leading to a to a natural 0.5m deep, 5m wide peat-filled channel, its surface rising north of borehole 23 for 40m to 8.6m OD where it merges with the surface of the NCT surface. It is called the dry valley because it carries no stream at the present day, though its floor is flooded in the winter. The southern moat is also connected to the outer ditch (Figure 25) *via* this channel. Figure 31 shows the sediment stratigraphies on a 75m long transect along the thalweg of the dry valley and southern side of the southern moat (Figure 25).

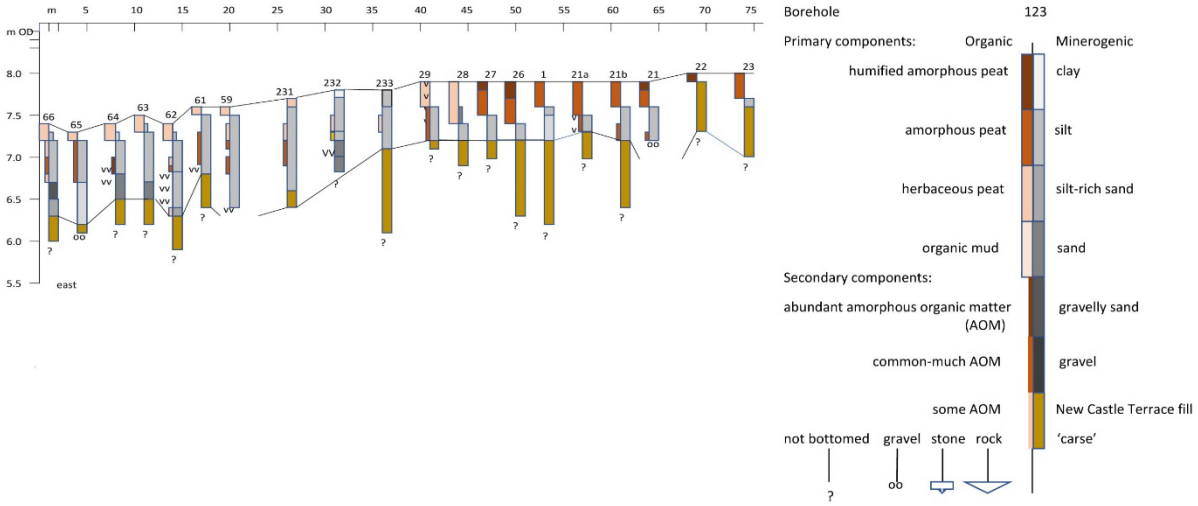


*Figure 31. Sediment stratigraphies along the thalweg of the dry valley (boreholes west of 40m distance) and the southern side of the southern moat (east of 25m distance).*

Boreholes 59-66 are at the east end of the southern moat. Borehole 66 is where the southern and eastern moats merge and the Old Castle Burn leads to the 'harbour'. The valley here is incised to 6.2m OD. Sediment overlying the NCT fill in boreholes 63 to 66 is a poorly sorted coarse sand with grit or gravel, impenetrable at 6.2m OD in borehole 65. This is sometimes bedded, though with some amorphous organic matter and wood fragments. Because the dry valley lies entirely within the NCT fill, and the NCT fill rarely contains sediment coarser than fine sand (Jardine 1980), the source of coarse sand and gravel is thought to lie on the coast, in the barrier beaches (above: Section 4.1.8). Diatom analyses have not been undertaken to confirm this. The coarse sand rises to around 6.7m OD in boreholes 63 to 66. The sediment then consistently fines up-profile, signalling either a change in sediment source or declining depositional energies, and it becomes increasingly organic, becoming an herbaceous peat at the surface, around 7.5m OD. In the west, the base of the dry valley lies on the NCT fill, incised a metre below the surrounding NCT surface. Borehole 21 bottomed on impenetrable gravel. The thin overlying silt is derived from the NCT fill. Rare brick-red concretions (building rubble?) and charcoal flecks suggest it accumulated with human activities close by, as does charred roundwood in borehole 232.

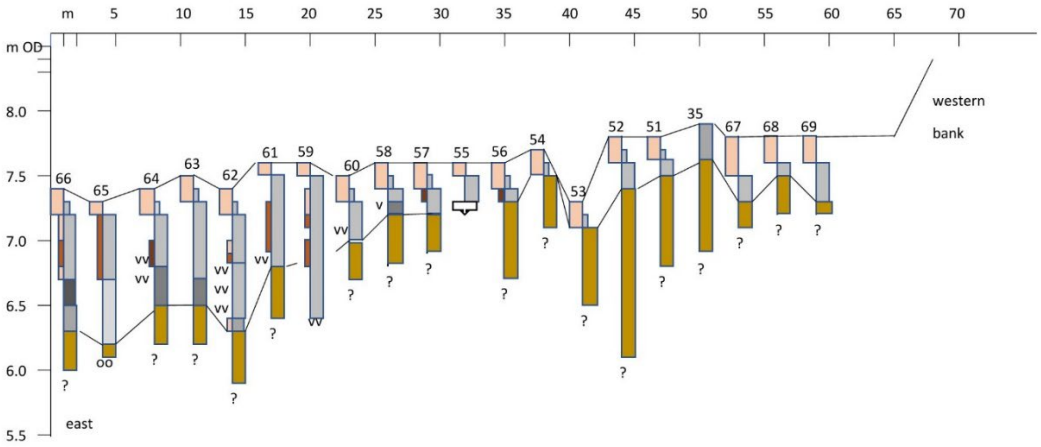


*Figure 32. Sediment stratigraphies along the axis of the southern moat. See Figure 31 for the key.*

Figure 32 shows the sediment stratigraphies recorded along the axis of the southern moat, parallel to and around 3m away from the line of the castle platform (Figure 25). Boreholes east of 22m distance are in the dry valley (Figure 31). In the west the transect ends 7m short of the bank separating the moat from the outer ditch, its crest at 10m OD. The castle platform is also at 10m OD.

The altitude of the NCT surface rises from 6.25m OD in borehole 62 to 7.25m OD by borehole 58. This is because on the northern side of the southern moat, nearest the Old Castle, the transect rises up the left (north) bank of the dry valley. Several points arise from this observation: (a) the builders of the moat system utilised the pre-existing, now dry, valley as part of the moat; (b) this and the Old Castle Burn, canalised within the eastern moat (Figure 25), both provided sources of water to the moat; (c) the southern moat is open in the west to incorporate the dry valley; (d) the southern and eastern moats meet where the natural watercourses met; (e) the east side of the castle platform was made to be parallel to the canalised Old Castle Burn, but this meant that the dry valley deviated from the square: this is why the west end of the southern moat is trumpet shaped; (f) it would have been very simple to steer the stream in the dry valley into a neater, square moat system but this was not done. In addition, there was no attempt to excavate the southern moat to the depth that the dry valley was. For water to have permanently covered the base of the southern moat, its surface would need to be higher than 7.9m OD, the base of the ditch at borehole 35 (Figure 32).

### 4.2.4. Sediments in the eastern moat

Five boreholes were sunk along the 40m length of this limb in 2004 (Tipping *et al* 2004; Figure 11.5). Towards the 'harbour', boreholes recorded medium sand to around 6.3m OD beneath 90cm of finer minerogenic sediments. The origin of this is probably coastal because the catchment of the Old Castle Burn is entirely within the NCT fill. Layers of gravel were recorded in finer sediment at around 7.0 and 7.15m OD in two boreholes. No borehole recorded peat except at the surface, where it was highly minerogenic. The surface of the fill is around 7.5m OD. The Old Castle Burn is incised some 50cm below this. The eastern moat was not examined in this re-analysis.

### 4.2.5. Sediments in the northern moat

The northern side of the moat system was not examined in this study. Seven Eijelkamp boreholes were made along its 30m length in 2004 (Tipping *et al* 2004; Figure 11.5). These recorded an 80cm thick sediment fill above the NCT fill, to a base at around 6.8m OD, slightly deeper in the east and higher (65cm) in the west. Ten or so centimetres of minerogenic sediment with much amorphous

organic matter and well preserved Cyperaceae leaves overlie the NCT fill in the east, succeeded everywhere by up to 60cm of peat. This becomes more minerogenic, with silt and very fine sand above 40cm depth. This sediment was probably derived from the NCT fill forming the sides and floor of the moat system.

Near the Old Castle Burn, at borehole 1 (Tipping *et al* 2004; Figure 11.5) with a sediment surface at 7.55m OD, sediment cores were obtained. Organic contents exceed 60% in the peat. Two AMS $^{14}$C assays on 1.0cm thick bulk peat samples (i.e. no organic fraction preferred) were obtained (Tipping *et al* 2004; table 10.1). At 82.0cm depth (6.7m OD), assay Beta-150692 gave an age for the basal peat of 850± 40 $^{14}$C BP, calibrated in 2021 to AD1050-1280. The age-range of the basal peat includes the felling date of the dendrochronologically dated oak timber in the western moat at AD1229-30 (below: Section 4.2.6). At 66.0cm depth (6.9m OD), where organic content falls below 25%, assay Beta-150693 gave an age of 660± 40 $^{14}$C BP, calibrated as with assay -150692 to AD 1270-1400. Spheroidal carbonaceous particles recorded above 13cm depth, generated by industrial coal burning since the mid-19th century (Rose *et al* 1995), indicate sediment accumulated close to the present.

Davies (2004, 107-110) recorded abundant *Lemna* (duckweed) spores in the moat, abundant only in the early years or decades of sediment infilling. They imply shallow water, warmed in the summer. Microscopic charcoal fragments were only abundant in these years or decades. Pollen and microfossil analyses indicate stagnant water. Sediment became more organic (60% organic content) after c. AD1300 as the moat was infilled with peat-forming plants like *Typha* (bulrushes) and Cyperaceae (sedges). The surrounding NCT surface was initially dominated by damp *Alnus* (alder) and *Salix* (willow) woodland with only limited evidence for anthropogenic disturbance. Proportions of alder were reduced after *c*. AD1300, possibly through purposeful clearance, but this did not create open ground. Trees like *Quercus* (oak) and *Fraxinus* (ash) replaced alder and willow in what may have a managed woodland. There is little evidence for open ground at any time. Around AD 1270-1400 (interpolated at *c*. AD1370) the organic mud received fine-grained mineral sediment, probably from the sides of the moat. This continued to suppress organic content to within 30cm of the ground surface.

### 4.2.6. Sediments in the western moat

#### Description and previous work

The western moat is around 70m long from the base of the southern bank in the dry valley to the northern moat bank (Figure 25). Its southern end is open to the southern moat and the dry valley. Its northern end is closed in a steep slope up to a track at 9.8m OD. The sediment surface is an average 7.9m OD, around 2m below the surface of the castle platform and the bank separating the western moat from the outer ditch. The moat is 10m wide and flat-bottomed, its floor of "blue-grey clay" (Brann 2004, 19) being truncated NCT fill some 40-60cm below the ground surface. RCAHMS archaeologists in 1978 and Brann in 2004 (pp. 18-19) excavated the western moat. Brann (figure 3.6) depicts his trench halfway (13-16m distance) along the 28m length of the castle platform. He found a horizontal oak timber lying on the NCT fill, part of the support structure for a bridge across the moat (Brann 2004, figure 3.4). He noted (2004, 19) its upper surface had rotted, suggesting that the moat sometimes dried out. Medieval potsherds were also recovered from the surface of the NCT fill. "Demolition rubble" was found in the silt that overlay the NCT fill with a thickness of 20-30cm.

Brann (2004) assumed the photographed timber was that which yielded a dendrochronological date of "*c* AD1229" (p. 18). He gave no more information, and there is no information in his reference to Baillie (1977). Mills (unpublished) identified that four timbers were sampled from the Old Castle and

reported for sample Q4348 a felling date in the winter of AD1229-1230, and for Q4345 a best estimate felling date of AD1225±9 years. The date of AD1229-30 is used here.

**Sediment stratigraphy**

Figure 33 shows the sediment stratigraphies of boreholes cored in 2021 and 2022 along the centre of the western moat. Boreholes 28 and 29 are in the dry valley (Figure 31); borehole 35 is also on the centre line of the southern moat (Figure 32). North of borehole 45 is upcast from Brann's excavation of the bridge. The transect was completed in 2022.

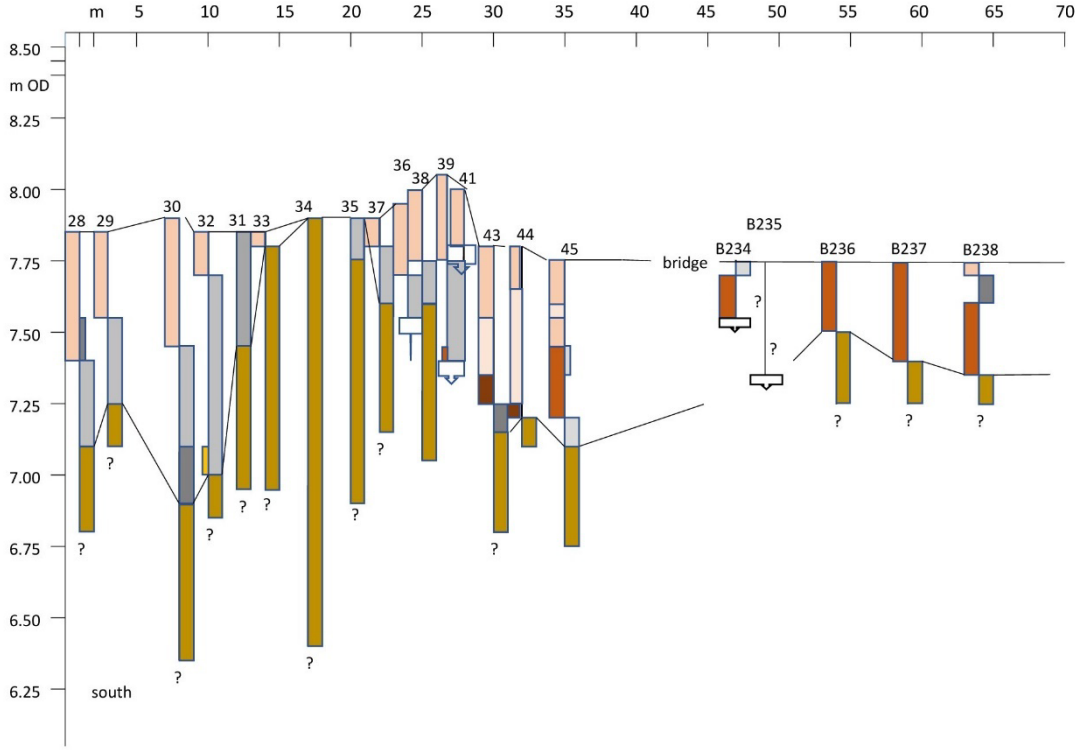


*Figure 33. Sediment stratigraphies along the axis of the western moat. See Figure 31 for the key.*

The surface of the NCT fill (e.g., the floor of the moat) is not at a uniform altitude. It is below 7.25m OD in the dry valley (boreholes 28–30), rising north of borehole 32 to form the ground surface in borehole 34 at 7.89m OD, then deepening to below 7.25m OD. North of the modern bridge the moat is much shallower with the NCT fill higher than 7.25m OD. South of borehole 34 this variation probably reflects the natural topography of the dry valley, before the castle was built. The ridge of NCT fill between boreholes 31 and 35 is interpreted as the left (north) bank of the dry valley, seemingly left as it was when the western moat was dug north of it. Figure 32 shows that this ridge extended north and south of borehole 35, between boreholes 56 and 68, to block the western moat. The NCT fill is progressively deeper north of borehole 35, to around 7.25m OD, and Brann (2004) recorded it to 6.9-7.0m OD at the bridge.

There is no source of water to the western moat other than from the dry valley to its south. To cover the floor of the western moat north of the ridge, the water surface would need to be a minimal 7.9m OD.

Closely spaced boreholes 36-41 (borehole 40 is not depicted in Figure 33 for clarity) at the western corner of the castle platform bottomed on stone at varying depths. Boreholes over a 5x5m grid with a spacing around 1m in this part of the moat also recorded stone, part of a sub-structure in the moat

to the castle platform. The relation of this to the splayed stonework bases on the castle platform (RCAHMS 1920, 11) is unknown. The stonework was mostly overlain by thick silt, that Brann (2004) also described at the bridge, although in borehole 41 herbaceous peat lay directly on stone. Stonework was also struck in boreholes 234 and 235 immediately north of the bridge.

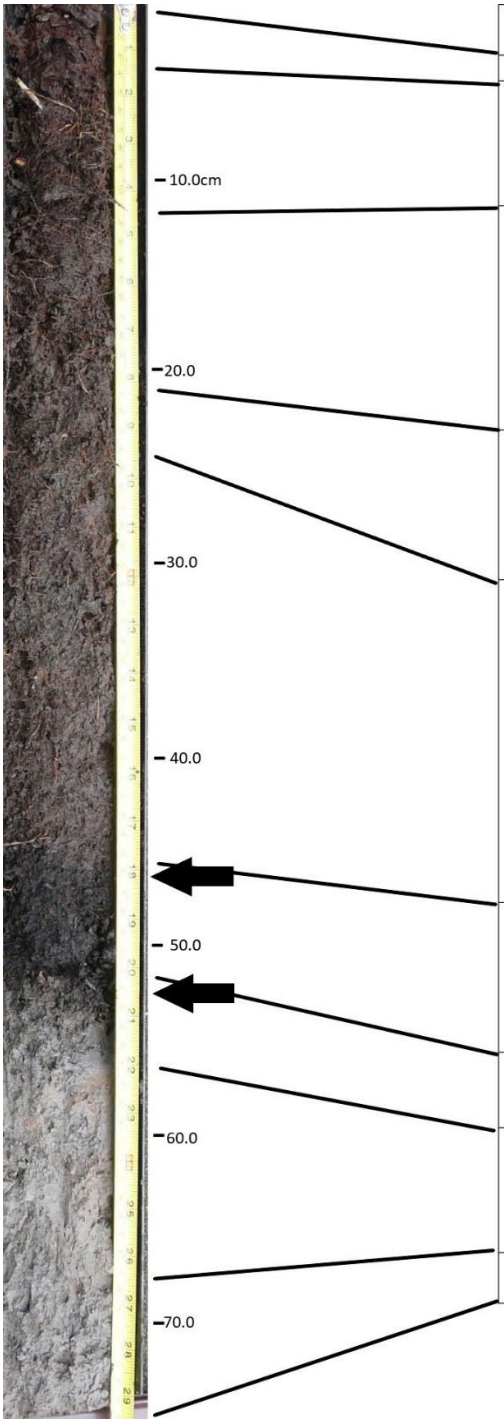


| Bed | Depth cm | Description |
|---|---|---|
| 10 | 0-3 | Leaf litter; gradual to |
| 9 | 3-12 | 7.5YR3/2 dark brown herb peat with abundant horizontal matted fine fibrous stems and rare coarse fleshy stems; gradual to |
| 8 | 12-21 | 7.5YR4/2 dark brown-brown herb peat with common horizontal matted fine fibrous stems in a matrix of amorphous organic matter with little mineral matter and a 10mm diam. subangular quartz/quartzite pebble at 19.5cm; gradual to |
| 7 | 21-25 | 7.5YR4/2 dark brown-brown herb peat with common horizontal matted fine fibrous stems in a matrix of amorphous organic matter with common mineral matter; gradual to |
| 6 | 25-45 | 5YR4/2 dark reddish grey amorphous peat/organic mud with few small horizontal and vertical fine fibrous stems, rare large wood fragments 45cm, rare to few sand grains below 32cm, common very coarse grit 39.25 to 42.5cm, an 8mm rounded rotted Locharbriggs Sst pebble 31-32cm and an 8mm diam. subangular quartz/quartzite pebble at 43cm; gradual to |
| 5 | 45-51/55 | 5YR2.5/1 black amorphous peat with common <2mm diameter roundwood (twigs) at 48cm and below 50cm and rare wood fragments; sharp sloping boundary to |
| 3 | 51/55-56 | 5YR5/1 grey structureless clay with silt, with rare-few vertical fine fibrous stems; sharp to |
| 2 | 56-67 | 5YR7.5/1 light grey structureless fine sand with silt, with common 7.5YR6/4 light brown mottling 57-59cm; gradual to |
| 1 | 67-74 | 5YR5/2 grey structureless silt with clay. |

Borehole 43 (Core 1)

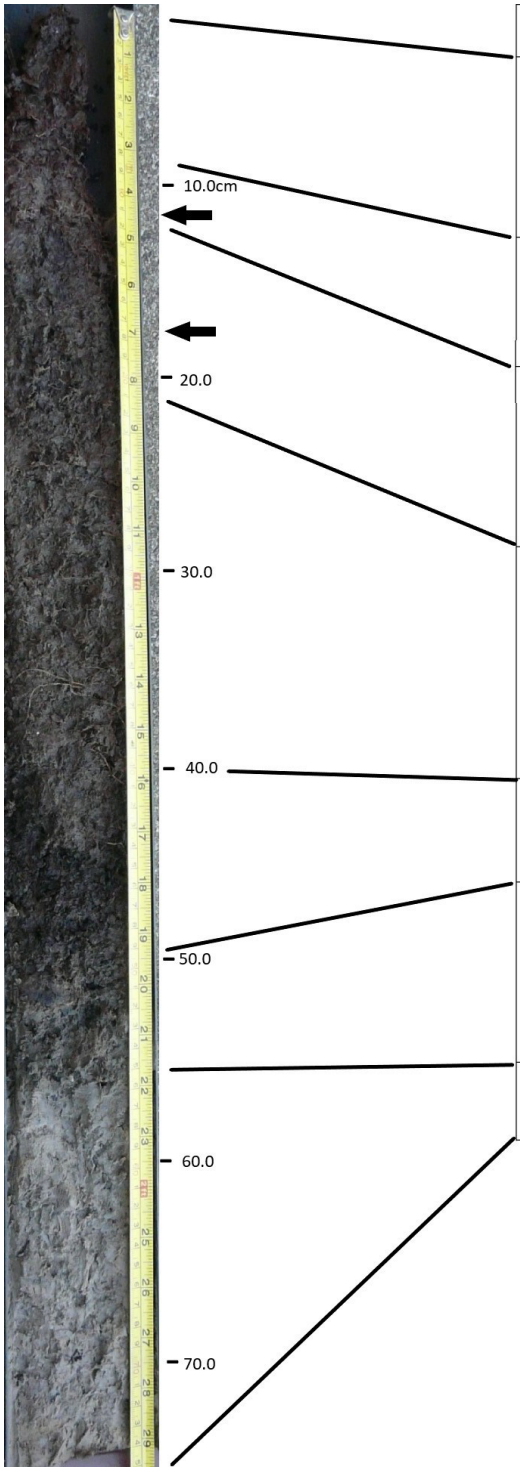


| Bed | Depth cm | Description |
|---|---|---|
| 9 | 0-9 | 10YR3/2 very dark greyish brown herb peat with abundant matted horizontal and vertical fine fibrous stems and common coarse fleshy stems and common leaf fragments; gradual to |
| 8 | 9-12 | 7.5YR4/2 brown-dark brown herb peat with abundant matted horizontal fine fibrous stems and rare mineral matter; sharp to |
| 7 | 12-21 | 5YR3/2 dark reddish brown herb peat with common matted horizontal fine fibrous stems, common amorphous organic matter and one 3mm diameter roundwood 17.5-19.0cm depth; gradual to |
| 6 | 21-40/45 | 5YR4/2 dark reddish grey amorphous peat/organic mud with few matted horizontal fine fibrous stems, rare small wood fragments and very rare small (<1mm diameter) roundwood (twigs) 26-27cm depth; boundary sharp sloping and curved across the core to |
| 5 | 40/45-49.5 | 5YR5/1 black amorphous peat with common-many small wood fragments and small roundwood (twigs); sharp to |
| 4 | 49.5-55 | 5YR4/2 dark reddish grey structureless silt with common very coarse sand and rare small charcoal fragments and one 20mm square wood fragment 50.0-51.5cm depth; sharp to |
| 2 | 55-74 | 5YR6/1 light grey-grey structureless silt with fine sand. |

Borehole 43 (Core 2)

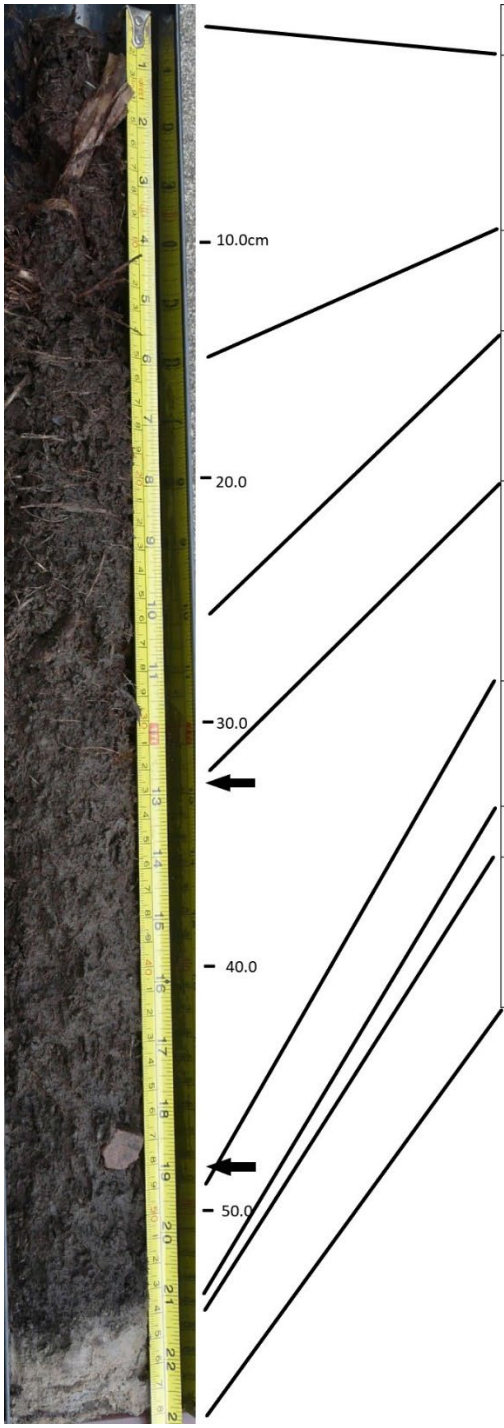


| Bed | Depth cm | Description |
|---|---|---|
| 9 | 0-15 | 5YR3/2 dark reddish brown herb peat with common matted horizontal and vertical fine fibrous stems and common horizontal and vertical coarse fleshy stems and rare leaf fragments; gradual to |
| 8 | 15-26 | 5YR3/2 dark reddish brown amorphous peat/organic mud with common horizontal fine fibrous stems; gradual to |
| 7 | 26-32 | 5YR4/2 dark reddish grey structureless organic mud with some horizontal fine fibrous stems and one 3mm square subrounded Locharbriggs Sst pebble 26-28cm; gradual to |
| 6 | 32-49 | 5YR4/2 dark reddish grey structureless organic mud with very rare vertical fine fibrous stems, common mica flakes, rare sand below 48cm and one 15mm square subrounded Locharbriggs Sst 46-48cm; gradual to |
| 5 | 49-53.5 | 5YR2.5/1 black amorphous peat with rare very fine fibrous stems, common silt and mica flakes; sharp horizontal irregular boundary to |
| 4 | 53.5-54 | 5YR5/2 reddish grey silt; sharp horizontal boundary to |
| 2 | 54-58 | 10YR6/4 light yellowish brown bedded fine-medium sand, coarsening down-unit, with one sub-horizontal band of amorphous organic matter 57-57.7cm. |

Borehole 44

*Figure 34. Photographs of prepared surfaces of 1.0m long, 6.0cm wide Russian cores at borehole 43 (cores 1 and 2) and borehole 44, with their sediment descriptions and positions of $^{14}C$ samples.*

Boreholes 43-45 (Figure 33) are stratigraphically the most complex, particularly at the base of the moat fill. Figure 34 shows prepared surfaces of three sediment cores taken with a 1.0m long Russian corer: cores 1 and 2 are within 0.5m of each other at borehole 43; that at B44 is 1m to the north. The ground surface (0m depth) is 7.80m OD at both boreholes. Beds 1-10 are seen to varying extents. Beds 1 to 3 represent the NCT fill beneath the moat: Bed 3 is affected by rootlet penetration from above. Bed 4 is seen in boreholes 43 (core 2) and 44. This is the basal sediment of the moat fill. It is minerogenic, a poorly sorted silt-rich sand. It is <5mm thick at borehole 44 where the sharp

irregular upper boundary suggests the bed may have been eroded: this may be why it is absent at borehole 43 (core 1).

Bed 5 is a distinctive black, highly humified amorphous peat. It was also recorded in the Eijelkamp gouge at boreholes 43 and 44 (Figure 33) but nowhere else on this transect. Its colour and humification suggest it to have been exposed to air before being sealed by Bed 6. It has many small wood macro-remains, both roundwood and fragments, unlike overlying sediment. This may reflect human activities around the moat. It has a conformable, gradual boundary to Bed 6 in borehole 43 (core 1) and borehole 44 but in borehole 43 (core 2) the upper boundary is erosional, probably a cut feature, indicative here of a hiatus between Beds 5 and 6.

Bed 6 records the appearance of minerogenic sediment within the peat, including occasional pebbles. Pebbles, including Galloway Granitic Suite stones, were also recorded in borehole 42. In borehole 40 the matrix is a 24cm thick structureless silt, overlying stonework. South of this, silt thins over the ridge of NCT fill before thickening in the southern moat and dry valley. East of borehole 41, silt is increasingly associated with amorphous organic mud, and peat at borehole 45. Silt was not found north of the bridge, although Tipping *et al* (2004; Figure 11.5) recorded gravel in one borehole north of the bridge. Silt deposition continued in Bed 7, with rare pebbles but was diminished in Bed 8 and above. Coarse herb peat caps most boreholes to the ground surface.

**AMS $^{14}$C dating**

Table 18 presents details of AMS $^{14}$C assays obtained for the western moat at borehole 43. All three cores were sampled because short-lived single entities, which are rare and increasingly so above the base of the fill were preferred for dating to peat (Ashmore 1999). Three assays are on the humic acid fraction of organic mud/peat. Although assay SUERC-101769 is deeper than assay SUERC-101768 it is stratigraphically higher.

| Borehole | Depth (cm) | Bed | Material | Description | Wt. (gms) | SUERC No. | $^{14}$C BP | $\delta^{13}$C (‰) | Cal BC/AD (95.4%) |
|---|---|---|---|---|---|---|---|---|---|
| 43 (2) | 11.5-12.0 | Base of 8 | herb peat | humic acid | 2.48 | 101775 | | -29.9 | modern |
| 43 (2) | 18.5-19.0 | in Bed 7 | wood (*Betula*) | one 3mm diam. short-lived horizontal twig | 0.25 | 101774 | 786 ±28 | -28.6 | AD1220-1278 |
| 43 (2) | 18.0-19.0 | Base of Bed 7 | herb peat | humic acid | *c.* 5 | 104410 | | -29.9 | modern |
| 43 (2) | 28.0-29.0 | In Bed 6 | organic mud | humic acid | *c.* 5 | 104409 | 224 ±26 | -30.2 | AD1640-1930 |
| 44 | 32.0-32.25 | In Bed 6 | organic mud | humic acid | 2.47 | 101773 | | -30.1 | modern |
| 44 | 48.0-48.75 | base of 6 | organic mud/ amorph peat | humic acid | 2.98 | 101769 | 664 ±28 | -30.9 | AD1279-1392 |
| 43 (1) | 45.75-46.25 | top of 5 | wood (*Alnus*) | one compressed horizontal fragment | 1.88 | 101768 | 692 ±28 | -28.4 | AD1272-1388 |

| | | | | | | | | | |
|---|---|---|---|---|---|---|---|---|---|
| 43 (1) | 52.0-53.0 | base of 5 | wood (*Alnus*) | one large compressed horizontal roundwood >10 and <50 years old | 1.68 | 101767 | 610 ±28 | -29.1 | AD1300-1403 |

*Table 18. Details of AMS $^{14}$C assays in boreholes 43 and 44 in the western moat, calibrated using Oxcal 4.4 (Bronk Ramsey 2009) with INTCAL20 (Reimer* et al *2020) and expressed at 95.4% probability*

The base of the western moat fill, the highly humified peat of Bed 5, is dated to AD1300-1403 (SUERC-101767). The top of Bed 5 is dated to AD1272-1388 (SUERC-101768) and the base of the overlying Bed 6 is dated by organic mud/peat to AD1279-1392 (SUERC-101769). These assays are indistinguishable, and from different materials are regarded as good estimates of the time that surviving peat began to accumulate in the western moat. Bed 5 is not significantly older than the overlying fill. Its humified state was through exposure to air, probably when the dendrochronologically dated timber became rotted (above), but this happened quite rapidly when, probably, the moat was not filled permanently with water. The re-cutting and truncation of Bed 5 also occurred before AD1279-1392. Together they indicate that peat accumulation was initially very rapid.

Above these assays there are severe interpretative problems. It has to be assumed that age-estimate SUERC-101773 is a product of contamination, though carefully sampled from a cleaned core (Figure 34b). Assay SUERC-104409 has an age range at 95.4% probability of AD1640-1930, influenced by the Suess effect: at 68.3% probability it has an interpretable range of AD1646-1799. A short-lived twig at 18.5-19cm depth has an age-range of AD1220-1278 (SUERC-101774: Table 2), older at 2σ than deeper $^{14}$C dates on cellulose. It cannot be used in chronology construction. It probably illustrates how assumptions of conformable deposition can be upset in an environment next to a range of intense human activities, and specifically suggests that twigs of an old tree fell into the western moat. The humic acid fraction of peat at 12cm depth has a modern age (SUERC-101775). It probably relates to very recent accelerated growth of peat. This phase may have begun above the sharp boundary at the base of Bed 8 at 12cm depth, peat with rare mineral matter.

Bayesian modelling with BACON software (Blauuw and Christen 2011) improves the temporal resolution of the $^{14}$C assays. Sediment at the base of the fill at 52.0cm depth has a modelled age of AD1287-1342. Sediment above this to 46.0cm depth has the same modelled age because the $^{14}$C assays are indistinguishable. Above these, the assays cannot be modelled. It is not possible to construct from these age estimates a chronology for the western moat independent to that for the outer ditch. The one internal test of this is encouraging: the age-estimate of assay SUERC-104409 at 68.3% probability (AD1646-1799) can be compared with the modelled age-range of sediment in the outer ditch at the same depth (29cm) of AD1633-1828. Sediment accumulation in the western moat is assumed to have been similar to that in the better understood outer ditch (Section 4.2.7). Ages quoted for sediment and diatom changes in the western moat are referred to as 'approx.'. Section 4.2.8 compares these assays with adjacent dated archaeological features.

**Quantitative sedimentological analyses**

Figure 35 presents data on the organic contents and particle size distributions <2.0mm (sand) of sediments in borehole 43 at contiguous 1.0cm increments. As a guide to interpretation, Tipping *et al* (2004, Figure 11.3) analysed the uppermost 7cm of NCT fill in the outer ditch, below 7.3m OD, and found it to have an organic content <5%, clay 15-20%, silts *c*. 60%, very fine and fine sand *c*. 20% with rare sand coarser than this.

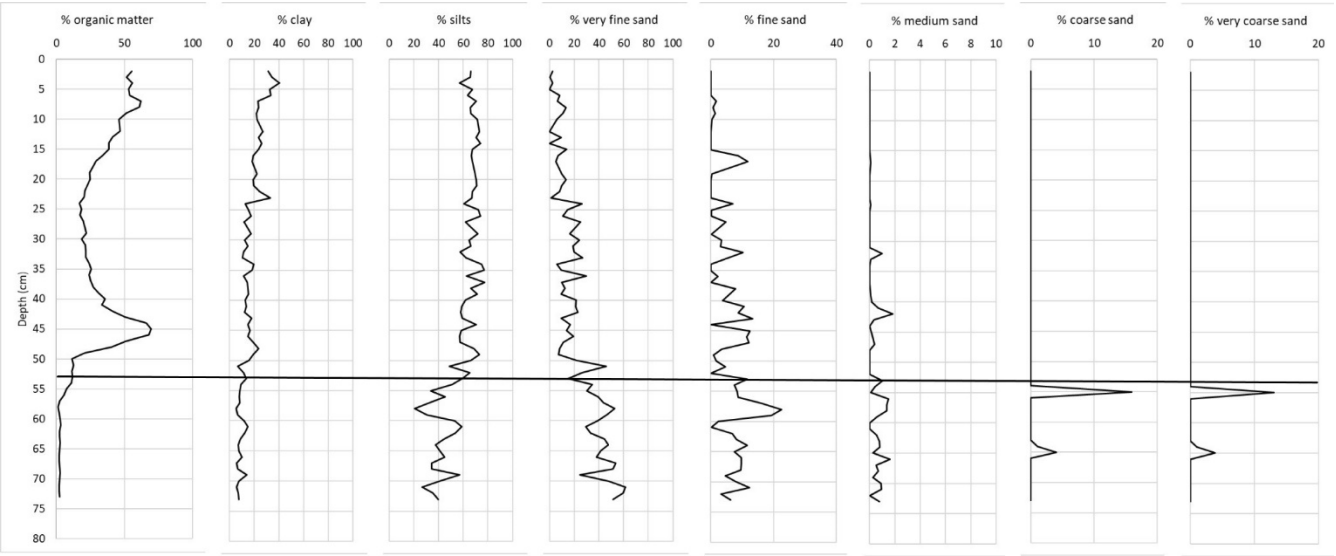


*Figure 35. Organic contents and particle size distributions of sediments in borehole 43 (core 1) at contiguous 1.0cm increments: note changes in horizontal scales.*

Sediments below the horizontal line at 53cm depth (7.27m OD) in Figure 35 are from Beds 1-3, from the NCT fill (Figure 34). They are very different to the NCT fill in the outer ditch recorded by Tipping *et al* (2004) with very fine and fine sand an average 53% and with two large peaks of much coarser sand at 65-64cm and 55m depth, the latter, though, a single sample. The differences suggest considerable variation in particle size distributions in the NCT fill over short distances.

Organic content increases gradually in the basal moat fill through increased aquatic biomass, algal, floral and faunal, to 70% at 45cm depth (7.35m OD) at AD AD1272-1388. It then falls to 33% in Bed 6 by 40cm depth (approx. AD1400). This is through deposition largely of silt in a low-energy depositional environment. The source of the silt may be from the moat sides and floor because minerogenic matter in Bed 6 is little different to the underlying NCT fill, but the Old Castle Burn and the dry valley drain only the NCT fill and would have been naturally turbid from re-deposited NCT fill, especially in winter months, so that a source allochthonous to the moat is also likely.

The proportion of organic matter gradually increased in Bed 7 (25-21cm depth: Figure 34) either because the supply of mineral sediment began to fall or aquatic biomass oce more increased, perhaps as water shallowed and warmed. Still-water depositional conditions above 24cm depth (7.56m OD; approx. AD1600) are implied by the settling out of more clay.

**Diatom analyses**

Thirty two sediment samples of 0.5cm thickness were removed at 1.5cm intervals from core borehole 43 (Core 1: Figure 34) from 4.25 to 58.5cm depth (Figure 36). The basal two samples are from Bed 2, the underlying 'natural' NCT fill. The uppermost 5 samples are from Bed 9, probably of modern age. Figure 36 is divided into five local diatom assemblage zones. Taxa are arranged left to right from marine to marine-brackish to fresh-brackish to fresh. Full ecological interpretations are awaited: here only broad changes in salinity are defined.

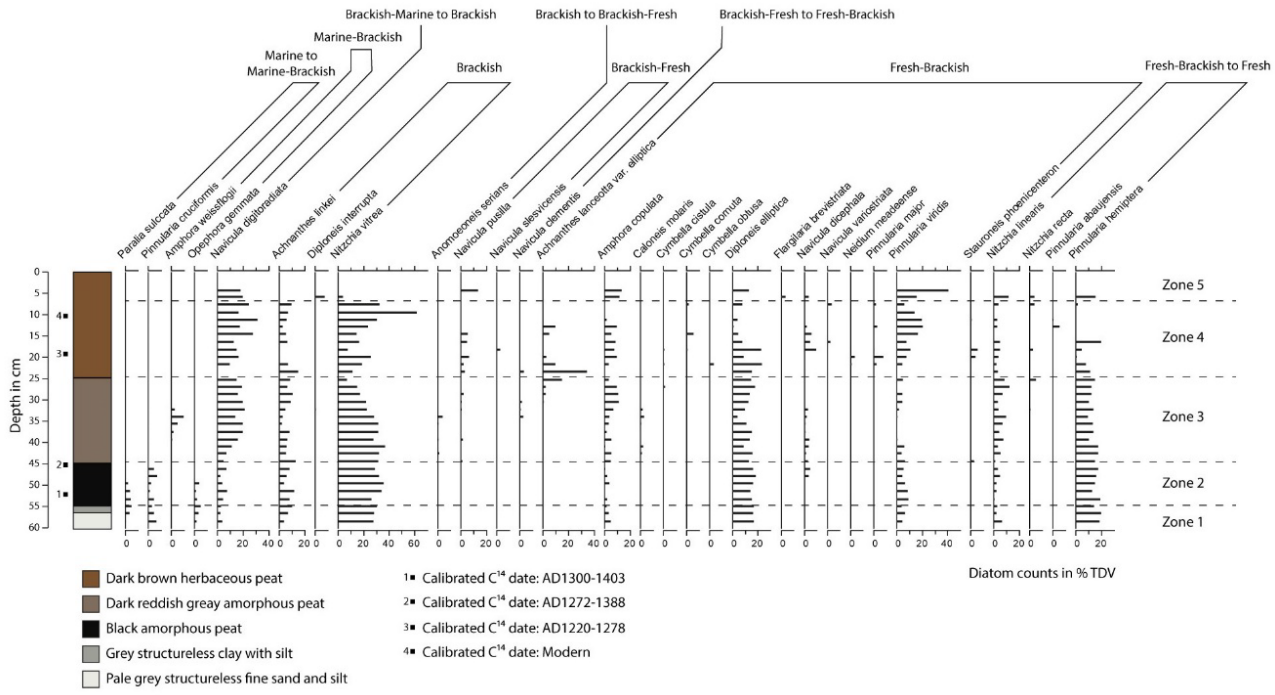


*Figure 36. Diatom analyses from sediments in borehole 43 (core 1) in the western moat. TDV = total diatom valves.*

A range of salinities from brackish-marine to fresh-brackish are represented throughout. Water in the moat was fresh, from the Old Castle Burn and the dry valley. But there were periods when taxa tolerant of much highe salinities were present. Marine to marine-brackish taxa, *Paralia sulcata* and *Pinnularia cruciformis*, and the marine-brackish *Opephora gemmata*, are confined to Zones 1 and 2 (58.5 to 45.25cm depth; 7.2 to 7.35m OD). Because all three are found in Bed 2 (56-67cm depth), the NCT fill, their occurrence in the basal peat of Bed 5 (45-53cm depth) may be through re-deposition of the NCT fill in the moat sides. This is true also for all taxa that are represented in both Zones 1 and 2. This may be too conservative an interpretation, however, because fresh-brackish taxa cannot have been reworked from the NCT fill and must represent diatom assemblages contemporary with moat sediments. In addition, Borehole 43 is some 5m away from the moat sides and Bed 5 has in part a high organic content, suggesting little erosion of the moat sides then (Figure 35). If contemporary with formation of Bed 5, the marine to marine-brackish taxa taxa represent an incursion of marine-estuarine water.

The Zone 2-3 boundary is dated to approx. AD1350. It coincides with the boundary between Beds 5 and 6, demonstrating a close relation between sediments and salinities. The water freshened slightly, dominated by brackish taxa, *Navicula digitoradiata* and *Nitzchia vitraea*. There are trends within Zone 3. The marine-brackish *Amphora weissflogl* peaks in mid-zone 35.75–32.25cm depth, around 7.45m OD and centred on approx. AD1475, suggesting an increased marine influence which checked the proportion of the brackish *Achnanthes linkei*, the fresh-brackish *Diploneis elliptica* and the fresh-brackish to fresh *Nitzchia linearis*. Above 32.25cm depth, percentages of *Nitzchia vitraea* declined, and fresh-brackish *Amphora copulata* and the fresh-brackish *Diploneis elliptica* increased.

The Zone 3-4 boundary at 24cm depth (7.5m OD) also coincides with the Bed 6-7 boundary at approx. AD1600. Valves of brackish taxa are recorded most but there is a clear fresh-brackish influence, particularly in the earlier half of Zone 4 with *Navicula pusilla* and *Achnanthes lanceolata var. elliptica*. The fresh-brackish assemblage changes above 20cm depth (7.6m OD: approx. AD1650), proportions of the brackish *Nitzchia vitraea* increase, with *Pinnularia viridis*, and the fresh-brackish

to fresh *Pinnularia hemitpera* is no longer recorded. Fresh-brackish and fresh-brackish to fresh forms dominate the two analyses in Zone 5, above 7cm depth, in recent sediment.

**Synthesis**

The NCT fill underlying the western moat is a very fine to fine sand with silt. At its deepest part at boreholes 34 and 44, below 7.25m OD, the moat began to fill with organic mud/peat at AD1287-1342. This is later than the felling date of AD1229-30 for a timber on the floor of the moat that was used in the bridge 10m away but it is not known if the peat was the earliest to form. The thin basal peat of Bed 5 is black and humified, suggesting with the poor preservation of bridge timber (Brann 2004, 19) that the deepest part of the moat was then sometimes dry. This might imply that water was yet to permanently fill the moat. Wood fragments suggest anthropogenic activity nearby. Despite being described as a peat, organic matter in Bed 5 (53-45cm depth) only slowly accumulated, peaking at AD1272-1388. One interpretation of the diatom flora in Zone 1 (58.5-45.0cm depth) is that it was reworked by erosion of the NCT fill in moat sides and floor, but Figure 35 shows Bed 5 to have higher silt and much less fine sand than the underlying NCT fill, so that some mineral matter may be contemporary and introduced, and possibly with it, marine-brackish diatoms.

The moat floor was possibly re-cut before deposition of Bed 6 at AD1279-1392. Bed 6 is a waterlain organic mud that accumulated rapidly. North of the bridge, peat started to form above the NCT fill at 7.35m OD. By then water permanently filled the moat. If water entered the moat from the south end, as seems likely, the water surface in the dry valley/southern moat was higher than 7.9m OD.

As the organic mud of Bed 6 accumulated, abundant silt was introduced. By approx. AD1400 it was the dominant sediment at borehole 43. Silt covered the stonework in the moat. Erosion and re-deposition of the NCT fill in the sides of the moat could have been the source near borehole 43 but to the south, the sediment is much less organic, suggesting its source was south of the western moat. Mineral sediment is absent in boreholes north of the bridge: whether the bridge affected sediment accumulation is unknown. Silt was delivered in low-energy waterlain flows to borehole 43. Pebbles in Bed 6, including Galloway Granitic Suite stones, do not accord with low-energy sediment deposition and these may have been anthropogenically introduced.

The diatom assemblage in Zone 3 at approx. AD1350 suggests slight freshening of the water in the moat, with brackish forms. Sedimentological analyses (Figure 35) were undertaken at borehole 43 to identify pulses of mineral sediment into organic mud, but there was only one sustained phase from approx. AD1400 to approx. AD1600. Diatom analyses at borehole 43 suggest an increased marine influence around approx. AD1475. At approx. AD1600, diatoms describe a clear fresh-brackish influence and waning salinity. This accords with the boundary at 25cm depth (7.65m OD) between the organic mud of Bed 6 and the peat of Bed 7 but sedimentological analyses show Bed 7 not to be a peat, with a gradual increase only in organic matter. The sediment becomes peat with >50% organic matter in the modern Bed 9 above 12cm depth: sedimentological analyses do not indicate an hiatus at the Bed 8-9 boundary. On the ridge separating the southern moat from the western moat at 7.8m OD (boreholes 33-35), late-stage peat is not preserved or never grew.

### 4.2.7. Sediments in the outer ditch

**Description and previous work**

The western moat of the Old Castle runs parallel to a ditch some 15m to the north called the outer ditch (Figure 25). There is a superficially similar but much shallower and less distinct ditch bordering the eastern side of the moat. Grose (1797) had no difficulty in seeing a double ditch when he visited

in the later 18th century. The outer ditch is some 65m long (Figure 39). It falls at its southern end to the surface of the dry valley at 7.9m OD. A ridge of NCT fill rises between the dry valley and the outer ditch to 7.7m OD. It is closed at the northern end at borehole 20 where the NCT fill rises to 8.25m OD. Around 40cm of upcast is preserved to the north of the outer ditch, to around 9m OD, lying on disturbed ground lower by a metre than the 'natural' NCT fill. At the northern end the outer ditch abuts the surface of a track at 9.8-10m OD, which may be the natural NCT fill. This track also blocks the northern end of the western moat (Figure 30). The flat floor of the outer ditch is 3m wide. At a consistent average 8.3m OD, rising from 8.0 to 8.3m OD from south to north, the surface is 1.7m below the bank separating it from the western moat and a metre below the bank of upcast, and an average 40cm higher than the ground surface in the western moat. Brann (2004, 3) described the outer ditch as a defence, but it is easily skirted.

The southern 40m length of the outer ditch was examined in 2004 from nine Eijelkamp boreholes (Tipping *et al* 2004, 99-101). Its fill above the floor of NCT fill varied in thickness. To the north of the ridge the fill is largely minerogenic, a laterally continuous clay-rich silt with much fine sand, more organic in its lower part, increasingly poorly sorted and more minerogenic in its upper part and capped by thin peat. What was interpreted as building rubble within the sediment fill was seen over 15m in three boreholes.

Sedimentological and diatom analyses were undertaken at borehole 3, 12m north of the ridge, with a ground surface at 8.0m OD. Three AMS $^{14}C$ assays were obtained on sediment in borehole 3, on the humin fraction of the organic matter, because a concern was the intrusion of younger roots in this shallow fill. Humin is the most stable organic fraction, usually representing the most residual (oldest) material (Shore, Bartley and Harkness 1995; Pessenda, Gouveia and Aravena 2001). The age estimates are in Table 19, re-calibrated in 2021. Basal organic mud (organic content by l-o-I of 30%) at 73-71cm depth (7.28m OD) has a calibrated age-range of AD770-1160. A similar organic mud (30% organic matter) at 67-65cm depth has almost the same calibrated age-range: AD770-1020. Both assays are significantly older (at 2σ) than the dendrochronologically dated oak timber that was part of the bridge over the western moat (AD1229-30: above). At 30-28cm depth, organic mud has a calibrated age-range of AD1180-1400.

| Borehole | Depth (cm) | Bed | Material | Description | Wt. (gms) | Lab No. | $^{14}C$ BP | $\delta^{13}C$ (‰) | Cal BC/AD (95.4%) |
|---|---|---|---|---|---|---|---|---|---|
| 2004 | | | | | | | | | |
| 3 | 30-28 | | organic mud | humin | | AA-51353 | 735 ±55 | -29.0 | AD1180-1400 |
| 3 | 67-65 | | organic mud | humin | | AA-51352 | 1130 ±45 | -29.2 | AD770-1020 |
| 3 | 73-71 | | organic mud | humin | | AA-51351 | 1050 ±60 | -29.7 | AD770-1160 |
| 2021 | | | | | | | | | |
| 13 (Core 3) | 4.5 | in Bed 9 | wood (*Alnus*) | two very short-lived horizontal twigs | 0.53 | SUERC-101766 | | -30.1 | modern |
| 13 (Core 3) | 9 | base of Bed 9 | wood (*Alnus*) | one large horizontal twig | 0.91 | SUERC-101765 | | -30.1 | modern |
| 13 (Core 3) | 40-42 | base of Bed 7 | Well humified peat with much silt | humic acid | nd | SUERC-102230 | 357 ±21 | -29.6 | AD1460-1633 |
| 13 (Core 1) | 50.5 | top of Bed 6 | wood (*Alnus*) | one short-lived | 0.31 | SUERC-101763 | 292 ±28 | -28.2 | AD1499-1660 |

| | | | | | | | | | |
|---|---|---|---|---|---|---|---|---|---|
| | | | | horizontal twig | | | | | |
| 13 (Core 2) | 72 | top of Bed 2 | wood (nd) | two short-lived horizontal twigs | 0.35 | SUERC-101764 | 588 ±28 | -29.6 | AD1303-1411 |
| 13 (Core 2) | 88.5-90.0 | base of Bed 2 | Wood (*Alnus*) | two short-lived horizontal twigs | nd | SUERC-102137 | 743 ±24 | -29.7 | AD1228-1294 |

*Table 19. Details of AMS $^{14}$C assays obtained in 2004 and in 2022 in the outer ditch calibrated using Oxcal 4.4 (Bronk Ramsey 2009) with INTCAL20 (Reimer* et al *2020) and expressed at 95.4% probability: nd = not determined.*

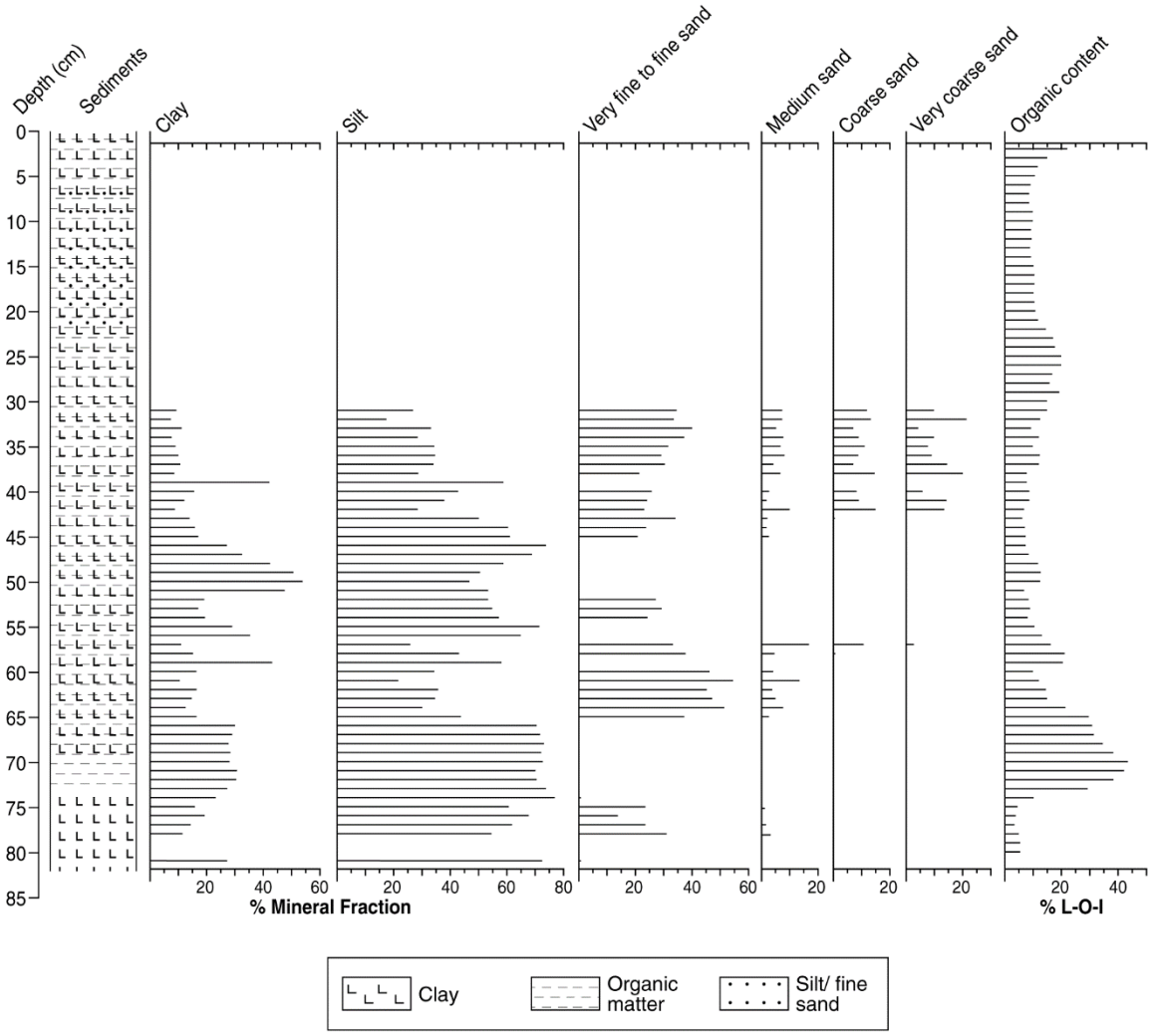


*Figure 37. Particle size data and organic contents of sediments in borehole 3 (2004): from Tipping* et al *(2004, Figure 11.3).*

Sedimentological data in borehole 3 (2004)(Figure 37) below 75cm depth are from the NCT fill underlying the outer ditch. They are clay-rich silts with very fine sand. The basal ditch fill is is similar and very uniform but lacks very fine sand. It has an organic content peaking at 45% at 70cm depth. Organic contents fall gradually thereafter. Abruptly at 65cm depth, fine-grained sediment is replaced by fine and medium sand until 56cm depth. Within this band there is a second, smaller peak in organic contents between 59 and 55cm depth. Clay-rich silt deposition resumes at 56cm depth, but there is another band of very fine to fine sand 54-52cm depth before a silt with more clay formed

until 45cm depth. A third pulse of coarse sediment above 45cm depth coarsens to include very coarse sand above 42cm depth, to 30cm depth: analyses ceased at this depth.

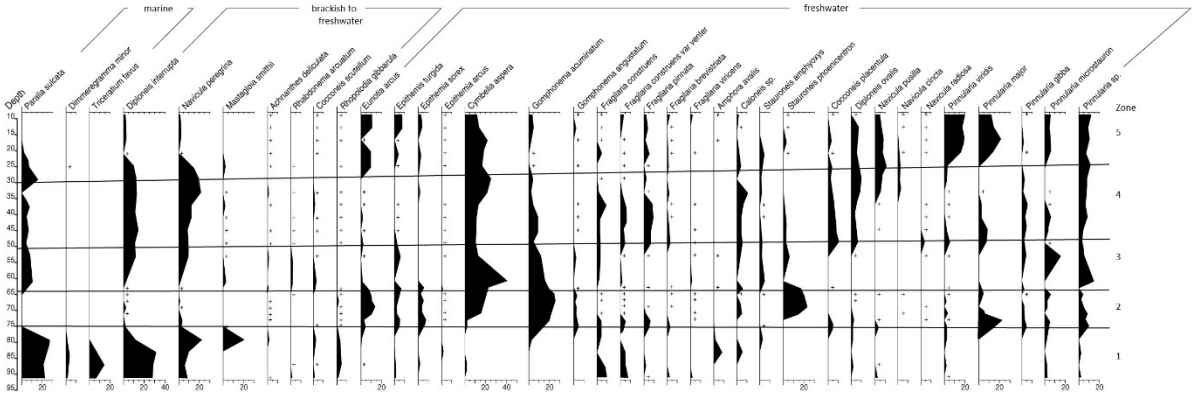


*Figure 38. Diatom taxa and zones plotted as % total diatom valves recorded in borehole 3 (2004): modified from Tipping* et al *(2004, Figure 11.4).*

Diatom analyses (Figure 38) also extended to the NCT fill (Zone 1: 91.0-75.0cm depth). This is dominated by marine to marine-brackish forms. The earliest fill of the outer ditch (Zone 2: 75.0-65.0cm depth) accumulated in fresh water ponded east of the ridge of NCT fill 12m to the south. *Paralia sulcata*, the only obligate marine species recorded, re-appears in Zone 3 (65.0-51.0cm depth), as do the more brackish *Diploneis interrupta* and *Navicula peregrina*, with *Cymbella aspera* and *Gomphonema acuminatum*, which both decline up-zone, but also with freshwater forms. Zone 4 (51.0-30.0cm depth) shows few changes in salinity, but freshwater taxa are more common. *Paralia sulcata* percentages start to decline at the Zone 4-5 boundary (30.0cm depth) and its valves are not recorded above 18.0cm depth, and freshwater taxa like *Eurotia arcus*, *Epithemia turgida*, *Pinnularia viridis*, *P*. *major* and *P*. *microstauron* dominate to the ground surface.

**Sediment stratigraphy (2021)**

Figure 39 presents the sediment stratigraphies of closely spaced boreholes along the axis of the outer ditch recorded in 2021. The ground surface north of borehole 11 is around 8.3m OD, some 30cm higher than surveyed in 2004: the 2004 data are probably incorrect. At borehole 4 the NCT fill is at 7.32m OD, marking the southern end of the ditch. The ridge separating the dry valley from the outer ditch is on borehole 5, at 8.05m OD. It is likely that this ridge was the left (north) bank of the dry valley, as on the western moat (above), and as there, water would need to overtop 8.05m OD to flow into the outer ditch. North of this, the base of the ditch first deepens to 7.25m OD and then rises to 7.8m OD at borehole 16. Amorphous peat is the basal deposit, black and well humified in boreholes 11, 12, 13.5 and 14. Above this is silt, though a silty clay initially at borehole 4, conformably and gradually sealing the peat. Stonework was struck at boreholes 6 and 9. Silt is found along all of the ditch, lying on the NCT fill at borehole 19. Borehole 20 shows that the ditch ends in a cut in the NCT fill. The silt becomes more organic at boreholes 6, 10 and 13 to 14 before silt was again deposited. The silt rises some 75cm higher than the ridge at borehole 5. A thin peat caps the ditch fill. The surface of the ditch fill is around 8.25m OD.

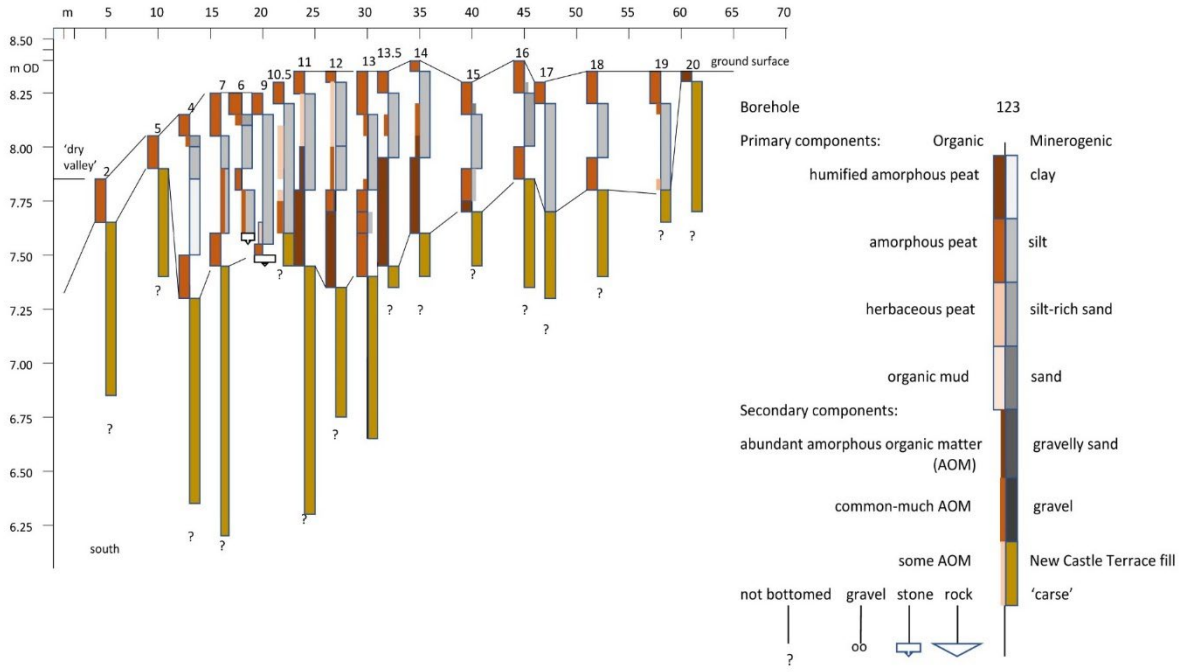


*Figure 39. Sediment stratigraphies along the axis of the outer ditch.*

Borehole 13 with a ground surface at 8.3m OD, 7m north of borehole 3 in 2004, was sampled for laboratory analyses because it is typical. It was sampled in two sets of cores, each 0-60; 60-120cm depth, <0.5m apart with an Abbey piston core: all depths and altitudes used are corrected for compression. The two sets of cores are very similar (Table 20). Organic contents and particle size analyses are presented in Figure 41. AMS $^{14}$C assays are presented in Table 19.

| Bed | Depth cm | Description |
|---|---|---|
| 9 | 0-13 | 5YR4/4 reddish brown amorphous peat with common-many scattered, un-orientated small and short (<2mm) wood fragments, one 4cm long, 2cm wide wood fragment 10.8-14.4cm and rare scattered mineral matter; gradual to |
| 8 | 13-25 | 10YR5/2 greyish brown structureless silt with common amorphous organic matter; gradual to |
| 7 | 25-42 | 10YR4/2 dark greyish brown structureless silt with little amorphous matter and rare rotted wood fragments at 32.4-34.2cm; gradual to |
| 6 | 42-49 | 10YR5/2 greyish brown structureless silt with common amorphous organic matter, few bark fragments 42.3-44.1cm, one 5cm long, <1mm fibrous root and two small wood fragments 45.0-46.8cm; gradual to |
| 5 | 49-58 | 5YR3/2 dark reddish brown structureless amorphous peat/organic mud, increasingly organic down-unit, with common >2mm rotted stones |
| 4 | 60-67 | 10YR4/2 dark greyish brown structureless amorphous peat/organic mud; gradual to |
| 3 | 67-71 | 10YR5/1 grey weakly stratified silt, scattered and in diffuse <2mm thick bands with much amorphous organic matter and few very small wood fragments; gradual to |
| 2 | 71-89 | 10YR3/1 very dark grey structureless amorphous peat with common-many small roundwood (twigs); sharp to |
| 1 | 89-120 | 10YR6/1 light grey to grey structureless fine sandy silt ('carse'): not bottomed |

| Bed | Depth cm | Description |
|---|---|---|
| 9 | 0-13 | 7.5YR3/2 dark brown amorphous peat with common small roundwood (twigs), common very small wood fragments and very rare vertical very fine fleshy roots/stems; gradual to |
| 8 | 13-33 | 10YR5/2 greyish brown structureless silt with little-common amorphous organic matter; gradual to |
| 7 | 33-46 | 10YR4/2 dark greyish brown structureless silt with common amorphous organic matter; gradual to |
| 6 | 46-59 | 5YR4/2 dark reddish grey amorphous peat/organic mud with common small wood fragments |
| 5 | 60-66 | 10YR3/2 very dark greyish brown amorphous peat with rare-few small roundwood, few very small wood fragments and little mineral matter; gradual to |
| 4 | 66-73 | 7.5YR3/0 very dark grey weakly stratified, block-structured amorphous peat with rare vertical very fine fibrous stems/roots, common small roundwood, common small wood fragments and some mineral matter in diffuse bands; gradual to |
| 3 | 73-82 | 10YR5/2 greyish brown amorphous peat with rare vertical very fine fibrous stems/roots, common small roundwood, common small wood fragments and some mineral matter in diffuse bands; gradual to |
| 2 | 82-88 | 7.5YR3/0 very dark grey weakly stratified amorphous peat with abundant small roundwood and rare horizontal very fine fibrous stems; sharp to |
| 1 | 88-120 | 10YR7/1 light grey fine sandy silt ('carse'): not bottomed |

*Table 20. Sediment descriptions of (a) cores 1 and 2 combined and (b) cores 3 and 4 combined at borehole 13 in the outer ditch. There is a 2.0cm gap between cores 1 and 2 between 58 and 60cm depth*

**AMS $^{14}$C dating (2021)**

The AMS $^{14}$C assays obtained in 2022 (Table 19) are on cellulose from slender short-lived twigs lying horizontally in the sediment, assumed because of this not to be intrusive. These were sampled because they are biochemically simple single short-lived entities (Ashmore 1999). One sample, assay SUERC-102230, was on peat with much silt, similar to the organic mud dated in 2004, but the humic acid fraction of this material was dated. There is no reason to question the $^{14}$C assays. They are considered correct estimates of the sediment age. Twigs at the base of the ditch fill have an age of AD1228-1294: SUERC-102137). Linear regression from this assay through assay SUERC-101764 and 'splitting the difference' between assays SUERC-101763 and -102230 has an $r^2$ value of >0.99 but a p-value of 0.083 because n = 4: the result is *not* significant at p <.05. This includes the humic acid fraction of peat dated by assay SUERC-102230. Assays SUERC-101765 and -766 on wood cellulose are also considered correct but they have not been used in the linear regression. They lie above a hiatus, taken to be at 13cm depth, the Bed 8-9 boundary, despite the boundary being described as gradual (Table 20).

Bayesian modelling with BACON software (Blauuw and Christen 2011) used assays SUERC-102137, -101764, -101763 and -102230 to extrapolate age estimates at contiguous 1.0cm intervals to 1.0cm depth with a step-size of 5.0cm (Figure 40). The likely hiatus between Beds 8 and 9 is marked at 13.0cm depth.

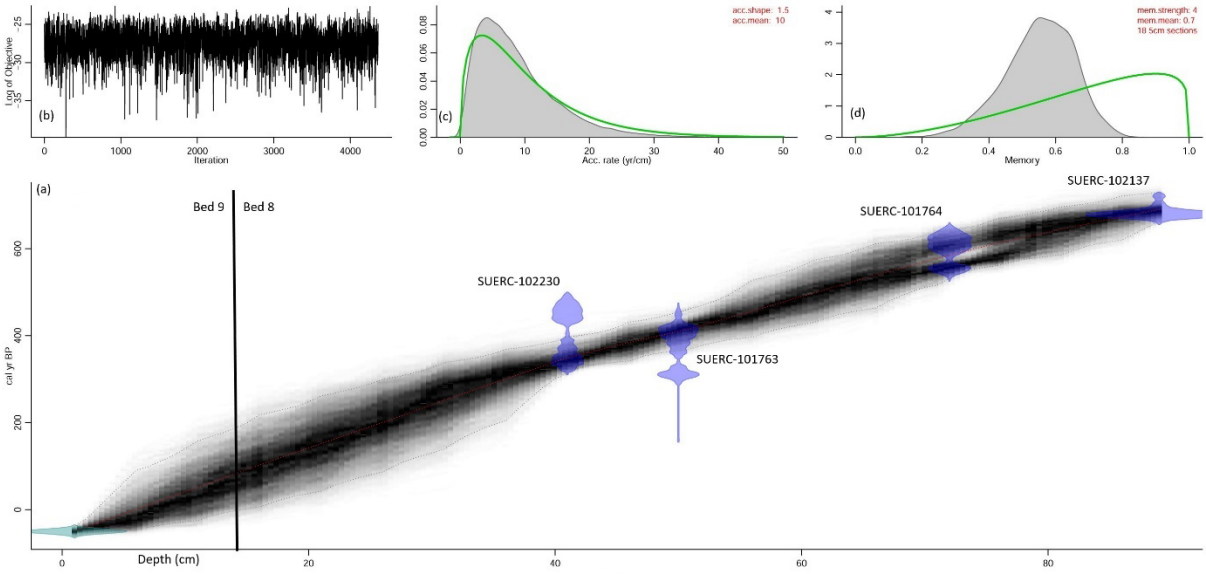


*Figure 40. (a) Bayesian modelled age-depth relation between the four calibrated AMS $^{14}$C assays to an extrapolated sediment surface at 0.0cm depth, with the probable hiatus between Beds 8 and 9 at 13.0cm depth marked: darker grey curves indicate more likely calendar ages; the width of the curve expresses the uncertainty of the age-range at any depth, wider above* c. *35cm depth where there are no age controls (only age estimates below the hiatus at 13.0cm depth are used; (b) MCMC iterations showing a broadly stationary distribution; (c) prior (green curve) and posterior (grey histogram) distributions for the accumulation rate and (d) prior (green curve) and posterior (grey histogram) distributions for the memory.*

Modelling gives an age of AD1220-1288 for basal organic sediment at 89cm depth (7.41m OD) and the following age estimates for the gross sedimentological changes described in Table 20:

(i) AD1311-1433 for the first marked appearance at 71cm depth (7.59m OD) of mineral matter at the base of Bed 3;

(ii) AD1335-1472 for a reduction in mineral matter at the base of Bed 4 at 67cm depth (7.55m OD);

(iii) AD1390-1524 for the deposition of common clasts >2mm diameter above 60 cm depth (7.70m OD) in Bed 5;

(iv) AD1503-1588 for an increase in mineral matter at the base of Bed 6 at 49cm depth (7.73m OD);

(v) AD1550-1625 for a large increase in mineral matter at the base of Bed 7 at 42cm depth (7.80m OD);

(vi) AD1783-1958 for the likely hiatus at the Bed 8-9 boundary at 13cm depth (8.27m OD).

To transpose this age modelling to the sediments analysed in 2004 (above), the ground surface at borehole 3 (2004) is assumed to have a correct altitude of 8.3m OD. Major environmental changes were:

(i) first appearance of estuarine-marine diatoms and much minerogenic sediment, including coarse sand above 65cm depth (7.65m OD) at AD1291-1392;

(ii) deposition of very poorly sorted sediment between 51 and 45cm depth (7.79 to 7.88m OD) between AD1377-1519 and AD1440-1556;

(iii) absence of estuarine-marine diatoms at 30cm depth (8.0m OD) after AD1563-1649.

Assays SUERC-102137, -101764 and -101763 are much younger than the equivalent assays obtained in 2004. Using mean calibrated age as a rough guide and bearing in mind the large age-ranges of assays AA-51351 and -51352, the age difference is *c*. 300 years at the base of the ditch fill, widening to >400 years at the depth-equivalent (40cm) to assay AA-51353, though the differences could be much larger or smaller. The assays obtained on the humin fraction of organic matter in 2004 are considered incorrect estimates of sediment age because the dating evidence suggests the outer ditch is broadly contemporary with the moat system (below: Section 4.2.7). Assay SUERC-102230, also on organic mud/peat with much silt, suggests that there is nothing inherently problematic in $^{14}C$ dating the humic acid fraction of the sediment. This is assumed to be generated from *in situ* organic matter. Assays on humin fractions are also correct, but the humin fraction is much older than the sediment in which it is found. It is also older than the outer ditch itself. As the NCT fill forming the sides and base of the ditch system has no discernible organic matter it cannot have contributed this material. Rather, it is thought that this most residual organic fraction originated in sediment outside the outer ditch, which was eroded and then re-deposited in the ditch after AD1228-1294, the more mobile humic acid fraction of this material having been washed away in transport. The calibrated ages show the source not to be long-lived unless only the younger sediment was eroded, and the $\delta^{13}C$ values show the source was terrestrial, but where it was, cannot be reconstructed. It is evidence, however, of the erosive force of water and sediment filling the outer ditch fill.

**Quantitative sedimentological analyses (2021)**

Figure 41 shows sedimentological data. It includes the numbers of roundwood (twigs) and wood fragments per contiguous 1.0cm sediment slice (*c*. 20cm$^3$) because these were seen to vary greatly during cleaning of the cores.

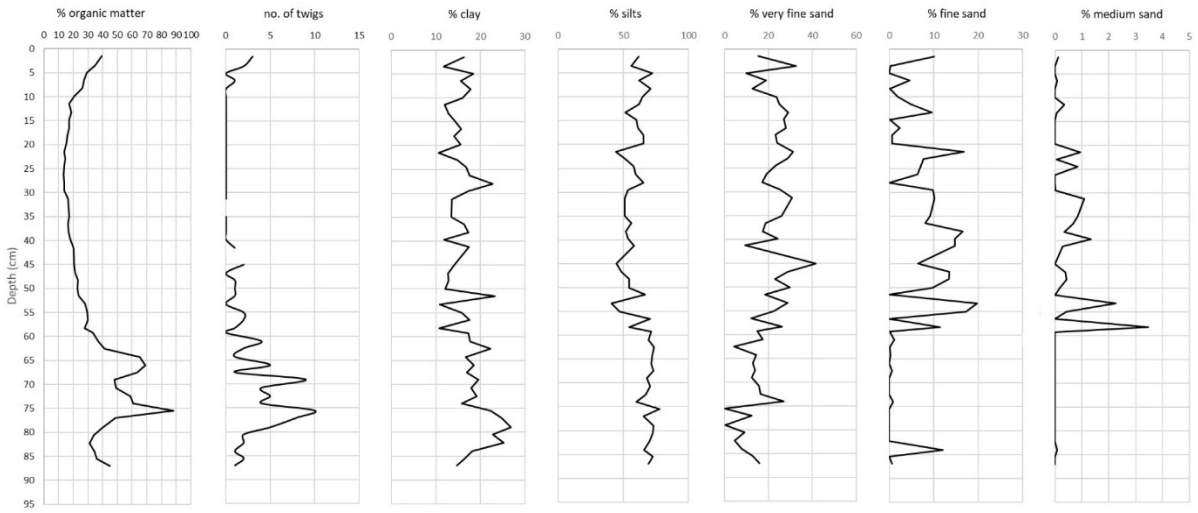


*Figure 41. Organic contents, particle size distributions and twigs in Cores 3 and 4 from borehole 13 in the outer ditch, plotted against depth. Note changes in horizontal scales.*

All analyses are from sediments in the ditch fill, above its base at 88cm depth (Table 20). Basal peat (Bed 2: Table 20) has a low organic content, perhaps because the NCT fill forming the ditch sides was initially unstable. Below 75cm depth (AD1291-1392) the fill is comparatively rich in clays from still-water deposition. Twigs are present from the base of the fill, and were used to date its inception, modelled to AD1220-1288. They probably represent trees overhanging the ditch as they do today (e.g. above 5cm depth: Figure 41). Organic contents and numbers of twigs track each other closely. Both rise above 80cm depth (AD1261–1367) to peak at 75cm depth (AD1291-1392). Very fine sand replaced clay at AD1291-1392.

The numbers of twigs fall from 69cm depth and organic contents fall from 66cm depth, between AD1327-1448 and AD1339-1487 as well-sorted very fine sandy silt was deposited. Twigs are rare or absent above 60cm depth (after AD1390-1524). Also above 60cm depth (AD1390-1524) there were abrupt but inconsistent increases in coarser sediment introduced by higher energy water flows. Two such pulses are seen in medium sand content at 58.3cm depth and 53.3cm depth, AD1405-1533 and AD1465-1563 respectively. Their loss may represent woodland clearance, although Davies (2004) did not detect woodland loss in her pollen diagram from the northern moat of the Old Castle, 25m away. From 58 to 45cm depth (AD1409-1535 to AD1531-1611) waning energy flows are suggested by steadily rising amounts of very fine sand (though not in silt). Organic contents fall smoothly and gradually to a nadir at 29.5cm depth (AD1633-1828). A second more sustained phase of elevated percentages of medium sand is seen between 40 and 30cm depth (AD1563-1649 to AD1624-1820) and a final peak in fine and medium sand at 21.5cm depth (AD1686-1902).

**Diatom analyses (2021)**

New diatom analyses from borehole 13 will become available in March-April 2023.

**Synthesis**

This section draws on the sedimentological data from borehole 13 (Figure 41) and the sedimentological and diatom analyses from borehole 3 (2004) (Figures 35, 36), applying to that statigraphy the Bayesian-modelled $^{14}$C chronology generated for borehole 13. The ditch fill in borehole 13 is 88cm thick and 75cm thick in borehole 3 (2004): depths in borehole 3 (2004) are made comparable by multiplying them by 1.17 (*c.* in the text).

The outer ditch was dug before AD1220-1288. Trees grew close to and overhung the ditch. Clay-rich silt settled out initially at both boreholes in still water. Though described as peat (Table 20), the earliest fill at borehole 13 (Bed 2: 89-71cm depth) has a low organic content until 80cm depth (AD1261-1367) as ditch sides took time to stabilise. At borehole 3 (2004) the earliest fill, overwhelmingly a silt with clay, has 40% organic matter at the base (AD1229-1330). Organic contents peaked at borehole 13 at 90% at 75cm depth (AD1291-1392). These events were almost certainly precisely synchronous, representing increases in aquatic biomass in the ditch. Differences are probably due to the higher amounts of mineral sediment in the south of the outer ditch. Diatom analyses from borehole 3 (Zone 2: *c*. 88-75cm in borehole 13) show the water to have been fresh. This was either rain-water ponded north of the buried ridge at the southern end or stream water from the dry valley that overtopped this ridge, at 7.7m OD. The deepest AMS $^{14}$C sample dated in 2004 (73-71cm depth, c. 84cm depth in borehole 13: Table 19) is from this diatom zone, eroded from an earlier freshwater peat and re-deposited in the outer ditch, it has been argued, indicating higher energy sedimentation than suggested from other analyses.

Towards the dry valley, very fine and medium sand abruptly overlay clay-rich silt at borehole 3 (2004) above 65cm depth (*c*. 76cm depth in borehole 13), AD1281-1389, until 57cm depth (*c*. 67cm in borehole 13) when the final deposit at AD1335-1472 included very coarse sand. Residual humin from eroded and re-deposited silt at 67-65cm depth in borehole 3 (2004) (Table 19) endorses the interpretation of this unit as a high energy deposit. Diatoms in Zone 3 at borehole 3 (2004) characterise the salinity of the environment coeval with this sand as brackish-marine (65.0-51.0cm depth; *c*. 76-60cm depth in borehole 13), until AD1390-1524. This sediment almost certainly entered the ditch from the dry valley. Organic contents fell sharply. Organic contents also fell in borehole 13 above 76cm depth (AD1281-1389) and mineral matter increased, weakly stratified from flowing water above 71cm depth (AD1312-1434: Table 20) but here a very fine sand replaced clay.

The small peaks in organic content 59-55cm depth in borehole 3 (2004) (*c*. 69-64cm depth in borehole 13: AD1327-1448 to AD1350-1491) and in borehole 13 (69-60cm depth: to AD1390-1524) are probably synchronous, representing a short period of reduced minerogenic sedimentation allowing aquatic organisms to re-establish. This may have lasted longer in the deeper water around borehole 13. Clay-rich silt sedimentation representative of quiescent conditions was established at borehole 3 (2004) at 56cm depth (*c*. 65.5cm in borehole 13) at AD1344-1488 but only briefly because sand was re-introduced for 2cm above 54cm depth (*c*. 63-61cm depth in borehole 13), AD1366-1501 to AD1377-1519.

Abruptly, two separate peaks in fine and medium sand were deposited in borehole 13 between (i) 59.3 and 56.5cm depth (AD1395-1535 to AD1418-1548) and (ii) 55.0 and 51.5cm depth (AD1440-1556 and AD1484-1575). The median grain size (not shown in Figure 41) more than doubles in samples above 60cm depth. Proportions of very fine sand increase between and after these peaks to 45cm depth (AD1531-1611). Bed 5 in borehole 13 contains common rotted stones >2mm in size between 58 and 49cm depth (Table 20), AD1409-1535 to AD1503-1588, similarly indicating high energy flows. The only rare twigs in borehole 13 above 60cm depth might be explained by high energy flows transporting twigs towards the north end of the ditch. There is, however, no equivalent to these events in borehole 3 (2004), which is problematic unless water flows were erosive towards the southern end of the ditch. These events post-date diatom Zone 3, which ends at 51.0cm depth, *c*. 60cm depth in borehole 13 at AD1390-1524, but the marine-brackish diatom flora continued in Zone 4 (Figure 38). It is very likely that the events between AD1395-1535 and AD1503-1588 represent at least one marine inundation.

Clay-rich silt was deposited above 51.0cm depth in borehole 3 (2004), *c*. 60cm depth in borehole 13. This may be younger than it appears if it formed after a hiatus. There was then a coarsening-up trend with successive peaks in clay at 50cm depth, silts at 46cm depth, very fine to fine sand at 43cm depth and poorly medium to very coarse sand at 42cm depth, equivalent to *c*. 58 to *c*. 49cm in borehole 13, from AD1409-1535 to AD1503-1588. The same trend is seen in borehole 13 above 60cm depth, sustained to 31cm depth. If synchronous, more sediment was deposited around borehole 13 than borehole 3 (2004). The marine-brackish environment of diatom Zone 3 became slightly fresher after AD1487-1580 in Zone 4 but more brackish within Zone 4 above 36cm depth (*c*. 42cm depth in borehole 13: AD1550-1625) in which the youngest evidence for re-deposited organic matter at borehole 3 (2004) is recorded (30-28cm; *c*. 34cm depth in borehole 13: Table 19). *Paralia sulcata*, the principal marine indicator, is not recorded at 33cm depth (*c*. 41cm in borehole 13) but is recorded after this with a brief peak at the Zone 4-5 boundary at 29cm depth (*c*. 34cm depth in borehole 13) at AD1598-1765.

Sediment in borehole 13 is a very fine sandy silt above 30cm depth, fine sand significant only between 15 and 10cm depth, probably in modern sediment. Diatom Zone 5 in borehole 3 (2004) above 30cm depth (*c*. 35cm in borehole 13: AD1591-1754) records predominantly fresh water taxa.

**4.2.8. The chronology of the moat system and the outer ditch**

There are three series of $^{14}$C assays on the basal fills of the northern moat, the western moat and the outer ditch. There is also a dendrochronological felling date of AD1229-30 for an oak timber that was found in 1977 at the base of the western moat and used in the drawbridge mechanism over the western moat (Brann 2004). The base of the peat in the northern moat has an age of AD1050-1280 (above: Section 4.2.5). This is older than the age of the basal peat in the western moat, modelled to AD1287-1342 and the two overlying calibrated assays in the western moat of AD1272-1388 and AD1279-1392 (Table 18). This is unlikely to be because the two moat limbs are of different ages. It may be that the inclusion of humin in assay Beta-150692 dragged the age estimate in the northern moat backward in time, although this would infer some re-deposition of old organic matter in a peat assumed to have been unaffected by this (Tipping *et al* 2004, 98). Assay Beta-150693 in the northern moat at 66cm depth has an age of AD1270-1400 (above), equivalent to around 42cm depth in the thinner sediments of the western moat fill, in agreement with assays SUERC-101767 to -101769 in the western Moat.

The age of the deepest and earliest peat in the outer ditch (SUERC-102137: Table 19) is modelled (Figure 40) to AD1220-1288. This overlaps by one year and is effectively significantly different to the modelled age of the deepest and earliest peat in the western moat (AD1287-1342) at 2σ. Both age estimates are on cellulose from young twigs. The cutting of the western moat was later than the cutting of the outer ditch.

All three $^{14}$C age estimates from the basal fills of the moat system and the outer ditch are younger than the felling date of AD1229-30 for the timber associated with the bridge to the Old Castle over the western moat. The calibrated age-range of assay SUERC-102137 in the outer ditch overlaps at 2σ by one year the felling date but the two are probably different. Bayesian modelling defines the age of the base of the western moat fill at 89.0cm depth as AD1219-1287 (above: Section 4.2.6). Assay SUERC-101767 at the base of the western moat is supported by overlying assays SUERC-101768 and -101769 (Table 18), neither of which extend in time to AD1229-30. Bayesian modelling re-defines slightly the age of the base of the western moat fill at 52.0cm depth as AD1287-1342 (above: Section 4.2.6). Either the moat system was systematically cleaned out (we thank Coralie Mills for this suggestion) before these dates (the evidence for re-cutting in the western moat (Section 4.2.6)

might suggest this) or the felling date of AD1229-30 was not the date the oak timber was incorporated in the drawbridge in the western moat. If the former, the basal peats in the moat may then reflect that sediment was no longer cleaned out, and that these dates relate to abandonment of the Old Castle as a place requiring a water-filled moat.

The series of assays from the moat system and the outer ditch place their construction overlapping that of the New Castle, taking a felling date of AD1277 as a maximal age for timbers used in Bridge 1 (MacIvor *et al* 1999; Section 4.5 below).

**4.2.9. Sediments next to the bailey**

Brann (2004, 6) briefly mentions a "ditched enclosure" north-east of the Old Castle "which may have served as the bailey" (Figure 25). Truckell (1950, 203) briefly described small excavations (where is not described) that "showed that the principal earthworks were of turf, clay, and rubble construction", undated "save for late medieval pottery in a house-floor built on an earlier raised platform", though he thought the site "could well be Roman by structure alone". The level ground of the bailey, on the NCT fill surface just below 10m OD, is ditched on its southern and northern sides and bordered by the Old Castle Burn to the east, but to the west is a very large 600m$^2$ rectangular basin, 36m long, 17m wide at its southern end and 0.9m deep. Its surface at 9.0m OD is peat. It floods in wet weather. The southern end of the basin faces the corner made by the western and northern sides of the moat system, separated from it by a track a few metres wide of unknown antiquity save for it being mapped by the Ordnance Survey in 1856. The basin surface is 1.2m higher than the floor of the northern end of the western moat. The south west corner of the basin faces the northern end of the outer ditch, though borehole 20 in the outer ditch (Figure 37) shows there was no connection between the two. The basin surface is also 1.2m higher than the floor of the northern end of the outer ditch. Because the basin surface is much higher than that in the northern moat, which is not truncated (Section 4.2.5), the basin is hydrologically independent of and separate from both the moat system and the outer ditch. The basin was always enclosed, and the southern end of the basin abutted a ridge of the NCT fill where the track now is.

Three parallel sediment-stratigraphic transects were made from east to west, at the southern end, in the centre and at the northern end. The depth of sediments shallows north of the southern end, so only the transect nearest the moat system and the outer ditch is depicted in Figure 42.

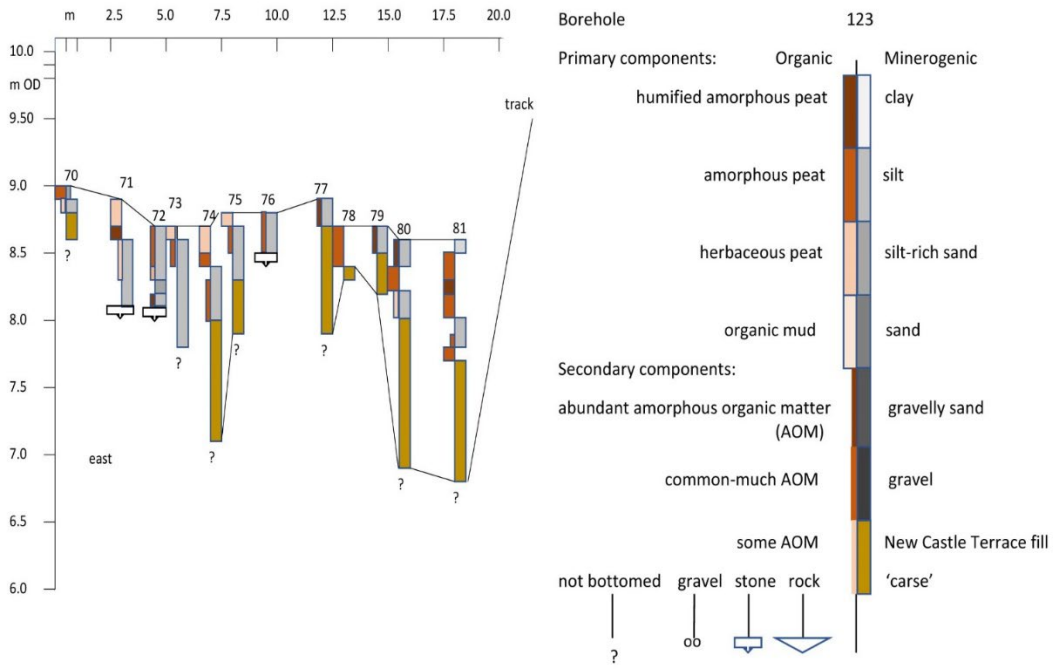


*Figure 42. Sediment stratigraphies along the southern side of the bailey basin.*

Beyond the eastern end of the basin, borehole 70 is in a much shallower ditch parallel to the track, a later feature. The altitudes of the NCT fill at the base of boreholes define two ditches beneath the basin surface: ditch (1) in boreholes 71 to 77 and ditch (2) in boreholes 77 to 81. These are also found beneath the centre of the basin but not at the northern end. Boreholes 71, 72 and 76 struck stonework. The fill of Ditch (1) is a uniform oxidised silt with amorphous organic matter, capped by peat. The fill of Ditch (2) has organic beds alternating with silt. Sediments at borehole 81, the deepest fill and nearest to the outer ditch, were sampled in two cores with a piston corer. Table 21 is the sediment description.

| Bed | Depth cm | Description |
|---|---|---|
| 12 | 0-0/8 | Dark grey weakly stratified (on colour differences) and deformed silt with <2mm laminae of dark brown amorphous organic matter; boundary sharp and sloping to |
| 11 | 0/8-23 | Reddish brown amorphous peat with very rare horizontal fine fleshy stems and common mineral matter; sediment cracked at the sharp horizontal boundary to |
| 10 | 23-31 | Dark brown to black amorphous peat; gradual to |
| 9 | 31-54 | Dark brown becoming mid-brown amorphous peat/organic mud with very rare horizontal fine fleshy stems and increasing mineral matter down-unit; gradual to |
| 8 | 54-56 | Stratified lenses of pale grey silt, increasing down-unit, in a matrix of pale brown amorphous organic matter; sharp to |
| 7 | 56-60 | Pale grey and dark grey weakly banded silt; gradual to |
| 6 | 60-61 | Pale grey and orange (oxidised) structureless silt; sharp to |
| 5 | 61-63 | Reddish brown organic mud/amorphous peat; sharp to |
| 4 | 63-74 | Grey-brown structureless silt with common amorphous matter; gradual to |
| 3 | 74-80 | Dark brown amorphous peat with much mineral matter, declining down-unit, with one lamina with sharp boundaries of grey-brown silt at 75.5cm; sharp to |
| 2 | 80-81 | Laminated brown amorphous organic matter and grey-brown mineral matter; sharp to |
| 1 | 81-120 | Pale grey stratified fine sandy silt ('carse'): not bottomed |

*Table 21. Sediment description of borehole 81 in the bailey basin.*

Beds 1 to 9 represent stratified alternations of minerogenic and organic matter in an undisturbed water body. Bed 10 is a well humified peat, probably formed in drier conditions with a lower water table inducing aerobic decay. In its complexity, this fill is difficult to relate to sediment stratigraphies

in the moat system and the outer ditch. To understand its relation to these sediments, three AMS $^{14}C$ assays were obtained (Table 22).

| Depth (cm) | Bed | Material | Description | Wt. (gms) | SUERC No. | $^{14}C$ BP | $\delta^{13}C$ (‰) | Cal BC/AD (95.4%) |
|---|---|---|---|---|---|---|---|---|
| 52.0-52.5 | base of Bed 8 | organic mud | humic acid | 11.63 | 101778 | 272 ±28 | -30.1 | AD1516-1797 |
| 61.0-61.5 | top of Bed 5 | organic mud/ amorphous peat | humic acid | 7.5 | 101777 | 849 ±28 | -29.7 | AD1158-1265 |
| 79.0-79.5 | base of Bed 3 | amorphous peat with some mineral matter | humic acid | 15.42 | 101776 | 1987 ±28 | -29.5 | 44BC-AD116 |

*Table 22. Details of AMS $^{14}C$ assays obtained on borehole 81 in the bailey basin using Oxcal 4.4 (Bronk Ramsey 2009) with INTCAL20 (Reimer* et al *2020) and expressed at 95.4% probability*

Assay -101776 dates the earliest peat in the deeper of the ditches to between the 1st century BC to the 2nd centuries AD. The ditch is earlier but assuming peat formed soon after its excavation, it was cut in the late pre-Roman Iron Age or, as Truckell (1950) thought, in the Roman Iron Age. The two ditches in the basin are parallel, suggesting that one was visible when the other was cut, so the entire basin probably dates to a time between 44 BC-AD116. It is possible that the owners of the Old Castle gained cachet from siting it so near to features they would have thought of Roman origin. The original function of the basin is unknown. It was enclosed and so was not a harbour.

Bed 2 (Table 21) indicates a waterlain beginning to sediment accumulation in the deeper of the ditches. Above this, organic mud and peat contain much mineral matter (descriptions are not supported by quantitative analyses). The slow rate of sediment accumulation (*c*. 65 yrs/cm) suggests that accumulation was not continuous and that there were depositional hiatuses. The top of organic sediment at 61cm depth is dated to AD1158-1265 (SUERC-101777: Table 22). This spans the period when the outer ditch, the Old Castle and its moat system were constructed. After this, Beds 7 and 8 are waterlain. Bed 7 has no organic content. Sediment accumulation was still slow at around 49 yrs/cm and possibly discontinuous. One probable origin for the mineral matter is disturbance to the NCT fill surface around the Old Castle during construction. Another may be the deposition of estuarine-marine mud from storm surges. If the former is demonstrated from diatom analyses, storm surges would have overtopped the NCT fill ridge at just under 10m OD. Cessation of silt deposition is dated to AD1516-1797 by assay SUERC-101778 (Table 22). This may be when human activities around the Old Castle ceased, or when coastal floods ceased affecting the basin. Sediment accumulation was rapid (*c*. 7 yrs/cm). Organic matter gradually increased to become peat at 31cm depth (*c*. AD1800; Table 21). Organic mud/peat at 61cm depth is Ditch 1 is underlain by stonework in boreholes 71, 72 and 76 (Figure 42): this cannot be radiocarbon dated because it is not associated with organic matter, and temporal correlation between the two ditches cannot be made from radiocarbon dating.

### 4.2.10. The New Castle

Caerlaverock New Castle was not investigated in this study. In 2004, SMC was granted to Tipping by Historic Scotland to core in one transect of 5-6 hand-sunk boreholes the sediment filling the outer ditch of the New Castle on its south side to establish whether storm-driven sediment reached this high. The base of the outer ditch by the southern bank of the outer earthwork is around 8.2m OD. The sediment fill is an organic mud, up to 80cm thick, to *c*. 9m OD. Still-water organic mud is interrupted by bands of silt and clay up to 30cm thick and to a consistent altitude of 8.50-8.60 m OD. Their origin is unknown.

The straight east and west sides of the outer earthwork, and its arcuate south bank (Figure 43) away from the rock-cut northern part have not been excavated or dated. They enclose an area of 1.9 ha. The eastern side is now a farm track, much disturbed. The ground surface east of the farm track barely falls south from 9.6 to 9.3m OD: it is assumed to be a natural surface. The NCT fill south of the south bank is at 9-9.5m OD (Figure 44). The ground surface just north of the New Castle is higher than 13m OD (Transect A-A': Figure 44). Within the outer ditch the ground surface falls south from 10.5m OD to level out at 9m OD and 9.5m OD (Transects A-A', B-B': Figure 44). The level surface is likely to be that of the sediment fill, cored in 2004 (above). Transect C-C' (Figure 44) records the altitude of the 200m long south bank of the outer earthwork. It is highest at the south east corner at 11.2m OD and much lower westward with the south west corner at 9.75m OD. If the south bank was intended to be a uniform height, which seems reasonable, it has been heavily eroded. Dumping of moat sediment by the Ministry of Works has been one disturbance but this was quite confined (Figure 43).

These altitudinal relations show that the New Castle itself is not significantly higher than the Old Castle. This does not mean that storm surges weren't a threat. The location of the New Castle was probably to take advantage of the spring-line to fill the moat (Section 2.7.1): it could not have been placed any higher up the slope. It could, thus, have been impacted by storm surges travelling several hundred metres inland. The minerogenic sediment trapped in the outer ditch could, therefore, be marine-estuarine. While the eastern and western banks of the outer earthwork are today insignicant features, but the south bank, nearest the coast, was built much higher, to more than 11m OD (Figure 44). Its erosion could have been anthropogenic – this is a castle after all. The likelihood of this might be tested by knowing the age of the outer earthwork, but there are questions concerning the chronology and function of the outer ditch from its excavation (MacIvor *et al* 1999). Only Trench II (Figure 43) described it, and that only partially. On the north west side it is an 11m wide rock-cut ditch with vertical sides 4.3m high towards the moat and 2.4m on the outside. Sediment in the outer ditch (context 506) is inadequately described as "grey-black soil with some gravel" (ibid, 155). In trench XIV a wooden bridge that crossed the outer ditch was $^{14}C$ and wiggle-match dated in 1999 at 2σ to AD1538-1613 but the bridge is later than the outer ditch. Trench XV sampled one of two projections from the primary earthwork around the moat, seen (ibid, 193) as later 16th century casements, part of a defensive circuit when the primary earthwork that ponded the moat was raised to create a high bank. "It may confidently be deduced that the outer bridge and ditch, and the high bank surrounding the castle, are contemporary one with the other" (ibid, 193), but no evidence for this was given by MacIvor: the casements are later additions to the primary earthwork. If the outer ditch is of later 16th and early 17th century age, after the recorded sieges and battles, erosion of its south bank is far more likely to have been natural, and storm surges the most likely impact. MacIvors' Trench I on the south side did not sample the outer ditch, but excavation found that the primary earthwork around the moat here had been extended southward after its initial construction by the deposition of some 3.5m of "clean sand" (ibid, 151). Since all other fills are far less 'clean', natural processes may have deposited the sand, later covered by more typical fills.

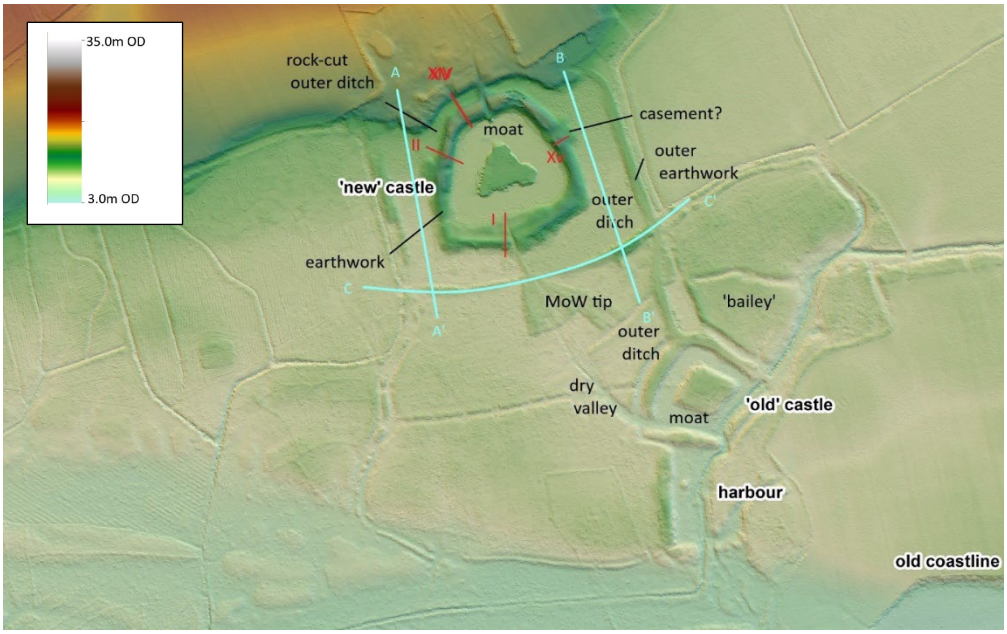


*Figure 43. Colour-contoured LiDAR image of the Old and New Castles and the surrounding ground surface. Excavated trenches I, II, XIV and XV at the New Castle (MacIvor* et al *1999) are depicted in red. LiDAR transects are in light blue. 'MoW tip' refers to the neat fan of moat sediment dumped by the Ministry of Works in the 1950s.*

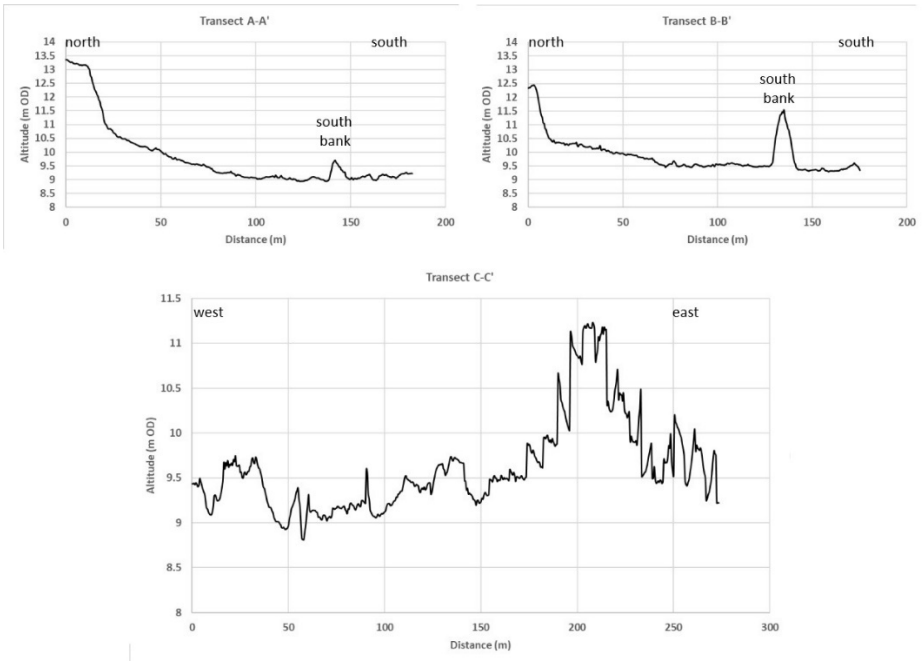


*Figure 44. LiDAR transects A-A' and B-B' from north to south across the outer ditch of the New Castle and C-C' along the south bank of the outer ditch of the New Castle.*

## 4.3. Discussion of events around the Old and New Castles

The undisturbed surface of the 'natural', the mid-Holocene New Castle Terrace (NCT) fill, is around 9m OD north of the outer ditch and west of the 'harbour' (Section 4.1.1). Around the Old Castle and its moat system, ground surfaces are higher (Figure 43: the green tinge represents surfaces at or higher than 10.0m OD). The west and north walls of the 'harbour' are a metre or so above the surface of the NCT fill. Brann (2004) recorded a metre or so of upcast overlying a buried ground surface in the north wall. The Old Castle platform reaches 10.m OD (Brann's (2004, 21) altitude of

approximately 9.3m OD is again inconsistent with LiDAR mapping). The bank separating the western moat and the outer ditch, the bank separating the northern moat from the bailey, and the bank separating the outer ditch from the basin next to the bailey reach 10.0m OD. These are all probably best seen as elevated by upcast from digging out the 'harbour' and the moat system and are probably not a natural rise in topography (cf. Brann 2004, 20). This might imply that the Old Castle platform excavated to the 'natural' (Brann 2004) may not be the 'natural: it is very hard to distinguish *in situ* from re-deposited NCT fill. There may be a buried ground surface here. Also, if the castle platform was raised by sediment from the moat system, the castle is younger than the moat system.

The bailey itself, whatever it was, also reaches 10.0m OD, higher by at least half a metre than the natural ground surface, over an area >1 hectare. If this is upcast it may represent a spread of archaeological features that Truckell (1950) tentatively explored. The deeper of two parallel ditches in the large rectangular basin next to the bailey was dug from this non-natural surface at 10m OD to around 6.8m OD (Figure 42). This was filled with peat and organic mud, not necessarily continuously, from 44 BC- AD116.

**4.3.1. High Medieval events**

1. The peats and organic muds filling the rectangular basin next to the bailey were replaced after AD1158-1265 (*c*. AD1200) by inorganic silty fine sand at 7.96m OD. The sediment is re-deposited NCT fill of unknown origin.

2. Slightly before and after AD1200-1300 sediment in the 'harbour' accumulated conformably, probably slowly and gradually, without disturbance, demonstrable hiatuses or sediment reworking (Section 4.2.1.4). The 'harbour' was not a conduit for Medieval or later storm surges (events 3, 13 and 16: below). This is very hard to explain because this is the easiest route for sea water to take in penetrating the moat system. It is probably necessary to explain this by hypothesising a barrier at the southern wall of the 'harbour' to prevent ingress of sea water during surges. There is no evidence now for such a barrier although the sediment that appears to have formed the southern wall (from one borehole: Section 4.2.1) is easily eroded and widened, and need not retain evidence.

If younger than AD 120-440, the latest time that MHWS lay at 4.6-5m OD, the sea would not have reached into the 'harbour' except during significantly high, and unpredictable, tides or surges. It could not have been a harbour. This is close to Marshall's (1961, 178) questioning of the 'harbour' as a harbour. She thought the low rock dome of Bowhouse Scar, 400m south of the 'harbour' at 4.2m OD, would have blocked passage. This is less relevant if passage was from the south west or the embayment south east of the 'harbour' (Figure 7). The inferred chronology for the formation of B5 (Section 4.1.5) is tentative, but suggests that a south west passage was blocked in the 1st millennium AD. Brann (2004) depicts from field survey, channels leading south east from the south end of the 'harbour' (Figure 30) but the LiDAR contours in Figure 25 suggest these are slight. It is not known if the embayment south east of the 'harbour' existed (above: Section 4.1.1).

Nevertheless, the Old Castle Burn exited to the sea, first in a tidal creek and later through whatever the 'harbour' was. To prevent storm surges entering, as the sedimentological evidence strongly suggests happened, the Old Castle Burn had to have been blocked or dammed. This is what the change in OSL net signal intensities just before AD1200-1300 is thought to relate to. This implies that at least in part the southern wall is a built, not natural, structure. Portable OSL analyses from sediments in boreholes along the southern wall could in future establish which parts might have accumulated conformably, naturally and where deposition was chaotic (anthropogenic), and how

wide the gap was that allowed the Old Castle Burn to drain. A good explanation for the 'bollards' on the line of the southern wall east of the Old Castle Burn (Figures 24, 40) would help here.

Blocking may have been a hasty protection from storm surges, the Old Castle Burn possibly culverted with a sluice within a built part of the southern wall, or blocking may have been an intended part of an undoubtedly artificial structure. Despite the damming of its south bank, 30cm of uniform mud continued to accumulate in the 'harbour' in Zone F after *c*. AD1250. This would have been primarily introduced in fresh water by the Old Castle Burn, the dry valley and the moat system at a time of accelerated geomorphic activity related to the building of the Old Castle, and also sea water from storm surges that impacted the moat system (cf. event 3: below).

The function of the 'harbour' remains unknown. One possibility is a fish pond, with the 'harbour' intended to hold water within it. The narrow and shallow moat system around the Old Castle would not have served this purpose as larger moat systems did elsewhere (Taylor 2000). This will have been filled with fresh water, with the location of the 'harbour' explained by its advantage in receiving water from both sources, though also downstream of any latrines at the Old Castle. The Old Castle Burn could have filled the 'harbour' to 8m OD, the altitude of the base of the shallow ditch on the northern wall of the 'harbour' and might have spilled over the southern wall if effectively dammed at its base, though incision would have been rapid unless somehow arrested.

However, salts would have leached from the surrounding NCT fill and from storm surges that still impacted the moat system (cf. event 3: below), so that salt water spilling into the 'harbour' immediately after these from the interior will have stressed the freshwater fish most popular in the Middle Ages.

Fish ponds increased in number in western Europe from the 12th century, associated with high-status settlements (Hoffmann 1996, Taylor 2000). CANMORE records 23 fish ponds in Scotland but only two are thought to be Medieval. Probable early 13th century ponds are close to but separate from the moat around Auchen Castle west of Moffat in Annandale (CANMORE ID 48391) and have been suggested below Sir John de Graham's Castle near Stirling (CANMORE ID 45283), though not proven at the latter by sediment-stratigraphic work (Tipping unpublished). The Auchen Castle example is a pair of ponds separated by a causeway, 0.14 ha in total area, compared to the 0.2 ha area of the 'harbour' at Caerlaverock. R.C. Reid (1927) excavated at Auchen Castle but did not draw the conclusion then or in 1946 that the Auchen and Caerlaverock structures were comparable in function, probably because Reid assumed Old Caerlaverock Castle had a harbour.

3. Close to its connection to the 'harbour', undated but early on in its infilling and probably close to AD1287-1342 (*c*. AD1320), fine gravel was deposited in the deeper fill of the southern moat to 6.2m OD and sand to 6.2m OD. Fine gravel was also deposited in the dry valley at 7.0m OD and in the eastern moat (Tipping *et al* 2004) to 6.3m OD. Although the depositional environment of the very coarse grained sediment at the base of the southern moat, closest to the 'harbour', has not been defined from diatoms, a coastal source is most likely (Section 4.2.3) as it is in fine gravels in other limbs of the moat, introduced by wave action from the coast. Since there is no evidence that the 'harbour' was impacted by this or later storm surges, they found another route into the moat system. The barrier-beaching event that created B5 and eroded the cliff is undated, but the scale of impact makes it comparable to this marine inundation. The barrier-beaching event probably raised the water surface to at least 9m OD (Section 4.1.6). At this altitude, surges could sweep across the level ground surface (Figure 43): evidence would be retained only in sediment traps like the moat system. The water surface in the moat system and the dry valley was at or higher than 7.9m OD, the altitude of the surface of the ridge separating southern and western moat: this can be compared to

the contemporary estimated MHWS of 4.6-5m OD. These events in two ditches were almost certainly precisely synchronous. Draining of the moat system after an inundation would have been *via* the Old Castle Burn and the 'harbour', but would have been slower and at lower rates of flow which might have been accommodated by the channel of the Old Castle Burn. The shallow ditch cut in the top of the nothern wall to 8m OD, connecting the dry valley/southern moat to the 'harbour' (Section 4.2.1) is fancied to have conveyed flood water from the moat system faster. The flows in the western moat were very unlikely to have structurally impacted the Old Castle. A greater threat may have been in the height of the storm surge, but we do not know this, only that it was above 8m OD and possibly higher than 9m OD. Whether this event provoked abandonment of the Old Castle is unclear but its apparent scale makes it feasible.

The marine inundation occurred after AD1287-1342 (*c*. AD1310) and before AD1272-1392 (*c*. AD1330). There is no mention of this event in the '*Siege of Caerlaverock'* (Scott-Giles 1960) in AD1300 (Section 2.7.1), which might indicate that the inundation post-dated the siege. Whether the event coincided with storms in the Solway Firth in 1292, 1302 or *c*. 1304 (Section 2.7.2) is unknown. The event occurred within the Medieval Climate Anomaly and before the climatic shift in western Scotland to the LIA at around AD1425. It coincides with the Wolf solar minimum AD1280-1350, which Van Vliet-Lanoë *et al* (2014b) identified as a period of frequent or severe storms in Brittany (Section 2.6). North Sea storms were prominent (Bailey 1991; Galloway 2009). It also coincides with the onset of stormy conditions in northernmost Scotland (Figure 6). Baker *et al* (2015) and Ortega *et al* (2015) reconstruct a positive NAO, but *c*. 1300 marks the beginning of a stepped decline in the former's reconstruction, with further steps at *c*. 1325 and *c*. 1400: unlike other solar minima, the Wolf minimum is not associated with a negative NAO (Anchukaitis *et al* 2019). Dawson *et al* (2007), however, thought the period from around AD1270 to AD1400 was one of low North Atlantic storminess and Alheit and Hagen (2002) inferred the period *c*. 1307-1330 to be one of weaker westerlies. The imprecision of radiocarbon dating controls at Caerlaverock does not encourage more detailed correlations, but parts of the early 14th century in western Europe were very harsh in climate, particularly in heavy rain and storms from the Atlantic and highly variable seasonal temperatures, and its impacts (Lyons 1989; Jordan 1996; Rosen 2014; Campbell 2016, 50-58; 198-208). Dawson *et al* (2007) attributed increased rainfall over western Europe to 'overheating' of western Atlantic waters which energised atmospheric circulation: warmer sea surface temperatures were prominent between 1315 and 1333. Sea surface temperatures seem not to have changed off western Scotland (Cage and Austin 2010).

4. Before AD1220-1288 (c. AD1250) the outer ditch was dug from a level natural surface of the NCT around 9m OD. The ditch was 3m wide. It ran for 65m from the 5m wide, shallow dry valley in the south, assumed to have then contained a small stream. The floor of the dry valley was maybe 1.5m below the floor of the outer ditch at around 7m OD. Where the outer ditch and the dry valley met, the north bank of the dry valley was left as a ridge at 8.25m OD. There is no source of water to the outer ditch other than the dry valley. This ridge allowed ponding of water in the outer ditch, but it also made it harder for the outer ditch to receive water from the dry valley. North of this ridge the ditch was dug deepest, almost a metre to 7.25m OD: it is <90cm deep everywhere else. It was not defensible. At its northern end, the outer ditch was dug to within 7m of the south west corner of the peat-filled basin next to the bailey. This left a narrow strip of land between the two. Today this surface is at 9.8-10.0m m OD: it was probably artificially raised above the 'natural' ground surface of the NCT fill at 9m OD.

5. The earliest $^{14}$C assay at the base of the northern moat is AD1050-1280 (*c*. AD1160). The northern moat is 30m long. It was dug to around 6.8m OD. Before AD1287-1342 (*c*. AD1300) the western

moat was dug. Although it is very likely that all four sides of the moat were dug at the same time, this cannot be demonstrated, probably because organic fractions differed between $^{14}C$ assays. The 50m long eastern moat incorporated the Old Castle Burn into it, presumably as a water source for the moat system. Its floor deepened south towards the 'harbour'. The southern moat incorporated the dry valley, also presumably a water source. Because the two stream valleys are not at right-angles to each other, the southern moat was made wider and asymmetric when it could easily have been symmetric. The north bank of the dry valley was preserved in the southern end of the western moat, as it had been in the outer ditch, with the same hydrological consequences. The 70m long western moat was dug to around 7.3m OD, 50cm higher than the northern moat.

The floor of the dry valley in the southern moat sloped down to 6.4m OD at the exit of the streams to the 'harbour'. This was around 1.8m higher than the altitude of contemporary mean high water at spring tides (MHWS). Fresh water from the streams was the only source of water to the moat system.

6. The earliest preserved fill in the outer ditch started to accumulate at AD1220-1288 (*c*. AD1250). Trees grew close to or in the ditch. Probable slumping of ditch sides had greatly slowed by AD1261-1367 (*c*.AD1310). The water in the ditch was undisturbed, still if not stagnant and fresh: water depth cannot be estimated.

The earliest preserved fill in the deepest part of the western moat started to accumulate at AD1287-1342 (*c*. AD1310). This was a thin humified peat (Bed 5). Probably slightly before this, though perhaps later than its felling date of AD1229-30, an oak timber formed part of a drawbridge over the western moat. The western moat was initially at times dry because the basal peat was humified and the upper surface of the bridge timber rotted. Water may not have entered the western moat at this time.

This was probably the time, after the moats were dug, that the corner of the southern and western moats, and probably all corners of the castle platform, were strengthened by stonework in the moat. There is no reason to think these were not part of the original architecture of the castle platform.

7. Archaeomagnetic dating in 2004 of a Phase 2/4 hearth at the Old Castle suggests firing after AD1250 and before AD1310 (Brann 2004, 24). A cut Scottish short-cross penny in circulation AD1210-1250 lay under Phase 4 cobbling. Three shards of a probable 13th century AD Syrian glass vessel come from archaeological deposits of Phase 2 on the castle platform at around 10m OD. Abandonment is not dated independent of a supposed narrative for foundation of the New Castle (Brann 2004, 37).

8. A construction date for the New Castle of *c*. AD1277 may be inferred from the dendrochronological dating of the primary bridge timbers (MacIvor *et al* 1999, 188).

9. The New Castle was besieged by Edward I in AD1300; Caerlaverock changed hands repeatedly until 1335 or 1336 (MacIvor *et al* 1999, 146).

10. In the western moat the organic content of the sediment peaked at AD1272-1388 (*c*. AD1330). In the outer ditch the same happened at AD1261-1367 (*c*. AD1310). This event too was probably synchronous. It represents high aquatic biological activity, either autogenic (successional change) or climatically induced by warm temperatures.

11. The earliest preserved peat in the western moat (Bed 6) was re-cut and a second peat formed at AD1279-1392 (*c*. AD1330).

12. At around this time (AD1281-1389; *c*. AD1335) still-water conditions in the outer ditch were disturbed as very fine to medium sand was deposited and the diatom flora changed to brackish-marine. This was a marine inundation. By *c*. AD1335 the water surface in the moat system had also risen to overtop the ridge at 7.7m OD in the outer ditch.

In the western moat increasing amounts of silt replaced organic matter after AD1272-1388 (*c*. AD1330) and before approx. AD1400. This was deposited by lower energy flows than those that delivered sand to the outer ditch at the same time. The organic mud in the Western Moat had elements of a marine-brackish diatom flora prior to AD1272-1392 (*c*. AD1330). While this may have been reworked by erosion of the NCT fill in the moat sides and floor or it may have been introduced by marine-estuarine water *via* the southern moat. The evidence at the outer ditch suggests the latter. This was a marine inundation, probably the same event as recorded in the outer ditch. It probably occurred in the latter half of the 14th century. It is not clear if this event was part of a climatic shift or was by chance. Britton (1937) and Brooks (1949) saw this period as one of heightened storminess but by then, the strength of the NAO had considerably declined (Baker *et al* 2015; Ortega *et al* 2015). Sea surface temperatures in the western Atlantic were less variable, with the last 'overheating' at 1378-80 (Dawson *et al* 2007) although sea surface temperatures off western Scotland cooled sharply in the last quarter of the century (Cage and Austin 2010). The extent of Arctic sea ice, which can intensify winter storms even within negative NAO phases (Trouet *et al* 2012), peaked at *c*. 1370 but shrank quickly after this (Campbell 2016, 207).

### 4.3.2. Later Middle Age (post *c*. AD1350) events

13. Water in the northern moat of the Old Castle that had been stagnant and undisturbed, became more oxygenated after *c*. AD1370 when the sediment surface was around 6.9m OD. The mineral content of the peat increased markedly, probably from erosion of the moat sides. What caused the erosion is not known. It may have been anthropogenic or by water forced into the moat system.

14. The second bridge at the New Castle is dated by dendrochronology to *c*. AD1370 (MacIvor *et al* 1999, 191). From this time, the earthwork which retained water in the New Castle moat was reinforced and greatly enlarged southward by the tipping of NCT fill and other material to create a broad 30m wide platform (MacIvor *et al* 1999, 191). The New Castle was further modified in the AD1450s (MacIvor *et al* 1999, 147).

15. There were small peaks in organic content in both analysed boreholes in the outer ditch from AD1327-1448 (*c*. AD1390) to AD1390-1524 (*c*. AD1460). Mineral sediment supply probably waned and quiescent conditions were established with deposition of clay-rich silt. In the western moat the diatom assemblage in Zone 3 after approx. AD1350 suggests slight freshening of the water in the moat, though with brackish forms. This is not seen in analyses at borehole 3 (2004) in the outer ditch.

### 4.3.3. Early modern events

16. In the outer ditch an extraordinary phase of quite violent deposition (and probably erosion) is recorded in sediments from AD1395-1535 (*c*. AD1460). Their accumulation, particularly of pebbles in Bed 5 must in part have been rapid if not instantaneous. There may have been more than one event, though this is not suggested by the data, and in particular by the underlying coarsening-up trend in sediments in the outer ditch that signify increasing depositional energies over a long time from AD1409-1535 (*c*. AD1470) to AD1503-1588 (*c*. AD1545). Fine gravel was deposited in the eastern moat at an altitude of 7.0-7.15m OD (Tipping *et al* 2004), perhaps in this event. The event/s represent a second marine inundation, though the brackish-marine diatom flora in Zones 3 and 4 do

not suggest that salinity was significantly reduced before c. AD1460. Diatom analyses from western moat sediments indicate only a short-lived marine influence at approx. AD1475. It is not known why there is such a contrast between the two parallel ditches, but the western moat is more protected from southerly storm surges by the ridge of upcast between the 'harbour' and the moat system. The marine inundation probably occurred in the Spörer solar minimum AD1450-1550.

17. Construction of a bridge over the outer ditch of the New Castle is $^{14}$C and wiggle-match dated to AD1538-1613 (MacIvor *et al* 1999, 193-4), re-calibrated in 2022 to AD1450-1620. The outer ditch of the New Castle itself is older but how much older is not known. It encloses a very large area to the south of the New Castle, an unnecessary shape and size for defence, unless defence from marine inundation was needed. Sediments in it are thought to contain a sedimentological signal comparable to marine-estuarine sediment around the Old Castle (Tipping unpublished 2004).

18. Water in the outer ditch once more became brackish after AD1550-1625 (*c*. AD 1590), within the trend to coarser sediments. Unless diatoms were reworked, this is a third marine inundation. It is not seen at all in western moat sediments. Its significance is uncertain.

19. After AD1516-1797 (*c*. AD1650) the inorganic silty fine sand that had accumulated, very slowly or discontinuously, in the basin next to the bailey from AD1158-1265 (*c*. AD1200), was replaced by peat. At approx. AD1600, diatoms indicate waning salinity in the western moat. Organic contents in the western moat slowly increase after approx. AD1600 but not in the outer ditch. The marine diatom *Paralia sulcata* is recorded in outer ditch sediments to AD1598-1765 (*c*. AD1680). Storm surges affecting the Old Castle moat system very likely ceased by *c*. AD1700 at the latest. In one way it is extraordinary that marine inundations in the 16th century are registered at all because the gravel spit R14 is dated by the youngest basal minerogenic fill in B6 to *c*. AD1560 (Section 4.1.5). Assuming formation of the eastern end of the spit is of this age, the moat system was by AD1560 some 200m from the coast. We do not know when R10 to R13 formed.

Sediment in the 'harbour' continued to accumulate, supplied by fresh water from the Old Castle Burn, possibly accelerated by the collapse of sluices that had ponded water in the moat system. Slight sedimentological changes in the western moat at approx. AD1600 and in the outer ditch after AD1591-1754 might, then, reflect the cessation of storm surges and abandonment of the moat system around the Old Castle.

20. Before 1634 the first Earl of Nithsdale created, within the New Castle, a new mansion decorated in the classical idiom (MacIvor *et al* 1999, 196).

21. The Old Castle Burn had completely incised through the dam made by or in the south bank of the 'harbour' before the mid-18th century when Roy's Military Survey depicted it. The earliest merse began to form before the mid-18th century.

## 4.4. Archaeological structures in Castle Wood

Figure 45a is a LiDAR LRM image of Castle Wood. It identifies positive features in red and negative features like ditches, channels and tracks in blue. Figure 44b defines the considerable evidence for archaeological structures. Some of these features have been considered by Mills, Quelch and Darrah (unpublished 2020, 44-62).


*Figure 44. A pair of LiDAR LRM images, the lower annotated to show the anthropogenic structures preserved in Castle Wood.*

Structure A is an enclosure on the level surface of the NCT fill, 15-20m west of the west bank of the 'harbour' (Brann 2004, 18; fig. 1.2) though not parallel to it. Fig. 1.2 of Brann (2004) shows the enclosure stopping at the ditched 'park pale'. He suggested that the enclosure post-dated the 'park pale'. The 'park pale' is in turn linked to the formation of beach deposits in Basin 5 which may date to the first half of the 1st millennium AD or in the high Middle Ages. Gaps in the 'park pale' are interpreted to provide access to the coast. Figure 44 shows the first of these (a), one of two tracks that descend obliquely the south bank of the 'harbour', presumably to the surface of Basin 5 after it had formed (b). The second entrance is not clear on Figure 45: it is where the west side of the enclosure changes orientation (c). This change may indicate an alteration to the existing structure. This boundary is tentatively traced across the marshy ground of Basin 5 north of the Old Castle Burn (d). It is more emphatic on the south side of Basin 5 and in the gap between Ridges 10 and 12 (e).

This boundary and the track (b) post-date peat formation in Basin 5, which was too recent to be $^{14}C$ dated (Section 4.1.10). Within the 'park pale' parallel, straight, north-south trending, post-Medieval cultivation traces overlie Structure A.

Ridge 10 is defined in Figure 44 by an irregular but continuous boundary (f) that is hard to interpret. To the east, the combined width of Ridges 12 and 13 shows a more emphatic boundary defining dry ground (g). The southern side is particularly emphasised, comparable to the sea wall across the high merse (h) but the two are offset and need not be of the same age. One slender arm of this enclosure (i) projects towards B7. This may be a trackway or a wall. Since B7 is still largely under water in the winter now, access to it in the past is most likely to have been for summer grazing. The small enclosures on Ridges 12 and 13 (j), most triangular in shape, may have been for livestock management.

To the west, R7 is crossed at right angles by nine 9-10m long parallel north-south trending boundaries, 5-6m apart, some crossing the wet ground of B4, seemingly unenclosed at their northern and southern ends (k: Figure 45). In the east there are some longer boundaries (l). These probably pre-date the woodland. R8 does not have these, despite being comparable to R7 in every way except age. Lines in the ground of Castlewood Cottage (m) are recent. North of the E-W ditch, these short north-south trending boundaries have their correlative on the western surface of R4 where they appear to be confined to the dry ground, most stopping at B3 and B2 (n). Three of these are found crossing B5 to lie on R5 (o). They cut earlier, longer, north east to south west trending boundaries on R5 and R6 (p). Their function is unknown save that they were parts of a farming landscape that was re-structured at least once. The eastern part of R4 is entirely different, showing one long east-west trending boundary (q) which stops at a N-S ditch. This change relates somehow to the lower altitude and flatter east end of R4 (Figure 21a), though how is unknown. It suggests an acute sensitivity to detail in the landscape. This less dense pattern of boundaries is possibly seen in the structures north of Basin 1 (r).

This sensitivity extends to Basin 2, north of R4. Wells (1775-6) depicts the surface as meadow and free of trees (Figure 4). It remained that way, probably because of poor drainage, until the late 19th century (Ordnance Survey 1898) when the entire surface of the peat was ploughed, broadly east-west (s) into 3-4m wide ridges and planted with deciduous trees, a very specific use for land that had resisted incorporation into the cultural landscape. The field boundaries seen on the ridges below are not found on or above Ridge 1, probably ploughed out. The NCT surface here was cut in parallel north-south trending ditches (t) and ploughed in narrower north-south ridges for forestry, something that didn't happen to the lower, always wetter, and more marginal ground. At u in Figure 45 a small, square structure overlies the ridges.

Some sense of time-depth for these disparate structures can be suggested from new dating and observations. Extensive field walls are only recorded on R4 and R7 on the earlier strandplain. R7 is not dated. R4 formed earlier and is likely to be late prehistoric in age because it is shoreward of the OSL dated B3 (Section 4.1.5). Some field walls may thus have some antiquity. Structure Q on R4 is different. It lies on a part of the ridge that may have suffered erosion in the event/s that carved out the embayment initially filled with sediments of B5 (Section 4.1.13). The extension d-e of Structure A crosses B5 and must post-date this time. The group of features e to j clinging to R10, R12 and R13, on the other hand, cannot significantly pre-date formation of these ridges, prior to the later 16th century at the earliest (Section 4.1.5). Until *c.* AD1600 the effects of the youngest storm surges seem to have impacted the moat system around the Old Castle (Section 4.3) and would have been felt more strongly on the strandplain. B7 is suggested to have been a focus for summer pasture. If

correct, this activity may pre-date the development of the much larger salt marsh of the merse before the mid-18th century.

It is probable that all these structures pre-date the dense scrubby woodland that grows today. Davies (2004) recorded oak-ash woodland, possibly managed, around the Old Castle, from the 14th century, but how extensive this was is not known. There was a wood south of the New Castle in 1640 (Fraser 1873, II, 137; MacIvor *et al* 1999, 150). However, Thomas Winter's chart of 1742 (https://maps.nls.uk/view/216444100: Moore 1983) uses the distinctive profile of the New Castle as a guide to sailors finding the deep channel of the River Nith to Dumfries: this profile would not have been seen was Castle Wood as it is today. Wells' detailed plan of Castle Wood in 1775-6 (Figure 3) depicts the area between B5 and R14 as meadow (M: Figure 3). To the west, woodland is depicted, suggesting a difference in land management perhaps caused by differential drainage: the ground between R4 and B6 is older and slightly higher. The surfaces of B5, B7 and B8 were still open when the Ordnance Survey first mapped Caerlaverock in 1856 and depicted trees growing on R12 and R13.

### 4.5. Some archaeological and archival implications of the work

1. Late Iron Age or Roman Iron Age activity has been attested for the first time from the large rectangular basin by the bailey (Section 4.2.8). Contemporary archaeological structures may be present on the bailey (Truckell 1950), which is elevated above the natural NCT ground surface. A defensive origin is unlikely fir the basin as it protects only one side of whatever was on the NCT surface to the east (Figure 25). The Old Castle Burn might be argued to protect the eastern side, but other ditches around the bailey are much smaller and shallower. The basin was not a harbour because (a) it was always enclosed and (b) its floor at 9m OD is at least 4m higher than contemporary MHWS (Section 2.3; Smith *et al* 2003a). If a harbour had been intended, it would have been in the valley of the Old Castle Burn and much deeper. Roman fishponds are known, though from villas in southern England where they probably defined high status (Locker 2007), at odds with a military setting like Caerlaverock.

2. Later prehistoric storm surges at Caerlaverock allow an understanding of the location of the Roman fortlet and fort annexe west of Castle Wood at Lantonside (Wilson 1999; CANMORE ID 66089; 66090). Rather than constructed on level ground it is perched on a slope at around 16-18m OD, above the Lantonside barrier beaches (Section 4.1.7). It may be that continuing coastal erosion and re-deposition made this a less vulnerable site.

3. On the surfaces of Basin 1 and Ridge 3 (Figure 7b) the bank and ditch of the southern side of the 'park pale' was constructed before the storm surge events that formed Basin 5 partially destroyed it. It has a clear entrance (Figure 19) allowing access to the south, to land that had some value. It is probable that this resource existed before the earliest preserved storm surge event in B5, which is not dated but may lie in the first half of the 1st millennium AD or the early 14th century.

4. Some workers have suggested a Medieval decline in salt panning on the northern Solway shore. Saltcote Hills on Blackshaw Bank, 3km east of Castle Wood, are Medieval sleeching mounds (Cranstone 2006), though when they were made is not known. Salt-panners along the inner Solway Firth are known from the 1170s (Oram 2012), specifically working the salt marsh at Caerlaverock but not recorded after AD1309 (McIntire 1942): McIntire assumed some political tension between Holm Cultram and Dundrennan Abbeys to account for this. Oram (2012) speculated that exhaustion of viable fuel sources may have provoked Melrose Abbey to shift its interests away from the inner Solway Firth in the late 13th or 14th centuries, but early modern salt-making was common (Cranstone 2006) and extensive and deep peat mosses still survive on the coast (Nichols 1967). Oram

(2012) noted the coincidence in timing of the failure of the Melrose pans with evidence for increased storminess and marine inundation. It is tempting to implicate some storm surge events, notably the formation of R10-13, perhaps, to this period.

5. Radiocarbon dating suggests that the outer ditch was cut before the western moat, perhaps a few decades earlier, though not the several hundred years suggested from $^{14}C$ assays on the humin fraction of organic matter suggested by Tipping *et al* (2004). The moat limbs were probably cut together at the same time, although this cannot be established from $^{14}C$ dating. Radiocarbon dating of the western moat suggests either that the moat system was no longer cleaned out after AD1287-1342 or that the oak timber felled in AD1229-30 was used in the drawbridge over the western moat some time, again perhaps decades, later. The Old Castle and moat system may be younger than argued by Brann (2004). How much younger is unknown: MacIvor *et al* (1999) suggested a delay of several decades between the felling of four timbers and their incorporation in the 14th century bridge 2 at the New Castle. This need not imply that the Old Castle and the New Castle were contemporary, but it makes the temporal gap smaller. MacIvor et al (1999, 188, 190) made the assumption that the New Castle followed abandonment of the Old Castle but he had no dating evidence from the Old Castle. Brann (2004) followed. Archaeomagnetic dating of the hearth in Phase 2 of the Old Castle gave age-ranges of AD1250-1310 for the first firing and AD1250-1275 (or AD1400-1440) for the last firing (Noel 2004). The most closely dated artefact retrieved from Brann's (2004) excavation is the cut Scottish short-cross penny (Bateson 2004), dated to AD1210-1250. Other less closely dated finds include a brooch from the late 13th or 14th centuries (Cox 2004, 57), a horseshoe "generally dated to the second half of the 13th century or the early part of the 14th" (ibid, 63), and Islamic glassware "from the late 12th century until 1400" (Murdoch 2004, 69) in a late phase. Circularities develop in discussion of the chronology of metalworking debris (Photos-Jones 2004, 81), which is based on the pottery (Hall 2004), which is in turn only dated by the assumed chronology of the Old Castle, which is then 'dated' by the pottery (e.g. Brann 2004, 37).

Timbers used in bridge 1 at the New Castle were felled in AD1277 (MacIvor *et al* (1999): these are not thought to have been re-used, and bridge 1 probably dates to AD1277. The earliest preserved occupation level of the New Castle contained a long-cross penny (AD1251-1272), relatively unworn and probably lost not long after 1272 at the latest.

6. A storm surge impacted the moat system of the Old Castle and the outer ditch after AD1287-1342 (*c*. AD1320) and before AD1272-1392 (*c*. AD1330). It raised the water surface around the Old Castle higher than 8m OD (event 12: Section 4.3.1): the ground floor of the Old Castle stood around 10m OD. Whether this forced abandonment is unknown: abandonment of the Old Castle itself is not dated. Of equal interest given the close proximity of the contemporary coast is why the Old Castle was built there. We do not yet understand the complete chronology of Medieval storm surges because deposits in B5 to B8 are not dated, sediments in the 'harbour' have proved interpretatively problematic with many hiatuses, and the moat system can only record storm surge events after it was dug. These mean that the frequency and scale of storm surges when the site of the Old Castle was being considered, but if they occurred, the vulnerability of the Old Castle to these was either unrecognised or its strategic position with regard to sea-lanes in the inner Solway Firth overruled this.

7. There are instances in the construction of the moat system that suggest a rather 'slap-dash' design or execution at odds with its apparent high status. One is in the way that the bank separating the 'harbour' and southern moat is not parallel to the castle platform. This leaves the southern moat asymmetrical, when it would have been easy to incorporate the dry valley into a neater design. A second is the way that the left (north) bank of the dry valley was left as an upstanding ridge at the

southern ends of the western moat and the outer ditch, so that the floors of these were not uniform when they could easily have been. These ridges may have been left in order to pond water in these ditches, although this might imply that water supply to the moat system was not reliable or that any sluice between the moat system and the 'harbour' was not reliable. But this decision rendered the ditches indefensible. Davies' (2004) pollen record from the northern moat throws up more puzzles regarding status of the Old Castle, because the land immediately around the Old Castle was full of trees, though not the possibly managed oak wood it eventually became but wetland alders and willows on poorly drained marshy ground. The appearance must have been drab, in the winter waterlogged and in the summer midge-ridden.

8. The absence of imported pottery recovered from the Old Castle excavations is also surprising if it was of high status. Hall (2004, 49) circumvented this by explaining that Caerlaverock was distant from trade routes, but a high-status site would attract trade to it. And in any case, Caerlaverock "lay at the northern terminus of an important crossing-point of the Solway" (MacIvor *et al* 1999, 144). High status seems implicit in the recovery of very rare Islamic glass (Murdoch 2004, 68-69), but this does not mean that the Old Castle was the intended destination, only that it passed through the Old Castle and went no further. That the Old Castle was not only high-status but also the home of the Maxwells pervades Brann's (2004) text, even in the description of archaeological fieldwork in Chapter 3. Thus a two-storey 'chamber block' is invoked on slender archaeological evidence with "the Maxwell's quarters at first-floor level" (p. 21). The assumed status of the site is the sole circular reason for identifying one structure a "great hall" (p. 23). Yet some details of construction on the castle platform are also slap-dash. A stone "curtain wall" at least 4.4m high was built in Phase 3 "directly onto the surface of the mound, or at best a shallow trench or terrace" (Brann 2004, 25). The Phase 4 "great hall" was not "the politest of architecture" (ibid, 29). Platt (2010) questioned whether moated sites were connected to status, suggesting that security from attack or theft was a more practical concern. Though the Old Castle pre-dates the early 14th century social stresses that Platt built his thesis around, and in its depth the moat system would not have provided much defence or protection, it may have appeared so. The argument is of some significance at Caerlaverock because the assumption that the Old Castle was equivalent in status to the New Castle drives the idea of abandonment and substitution. If the Old Castle was of lower status, serving a different function, it need not have been replaced by the New Castle.

9. The 'harbour' remains a frustrating hole in the ground. It has to be assumed that normal high tides at any time in the historic period did not reach it. This does not contradict mid-16th century archival reports that "bootes as said ys of ten tonnes will come to the foote of this hill [Wardlaw] at the full sea" (Watson 1923, 29) because the Lochar Water, east of Caerlaverock, flows at the foot of Wardlaw. Nielson (1899) also thought large ships may have moored at the mouth of the Lochar Water. Approaches to Dumfries up the much more powerful River Nith were problematic in the mid-17th century, the acerbic Thomas Tucker describing in 1655 that "The badness of coming into the river [Nith] upon whiche it [Dumfries] lyes … hinders … theyr commerce by sea, soe as whatever they have come that way is commonly and usually landed at Kirkcowbright" (Hume Browne 1891, 180).

10. There is an apparent dearth of contemporary accounts of the Medieval and later marine inundations recorded at Caerlaverock. The search for these in this study has been limited and largely confined to secondary sources (*Transactions of the Dumfries and Galloway Natural History & Antiquarian Society*; Fraser 1873; McDowall 1906; Shirley 1915, Reid (ed) 1915): Reid (1915) was editing Edgar's (*c*. 1746) history, much closer in time to the youngest storm surges, but Edgar reported nothing. Smith (2015) showed for the historic period that systematic archival searches can

yield many more reports than expected, albeit in the comparatively urban Severn estuary. Did the Caerlaverock storm surges have no lasting impact that no one described them?

## 5. Recommendations

A number of new, fruitful lines of enquiry germane to the archaeology.

1. The potential for environmental reconstruction of the peat-filled basin next to the bailey is enormous. It is shown to be of late Iron Age or Roman Iron Age date (Section 4.2.9). Roman origins for some structures around the Old Castle have been postulated (Reid 1946; Truckell 1950). We can now define activities and their durations from $^{14}C$ dated and Bayesian defined pollen analyses. When people later became interested in the site of the Old Castle can now be defined as well as what happened during castle construction itself from a site within a few metres of it. This basin is the only terrestrial deposit identified which pre-dates the Old Castle and which might contain sedimentological and diatom records of storm surges preceding the Old Castle (point 6 in Section 4.5). There is a pressing need in any case to undertake detailed diatom and pollen analyses on the minerogenic band dated between AD1158-1265 and AD1516-1797 to define its origin.

2. The south bank of the 'harbour' has become central to explanations of Medieval storm surges. Some workers have pretended it didn't exist but it did, of course, and still does. We do not know whether this bank was was part of the original structure of the 'harbour', cut from pre-existing NCT fill, whether the south bank was original but shorter, making a wider gap than at present, or whether it was an after-thought, built later, in the 13th century as argued in Section 4.3.1. LiDAR imagery shows the south bank to be more lumpy and less well made than other, more linear banks. One borehole only was cored into it (Section 4.2.1) because it is impossible visually to distinguish between *in situ* NCT fill and re-deposited NCT fill. But luminescence profiling can, quickly, easily and cheaply. *In situ* NCT fill will be dominated by a conformable profile, with declining up-profile OSL net signal intensities: sediment that has been dug and re-used in an articial structure will have a chaotic profile. To test all three reconstructions, we might take 4-5 cores along its crest and measure luminescence properties at, say, 10cm intervals, compare the cores to detect whether they are all *in situ* or all re-deposited, or whether only some are.

3. There is a need to better understand the sediments in the 'harbour' above 173cm depth (3630-3210 BC). We did not undertake quantitative sedimentological analyses of the vibrocores sampled in 2021 because the sediment is visually a uniform inorganic mud. We know that medium-coarse sand of probable marine-estuarine origin is absent in all boreholes. We might expect, however, to find some coarsening of sediment in Zones D and E (Section 4.2.1.4). With proposed blocking of the 'harbour' around AD1250, it would be useful to understand what effect this had on 'harbour' sedimentation: we might hypothesise a change to more fine-grained sediment as storm surges were excluded. Contiguous close-spaced samples might also test and define the idea that surge-generated coarse sediment drained back through the 'harbour', as it must have. Particle size characteristics should also have changed above 121cm depth when, it is hypothesised, only freshwater entered the harbour. Diatom analyses above 152cm depth, after AD1200-1300, would also test these reconstructions.

We do not know if the 'harbour' ever retained water. If the south bank was not an original part of the structure, it could not, at any time in the historic period because it was higher than the sea. It might have when the south bank was added if the south bank also blocked the Old Castle Burn at its exit. Diatom analyses would test the presence of water and its salinity. Blocking of the 'harbour' should have excluded sea water although the 'harbour' must have been the route by which saline water drained back to the sea from the interior. Very detailed diatom analyses from 'harbour' sediment after AD1200-1300 might define how many such events there had been, and also identify the last event, predicted to be in the 16th century. Geochemical analyses might also define when the

'harbour' was dry because *in situ* weathering and incipient soil formation would occur only when the 'harbour' was empty.

4. There is the need for sediment-stratigraphic work and diatom analyses of the outer ditch of the New Castle (Section 4.2.10). The moat was drained and sediments removed in the 1950s. The outer ditch was thought to date from *c*. AD1600, seemingly too late to receive estuarine-marine sediment (Section 4.3.3), but this date relates to a bridge over an earlier ditch. Tipping (unpublished 2004) reported to Historic Scotland that the outer ditch on the south side of the New Castle contained mineral sediments similar to those in ditches around the Old Castle. If confirmed and demonstrated to be estuarine-marine from diatom analyses, and dated, this would establish a higher minimum altitude for coastal floods significantly higher than possible from existing analyses.

## 6. Conclusions

1. In Castle Wood there are very well-preserved coastal landforms and sediment bodies, barrier beaches and 'lagoons', relating to severe storm surges. These formed two successive prograding strandplains. Only one remnant of a salt marsh pre-dating the storm surges survives, probably around 2500 BC in age.

2. The first strandplain began to form at a time before, probably only slighly before *c*. 200 BC, in the late Iron Age. From this time onward, relative sea level has been where it is today. The Caerlaverock strandplains were thus not formed by relative sea level fall as are all other dated strandplains in the British Isles known to the writer. Sediment supply to the coast and its reworking by storm surges were the controlling factors.

3. The barrier beaches of the first strandplain probably took the form of spits which extended east from the Nith estuary through longshore drift, which is clockwise in the inner Solway Firth. The spits cannot be traced east across the entire Caerlaverock peninsula but it is likely that they did.

4. The coarse clastic (fine sandy gravel and sand) spits received sediment from glacial and glaciofluvial sources in the lower Nith valley. These had probably begun to be eroded by the river responding to climatic or land use changes. There are at least five preserved spits. Three have 'lagoons' to shoreward. In total some 150-200m of new coast was created. Only the second is dated, by OSL to 160 ± 70 BC. Minimal AMS $^{14}$C assays on peat overlying 'lagoonal' sediment gave unrealistic results.

5. Minimal water depths in these storm surges may have been 2.5m higher than contemporary MHWS, exceeding 7m OD.

6. There is no direct evidence that salt marsh grew between the development of the first and second strandplains but the entrance through the 'park pale' on R3 hints that access was needed to coastal sediment that was destroyed by the subsequent barrier breaching event, and there is a record of salt-panners at Caerlaverock prior to AD1304 (McIntire 1942).

7. The spits and 'lagoons' of the first stranplain were then truncated by a much more energetic storm surge or surges which breached them and possibly eroded *c*. 1.5m of underlying bedrock on the foreshore, and impacted on the later prehistoric cliff, forming a beach in front of and on top of it. The surge hit the coast head-on from the south or south west. It partially destroyed archaeological structures. It had a minimum water depth of around 9m OD. The age of this event is not known. It may date to the first half of the 1st Millennium AD or around AD1300. However, it may also be the earliest event to have impacted the moat system of the Old Castle (below). A few hours or days later, a barrier beach (R10) formed shoreward of the 'harbour' and the Old Castle Burn.

8. The Old Castle Burn tidal creek had accumulated from long before this. Disturbed sediment, including erosional hiatuses, may have been caused by storm surges before and including the barrier-breaching event. One hiatus may have been created by people digging and widening the tidal creek, making the 'harbour'. However, throughout the historic period, any likely 'harbour' floor was higher than contemporary MHWS.

9. Sediment deposited in the 'harbour' in the Middle Ages shows no disturbance, only conformable, probably gradual and possibly continuous slow sedimentation. This is very problematic for what happened inland of the 'harbour' from the high Medieval period onward.

10. Later prehistoric archaeology around the Old Castle has been confirmed for the first time, a large rectangular basin, not unlike a harbour though it could not have been one. It is either late Iron Age or Roman Iron Age in date. It filled with peat and organic mud.

11. The late prehistoric basin close to the Old Castle filled with organic sediment until AD1158-1265 (*c*. AD1200) when this was replaced by an inorganic silty fine sand. We do not know but we speculate that this marked the earliest Medieval storm surge.

12. Around the Old Castle itself is a moat system and a very odd ditch, the outer ditch. It had been thought in 2004 from $^{14}$C assays on the humin fraction of peats that this ditch might be several hundred years older than the Old Castle. New Bayesian-modelled AMS $^{14}$C assays show this to be incorrect: these assays are thought to have been residual from peats that formed before the outer ditch was dug and which were transported into it by high Medieval and later storm surges.

13. The earliest preserved peat in the outer ditch is $^{14}$C dated to AD1220-1288. The assumed age of the Old Castle is AD1229-30, from dendro-chronology. The earliest preserved peat in the western moat is closely $^{14}$C dated by three assays to AD1287-1342. One interpretation of these dates is that (a) the outer ditch is very likely to be older by a few decades than the moat system of the Old Castle and (b) the Old Castle is younger than the felling date of the timber. However, it may also be that sediment in the moat system (but apparently not in the outer ditch) was cleaned out until AD1287-1342. If so, the last date-range may indicate a change in function of the Old Castle.

14. A number of archaeological and environmental factors question the assumed high status of the Old Castle.

15. At least one storm surge impacted the moat system of the Old Castle after AD1272-1388 (*c*. AD1300) and before AD1327-1448 (c. AD1390). If minerogenic sediments in the basin next to the bailey do record storm surges AD1158-1265, this event was not the first to impact the area, only the first to impact the Old Castle. It did not impact the moat system *via* the 'harbour'. The 'harbour' was there then but its exit to the sea must somehow have been blocked. The surge travelled to the moat system over the cliff and across the natural ground surface. It inundated the moat system above 8m OD: the height of its water surface is not known. If prodigiously high, this rather than strength of the flow might have encouraged abandonment, but the New Castle, though inland, is not significantly higher than the Old Castle.

15. Later storm surges are recorded impacting the moat system, between AD1395-1535 (*c*. AD1460) and approx. AD1475, and much less distinctly after AD1550-1625 (*c*. AD. 1590) and before AD1598-1765 (*c*. AD1680). It is thought that storm surges ceased to impact the Old Castle and its environs after AD1516-1797 (*c*. AD1650).

16. Some of these storm surges probably played a major part in the formation of the younger strandplain at Caerlaverock. This developed through a system of five parallel elongate barrier beaches and three 'lagoons'. These were not spits but swash-aligned storm ridges. Their age is unknown save that they post-date the barrier-breaching event in, perhaps, the 1st millennium AD and pre-date AD1560 ± 20. They may all be high Medieval and later. The indistinct character of later storm surges, detected only from their diatom floras and not from sedimentology, may be due to surges a long way south of the moat system.

17. The final barrier beach at Caerlaverock marks a return to the later prehistoric because it is an exceptionally long recurved drift-aligned spit which wraps around and protects the earlier strandplains. It formed around AD1560.

18. The development of salt marsh at Caerlaverock from before the mid-18th century was encouraged by strong south westerly winds driving sand and silt onshore. This was described by contemporaries. No one it seems wrote about the much larger events described in this report.

**Acknowledgements**

We would like to thank Historic Environment Scotland, and particularly Morvern French and Stefan Sagrott, for support and assistance in every aspect of the work, and the Trustees of the Castle Studies Trust for their generous financial support and interest. Stefan Sagrott's LiDAR imagery of Castle Wood was the catalyst to this work. The Caerlaverock Estate provided access to Castle Wood. Grateful thanks for help with fieldwork go to Valerie Bennett, Finn Thompson, Kath Usher, Richard and Laura Bates, Tim Kinnaird, Aayush Srivastava, Morvern French and Steve Farrar. Lisa Brown (HES) facilitated the $^{14}C$ dating programme and the re-assessment of archaeomagnetic dating at the Old Castle. The staff at the SUERC $^{14}C$ Laboratory, University of Glasgow) are thanked for the provision of $^{14}C$ assays. Carla Ferreira is thanked for assistance with BACON software. Tim Kinnaird and Aayush Srivastava (University of St. Andrews) provided more than just OSL age estimates. Jason Jordan (University of Coventry) supervised the diatom analyses in the Western Moat undertaken by Busie Gisanrin. Neil McDonald undertook particle size analyses from the Western Moat and the Outer Ditch. Steve Farrar (then at HES) and Andrew Burnett enthused over the interpretations.

**References**

*A Platt of the opposete Borders of Scotland to ye west marches of England.* http://www.bl.uk/onlinegallery/onlineex/unvbrit/a/001roy000018d03u00076000.html. Accessed 26/01/2022.

Alheit J. and Hagen E. 2002. Climate variability and historical NW European fisheries. *In* Wefer, G. (ed.) *Climate Development and History of the North Atlantic Realm*. Berlin: Springer-Verlag, 435-445.

Allen, J.R.L. 2000. Morphodynamics of Holocene salt marshes: a review sketch from the Atlantic and Southern North Sea coasts of Europe. *Quaternary Science Reviews* 19, 1155-1231.

Anchukaitis, K.J., Cook, E.R., Cook, B.I., Pearl, J.K., D'Arrigo, R. and Wilson, R 2019. Coupled modes of North Atlantic Ocean-atmosphere variability and the onset of the Little Ice Age. *Geophysical Research Letters*, 46 (21), 12417-12426. https://doi.org/10.1029/2019GL08435

Armstrong, R.B. 1883. *The history of Liddesdale, Eskdale, Wauchopdale and the Debatable Land*. Edinburgh.

Ashmore, P. 1999. Radiocarbon dating: avoiding errors by avoiding mixed samples. *Antiquity* 73, 124-130.

Axelsson, M., Dewey, S., Tourell, A. and Karpouzli, E. 2006. Site condition monitoring—the sublittoral sandbanks of the Solway Firth. *Scottish Natural Heritage Commissioned Report* 155. Inverness: Scottish Natural Heritage.

Bailey, M. 1991. *Per impetum maris*: natural disaster and economic decline in eastern England, 1275-1350. *In* Campbell, B.M.S. (ed.) *Before the Black Death. Studies in the 'crisis' of the early 14th century*. Manchester: University Press, 184-208.

Bailey, S.D., Wintle, A.G., Duller, G.A.T. and Bristow, C.S. 2001. Sand deposition during the last Millennium at Aberffraw, Anglesey, North Wales as determined by OSL dating of quartz. *Quaternary Science Reviews* 20 (5–9), 701–704.

Bailiff, I.K., French, C.A. and Scarre, C.J. 2013. Application of luminescence dating and geomorphological analysis to the study of landscape evolution, settlement and climate change on the Channel Island of Herm. *Journal of Archaeological Science* 41, 890-903.

Baillie, M.G.L. 1977. An oak chronology for south central Scotland. *Tree-Ring Bulletin* 37, 33-44.

Baker, A., Caseldine, C.J., Gilmour, M.A., Charman, D., Proctor, C.J., Hawkesworth, C.J. and Phillips, N. 1999. Stalgmite luminescence and peat humification records of palaeomoisture for the last 2500 years. *Earth and Planatery Science Letters* 165, 157-162.

Baker, A., Hellstrom, J.C., Kelly, B.F.G., Mariethos, G. and Trouet, V. 2015. A composite annual-resolution stalagmite record of North Atlantic climate over the last three millennia. *Scientific Reports* 5, 10307; doi: 10.1038/srep10307. (https://www-nature-com.ezproxy.stir.ac.uk/articles/srep10307).

Ball, T., Edwards, A. and Werritty, A. 2014. Coastal flooding in Scotland: towards national-level hazard assessment. *Natural Hazards* 70, 1133-1152.

Bampton, M., Kelley, A., Kelley, J., Jones, M. and Bigelow, G. 2017. Little Ice Age catastrophic storms and the destruction of a Shetland Island community. *Journal of Archaeological Science* 87, 17-29.

Barlow, N.L.M., Long, A.J., Saher, M.H., Gehrels, W.R., Garnett, M.H. and Scaife, R.G. 2014. Salt-marsh reconstructions of relative sea-level change in the North Atlantic during the last 2000 years. *Quaternary Science Reviews* 99, 1-16.

Bateman, M.D. and Godby, S.P. 2004. Late-Holocene inland dune activity in the UK: a case study from Breckland, East Anglia. *The Holocene,* 14 (4), 579-588.

Bateson, D. 2004. Coin. *In* Brann, M. *Excavations at Caerlaverock Old Castle, Dumfries and Galloway, 1998-9*. Dumfries: Dumfries and Galloway Natural History and Antiquarian Society, 68.

Bellhouse R.L. 1962. Moricambe in Roman times and Roman sites along the Cumberland coast. *Transactions of the Cumberland & Westmorland Antiquarian & Archaeological Society* 62, 56-72.

Billeaud, I., Tessier, B. and Lesueur, P. 2009. Impacts of Late Holocene rapid climate changes as recorded in a macrotidal coastal setting (Mont-Saint-Michel Bay, France). *Geology* 37, 1031–1034.

Bjorck, S. and Clemmensen, L.B. 2004. Aeolian sediment in raised bog deposits, Halland, SW Sweden: a new proxy record of Holocene winter storminess variation in southern Scandinavia? *The Holocene* 14 (5), 677-688.

Blaauw, M. and Christen, J.A. 2011. Flexible paleoclimate age-depth models using an autoregressive Gamma process. *Bayesian Analysis* 6, 1-18.

Bond, G., Showers, W., Cheseby, M., Lotti, R., Almasi, P., deMenocal, P., Priore, P., Cullen, H., Hajdas, I. and Bonani, G. 1997. A pervasive millennial-scale cycle in North Atlantic Holocene and glacial climates. *Science* 278, 1257-1266.

Borja, F., Zazo, C., Dabrio, C.J., Dı´az del Olmo, F. Goy, J.L. and Lario, J. 1999. Holocene aeolian phases and human settlements along the Atlantic coast of southern Spain. *The Holocene* 9 (3), 333-339.

Brampton, A.H., Lees, R.G. and Ramsay, D.L. 1999. The coastal cells of Scotland and their application. *In* Baxter, J.M. *et al*. (eds) *Scotland's Living Coastline*. London: The Stationery Office, 69-78.

Brann, M. 2004. *Excavations at Caerlaverock Old Castle, Dumfries and Galloway, 1998-9*. Dumfries: Dumfries and Galloway Natural History and Antiquarian Society.

Brażdil, R., Pfister, C., Wanner, C., von Storch, H. and Luterbacher, J. 2005. Historical climatology in Europe – the state of the art. *Climatic Change* 70 (3), 363-430.

Bridges, P.H. and Leeder, M.R. 1976. Sedimentary model for intertidal mudflat channels, with examples from the Solway Firth, Scotland. *Sedimentology* 23, 533-552.

Bridson, R.H. 1979. Saltmarsh: its accretion and erosion at Caerlaverock National Nature Reserve, Dumfries. *Transactions of the Dumfries & Galloway Natural History and Antiquarian Society* 55, 60-67.

British Geological Survey 2005. *Solway West*. Scotland Special Sheet. Superficial Deposits and Simplified Bedrock. 1:50 000 Geology Series. Keyworth, Nottingham: British Geological Survey.

Britton, C.E. 1937. *A Meteorological Chronology to A.D. 1450*. Geophysical Memoirs No. 70. London: HMSO for Meteorological Office.

Bronk Ramsey, C. 2009. Bayesian analysis of radiocarbon dates. *Radiocarbon* 51 (1), 337-360.

Brookfield, M.E. 1979. Anatomy of a Lower Permian aeolian sandstone complex, Southern Scotland. *Scottish Journal of Geology* 15, 81-96.

Brookfield M.E. 1980. Permian intermontane basin sedimentation in southern Scotland. *Sedimentary Geology* 27,167–194.

Brookfield, M., Merritt, J.W. and McMillan, A. 2010. The Powfoot boulder pavement. *In* Livingstone, S.J., Evans, D.J.A. and Ó Cofaigh, C. (eds) *The Quaternary of the Solway Lowlands and Pennine Escarpment – Field Guide*. South Wales: Quaternary research Association, 113-116.

Brooks, C.E.P. 1949. *Climate Through the Ages*. London: Ernest Benn. 2nd Edition.

Brown, M. unpublished. *"The Seate and Stait of Carlaverok: The Castle in its Setting*. Report to Historic Environment Scotland.

Brown, N. 2001. *History and Climate Change*. A Eurocentric perspective. London: Routledge.

Brown, P.J. 2015. Coasts of catastrophe? The incidence and impact of aeolian sand on British medieval coastal communities. *European Journal of Post Classical Archaeologies* 5, 127-148.

Brown, P.J. 2019. *Weathering a Medieval Climate: Gauging the impact of natural hazards on northern European society through archaeology and history, AD 1000-1550*. Durham theses, Durham University. Available at Durham E-Theses Online: http://etheses.dur.ac.uk/13194/

Büntgen, U., Tegel, W., Nicolussi, K., McCormick, M., Frank, D., Trouet, V., Kaplan, J.O., Herzig, F., Heussner, K-A., Wanner, H., Luterbacher, J. and Esper, J. 2011. 2500 Years of European climate variability and human susceptibility. *Science* 331, 578-582.

Büntgen, U., Myglan, V.S., Charpentier Ljunqusit, F., McCormick, M., di Cosmo, N., Sigl, M., Jungclaus, J., Wagner, S., Krusic, P.J., Esper, J., Kaplan, J.O., de Vaan, M.A.C., Luterbacher, J., Wacker, L., Tegel, W. and Kirdyanov, A.V. 2016. Cooling and societal change during the Late Antique Little Ice Age from 536 to around 660 AD. *Nature Geoscience* 9, 231-236.

Burn, M. and Palmer, S. 2015. Atlantic hurricane activity during the last millennium. *Scientific Reports* 5**,** 12838. https://doi.org/10.1038/srep12838

Cage, A.G. and Austin, W.E.N. 2010. Marine climate variability during the last millennium: The Loch Sunart record, Scotland, UK. *Quaternary Science Reviews* 29 (13-14), 1633-1647.

Campbell, B.M.S. 2016. *The great transition. Climate, disease and society in the late-medieval world*. Cambridge: Cambridge University Press.

CANMORE. National Record of the Historic Environment. https://canmore.org.uk/

Carter, R.W.G. 1983. Raised coastal landforms as products of modern process variations and their relevance in eustatic sea level studies: examples from eastern Ireland. *Boreas* 12, 167-182.

Carter, R.W.G. and Orford, J.D. 1981. Overwash processes along a gravel beach in southeast Ireland. *Earth Surface Processes and Landforms* 6, 413--426.

Carter, R.W.G. and Orford, J.D. 1984. Coarse clastic barrier beaches: a discussion of the distinctive dynamic and morphosedimentary characteristics. *Marine Geology* 60, 377-389.

Carter, R.W.G. and Orford, J.D. 1988. Conceptual model of coarse clastic barrier formation from multiple sediment sources. *Geographical Review* 78, 221-39.

Carter, R.W.G., Johnston, T.W., McKenna, J. and Orford, J.D. 1987. Sea-level, sediment supply and coastal changes: examples from the coast of Ireland. *Progress in Oceanography* 18, 79–101.

Carter, R.W.G., Forbes, D.L., Jennings, S.C., Orford, J.D., Shaw, J. and Taylor, R.B. 1989. Barrier and lagoon evolution under differing relative sea-level regimes: examples from Ireland and Nova Scotia. *Marine Geology* 88, 221-242.

Chambers, R. 1855. *Domestic Annals of Scotland*. Edinburgh: W. & R. Chambers (Abridged).

Charman, D.J., Blundell, A., Chiverrell, R.C., Hendon, D. and Langdon, P.G. 2006. Compilation of non-annually resolved Holocene proxy climate records: stacked Holocene peatland palaeo-water table reconstructions from northern Britain. *Quaternary Science Reviews* 25, 336-350.

Clare T. 2004. Coastal change and the western end of Hadrian's Wall. *In* Wilson, R.J.A. and Careura, I.D. (eds) *Romans and the Solway. Essays in Honour of Richard Bellhouse*. Kendal: Cumberland & Westmorland Antiquarian and Archaeological Society, 39-51.

Clarke, M.L. and Rendell, H.M. 2006. Effects of storminess, sand supply and the North Atlantic Oscillation on sand invasion and coastal dune accretion in western Portugal. *The Holocene*, 16 (3), 341-355.

Clarke M.L. and Rendell, H.M. 2009. The impact of North Atlantic storminess on western European coasts: A review. *Quaternary International* 195 (1–2), 31-41. https://doi.org/10.1016/j.quaint.2008.02.007

Clarke, M., Rendell, H., Tastet, J-P., Clave, B. and Masse, L. 2002. Late Holocene sand invasion and North Atlantic storminess along the Aquitaine coast, southwest France. *The Holocene* 12, 231-238.

Clemmensen, L.B., Murray, A., Heinemeier, J. and de Jong, R. 2009. The evolution of Holocene coastal dunefields, Jutland, Denmark: A record of climate change over the past 5000 years. *Geomorphology* 105, 303-313.

Comber, P.M. 1993. *Shoreline response to relative sea level change, Culbin Sands, Northeast Scotland*. Unpublished PhD Thesis, University of Glasgow.

Comber, P.D. 1995. Culbin Sands and the Bar. *Scottish Geographical Magazine* 111 (1), 54-57.

Cook, E.R. 2003. Multi-proxy reconstructions of the North Atlantic Oscillation (NAO) Index: a critical review and a new well-verified winter NAO index reconstruction back to AD1400. *Geophysics Monograph* 134, 63-79.

Cook, E. R., Seager, R., Kushnir, Y., Briffa, K. R., Büntgen, U., Frank, D., Krusic, P. J., Tegel, W., van der Schrier, G., Andreu-Hayles, L., Baillie, M., Baittinger, C., Bleicher, N., Bonde, N., Brown, D., Carrer, M., Cooper, R., Čufar, K., Dittmar, C., ... Zang, C. 2015. Old World megadroughts and pluvials during the Common Era. *Science Advances* 1 (10), 1-9. https://doi.org/10.1126/sciadv.1500561

Cooper, J.A.G. and Jackson, D.W.T. 1999. Wave spray-induced sand transport and deposition during a coastal storm, Magilligan Point, Northern Ireland. *Marine Geology* 161 (2–4), 377-383.

Cooper, J.A.G., Jackson, D.W.T., Navas, F., McKenna, J. and Malvarez, G. 2004. Identifying storm impacts on an embayed, high-energy coastline: examples from western Ireland. *Marine Geology* 210, 261-280.

Costa, P.J.M., Dawson, S., Ramalho, R.S., Engel, M., Dourado, F., Bosnic,I. and Andrade, C. 2021. A review on onshore tsunami deposits along the Atlantic coasts. *Earth-Science Reviews* 212, 103441. https://doi.org/10.1016/j.earscirev.2020.103441.

Costas, S., Naughton, F., Goble, R. and Renssen, H. 2016. Windiness spells in SW Europe since the last glacial maximum. *Earth and Planetary Science Letters* 436, 82-92. https://doi.org/10.1016/j.quascirev.2012.03.008

Cox, A. 2004. Copper-alloy objects. *In* Brann, M. *Excavations at Caerlaverock Old Castle, Dumfries and Galloway, 1998-9*. Dumfries: Dumfries and Galloway Natural History and Antiquarian Society, 57-61.

Cracknell B.E. 2005. '*Outrageous Waves'. Global Warming and Coastal Change in Britain through Two Thousand Years*. London: Phillimore.

Cranstone, D. 2006. *Solway Salt Project 2005-6*. Unpublished.

Cunningham, A.C., Bakker, M.A.J., van Heteren, S., van der Valk, B., van der Spek, A.J.F., Schaart, D.R. and Wallinga, J. 2011. Extracting storm-surge data from coastal dunes for improved assessment of flood risk. *Geology* 39 (11), 1063-1066.

Cunningham, L.K., Austin, W.E.N., Knudsen, K.L., Eiriksson, J., Scourse, J.D., Wanamaker, A.D., Butler, P.G., Cage, A.G., Richter, T., Husum, K., Hald, M., Andersson, C., Zorita, E., Linderholm, H.W., Gunnarson, B.E., Sicre, M-A., Sejrup, H.P., Jiang, H. and Wilson, R.J.S. 2013. Reconstructions of surface ocean conditions from the northeast Atlantic and Nordic seas during the last millennium. *The Holocene* 23 (7), 921-935. https://doi.org/10.1177/0959683613479677

Davies, A.L. 2004. Medieval and later vegetational history around Caerlaverock Old Castle. *In* Brann, M. *Excavations at Caerlaverock Old Castle, Dumfries and Galloway, 1998-9*. Dumfries: Dumfries and Galloway Natural History and Antiquarian Society, 109-112.

Dawson, A.G., Dawson, S., Cressey, M., Bunting, J., Long, D. and Milburn, P. 1999. Newbie Cottages, Inner Solway Firth: Holocene relative sea level changes. *In* Tipping, R.M. (ed) *The Quaternary of Dumfries and Galloway. Field Guide.* London: Quaternary Research Association, 98-104.

Dawson, A.G., Elliott, L., Mayewski, P., Lockett, P., Noone, S., Hickey, K., Holt, T., Wadhams, P. and Foster, I. 2003. Late-Holocene North Atlantic climate 'seesaws', storminess changes and Greenland ice sheet (GISP2) palaeoclimates. *The Holocene* 13, 381-392.

Dawson, A.G., Elliott, L., Noone, S., Hickey, K., Holt, T., Wadhams, P. and Foster, I. 2004. Historical storminess and climate 'see-saws' in the North Atlantic region. *Marine Geology* 210, 247-259.

Dawson, A.G., Hickey, K., McKenna, J. and Foster, I.D.L. 1997. A 200-year record of gale frequency, Edinburgh, Scotland: possible link with high-magnitude volcanic eruptions. *The Holocene* 7 (3), 337-341.

Dawson, A.G., Hickey, K., Mayewski, P.A. and Nesje, A. 2007. Greenland (GISP2) ice core and historical indicators of complex North Atlantic climate changes during the fourteenth century. *The Holocene* 17 (4), 427-434.

Dawson, A.G., Smith, D.E. and Dawson, S. 2001. *Potential impacts of climate change on sea level around Scotland*. Perth: Scottish Natural Heritage, Research, Survey and Monitoring Report, No. 178.

Dawson, S., Smith, D.R., Jordan, J. and Dawson, A.G. 2004. Late Holocene coastal sand movements in the Outer Hebrides, N.W. Scotland. *Marine Geology* 210, 281-306.

Dawson, S., Dawson, A.G.and Jordan, J.T. 2011. North Atlantic climate change and Late Holocene windstorm activity in the Outer Hebrides, Scotland. *In* Griffiths, D. & Ashmore, P.A. (eds) *Aeolian Archaeology: The Archaeology of Sand Landscapes in Scotland*. Scottish Archaeological Internet Report 48, 25-36.

Delaney C. and Devoy, R. 1995. Evidence from sites in Western Ireland of late Holocene changes in coastal environments. *Marine Geology* 124, 273-287.

Devoy, R.J.N., Delaney, C., Carter, R.W.G. and Jennings, S.C. 1996. Coastal stratigraphies as indicators of environmental changes upon European Atlantic coasts in the late Holocene. *Journal of Coastal Research*, 12, 564-588.

Donnelly, J.P., Butler, J., Roll, S., Wengren, M. and Webb, T III. 2004. A backbarrier overwash record of intense storms from Brigantine, New Jersey. *Marine Geology* 210, 107-121.

Donnelly, C., Kraus, N. and Larson, M. 2006. State of knowledge on measurement and modeling of coastal overwash. *Journal of Coastal Research* 22, 965–991.

Dugmore, A.J., Borthwick, D.M., Church, M.J., Dawson, A., Edwards, K.J., Keller, C., Mayewski, P., McGovern, T.H., Mairs, K-A. and Sveinbjarnardottir, G. 2007. The role of climate in settlement and landscape change in the North Atlantic Islands: An assessment of cumulative deviations in high-resolution proxy climate records. *Human Ecology* 35**,** 169–178. https://doi.org/10.1007/s10745-006-9051-z

Dumayne, L. and Barber, K.E. 1994. The impact of the Romans on the environment of northern England: pollen data from three sites close to Hadrian's Wall. *The Holocene* 4, 165-173.

Dunbar, E., Cook, G.T., Naysmith, P., Tripney, B.G. and Xu, S. 2016. AMS $^{14}$C dating at the Scottish Universities Environmental Research Centre (SUERC) Radiocarbon Dating Laboratory. *Radiocarbon* 58 (1), 9-23.

Dyer, K.R., Christie, M.C. and Wright, E.W. 2000. The classification of intertidal mudflats. *Continental Shelf Research* 20, 1039-1060.

Eiríksson,J., Bára Bartels-Jónsdóttir,H., Cage, A.G., Gudmundsdóttir, E.R., Klitgaard-Kristensen, D., Marret, F., Rodrigues, T., Abrantes, F., Austin, W.E.N., Jiang, H., Knudsen, K-L. and Sejrup, H-P. 2006. Variability of the North Atlantic Current during the last 2000 years based on shelf bottom water and sea surface temperatures along an open ocean/ shallow marine transect in western Europe. *The Holocene* 16 (7), 1017- 1029.

Evans, D.J.A., Livingstone, S.J., Vieli, A. and Ó Cofaigh, C. 2009. The palaeoglaciology of the central sector of the British and Irish Ice Sheet: reconciling glacial geomorphology and preliminary ice sheet modelling. *Quaternary Science Reviews* 28, 737-757.

Faust, J.C., Fabian, K., Milzer, G., Giraudeau, J. and Knies, J. 2016. Norwegian fjord sediments reveal NAO related winter temperature and precipitation changes of the past 2800 years. *Earth and Planetary Science Letters* 435, 84-93. https://doi.org/10.1016/j.epsl.2015.12.003

Firth, C.R., Smith, D.E., Hansom, J.D. and Pearson, S.G. 1995. Holocene spit development on a regressive shoreline, Dornoch Firth, Scotland. *Marine Geology* 124 (1–4), 203-214. https://doi.org/10.1016/0025-3227(95)00041-V

Firth, C.R., Collins, P.E.F. and Smith, D.E. 2000. *Focus on Firths: Coastal Landforms, Processes and Management Options. V. The Solway Firth*. SNH Review No. 128. Edinburgh: Scottish Natural Heritage.

Fitton, J.M., Hansom, J.D. and Rennie, A.F. 2016. A national coastal erosion susceptibility model for Scotland. *Ocean & Coastal Management* 132, 80-89. https://doi.org/10.1016/j.ocecoaman.2016.08.018

Fletcher, M. and Miller, I. 1997. Recent archaeological work on the Holm Cultram sea dyke, Skinburness, Cumbria. *Transactions of the Cumberland & Westmorland Antiquarian & Archaeological Society* 97, 203-216.

Forbes, D.L., Orford, J.D., Carter, R.W.G., Shaw, J. and Jennings, S.C. 1995. Morphodyamic evolution, self-organization, and instability of coarse-clastic barriers on paraglacial coasts. *Marine Geology* 126, 63–85.

Fraser, G.W. 1873. *The Book of Carlaverock. Memoirs of the Maxwells, Earls of Nithsdale, Lords Maxwell and Herries*. Edinburgh: Privately Printed. https://digital.nls.uk/jacobite-prints-and-broadsides/archive/75242024#?c=0&m=0&s=0&cv=498&xywh=-1061%2C-172%2C4621%2C3425. Accessed 23/01/22.

Fridlington, M.A. 1998. Radiometric depositional history of the Solway Firth, UK. *Radioprotection–Colloques* 32 (3), 293-298.

Fruergaard M., Andersen T.J., Johannessen P.N., Nielsen, L.H. and Pejrup, M. 2013. Major coastal impact induced by a 1000-year storm event. *Scientific Reports* 3, 1051.

Galloway, J.A. 2009. Storm flooding, coastal defence and land use around the Thames estuary, *c*.1250-1450. *Journal of Medieval History* 35, 171-188.

Garbutt, P.A. 1993. *Ituna: a model of the Solway Firth*. Lowestoft: Directorate of Fisheries Research.

Garcia-Oliver, M., Tabor, G. and Djordjevic, S. 2014. Modelling the impact of tidal farms on flood risk in the Solway Firth estuary. *Proceedings of the 2nd International Conference on Environmental Interactions of Marine Renewable Energy Technologies (EIMR2014)*, 1-3.

Gehrels, W.R. and Shennan, I. 2015. Sea level in time and space: revolutions and inconvenient truths. *Journal of Quaternary Science* 30 (2), 131-143.

Geological Survey of Scotland 1879. *1:63360 Series Sheet 6: Annan (Solid).* https://largeimages.bgs.ac.uk/iip/mapsportal.html?id=1001406. Accessed 12/01/22.

Gilbertson, D.D., Schwenninger, J-L., Kemp, R.A. and Rhodes, E.J. 1999. Sand-drift and soil formation along an exposed North Atlantic coastline: 14,000 years of diverse geomorphological and human impacts. *Journal of Archaeological Science* 26, 439-469.

Glueck, M.F. and Stockton, C.W. 2001. Reconstruction of the NAO, 1429-1983. *International Journal of Climatology* 21, 1453-1465.

Gordon, J. 1845a (ed.) *The New Statistical Account of Scotland / by the ministers of the respective parishes, under the superintendence of a committee of the Society for the Benefit of the Sons and Daughters of the Clergy.* Cummertrees, Dumfries, Vol. 4, Edinburgh: Blackwoods and Sons, 1845, p. 244. University of Edinburgh, University of Glasgow. (1999) The Statistical Accounts of Scotland online service: https://stataccscot.edina.ac.uk:443/link/nsa-vol4-p244-parish-dumfries-cummertrees

Gordon, J. 1845b (ed.) *The New Statistical Account of Scotland / by the ministers of the respective parishes, under the superintendence of a committee of the Society for the Benefit of the Sons and Daughters of the Clergy.* New Abbey, Kirkcudbright, Vol. 4, Edinburgh: Blackwoods and Sons, 1845, p. 345. University of Edinburgh, University of Glasgow. (1999) The Statistical Accounts of Scotland online service: https://stataccscot.edina.ac.uk:443/link/nsa-vol4-p244-parish-kirkcudbright-new_abbey

Gordon, J. 1845c (ed.) *The New Statistical Account of Scotland / by the ministers of the respective parishes, under the superintendence of a committee of the Society for the Benefit of the Sons and Daughters of the Clergy.* Graitney, Dumfries, Vol. 4, Edinburgh: Blackwoods and Sons, 1845, p. 263. University of Edinburgh, University of Glasgow. (1999) The Statistical Accounts of Scotland online service: https://stataccscot.edina.ac.uk:443/link/nsa-vol4-p263-parish-dumfries-graitney

Goslin, J. and Clemmensen, L.B. 2017. Proxy records of Holocene storm events in coastal barrier systems: storm-wave induced markers. *Quaternary Science Reviews* 174, 80–119.

Goslin, J., Fruergaard, M., Sander, L., Gałka, M., Menviel, L., Monkenbusch, J., Thibault, N. and Clemmensen, L.B., 2018. Holocene centennial to millennial shifts in North Atlantic storminess and ocean dynamics. *Scientific Reports* 8, 1–12.

Graham, A. and Truckell, A.E. 1976-7. Harbours in the Solway Firth. *Transactions of the Dumfries and Galloway Natural History and Antiquarian Society* 3rd Series 52, 109-142.

Graham, N.E., Ammann, C.M., Fleitmann, D., Cobb, K.M. and Luterbacher, J. 2011. Support for global climate reorganization during the "Medieval Climate Anomaly". *Climate Dynamics* 37, 1217-1245.

Grainger, F. and Collingwood, W.G. 1929. *Register and Records of Holm Cultram*. Kendal: T. Wilson and Sons. https://www.british-history.ac.uk/n-westmorland-records/vol7/pp136-148

Griffiths, D. 2015. Medieval coastal sand inundation in Britain and Ireland. *Medieval Archaeology* 59 (1), 103-121.

Grose, F. 1797. *The Antiquities of Scotland*. London: Hooper and Wigstead. (Vol 1).

Haigh, I., Wadey, M., Wahl, T., Ozsoy, O., Nicholls, R.J., Brown, J.M., Horsburgh, K. and Gouldby, B. 2016. Spatial and temporal analysis of extreme sea level and storm surge events around the coastline of the UK. *Science Data* 3**,** 160107. https://doi.org/10.1038/sdata.2016.107

Hall, D.W. 2004. The pottery. *In* Brann, M. *Excavations at Caerlaverock Old Castle, Dumfries and Galloway, 1998-9*. Dumfries: Dumfries and Galloway Natural History and Antiquarian Society, 47-56.

Hansom, J.D. 1999. The coastal geomorphology of Scotland: options for coastal management. *In* Baxter, J.M. *et al* (eds) *Scotland's Living Coastline*. London: The Stationery Office, 34-44.

Hansom, J.D. 2001. Coastal sensitivity to environmental change: a view from the beach. *Catena* 42, 291-305.

Hansom, J.D. 2003. Morrich More, Ross and Cromarty (NH 803 835-NH 892 830). *In* May, V.J. and Hansom, J.D. (eds), *Coastal Geomorphology of Great Britain*. Geological Conservation Review Series No. 28. Peterborough, Joint Nature Conservation Committee, 576- 583.

Hansom, J.D. 2021. Beaches and dunes of the Moray Firth coast. *In* Ballantyne, C.K. and Gordon, J.E. (eds) *Landscapes and Landforms of Scotland*. World Geomorphological Landscapes. Springer, Cham. https://doi.org/10.1007/978-3-030-71246-4_22

Hansom, J.D. and Hall, A.M. 2009. Magnitude and frequency of extra-tropical North Atlantic cyclones: A chronology from cliff-top storm deposits. *Quaternary International* 195 (1-2), 42-52.

Hansom, J.D. and McGlashan, D.J. 2004. Scotland's coast: understanding past and present processes for sustainable management. *Scottish Geographical Journal* 120 (1), 99-116.

Harrison, J. 1997. Central and southern Scotland. *In* Wheeler, D. and Mayes, J. (eds) *Regional Climates of the British Isles*. London: Routledge, 205-227.

Harvey, M.M. 2000. *Geomorphological controls on the sedimentation patterns of, and distribution of anthropogenic radionuclides in, coastal saltmarshes, south-west Scotland*. Unpublished PhD. Thesis, University of Glasgow.

Harvey, M.M. and Allan, R.K. 1998. The Solway Firth saltmarshes. *Scottish Geographical Magazine* 114, 42-45.

Haslett, S.K. and Bryant, E.A. 2007. Reconnaissance of historic (post-AD 1000) high-energy deposits along the Atlantic coasts of southwest Britain, Ireland and Brittany, France. *Marine Geology* 242, 207–220.

Haslett, S.K. and Bryant, E.A. 2008. Historic tsunami in Britain since AD 1000: a review. *Natural Hazards and Earth System Science*, 8, 587–601.

Hickey, K.R. 1997. *Documentary Records of Coastal Storms in Scotland, 1500-1991 AD.* Unpublished Ph D Thesis, Coventry University.

Hodgson, J.M. 1974. *Soil Survey Field Handbook*. Harpenden: Lawes Agricultural Trust.

Hoffmann, R.C. 1996. Economic development and aquatic ecosystems in Medieval Europe. *American Historical Review* 101, 630-669.

Hough, C. 2020. Place-Name evidence for the etymology of Scots *Carse*. *Notes and Queries* 67 (1), March 2020, Pages 31–32. https://doi-org.ezproxy-s1.stir.ac.uk/10.1093/notesj/gjz162

Hughes, R. 1995. *A synoptic account of the revision of the Scottish 1:50,000 series Sheet 6W (Kirkbean), with a summary of the Flandrian history*. BGS Technical Report WA/95/21.

Hume Brown, P. 1891. *Early Travellers in Scotland*. Edinburgh: David Douglas.

Hurrell, J.W. 1995. Decadal trends in the North Atlantic Oscillation: regional temperatures and precipitation. *Science* 269, 676-679.

Jackson, D.W.T., Costas, S. and Guisado-Pintado, E. 2019. Large-scale transgressive coastal dune behaviour in Europe during the Little Ice Age. *Global and Planetary Change* 175, 82-91. https://doi.org/10.1016/j.gloplacha.2019.02.003

James, A. unpublished. *Caerlaverock*. Report to Historic Environment Scotland.

Jardine, W.G. 1975. Chronology of Holocene marine transgression and regression in south-western Scotland. *Boreas* 4, 173-96.

Jardine, W.G. 1980. Holocene raised coastal sediments and former shorelines of Dumfriesshire and eastern Galloway. *Transactions of the Dumfries & Galloway Natural History and Antiquarian Society* 55, 1-59.

Jong, R. de, Bjorck, S., Bjorkman, L. and Clemmensen, L.B. 2006. Storminess variation during the last 6500 years as reconstructed from an ombrotrophic peat bog in Halland, southwest Sweden. *Journal of Quaternary Science* 21 (8), 905-919.

Jong, R. de, Schoning, K. and Bjorck, S. 2007. Increased aeolian activity during humidity shifts in a raised bog in south-west Sweden during the past 1700 years. *Climates of the Past Discussions* 3, 383-408.

Jones, G.D.B. 1980. Archaeology and coastal change in the north-west. *In* Thompson, F.H. (ed.) *Archaeology and Coastal Change*. London: Society of Antiquaries, 87-102.

Jordan, W.C. 1996. *The great famine: Northern Europe in the early fourteenth century*. Princeton: Princeton University Press.

Kington, J. 1988. *The weather of the 1780s over Europe*. Cambridge: Cambridge University Press.

Kontrowitz, M. and Griffiths, H. 2009. Ostracods from the wet moat at Caerlaverock Castle. *Transactions of the Dumfries & Galloway Natural History and Antiquarian Society* 83, 1-4.

Kraker, A.M.J. de. 2002. Historic Storms in the North Sea area, an assessment of the storm data, the present position of research and the prospects for future research. *In* Wefer, G., Berger, W., Behre, K-E. and Jansen, E. (eds) *Climate Development and History of the North Atlantic Realm*. Berlin: Springer-Verlag, 415-434.

Kreutz, K.J., Mayewski, P.A., Meeker, L.D., Twickler, M.S., Whitlow, S.I. and Pittalwala, I.I. 1997. Bipolar changes in atmospheric circulation during the Little Ice Age. *Science* 277, 1294-1296.

Lamb, H.H. 1977. *Climate: Present, Past and Future*. *Volume 2. Climatic History and the Future*. London: Methuen.

Lamb, H.H. 1979. Climate variation and changes in the wind and ocean circulation: the Little Ice Age in the NE Atlantic. *Quaternary Research* 11, 1-20.

Lamb, H.H. 1995. *Climate, History and the Modern World*. London: Methuen. 2nd Ed.

Lamb, H.H. and Frydendahl, K. 1991. *Historic Storms of the North Sea, British Isles and Northwest Europe*. Cambridge: University Press.

Lawrence, T., Long, A.J., Gehrels, W.R., Jackson, L.P. and Smith, D.E. 2016. Relative sea-level data from southwest Scotland constrain meltwater-driven sea-level jumps prior to the 8.2 kyr BP event. *Quaternary Science Reviews* 151, 292-308.

Lehner, F., Raible, C.C. and Stocker, T.F. 2012. Testing the robustness of a precipitation proxy-based North Atlantic Oscillation reconstruction. *Quaternary Science Reviews* 45, 85-94. https://doi.org/10.1016/j.quascirev.2012.04.025

Lennon, G.W. 1963a. The identification of weather conditions associated with the generation of major storm surges along the west coast of the British Isles. *Quarterly Journal of the Meteorological Society* 89, 381-394.

Lennon, G.W. 1963b. A frequency investigation of abnormally high tidal levels at certain west coast ports. *Proceedings of the Institution of Civil Engineers* 25, 481-494.

Livingstone, S.J., Ó Cofaigh, C. and Evans, D.J.A. 2008. Glacial geomorphology of the central sector of the last British-Irish Ice Sheet. *Journal of Maps* 2008, 358-377.

Lloyd, J.M., Shennan, I., Kirby, J.R. and Rutherford, M.M. 1999. Holocene relative sea-level changes in the inner Solway Firth. *Quaternary International* 60, 83-100.

Locker, A. 2007. *In piscibus diversis*; the bone evidence for fish consumption in Roman Britain. *Britannia* 38, 141-180.

Long, A.J., Innes, J.B, Kirby, J.R., Lloyd, J.M., Rutherford, M.M.. Shennen, I. and Tooley, M.J. 1998. Holocene sea-level change and coastal evolution in in the Humber estuary, eastern England: an assessment of rapid coastal change. *The Holocene* 8 (2), 229-247.

Long, A., Waller, M. and Plater, A.J., 2007. *Dungeness and Romney Marsh: barrier dynamics and marshland evolution*. Oxford: Oxbow books.

Lund, D.E., Lynch-Steiglitz and Curry, W.B. 2006. Gulf Stream density structure and transport during the past millennium. *Nature* 444 (01 Nov 2006), 601-604.

Luterbacher, J., Xoplaki, E., Dietrich, D., Jones, P.D., Davies, T.D., Portis, D., Gonzalez-Rouco, J.F., von Storch, H., Gyalistras, D., Casty, C. and Wanner, H. 2002. Extending North Atlantic Oscillation reconstructions back to 1500. *Atmospheric Science Letters* 2, 114-124.

Lyons, M. 1989. Weather, famines, pestilence and plague in Ireland, 900-1500. *In* Crawford, R.M. (ed.) *Famine: The Irish experience 900-1900*. Edinburgh: John Donald, 31-74.

MacIvor, I., Gallagher, D., Laing, L., Caldwell, D., Gabra-Saunders, T., Haggarty, G., Hurst-Vose, R., McQ. Holmes, N.M. and Ruckley, N.A. 1999. Excavations at Caerlaverock Castle, 1955–66, *Archaeological Journal* 156 (1), 143-245.

Macklin, M.G., Johnstone, E. and Lewin, J. 2005. Pervasive and long-term forcing of Holocene river instability and flooding in Great Britain by centennial-scale climate change. *The Holocene* 15, 937-943.

Macklin, M.G., Jones, A.F. and Lewin, J. 2010. River response to rapid Holocene environmental change: evidence and explanation in British catchments. *Quaternary Science Reviews* 29, 1555-1576.

Macklin, M.G. and Rumsby, B.T. 2007. Changing climate and extreme floods in the British uplands. *Transactions of the Institute of British Geographers* NS 32, 168-186.

Macleod, I. 2001. *Where the Whaups are Crying. A Dumfries and Galloway Anthology*. Edinburgh: Birlinn.

Madsen, A. T., Murray, A. S., Andersen, T. J. and Pejrup, M. 2010. Luminescence dating of Holocene sedimentary deposits on Rømø, a barrier island in the Wadden Sea, Denmark. *Holocene* 20, 1247–1256.

Marshall, J.R. 1961. *Investigations int Some Aspects of the Physiography of the Upper Solway Marshes and Mosses*. Unpublished Ph D Thesis, University of Newcastle-upon-Tyne.

Marshall, J.R. 1962a. The morphology of the upper Solway salt marshes. *Scottish Geographical Magazine* 78, 81-99.

Marshall, J.R. 1962b. The physiographic development of Caerlaverock Merse. *Transactions of the Dumfries & Galloway Natural History and Antiquarian Society* 39, 62-123.

Marusek, J.A. 2010. *A Chronological Listing of Early Weather Events*. http://www.breadandbutterscience.com/ weather.pdf: accessed 23/04/2022.

Masse, G., Rowland, S.J., Sicre, M.A., Jacob, J., Jansen, E. and Belt, S.T. 2008. Abrupt climate changes for Iceland during the last millennium: evidence from high resolution sea ice reconstructions. *Earth and Planetary Science Letters* 269, (3–4), 565-569.

Maxwell, H. Sir 1913. *The Chronicle of Lanercost 1272-1346*. Glasgow: James Maclehose and Sons.

May, V.J. and Hanson, J.D. 2003. *Coastal Geomorphology of Great Britain*. Peterborough: Joint Nature Conservation Committee.

Mayewski, P.A. *et al* 2004. Holocene climate variability. *Quaternary Research* 62, 243-255.

McDermott, F., Mattey, D.P. and Hawkesworth, C. 2001. Centennial-scale Holocene climate variability revealed by a high-resolution speleothem $\delta^{18}O$ record from SW Ireland. *Science* 294, 1328-1331.

McDowall, W. 1906. *History of the Burgh of Dumfries*. Dumfries: Thomas Hunter & Co.

McIlvenny, J.D., Muller, F.L.L. and Dawson, A. 2013. A 7600 year sedimentary record of climatic instability in Dunnet Bay, north Scotland. *Marine Geology* 335, 100-113.

McIntire, W.T. 1942. The salt pans of the Solway. *Transactions of the Cumberland & Westmorland Antiquarian & Archaeological Society* 42, 1-12.

McIntire, W.T. 1943. The old port of Sandsfield. *Transactions of the Cumberland and Westmorland Antiquarian and Archaeological Society* 43, 71-81.

McKenna, J., Cooper, G.A.J. and Jackson, D.W.T. 2012. Storm swash terraces: A previously overlooked element of the cliff-shore platform system. *Journal of Sedimentary Research* 82: 260–269.

McMillan, A.A., Merritt, J.W., Auton, C.A. and Golledge, N.R. 2011. The Quaternary geology of the Solway. *British Geological Survey Research Report* RR/11/04. Keyworth, Nottingham: British Geological Survey.

Meeker, L.D. and Mayewski, P.A. 2002. A 1400-year high-resolution record of atmospheric circulation over the North Atlantic and Asia. *The Holocene* 12, 257-266.

Miller, G.H. *et al* 2012. Abrupt onset of the Little Ice Age triggered by volcanism and sustained by sea-ice/ocean feedbacks. *Geophysics Research Letters* 39, L02708.

Mills, C. unpublished. The dendrochronological evidence. In Mills, C., Quelch, P. and Darrah, H. (eds) *Caerlaverock Interpretation Project: Woodland and Landscape*. Report to HES.

Mills, C., Quelch, P. and Darrah, H. unpublished. *Caerlaverock Interpretation Project: Woodland and Landscape*. Report to HES.Moffat *et al* 2020

Moffat, C., Baxter, J., Berx, B., Bosley, K., Boulcott, P., Cox, M., Cruickshank, L., Gillham, K., Haynes, V., Roberts, A., Vaughan, D. and Webster, L. 2020. *Scotland's Marine Assessment 2020*. Scottish Government. https://marine.gov.scot/sma. Accessed 24/12/21.

Moore, J.N. 1983. Thomas Winter's chart of the Solway Firth. *Trans. Dumfries & Galloway Natural History and Antiquarian Society* 59, 57-63.

Morss, W.L. 1927. The plant colonisation of Merse Lands in the estuary of he River Nith. *Journal of Ecology* 13, 310-343.

Moskalewicz, D., Szczuciński, W., Mroczek, P. and Vaikutienė, G. 2020. Sedimentary record of historical extreme storm surges on the Gulf of Gdańsk coast, Baltic Sea. *Marine Geology* 420, 106084. https://doi.org/10.1016/j.margeo.2019.106084

Mowbay, T. de. 1983. The genesis of lateral accretion deposits in recent intertidal mudflat channels, Solway Firth, Scotland. *Sedimentology* 30, 425-435.

Munyikwa, K., Kinnaird, T. C. and Sanderson, D. C. W. 2021. The potential of portable luminescence readers in geomorphological investigations: a review. *Earth Surface Processes and Landforms*, 46 (1), 131-150. https://doi.org/10.1002/esp.4975

Murdoch, R. 2004. Glass. *In* Brann, M. *Excavations at Caerlaverock Old Castle, Dumfries and Galloway, 1998-9*. Dumfries: Dumfries and Galloway Natural History and Antiquarian Society, 68-69.

Murray, A.S. and Clemmensen, L.B. 2001. Luminescence dating of Holocene aeolian sand movement, Thy, Denmark. *Quaternary Science Reviews* 20, 751–754.

Newell, W. 1845. Untitled [Plan of River Nith from Dumfries to Southerness. https://maps.nls.uk/estates/rec/5760. Accessed 24/22/2021.

Nichols, H. 1967. Vegetational change, shoreline displacement and the human factor in the Late Quaternary history of south-west Scotland. *Transactions of the Royal Society of Edinburgh* 67, 145-187.

Nielsen, A., Murray, A.S., Pejrup, M. and Elberling, B. 2006. Optically stimulated luminescence dating of a Holocene beach ridge plain in Northern Jutland, Denmark. *Quaternary Geochronology* 1 (4), 305-312. https://doi.org/10.1016/j.quageo.2006.03.001.

Nielson, G. 1899. *Annals of the Solway until AD1307*. Privately Printed.

Noel, M.J. 2004. Archaeomagnetic dating. *In* Brann, M. *Excavations at Caerlaverock Old Castle, Dumfries and Galloway, 1998-9*. Dumfries: Dumfries and Galloway Natural History and Antiquarian Society, 95-98.

Nott, J., Smithers, S., Walsh, K. and Rhodes, E. 2009. Sand beach ridges record 6000 year history of extreme tropical cyclone activity in northeastern Australia. *Quaternary Science Reviews* 28, 1511-1520.

O'Brien, S.R., Mayewski, P.A., Meeker, L.D., Meese, D.A., Twickler, M.S. and Whitlow, S.I. 1995. Complexity of Holocene climate as reconstructed from a Greenland ice core. *Science* 270, 1962-1964.

Ogilvie, A. and Farmer, G. 1997. Documenting the Medieval climate. *In* Hulme, M. and Barrow, E. (eds) *Climates of the British Isles Present, Past and Future*. London: Routledge, 112-133.

Oliver, T.S.N., Thom, B.G. and Woodroffe, C.D. 2016. Formation of beach-ridge plains: an appreciation of the contribution by Jack L. Davies. *Geographical Research* 55 (3), 305-320.

Olsen, J., Anderson, N.J. and Knudsen, M.F. 2012. Variability of the North Atlantic Oscillation over the past 5,200 years. *Nature Geoscience* 5, 808-812.

Oppo, D.W., McManus, J.F. and Cullen, J.L. 2003. Deepwater variability in the Holocene epoch. *Nature* 422, 277-278.

Oram, R. 2012. The sea-salt industry in Medieval Scotland. *Studies in Medieval and Renaissance History*, 3rd Series, 9, 211-234.

Orford, J.D., Carter, R.W.G. and Jennings, S. 1991. Coarse clastic barrier environments: evolution and implications for Quaternary sea level interpretation. *Quaternary International* 9, 87–104.

Orford, J.D., Murdy, J. and Freel, R. 2006. Developing constraints on the relative sea-level curve for the north-east of Ireland from the mid-Holocene to the present day. *Philosophical Transactions of the Royal Society of London* A364, p. 857–866.

Orford, J.D., Wilson, P., Wintle, A.G., Knight, J. & Braley, S. 2000. Holocene coastal dune initiation in Northumberland and Norfolk, eastern UK: climate and sea-level changes as possible forcing agents for dune initiation. *In* Shennan, I. and Andrews, J. (eds) *Holocene Land-Ocean Interaction and Environmental Change around the North Sea*. London: Geological Society of London Special Publication 166, 197-218.

Orme, L.C., Davies, S.J. and Duller, G.A.T. 2015. Reconstructed centennial variability of late Holocene storminess from Cors Fochno, Wales. *Journal of Quaternary Science* 30 (5), 478-488.

Orme, L.C., Reinhardt, L., Jones, R.T., Charman, D.J., Barkwith, A. and Ellis, M.A. 2016. Aeolian sediment reconstructions from the Scottish Outer Hebrides: Late Holocene storminess and the role of the North Atlantic Oscillation. *Quaternary Science Reviews* 132, 15-25.

Ortega, P., Lehner, F., Swingedouw, D.., Masson-Delmotte, V., Raible, C.C., Casado, M. and You, P. 2015. A model-tested North Atlantic Oscillation reconstruction for the past millennium. *Nature* 523, 71-74.

Otvos, E.G. 2020. Coastal barriers - fresh look at origins, nomenclature and classification issues. *Geomorphology* 355, 107000. https://doi.org/10.1016/j.geomorph.2019.107000

Pennant, T. 1998. *A Tour in Scotland and Voyage to the Hebrides 1772*. Edinburgh: Birlinn.

Pessenda, L.C.R., Gouveia, S.E.M. and Aravena, R. 2001. Radiocarbon dating of total soil organic matter and humin fraction and its comparison with $^{14}C$ ages of fossil charcoal. *Radiocarbon* 43 (2B), 595-601.

Pfister, C., Luterbacher, J., Schwarz-Zanetti, G. and Wegmann, M. 1998. Winter air temperature variations in western Europe during the Early and high Middle Ages (AD 750-1300). *The Holocene* 8 (5), 535-552.

Phillips, M.R., Rees, E.F. and Thomas, T. 2013. Winds, sea levels and North Atlantic Oscillation (NAO) influences: An evaluation. *Global and Planetary Change* 100, (2013) 145–152.

Photos-Jones, E. 2004. The technical characterisation of the Old Caerlaverock Castle metallurgical waste. *In* Brann, M. *Excavations at Caerlaverock Old Castle, Dumfries and Galloway, 1998-9*. Dumfries: Dumfries and Galloway Natural History and Antiquarian Society, 81-88.

Plater A.J., Long, A.J., Spencer, C.D. and Delacour, R.A.P. 1999. The stratigraphic record of sea-level change and storms during the last 2000 years: Romney Marsh, southeast England. *Quaternary International* 55, 17-27.

Plater, A.J., Stupples, P. and Roberts, H.M. 2009. Evidence of episodic coastal change during the Late Holocene: The Dungeness barrier complex, SE England. *Geomorphology* 104 (1–2), 47-58.

Platt, C. 2010. The homestead moat: security or status? *Archaeological Journal* 167 (1), 115–133.

Poirier, C., Tessier, B. and Chaumillon, E. 2017. Climate control on late Holocene high-energy sedimentation along coasts of the northeastern Atlantic Ocean. *Palaeogeography, Palaeoclimatology, Palaeoecology* 485, 784-797. https://doi.org/10.1016/j.palaeo.2017.07.037

Pont, T. *c*. 1596. *Nithsdale: part of Teviotdale (Pont 35)*. https://maps.nls.uk/rec/298. Accessed 24/01/22.

Preston, J., Sanderson, D., Kinnaird, T., Newton, A., Nitter, M., Coolen, J., Mehler, N. and Dugmore, A. 2020. Dynamic beach response to changing storminess of Unst, Shetland: implications for landing places exploited by Norse communities. *The Journal of Island and Coastal Archaeology* 15 (2), 153-178.

Proctor, C.J., Baker, A., Barnes, W.L. and Gilmour, M.A. 2000. A thousand year speleothem record of North Atlantic climate from Scotland. *Climate Dynamics* 16, 815-820.

Pye, K. and Neal, A. 1993. Late Holocene dune formation on the Sefton coast, northwest England. *In* Pye, K. (ed.) *The dynamics and environmental context of aeolian sedimentary systems*. Geological Society Special Publication 72. London: Geological Society of London, 201–217.

RCAHMS 1920. *An Inventory of Monuments and Constructions in the County of Dumfries*. Edinburgh.

Reid, C. (ed) 1915. *An Introduction to the History of Dumfries* by Robert Edgar 1746. Dumfries: Maxwell & Sons.

Reid, C. 1946. The old castle site at Caerlaverock. *Transactions of the Dumfries & Galloway Natural History and Antiquarian Society* 23, 66-82.

Reid, R.C. 1927. The excavation of Auchencas. *Transactions of the Dumfries & Galloway Natural History and Antiquarian Society* 13 (1925-6), 104-124.

Reimann, T., Tsukamoto, S., Harff, J., Osadczuk, K. and Frechen, M. 2011. Reconstruction of Holocene coastal foredune progradation using luminescence dating - An example from the Świna barrier (southern Baltic Sea, NW Poland). *Geomorphology* 132 (1–2), 1-16. https://doi.org/10.1016/j.geomorph.2011.04.017

Reimer, P., Austin, W.E.N., Bard, E., Bayliss, A., Blackwell, P.G., Bronk Ramsey, C., Butzin, M., Cheng, H., Edwards, R.L., Friedrich, M., Grootes, P.M., Guilderson, T.P., Hajdas, I., Heaton, T.J. and Hogg, A.G. 2020. The IntCal20 Northern Hemisphere radiocarbon age calibration curve (0-55 kcal BP). *Radiocarbon*, 62 (4), pp. 725-757. https://doi.org/10.1017/RDC.2020.41

Rennie, A.F., and Hansom, J.D. 2011. Sea level trend reversal: land uplift outpaced bu sea level rise on Scotland's coast. *Geomorphology* 125 (1), 193-202.

Retallack, G.J. and Roering, J.J. 2012. Wave-cut or water-table platforms of rocky coasts and rivers? *GSA Today* 22 (6), 4–10.

Roberts, H.M. and Plater, A.J. 2007. Reconstruction of Holocene foreland progradation using optically stimulated luminescence (OSL) dating: an example from Dungeness, UK. *The Holocene* 17 (4), 495-505.

Rose, N.L., Harlock, S., Appleby, P.G. and Battarbee, R.W. 1995. Dating of recent lake sediments in the United Kingdom and Ireland using spheroidal carbonaceous particle (SCP) concentration profiles. *The Holocene* 5, 328-355.

Rosen, W. 2014. *The third horseman: Climate change and the great famine of the 14th century*. New York: Viking.

Rowe, S.M. 1978. *An Investigation of the Erosion and Accretion Regime on the Saltmarshes of the Upper Solway Firth from 1946 to 1975*. Edinburgh: Nature Conservancy Council.

Roy, P.S., Cowell, P.J., Ferland, M.A. and Thom, B.G. 1994. Wave-dominated coasts. *In* Carter, R.W.G. and Woodroffe, C.D. (eds) *Coastal Evolution*. Cambridge: Camridge University Press, 121–186.

Roy's Military Survey of Scotland, 1752-55. Roy Map Strip 5. Section: 1f. https://maps.nls.uk/geo/roy/#zoom=11&lat=55.0055&lon=-3.4201&layers=1&point=54.9448,-3.4200. Accessed 10/10/21.

Sanderson, D.C.W. and Murphy, S. 2010. Using simple portable OSL measurements and laboratory characterisation to help understand complex and heterogeneous sediment sequences for luminescence dating. *Quaternary Geochronology* 5, 299-305.

Schumm, S.A. 1976. Episodic erosion: a modification of the geomorphic cycle. *In* Melhorn, W. and Flemal, R. (eds) *Theories of Landform Development*. New York: Allen & Unwin, 69-85.

Scott-Giles, C.W. (transl.) 1960. *Siege of Caerlaverock*. https://www.theheraldrysociety.com/articles/the-siege-of-caerlaverock/. Accessed 26/01/2022.

Seager, R., Graham, N., Herweijer, C., Gordon, A.L., Kushnir, Y. and Cook, E. 2007. Blueprints for Medieval hydroclimate. *Quaternary Science Reviews* 26, 2322-2336.

Sedgwick, P.E. and Davis, R.A.Jr. 2003. Stratigraphy of washover deposits in Florida: Implications for recognition in the stratigraphic record. *Marine Geology* 200, 31–48.

Shennan, Bradley, S.L. and Edwards, R. 2018. Relative sea-level changes and crustal movements in Britain and Ireland since the Last Glacial Maximum. *Quaternary Science Reviews* 188, 143-159.

Shirley, G.W. 1915. *The growth of a Scottish burgh: a study in the early history of Dumfries*. Dumfries: Privately Printed.

Shore, J.S., Bartley, D.D. and Harkness, D.D. 1995. Problems encountered with the $^{14}C$ dating of peat. *Quaternary Science Reviews* 14, 373-383.

Sicre, M.A., Jacob, J., Ezat, U., Rousse, S., Kissel, C., Yiou, P., Eiríksson, J., Knudsen, K.L., Jansen, E. and Turon, J-L. 2008. Decadal variability of sea surface temperatures off North Iceland over the last 2000 years. *Earth and Planetary Science Letters* 268, 137-142.

Simpson, W.D. 1953 Caerlaverock Castle. *Scottish Historical Review* 32, 123-27.

Sinclair, Sir John. 1794. *The Statistical Account of Scotland*, Ruthwell, Dumfries, Vol. 10, Edinburgh: William Creech, 1794, pp. 218. University of Edinburgh, University of Glasgow. (1999) The Statistical Accounts of Scotland online service: https://stataccscot.edina.ac.uk:443/link/osa-vol10-p218-parish-dumfries-ruthwell. Accessed 17/02/2022.

Sinclair, Sir John 1795. *The Statistical Account of Scotland*, Kirkbean, Kirkcudbright, Vol. 15, Edinburgh: William Creech, 1795, p. 119. University of Edinburgh, University of Glasgow. (1999) The

Statistical Accounts of Scotland online service: https://stataccscot.edina.ac.uk:443/link/osa-vol15-p119-parish-kirkcudbright-kirkbean. Accessed 17/02/2022.

Sinclair, Sir John. 1796. *The Statistical Account of Scotland*, Colvend and Southwick, Kirkcudbright, Vol. 17, Edinburgh: William Creech, 1796, p. 113. University of Edinburgh, University of Glasgow. (1999) The Statistical Accounts of Scotland online service: https://stataccscot.edina.ac.uk:443/link/osa-vol17-p113-parish-kirkcudbright-colvend_and_southwick. Accessed 17/02/22.

Singh, P.P. 1996. *Morpho-sedimentary evolution of a Flandrian macro-tidal spit-bay complex, Moricambe Bay, northwest England, UK*. Unpublished Ph D Thesis, University of Reading.

Smith, R.A.E. 2015. *The use of historical data in coastal flood modelling : a study on the Somerset coast of the Severn Estuary, UK*. Ph D Thesis, University of Bristol.

Smith, D.E., Cullingford, R.A., Haggart, B.A., Tipping, R., Wells, J.M., Mighall, T.M. and Dawson, S. 2003a. Holocene relative sea level changes in the lower Nith valley and estuary. *Scottish Journal of Geology* 39, 97-120.

Smith, D.E., Fretwell, P.T., Cullingford, R.A. and Firth, C.R. 2006. Towards improved empirical isobase models of Holocene land uplift for mainland Scotland, UK. *Philosophical Transactions of the Royal Society*, Series A 364, 949-972.

Smith, D.E., Hunt, C., Firth, C.R., Jordan, J.T., Fretwell, P.T., Harman, M. Murdy, J., Orford, J.D. and Burnside, N.G. 2012. Patterns of Holocene relative sea level change in the North of Britain and Ireland. *Quaternary Science Reviews* 54, 58-76.

Smith, D.E., Wells, J.M., Mighall, T.M., Cullingford, R.A., Holloway, L.K., Dawson, S. and Brooks, C.L. 2003b. Holocene relative sea levels and coastal changes in the lower Cree valley and estuary, SW Scotland, U.K. *Transactions of the Royal Society of Edinburgh: Earth Sciences* 93. 301-331.

Smith, D.E., Tipping, R.M., Jordan, J.T. and Blackett, M. 2020. Holocene relative sea level changes and coastal evolution at Luce Bay, South West Scotland. *Journal of Quaternary Science* 35 (6), 743-759.

Solway Firth Partnership 1996. *Solway Firth Review*. Dumfries: Solway Firth Partnership.

Sommerville, A.A., Hansom, J.D., Sanderson, D.C.W and Housley, R.A. 2003. Optically stimulated luminescence dating of large storm events in Northern Scotland. *Quaternary Science Reviews* 22, 1085-1092.

Sommerville, A.A., Hansom, J.D., Housley, R.A. and Sanderson, D.C.W. 2007. Optically stimulated luminescence (OSL) dating of coastal aeolian sand accumulation in Sanday, Orkney Islands, Scotland. *The Holocene* 17 (5), 627-637.

Sorrel, P., Tessier, B., Demory, F., Delsinne, N. and Mouazé, D. 2009. Evidence for millennial-scale climatic events in the sedimentary infilling of a macrotidal estuarine system, the Seine estuary (NW France). *Quaternary Science Reviews* 28, 499–516.

Sorrel, P., Debret, M., Billeaud, I., Jaccard, S.L., McManus, J. and Tessier, B. 2012. Persistent non-solar forcing of Holocene storm dynamics in coastal sedimentary archives. *Nature Geoscience* 5 (12), 892-896. https://doi.org/10.1038/ngeo1619

Spencer, C.D., Plater, A.J. and Long, A.J. 1998. Rapid coastal change during the mid- to late Holocene: the record of barrier estuary sedimentation in the Romney Marsh region, southeast England. *The Holocene* 8 (2), 143–163.

Srivastava, A., Kinnaird, T. and Bates, R. 2022. *OSL dating of sediments from the landscape of Caerlaverock Castle, southwest Scotland.* Report to Historic Environment Scotland.

Steers, J.A. 1973. *The Coastline of Scotland*. London: Cambridge University Press.

Stone, J.C. 1968. An evaluation of the 'Nidisdale' manuscript map by Timothy Pont. *Scottish Geographical Magazine* 84, 160-171.

Stone, J.C. 1973. The settlements of Nithsdale in the 16th century by Timothy Pont: a complete or partial record? *Transactions of the Dumfries & Galloway Natural History and Antiquarian Society* 50, 82-90.

Swindles, G.T. *et al* (32 authors) 2013. Centennial-scale climate change in Ireland during the Holocene. *Earth-Science Reviews* 126, 300-320.

Szkornik, K., Gehrels, W.R. and Murray, A.S., 2008. Aeolian sand movement and relative sea-level rise in Ho Bugt, western Denmark, during the 'Little Ice Age'. *The Holocene* 18 (6), 951-965.

Taylor, C. 2000. Medieval ornamental landscapes. *Landscapes* 1 (1), 38-55.

Tipping, R. 1995. Holocene evolution of a lowland Scottish landscape: Kirkpatrick Fleming. III. Fluvial history. *The Holocene* 5, 184-195.

Tipping, R. 1997. Pollen analysis, late Iron Age and Roman agriculture around Hadrian's Wall. *In* Gwilt, A. and Haselgrove, C. (eds) *Reconstructing Iron Age Societies*. Oxford: Oxbow, 239-247.

Tipping, R. 1999. Moffat Basin: Holocene fluvial stratigraphy and chronology. *In* Tipping, R. (ed) *The Quaternary of Dumfries & Galloway. Field Guide*. London: Quaternary Research Association, 153-159.

Tipping, R. and Adams, J. 2007. Structure, composition and significance of Medieval storm beach ridges at Caerlaverock, Dumfries & Galloway. *Scottish Journal of Geology* 43, 115-123.

Tipping, R., Davies, A., Dawson, A., Dawson, S., Smith, D., Tisdall, E. and Tyler, A. 2004. Landscape development and the Medieval coastline. *In* Brann, M. (ed.) *Excavations at Caerlaverock Old Castle 1998-99, 9-15*. Dumfries: Dumfries & Galloway Natural History and Antiquarian Society, 9-14.

Tipping, R., Haggart, B.A. and Milburn, P. 2007. The interaction of site and landscape around Pict's Knowe. *In* Thomas, J. (ed.) *Place and Memory: Excavations at the Pict's Knowe, Holywood and Holm Farm, Dumfries & Galloway, 1994-8*. Oxford: Oxbow Books, 6-36.

Tipping, R., Milburn, P. and Halliday, S. 1999. Fluvial processes, land use and climate change 2000 years ago in upper Annandale, southern Scotland. *In* Brown, A.G. & Quine, T. (eds) *Fluvial Processes and Environmental Change*. Chichester: Wiley, 311-328.

Tisdall, E.W., McCulloch, R.D., Sanderson, D.C.W., Simpson, I.A. and Woodward, N.L. 2013. Living with sand: A record of landscape change and storminess during the Bronze and Iron Ages, Orkney, Scotland. *Quaternary International* 301, 1-11.

Tooley, M.J. 1978. *Sea-level Changes: North-West England during the Flandrian Stage*. Oxford: Clarendon Press.

Trenhaile, A.S. 1997. *Coastal Dynamics and Landforms*. Oxford: Clarendon Press.

Trotter, F.M. 1929. The glaciation of the eastern Edenside, the Alston Block, and the Carlisle Plain. *Quarterly Journal of the Geological Society of London* 85, 549-612.

Trouet, V., Esper, J., Graham, N.E., Baker, A., Scourse, J.D. and Frank, D.C. 2009. Persistent positive North Atlantic Oscillation mode dominated the Medieval Climate Anomaly. *Science* 324, 78-80.

Trouet, V., Scourse, J.D. and Raible, C.C. 2012. North Atlantic storminess and Atlantic Meridional Overturning Circulation during the last Millennium: Reconciling contradictory proxy records of NAO variability. *Global and Planetary Change* 84-85, 48–55.

Truckell, A.E. 1950. Excavation Notes. *Transactions of the Dumfries & Galloway Natural History and Antiquarian Society* 27, 203.

Tsimplis, M.N., Woolf, D.K., Osborn, T.J., Wakelin, S., Wolf, J., Flather, R., Shaw, A.G.P., Woodworth, P., Challenor, P., Blackman, D., Pert, F., Yan, Z. and Jevrejeva, S. 2005. Towards a vulnerability assessment of the UK and northern European coasts: the role of regional climate variability. *Philosophical Transactions of the Royal Society of London* A363, 1329-1358.

Tufnell, L. 1983. Environmental observations by the Rev. William Hutton of Beetham, Cumbria. *Transactions of the Cumberland and Westmorland Antiquarian and Archaeological Society* 83, 141-150.

Tyler, A.N. 1999. Monitoring anthropogenic radioactivity in salt marsh environments through *in situ* gamma-ray spectrometry. *Journal of Environmental Radioactivity* 45, 235-252.

Van Vliet-Lanoë, B., Goslin, J., Hallégouët, B., Hénaff, A., Delacourt, C., Fernane, A., Franzetti, M., Le Cornec, E., Le Roy, P. and Penaud, A. 2014a. Middle- to late-Holocene storminess in Brittany (NW France): Part I – morphological impact and stratigraphical record. *The Holocene* 24 (4),413-433.

Van Vliet-Lanoë, B., Penaud, A., Hénaff, A., Delacourt, C., Fernane, A., Goslin, J., Hallégouët, B. and Le Cornec, E. 2014b. Middle- to Late-Holocene Storminess in Brittany (NW France): Part II – The chronology of events and climate forcing. *The Holocene* 24 (4), 434-453.

Van Vliet-Lanoë, B., Henaff, A., Hallegouet, B., Delacourt, C., LeCornec, E. and Meurisse-Fort, M. 2016. Holocene formation and evolution of coastal dune ridges, Brittany, France. *Comptes Rendus Geoscience* 348, 462-470.

Wang, T., Surge, D. and Mithen, S. 2011. Seasonal temperature variability of the Neoglacial (3300–2500 BP) and Roman Warm Period (2500–1600 BP) reconstructed from oxygen isotope ratios of limpet shells (Patella vulgata), Northwest Scotland. *Palaeogeography, Palaeoclimatology, Palaeoecology* 317-318, 104-113.

Watson, G.P.H. 1923. The development of Caerlaverock Castle. *Proceedings of the Society of Antiquaries of Scotland* 57, 29-40.

Wells, J.M., Mighall, T.M., Smith, D.E. & Dawson, A.G. 1999. Brighouse Bay, southwest Scotland: Holocene vegetational history and human impact at a small coastal valley mire. *In* Andrews, P. & Banham, P. (Eds) *Late Cenozoic Environments and Hominid Evolution: a Tribute to Bill Bishop*. London: Geological Society, 217-233.

Wells, J. 1775-6. Plans of the Barony of Caerlaverock. Castle Wood, Wood Back and Greenhead. https://maps.nls.uk/view/217626568. Accessed 24/01/22.

Wilson, A. 1999. Roman penetration in eastern Dumfriesshire and beyond. *Transactions of the Dumfries & Galloway Natural History and Antiquarian Society* 73, 33-66.

Wilson, J. 1905 (ed.). Houses of Austin canons: The priory of Carlisle. *In A History of the County of Cumberland: Volume 2,* ed. J Wilson (London, 1905), pp. 131-151. British History Online http://www.british-history.ac.uk/vch/cumb/vol2/pp131-151. Accessed 17/08/21.

Wilson, J.B. 1965. *The palaeoecological significance of infaunas and their associated sediments*. Unpublished Ph D Thesis, University of Edinburgh.

Wilson, P. 1990. Coastal dune chronology in the north of Ireland. *Catena Supplement* 18, 71-79.

Wilson, P. 2002. Holocene coastal dune development on the South Erradale peninsula, Wester Ross, Scotland. *Scottish Journal of Geology* 38, 5-12.

Wilson, P. and Braley, S. M. 1997. Development and age structure of Holocene coastal sand dunes at Horn Head, near Dunfanaghy, Co Donegal, Ireland. *The Holocene*, 7 (2), 187-198.

Wilson, P., McGourty, J. and Bateman, M.D. 2004. Mid- to late-Holocene coastal dune event stratigraphy for the north coast of Ireland. *The Holocene* 14 (3), 406-416.

Wilson, P. and McKenna, J. 1996. Holocene evolution of the River Bann estuary and adjacent coast, Northern Ireland. *Proceedings of the Geologists' Association* 107, 241-252.

Wilson, P., Orford, J. D., Knight, J., Braley, S. M. and Wintle, A. G. 2001. Late Holocene (post-4000 years BP) coastal dune development in Northumberland, northeast England. *The Holocene*, 11 (2), 215-230.

Wintle, A.G., Clarke, M.L., Musson, F.M., Orford, J.D. and Devoy, R.J.N. 1998. Luminescence dating of recent dunes on Inch Spit, Dingle Bay, southwest Ireland. *The Holocene* 8 (3), 331-339.

Woodworth, P.L. and Blackman, D.L. 2002. Changes in extreme high waters at Liverpool since 1768. *International Journal of Climatology* 22, 697-14.

Woodworth, P.L., Flather, R.A., Williams, J.A., Wakelin, S.L. and Jevrejeva, S. 2007. The dependence of UK extreme sea levels and storm surges on the North Atlantic Oscillation. *Continental Shelf Research* 27 (7), 935-946.

Yates, M.J. 1979. The discovery of two Flat Axes near Caerlaverock Castle. Dumfries. *Transactions of the Dumfries & Galloway Natural History and Antiquarian Society* 54, 147-148.

Zong, Y. and Tooley, M.J. 2003. A historical record of coastal floods in Britain: frequencies and associated storm tracks. *Natural Hazards* 29, 13-36.

**Figure Captions**

Figure 1. The topographic setting of Caerlaverock: (a) the inner Solway Firth, north east of a line between Southerness in Scotland and Silloth in England; (b) Caerlaverock in relation to Dumfries, the River Nith and the Lochar Water.

Figure 2. Solid and superficial geology around Caerlaverock.

Figure 3. Superficial sediments around the Old and New Caerlaverock Castles.

Figure 4. Wells' 1775-6 estate plan of Castle Wood, Wood Back and Greenhead (https://maps.nls.uk/view/217626568)

Figure 5. Distribution and approximate orientations of coastal gravel ridges on the Scottish side of the Solway Firth mapped by Jardine (1980) and Smith *et al* (2003a).

Figure 6. (a) the distribution along the coastal Atlantic façade of dated (rounded to 50 years) natural sediment accumulations between 400BC and AD1800 argued by the authors to describe past storminess.

Figure 7. (a) a LiDAR MHS image of the topography of Castle Wood and surroundings, identifying the features named in this work; (b) interpretation of the topography of Castle Wood and surroundings showing the cliff-line that was the coast prior to the events in this work, basins B1 to B8 and ridges R1 to R14 that define them, and the subdued ridges Ra to Rf at Lantonside; (c) natural channels that cut ridges; (d) the locations of sediment-stratigraphic transects across the basins and of gravel samples in ridges, with the single transect reported by Tipping and Adams (2007: figure 3).

Figure 8. Altitudes (m OD) of buried bedrock surfaces encountered along north-south sediment-stratigraphic transects (a) from north of Basin 2 to Ridge 14 in the west, (b) along Tipping and Adams' (2007) transect and (c) from Basin 5 to Basin 8 in the east.

Figure 9. Sediment-stratigraphic borehole transects across (a) Basin 1 (boreholes 104 to 110) and Ridge 3 (boreholes 111 to 113), and (b) north of Basin 2 (borehole 91) and across Basin 2 (boreholes 92 to 103).

Figure 10. Sediment-stratigraphic borehole transects across Basin 3 (boreholes 114 to 127). See Figure 9 for key.

Figure 11. Sediment-stratigraphic borehole transects across Basin 3 (boreholes 123 and 198 to 201), Ridge 5 (boreholes 197 and 202 to 205) and Basin 4 (boreholes 206 to 212). See Figure 9 for key.

Figure 12. Sediment-stratigraphic borehole transects across Basin 5 along three north-south transects, arranged from west to east (Figure 7d): (a) transect 5(i) from Ridge 3 (boreholes 112–113) south; (b) transect 5(ii) north of the Old Castle Burn from the cliff north of Basin 5 (boreholes 134 to 138) across Basin 5 (boreholes 139 to 157); (c) transect 5(iii) from the cliff (boreholes 167 to 172) to Basin 5 (borehole 173). See Figure 9 for key.

Figure 13. Sediment-stratigraphic borehole transect across Basin 5 at transect 5(ii) showing the relation between sediments (a) north of the Old Castle Burn and (b) south of the Old Castle Burn (see Figure 7d).

Figure 14. Sediment-stratigraphic borehole transect from Ridge 8 across Basin 6 (boreholes 183 to 194). See Figure 12 for key.

Figure 15. Sediment-stratigraphic borehole transect across Ridge 10, Basin 7 (boreholes 217 to 224), Ridge 11 (boreholes 225 to the modified golf-hole corer boreholes R11 and B8. See Figure 12 for key.

Figure 16. Photographs of the sediment in B2 at borehole 101 (Figure 8), B3 at borehole 123 (Figure 9), B5 (south) at borehole 162 (below: Figure 18), B7 at borehole 214 (Figure 11) and B8 (Figure 11).

Figure 17. OSL net signal intensities in the uppermost c. 50cm of the NCT fill in Basins 2, 3 and 5-8 inc. Note changes in horizontal scale.

Figure 18. A contoured LiDAR image (0.25m intervals) of the ground around Basin 5 showing geomorphological features, some archaeological features, the locations of Transects 5(i) to 5(iv) and the conjectured extent of erosion of the NCT fill on the north side of Basin 5.

Figure 19. Natural and archaeological features at and east of Ridge 3.

Figure 20. A photograph looking east from the crest of the lower bank, with the ditch to the north and with the staff in the entrance gap in the bank.

Figure 21. Plots of LiDAR-defined long profiles (west-east) on (a) R4, (b) R6, (c) along R10 and R12 and (d) along 600m, within Castle Wood, of R14.

Figure 22. 2018 aerial photograph of the fields west of Castle Wood at Lantonside with the interpretation of subdued ridge crests and their appearance (a-f) on the LiDAR image of Figure 7b.

Figure 23. Percentages of GGS, Permian and Silurian clasts in ridges and beaches.

Figure 24. Map of the Caerlaverock peninsula showing prominent buildings, the Shore Road, areas of bedrock and of the New Castle Terrace north of the Lantonside storm beaches and their continuation in Castle Wood (only schematically represented), emphasising the area east of Ridges 4 to 8 that was eroded after their formation, and the area east of the subsequent Ridges 10 to 13 that was eroded after their formation (arrowed): modified from Brann (2004) figure 2.1.

Figure 25. Archaeological features at and around Old Caerlaverock Castle picked out by contours at 0.25m intervals.

Figure 26. Lidar transects at 0.5m intervals across the floor of the ‘harbour’ from north to south at (a) Transect 10 and (b) to the east.

Figure 27. Particle size distributions in harbour sediment.

Figure 28. (a) IRSL:OSL ratios, (b) OSL net signal intensities, (c) and (d) apparent doses of selected samples, and (e) IRSL:OSL depletion ratios plotted against depth.

Figure 29 [draft]. Age (BP) - altitude curve of Holocene RSL change in the lower Nith valley (modified from Smith et al 2003a; Figure 16) with the altitudes and age-ranges of OSL ages CERSA-752 and -751 and apparent change in RSL at these times shown in red.

Figure 30. Surveyed earthworks (Fig. 1.2 of Brann 2004).

Figure 31. Sediment stratigraphies along the thalweg of the dry valley (boreholes west of 40m distance) and the southern side of the southern moat (east of 25m distance).

Figure 32. Sediment stratigraphies along the axis of the southern moat. See Figure 31 for the key.

Figure 33. Sediment stratigraphies along the axis of the western moat. See Figure 31 for the key.

**Table Captions**

Table 1. Mean altitudes and single standard deviations of Basins 1-2 and 4-8 inc.

Table 2. Sediment descriptions of modified golf-hole cores in B2, B3 and B5 (south) to B8.

Table 3. Luminescence data from B2, B3, and B5-8 inclusive.

Table 4. ICP-MS and ICP-OES determinations of K (%), U and Th (ppm) concentrations, cosmic dose contributions, effective beta and gamma dose rates (wet) following water correction, burial doses, total effective environmnetal dose rates and corresponding depositional ages of two sediment samples in B3 and B6.

Table 5. Comparisons in luminescence between B2, B3 and B5-8 inclusive, and the 'harbour' in aliquot 1 apparent doses, calculated as percentages of the maximum (% max: 10.44 at 4.27m OD in the 'harbour'), plotted by increasing % max, with depths and altitudes of the samples. Aliquot 2 data are similar.

Table 6. Characteristics of R3 to R14: preserved height (a) is the height of the ridge above the surface of its shoreward basin; preserved height (b) is the height of the ridge above the surface of its seaward basin.

Table 7. Spatial and altitudinal correlation of the Lantonside ridges (Smith et al 2003a) and those in Castle Wood (this study).

Table 8. Details of gravel sampling sites on ridges and of samples: thickness is the thickness of the augered sample.

Table 9. Percentages of GGS, Permian and Silurian clasts in ridges and beaches.

Table 10. Shape characteristics in the three recorded lithologies of all clasts with a-axes >16.0mm.

Table 11. Percentages of all clasts and those of Galloway Granitic Suite, Permian and Silurian lithologies in three divisions: a-axis lengths 16-25mm, 25-50mm and >50mm.

Table 12. Mean and modal a-axis values (mm) for all clasts and percentages of angular (ang), subangular (suba), subrounded (subr) and rounded (r'nd) clasts of Galloway Granitic Suite, Permian and Silurian clasts with a-axes >16.0mm.

Table 13. Descriptive statistics of minerogenic clasts with a-axes >1.0mm in Bed 3, borehole 101, Basin 2.

Table 14. Details of AMS $^{14}$C assays in B2, B3, B6 and B7 using Oxcal 4.4 (Bronk Ramsey 2009) with INTCAL20 (Reimer *et al* 2020) and expressed at 95.4% probability.

Table 15. Sediment stratigraphy of the core from the 'harbour'.

Table 16. Luminescence data from sediments in the 'harbour'.

Table 17. ICP-MS and ICP-OES determinations of K (%), U and Th (ppm) concentrations, cosmic dose contributions, effective beta and gamma dose rates (wet) following water correction, burial doses, total effective environmental dose rates and corresponding depositional ages of three sediment samples from the 'harbour'.

Table 18. Details of AMS $^{14}$C assays in boreholes 43 and 44 in the western moat using Oxcal 4.4 (Bronk Ramsey 2009) with INTCAL20 (Reimer *et al* 2020) and expressed at 95.4% probability.